EFFECTS OF FRAME ASPECT RATIO ON
THE SEISMIC PERFORMANCE IMPROVEMENT OF
PANEL STRENGTHENING TECHNIQUE

A THESIS SUBMITTED TO
THE GRADUATE SCHOOL OF NATURAL AND APPLIED SCIENCES
OF
MIDDLE EAST TECHNICAL UNIVERSITY

BY

DİLEK OKUYUCU

IN PARTIAL FULFILLMENT OF THE REQUIREMENTS
FOR
THE DEGREE OF PHILOSOPHY OF DOCTORATE
IN
CIVIL ENGINEERING

AUGUST 2011

Approval of the thesis:

EFFECTS OF FRAME ASPECT RATIO ON
THE SEISMIC PERFORMANCE IMPROVEMENT OF
PANEL STRENGTHENING TECHNIQUE

submitted by **DİLEK OKUYUCU** in partial fulfillment of the requirements for the degree of **Doctor of Philosophy in Civil Engineering Department, Middle East Technical University** by,

Prof. Dr. Canan Özgen   _____
Dean, Graduate School of **Natural and Applied Sciences**

Prof. Dr. Güney Özcebe   _____
Head of Department, **Civil Engineering**

Prof. Dr. Tuğrul Tankut   _____
Supervisor, **Civil Engineering Dept., METU**

Examining Committee Members:

Prof. Dr. Güney Özcebe   _____
Civil Engineering Dept., METU

Prof. Dr. Tuğrul Tankut   _____
Civil Engineering Dept., METU

Prof. Dr. Hüsnü Can   _____
Civil Engineering Dept., GAZİ UNV.

Assoc. Prof. Dr. Barış BİNİCİ   _____
Civil Engineering Dept., METU.

Assist.. Prof. Dr. A. Cüneyt Aydın   _____
Civil Engineering Dept., ATATÜRK ÜNV.

Date : ———— 19.08.2011 ————

I hereby declare that all information in this document has been obtained and presented in accordance with academic rules and ethical conduct. I also declare that, as required by these rules and conduct, I have fully cited and referenced all material and results that are not original to this work.

Name, Last Name : Dilek OKUYUCU

Signature   :

ABSTRACT

EFFECTS OF FRAME ASPECT RATIO ON
THE SEISMIC PERFORMANCE IMPROVEMENT OF
PC PANEL STRENGTHENING TECHNIQUE

OKUYUCU, Dilek

Ph.D., Department of Civil Engineering
Supervisor: Prof. Dr. Tuğrul TANKUT
August 2011, 350 pages

PC panel strengthening technique was developed in M.E.T.U. Structural Mechanics Laboratory in order to respond the need of practical and efficient pre-quake seismic strengthening procedures applicable to RC framed structures. The idea behind the method is simply to convert the non-structural infills into load bearing structural elements by gluing PC panels over the existing infill wall surface. The remarkable advantages of the procedure is not only the considerable amount of seismic performance improvement but also the simplicity of application, very low levels of disturbance to the occupants and most importantly, the applicability during service.

A number of PC panel application parameters were experimentally investigated by previous researchers. The success of PC panel method on seismic performance improvement of RC frames with different aspect ratios was experimentally investigated in the present study. Total of fifteen, 1:3 scaled, one-bay, two-storey RC frames were tested in three various aspect ratio series. Constant axial load was applied to the columns and reversed cyclic load was applied in the lateral direction. Hollow brick

infilled frame and cast-in-place RC infilled frame were the lower and upper bound reference specimens, respectively.

Seismic performance indicators such as response envelope curves, lateral load carrying capacities, cumulative energy dissipations, initial stiffness indicators and ductility values clearly showed the effectiveness of PC panel application over different geometry of RC frames of concern. Moreover, PC panel application either with rectangular or with strip shaped PC panels provided seismic performance improvement to be almost equal to that of cast-in-place RC infill application for all series.

Equivalent diagonal strut concept was followed in analytical studies to simulate the infills of RC frame openings. The required strut material properties were estimated from total of eighteen individual wall panel tests. The bond-slip effect, due to utilization low strength of concrete and plain rebars, was also investigated and introduced to the analytical frame models. Non-linear push over analysis was performed for all specimens in OpenSees computer software. The analytical results were compared with that of experimental response envelopes.

Keywords: Pre-quake seismic retrofit, aspect ratio, precast concrete panel, hollow brick infill wall, cast-in-place RC infill.

ÖZ

ÇERÇEVE BOYUTLARI ORANININ ÖNÜRETİMLİ BETONARME PANELLERLE GÜÇLENDİRME TEKNİĞİNİN SAĞLADIĞI DEPREM PERFOMANSI ÜZERİNDEKİ ETKİSİ

OKUYUCU, Dilek

Doktora, İnşaat Mühendisliği Bölümü
Tez Yöneticisi : Prof. Dr. Tuğrul TANKUT
Ağustos 2011, 350 sayfa

Önüretimli betonarme panel tekniği, betonarme çerçeve türü yapılara uygulanabilecek pratik ve etkin deprem öncesi güçlendirme yöntemi ihtiyacını cevaplamak amacıyla O.D.T.Ü. Yapı Mekaniği Laboratuvarı' nda geliştirilmiştir. Yöntemin ana fikri, yük taşımayan dolgu duvarların, basit bir uygulama ile, duvar yüzeylerine önüretimli betonarme panel yapıştırmak suretiyle yük taşıyan yapısal elamanlara dönüştürülmesidir. Uygulamanın dikkat çekici yönü sadece önemli ölçüde sismik performans iyileşmesi sağlaması değil, aynı zamanda basit işçilik gereksimi, kullanıcıya çok az rahatsızlık verilmesi ve tüm bunlardan daha da önemli olacak şekilde, uygulama esnasında yapı işlevselliiinin kesintiye uğratılmaması gibi üstünlükler sağlıyor olmasıdır.

Önüretilmi betonarme panel yönemine ilişkin pek çok parametre önceki dönem araştırmacıları tarafından deneysel olarak incelenmiştir. Bu çalışmaların sonuçlarını temel alarak, önüretimli betonarme panel uygulamasının farklı boyut oranına sahip betonarme çerçevlerin sismik performanslarındaki iyileşme üzerindeki etkisi bu tez çalışması kapsamında deneysel olarak incelenmiştir. Toplam on beş adet, üç farklı

çerçeve boyut oranına sahip,1:3 ölçekli, tek-açıklık, iki-katlı betonarme çerçeve numunesi deneye tabi tutulmuştur. Deney süresince kolonlara sabit eksenel yük uygulanmış, yatay doğrultuda deprem yüklerini benzeştirir nitelikteki tersinir tekrarlı yük çevrimleri uygulanmıştır. Boşluklu tuğla dolgulu çerçeve ve yerinde dökme betonarme dolgulu çerçeve elemanları her seri için alt ve üst limit referans elemanları olarak test edilmişlerdir.

Tepki zarf eğrileri, yatay yük taşıma kapasiteleri, toplam enerji sönümleme değerleri ve başlangıç rijitliği göstergeleri gibi sismik performans bildiricileri, önüretimli betonarme panel uygulamasının farklı boyut oranlarına sahip çerçeveler üzerinde yapısal performansı önemli ölçüde iyileştirici yönde etkili olduğunu göstermiştir. Bununla birlikte, şerit ya da dikdörtgen şekilli önüretimli betonarme panel uygulaması ile, tüm çerçeve serilerinde, yerinde dökme betonarme dolgu duvar uygulamasına eşdeğer oranda sismik performans iyileşmesi sağlandığı gözlemlenmiştir.

Kuramsal çalışmalarda, çerçeve açıklıklarındaki dolgu duvarlar eşdeğer çapraz çubuk yöntemi kullanılarak modellenmiştir. Eşdeğer çubuklar için gerekli olan malzeme özellikleri ise, toplam on sekiz adet tekil dolgu duvarı testi sonuçlarından elde edilmiş ve kullanılmıştır. Ayrıca, düşük dayanımlı beton ve düz donatı kullanımı nedeni ile etkili olan aderans kayması etkisi öncelikli olarak boş çerçeveler üzerinde incelenmiş ve kuramsal çerçeve modellerine yansıtılmıştır. Tüm deney elemanları için, OpenSees bilgisayar programı kullanılarak lineer olmayan itme analizleri yapılmıştır. Kuramsal olarak elde edilen sonuçlar, deneysel zarf eğrileri ile karşılaştırılmıştır.

Anahtar Kelimeler: Deprem öncesi iyileştirme, çerçeve boyutları oranı, önüretimli betonarme panel, boşluklu tuğla duvar , yerinde dökme betonarme dolgu.

Dedicated to Mrs. Nimet Taşmasor OKUYUCU

My Beloved Mother

ACKNOWLEDGEMENTS

and adopted me as their academic daughter. It is really a very heavy responsibility to be worth of them. I hope, I can get over it. I love both of them, very much.

I can never forget the moral supports and interests of Prof. Dr. Mustafa Tokyay and Prof. Dr. Yener Özkan during my thesis work. They have always been the invisible motivating power to their dadash girl; as their recognition. Thanks them for everything.

I owe a very special thank to Prof. Dr. Uğurhan Akyüz. I can never forget his help and enchouragement at the very beginning of my graduate studies. Assist. Prof. Dr. A. Cüneyt Aydın has always been my biggest out-of-M.E.T.U support. His existence has always given trust to me. Special thanks to him for his friendly attitude.

Cordial thanks are due to Asst. Prof. Dr. Mehmet Baran. It will be always an honour for me to be in contact for further achievements. Burhan Avcı, the man who taught me to smile even at the worst times that your experiment totaly failed, deserves my very special thanks. M.E.T.U. Structural Mechanics Laboratory stuff Hasan Metin, Ömer Metin, Osman Keskin, Murat Pehlivan, H. Hüseyin Güler, Murat Demirel and Barış Esen are the technical power behind the work. My special thanks always go to all of them.

I owe to present my thanks to my dear friends Barış Erdil, Ramazan Özçelik, Tuba Eroğlu, Ceren Katipoğlu, Ali Şahin Taşlıgedik, Burhan Alam, Nazan Yılmaz, Emre Akın and Seval Pınarbaşı. Sebay Durul deserves very special thanks for his administrative guidance. Heplful guidance of the administrative staff of the department will always be memorized.

Judo is the other half of my life. It has thought me to never give up, even up to the last second and resist. I think, it is the time to start giving back to Judo.

TABLE OF CONTENTS

CHAPTERS

LIST OF TABLES

TABLES

LIST OF FIGURES

FIGURES

xxii

xxiii

LIST OF SYMBOLS

α	:	Frame Aspect Ratio
L	:	Beam Length of the Frame
Φ, d_b	:	Bar Diameter
f_y	:	Yield Strength of Steel
f_u	:	Ultimate Strength of Steel
f_s	:	Steel Stress
ε_y	:	Yield Strain of Steel
P	:	Equivalent Lateral Load on Column
PG	:	Pressure Gage
DG	:	Dial Gage
$LVDT$	:	Linear Variable Displacement Transducer
$1D$	:	One Dimensional
$2D$	:	Two Dimensional
$3D$	:	Three Dimensional
g	:	Gravitational Acceleration
N	:	Applied Column Axial Load
N	:	Column Axial Load Capacity
Δ_1	:	First Storey Level Lateral Displacement
Δ_2	:	Second Storey Level Lateral Displacement
h_1	:	First Storey Height
h_2	:	Second Storey Height
Δ_u	:	Ultimate displacement taken from bilinear representation of the response envelope curve on the forward loading direction which corresponds to post-peak load level corresponding to 15% strength loss
Δ_y	:	Yield displacement taken from bilinear representation of the response envelope curve on the forward loading direction
S_1	:	Tangent Slope of First Cycle

S_2	:	Tangent Slope of Second Cycle
F_{max}	:	Maximum Lateral Load
μ_Δ	:	Displacement Ductility Ratio
K_e	:	Effective Elastic Stiffness of Bilinear Representation of Response Envelope Curve
V_b	:	Base Shear
Δ_{top}	:	Top Displacement
Δ_{flex}	:	Lateral Flexural Deformation of a Column
Φ_y	:	Yield Rotation at the Column End
Δ_{slip}	:	Lateral Bond-Slip Deformation of a Column
δ_{slip}	:	Vertical Bond-Slip Deformation of a Column
u	:	Bond Stress
L	:	Column Height
l	:	Strain Penetration Length at Column End Zone
C	:	Compressive Force
T	:	Tensile Force
C_u	:	Compressive Force on the Column at Maxium Lateral Load Level
T_u	:	Tensile Force on the Column at Maxium Lateral Load Level
f_c, f_c'	:	Compressive Strength of Concrete
α_i	:	Parameter used in the Local Bond-Slip Relation
S_y	:	Slip corresponding to yield strength of longitudinal reinforcement
S_u	:	Slip corresponding to ultimate strength of longitudinal reinforcement
h_{col}	:	Column Clear Height
h_{inf}	:	Infill Height
L_{inf}	:	Infill Width
λ_1	:	Coefficient used to determine equivalent width of strut.
E_{inf}	:	Expected modulus of elasticity of infill material
E_{fe}	:	Expected modulus of elasticity of frame material
I_{col}	:	Moment of inertia of column
t_{inf}	:	Thickness of infill panel and equivalent strut
θ	:	Angle whose tangent is the infill height-to-length aspect ratio
a_{inf}	:	Width of diagonal compression strut
d_{inf}	:	Diagonal length of infill panel

$f_{c,frame}$	:	The compressive strength of the frame concrete
$f_{c,panel}$	:	Compressive strength of PC panel concrete
$f_{c,plaster}$	:	Compressive strength of infill plaster/mortar
$f_{c,strut}$	:	Compressive Strength of Strut Material
w_{strut}	:	Best-fitting strut width with the experimental data
$C_{w,strut}$	:	Strut width coefficient
ε_m	:	Strain Corresponding to Compressive Strength of Strut
ε_m	:	Ultimate Strain for Strut Material
b_s, c_s	:	Coefficients for Strain Calculations of the Strut Material Model
F_{strut}	:	Axial Load Carrying Capacity of a Compression Strut
k_{strut}	:	Axial Rigidity of a Compression Strut
RC	:	Reinforced Concrete
PC	:	Precast Concrete
M.E.T.U.	:	Middle East Technical University
NATO	:	North Atlantic Treaty Organisation
PEER	:	Pacific Earthquake Engineering Research Centre
IZIIS	:	Institute of Earthquake Engineering and Engineering Seismology

CHAPTER 1

INTRODUCTION

1.1. General

Public settlement area of Turkey is mostly located in one of the highly seismic zones of the earth. Earthquakes of varying intensities frequently occur and sometimes result in high amount of life and financial losses. The lack of the adequate lateral strength and stiffness of the RC (reinforced concrete) framed structures was evident to cause life losses together with moral and economical damages by the post-quake observations of the recent urban ground motions; for instance 1992 Erzincan, 1995 Dinar, Ceyhan, 1999 Izmit and Gölcük and 2003 Bingöl. Extensive post-quake rehabilitation was applied to the damaged structures and the large volume of seismically deficient structures was realized to be in need of seismic behaviour evaluation and retrofit. Consequently, development of new, practical and efficient pre-quake seismic strengthening methods and vulnerability assessment techniques for existing RC buildings became an important research area for Turkish structural engineering.

Majority of the existing seismically deficient building stock consists of RC framed structures with hollow brick infills which are constructed for architectural needs or aesthetic reasons. Investigating the damages caused by the above mentioned earthquakes, replacement of existing non-structural brick infill walls by cast-in-place RC infills aroused as the most commonly applied seismic system behaviour improvement method for this type of structures in Turkey. Positive contribution of this application on seismic performance of RC framed structures is evidently clarified by comprehensive experimental studies and earthquake experienced real applications. However, when cast-in-place RC infill application is evaluated as *an engineering solution*, some disadvantages of the procedure are realized together with the positive

1

contributions of the method on the overall system behaviour. Replacement of existing brick walls by cast-in-place RC infills is a time consuming engineering work; and necessitates evacuation and qualitative workmanship. Non-stop functioning of the building during the retrofit work is very important for the occupants of the residential buildings by means of moving and hiring costs and as well as the moral disturbances. Moreover, this issue is somehow more pronounced for public service buildings such as hospitals, education facilities and military structures. The managing authorities of these buildings may not easily decide for necessary retrofit applications because of the possible stop in functioning.

Considering the need of more practical and efficient pre-quake retrofitting techniques for RC framed structures, high strength PC (precast concrete) panel application was developed in M.E.T.U. Structural Mechanics Laboratory as an engineering solution being an applicable, practical and efficient pre-quake strengthening method for RC framed structures. This method was initially proposed as an alternative to cast-in-place RC infill application due to its occupant friendly fashion without evacuation requirement and with ease of application. The philosophy behind the technique is to make *a simple conversion* of existing non-structural hollow brick infill into a load bearing structural member by manageable sized high strength PC panels that are epoxy-glued to the existing infill wall and dowel connected to the enchasing frame elements.

Previous researchers matured PC panel application by performing comprehensive experimental research on 1:3 scaled RC frame specimens. **Duvarcı (2003), Süsoy (2004), Baran (2005)** Test specimens were prepared by introducing the most commonly observed structural weaknesses as to represent the vulnerable target buildings. The frame elements were subjected to the constant column axial load and reversed cyclic loading in the lateral direction to simulate earthquake forces. A number of PC panel application parameters such as panel geometry, connection details, etc. were experimentally investigated. The quasi-static test results indicated that the seismic performance indicators as lateral strength and stiffness, energy dissipation and ductility were considerably improved by PC panel application when compared to that of hollow brick infilled RC frame reference specimen.

The previous experimental research simplified the number of PC panel application parameters to be further investigated by showing superiority of the technique over the lower bound reference of hollow brick infilled specimen. Moreover, the previous research was carried out on the one-bay one-storey and one-bay two-storey RC frame elements with unique aspect ratio, as called standard frame, for simplification of the initial work. The main research topic of the current study is to compare the performance improvement gained by PC panel application over that of the upper bound reference of cast-in-place RC infilled frame specimens and the effect of the frame aspect ratio on the composite frame-PC panel strengthened infill system behaviour.

Strip and rectangular shaped, high strength PC panels without shear keys were the properly survived ones from the past research and used in the current study to evaluate the effect of frame aspect ratio on seismic performance improvement PC panel application. The performance improvement gained by PC panel application was compared with that of the cast-in-place RC infilled frame specimens with three different aspect ratios, by quasi-static RC frame tests. Individual infill wall panels were also tested under diagonal compression to obtain experimental data based material characteristics of infills for analytical studies.

PC panel method is proposed to be a pre-quake seismic strengthening method for RC framed structures. However, this is not the first stage of the engineering solution for the seismic risk reduction by pre-quake retrofitting of RC framed structures. The retrofit need of the building is to be assessed first and then the method to improve seismic performance should be decided. The object and scope of the thesis research are below presented.

1.2. Object and Scope of the Study

The basic idea of PC panel method is to convert existing hollow brick infill into a load bearing structural component by PC panels which are epoxy glued to the existing infill and connected to the surrounding frame elements by means of anchorage dowels. Besides significant seismic performance improvement, the major advantage of the technique is that it can suitably be applied to buildings still in the use with minimal disturbance to the occupant. Considering the previous experimental research results and recommendations, the present study basically aimed the following objectives:

- To investigate the effect of frame aspect ratio on seismic performance improvement of seismically deficient RC framed structures by PC panel application.
- To make a comparison in between the seismic performance improvement levels of RC frames strengthened by PC panel application and the upper bound reference of cast-in-place RC infilled frames
- Verification of seismic performance improvement in RC framed structures with PC panel method by performing 3D shake table tests under seismic excitations.

In the scope of the study, two other one-bay two-storey RC frames with a lower and a higher aspect ratio besides that of the previous standard specimen were designed and constructed in 1:3 scale. In each size of RC frame series, the following specimens were prepared and subjected to reversed cyclic lateral loading together with constant column axial load.

- Bare frame; *for verification of analytical modelling.*
- Hollow brick infilled frame; *the lower bound reference.*
- Rectangular PC panel applied frame; *strengthened specimen.*
- Strip PC panel applied frame; *strengthened specimen.*
- Cast-in-place RC infilled specimen; *the upper bound, target reference.*

Quasi-static test specimens were prepared by introducing the most commonly observed structural deficiencies such as:

- Poor concrete quality with low strength and ordinary pouring workmanship.
- Utilization of plain bars as both transverse and longitudinal reinforcement.
- Inadequate confinement (insufficient transverse reinforcement, 90° hooks which were not anchored to the core, insufficiently confined joint regions and column ends)
- Stronger beams and weaker columns

Total of eighteen individual infill wall panels were prepared and tested under diagonal compression, in the scope of infill panel tests. Plastered hollow brick infills, strip and rectangular PC panel strengthened hollow brick infill wall panels and pure RC infills were the test specimens as to reflect all of the infill types of quasi-static RC frame test specimens. These experiments were carried out to obtain rough information about general material characteristics of the infills which was further valued for analytical studies.

In addition, dynamic shake table tests were carried out on 3D rectangular PC panel strengthened specimen at IZIIS- Skopje, Republic of Macedonia in order to check the validity of the proposed method under seismic excitations.

CHAPTER 2

LITERATURE REVIEW

2.1. General

The starting point of the literature survey of the thesis research was to understand the behaviour of the infilled frames under lateral loads in the light of the published studies. Subsequently, the literature review was extended and focused on to understand the contribution of RC infills on RC frame behaviour under the lateral earthquake loadings. The previous studies on PC panel method development are also presented.

2.2. Infilled Frame Behaviour

Effect of infills on lateral strength and stiffness of the framed structures was initially investigated on steel frames. This approach was an important simplification for the beginning to start the research conducted on a frame made of a well known, homogenous and isotropic material in order to point out the first facts of the composite infill-frame system behaviour. It was logical so that there are great numbers of variables which influence the behaviour of such a composite structure. Studies on behaviour of RC infilled frames under lateral loads were observed to be conducted in the later stages with reasonable assumptions taken out from the infilled steel frame tests.

In the light of the comprehensive experimental and analytical research, it is widely recognized that masonry infill panels substantially alter the behaviour of RC or steel frame type structural assemblages under lateral loads. However, due to the lack of

information on various parameters affecting such structural systems, the beneficial effects of infills are not normally considered by engineers in actual design methods. Although considerable research has been devoted to the study of infilled frames for more than five decades, there is no widely accepted design method for such structures. Because infill panels are often considered to be structurally inactive and they are rarely taken into consideration during the design process as exampled in **FEMA-356 (2000).** This is explained partly by the complexity of interaction between frame and infill and the great number of variables which influence the behaviour of such a composite structure.

The very first breakthrough in the research of RC infilled frames may be attributed to the studies of **Polyakov** as many researchers stated. **Altın (1990)** In his early studies, Polyakov performed experiments on hinged steel frames with brick infills without openings subjected to monotonic lateral loads. The results of the tests indicated that infills loosed their load carrying capacities by cracking of the mortar along the compressive diagonal. Moreover, the equivalent diagonal strut concept was initially mentioned by Polyakov, as well. **Polyakov (1956)** Studies of the later times' distinguished researchers as **Holmes (1961), (1963)** and **Smith (1962), (1966), (1966), (1967), (1968)** and Smith and Carter **(1969)** made very important scientific contributions on the topic of infilled frame behaviour, mainly condensed over 1960. The equivalent diagonal strut concept was early formulized by studies of Smith and his colleagues and then further developed by contributions of **Mainstone (1971),** for instance.

In early experiments **Ockleston (1955)** and **Thomas (1955)** investigated the contribution of infilled panels to the strength of the frames subjected to in-plane lateral loading. It was found that masonry infills have a significant effect on both strength and stiffness of the composite system.

Benjamin and Williams (1957) carried out extensive tests on scaled models of infilled frames. Scale effect, panel aspect ratio, brick size, column strength and panel reinforcement were the investigated parameters. Both steel and concrete frames ranging

from 1:8 scale to 1:1 scale and infilled either with masonry walls or concrete were tested. While they concluded that the aspect ratio of the system markedly affected the strength and stiffness of the infilled frames, results indicated that column strength did not alter the stiffness of such systems in the elastic range. Although the scale effect was investigated, the study concludes that the scaling factor was not significant as long as it was greater than **one-third.** They recommended approximate empirical relationships for prediction of ultimate strength and stiffness of infilled frames.

Benjamin and Williams (1958) extended their study on the behaviour of infilled frames, basically focusing on scale effect for infilled frames. They have tested bricks infilled RC frames varying from 1:3 scale to the full size prototype specimens. According to their study, the one-third scaled specimens were essentially alike but the ultimate strength when converted to full scale values varied together with a corresponding variation in the first crack load. They conclude that, this variation shows that any scale effect difference has little significance and the errors caused by scaling are not significant compared to variations resulting from workmanship. They have also stated that the aspect ratio of the frame has an important influence on ultimate strength and rigidity.

Wood (1958) pointed out that, the neglection of the composite action of infills in stiffening tall buildings might result in the difficulties in assessment of the correct behaviour of the infilled frame systems. He has suggested to follow the use of collapse design methods that take into consideration the contribution of the infill panels, in order to make a reliable design of the infilled frames.

Ersoy and Uzsoy (1971) tested one-bay one-storey RC infilled frames. The specimens were subjected to increasing monotonic loading in the lateral direction. Effect of vertical loads, ratio of beam stiffness to column stiffness, infill thickness and the connection type in between frame and infill were reported to be the investigated parameters. They have concluded that, the presence of infill considerably improved lateral strength and rigidity of the RC frame. They have further stated that, the bond in between frame and infill *did not affect* the lateral load capacity and rigidity. Pin ended

diagonal compression strut was suggested to represent the infill in the analytical investigations.

Mallick and Garg (1971) conducted an experimental investigation on scaled frame specimens to investigate the effects of openings on the lateral stiffness of infilled frames. Their model frame was constructed in duplicate form on the back-to-back principle. Since, the duplicate frame was tested as a beam which is simply supported at its ends and carrying a central point load, the arrangement simulates a pair of rigid frames with central column acting like a rigid base by virtue of its symmetry about centreline. They have observed that, the composite action between the frame and infill was adversely affected as the opening position was moved towards the compression diagonal. They have tested the infilled frames with and without the shear connectors ending up with the conclusion that, infilled frames with shear connectors were stiffer than the frames without shear connectors. The study, also, concluded that the presence of connectors would probably reduce the risk of lack of fit which is also responsible for the decrease in the initial stiffness of the infilled frames.

Mallick (1972) and **Liauw (1979)** conducted series of experiments reporting that the interface connectors increased the initial stiffness and strength of the structure. Improving the interface mechanical characteristics by packing mortar between the panel and the encasing frame or by using mechanical ties had little effect on major crack levels or the ultimate load of infilled frames as stated by **Dawe and Seah (1989)**.

Klingner and Bertero (1976) performed integrated experimental and analytical studies to investigate the hysteretic behaviour of infilled frames under the actions similar to those caused by severe earthquake ground motions. They have applied quasi-static loads simulating the principal effects of severe seismic excitations to their test specimens of 1:3 scaled RC frames and observed an increase in both strength and stiffness of infilled frames compared to that of reference bare frames.

Kligner and Bertero (1978) further widened their investigation on the earthquake resistance of infilled frames which were subjected to quasi-static loads simulating the

9

principal effects of severe seismic excitations. Their test specimens were in 1:3 scale representing a model of the subassemlage end frame of an eleven storey building. The models were not deficient RC frames so that deformed bars were utilized to avoid the superior bond-slip behaviour of plain bars; for instance. The bare and infilled frames with hollow-core blocks were designed to permit the geometric scaling of reinforcement by the factor of 1:3 maintaining the same mechanical characteristics in the model as in the prototype. The test was conducted by load controlled fashion in the initial cycles and then finalized by displacement controlled reversals. Positive contribution of infills on lateral load behaviour of RC frames was concluded by the research. Moreover, the increase in strength, energy absorption and dissipation capacities achieved by the addition of engineered infills was found to be so high that it was supposed to exceed the detrimental effects of possible increases in inertial forced due to increased stiffness and consequent decrease in period.

Makino, Kawano and Kurobane (1980) reported to conduct an experimental research with six, 1:3 scaled steel frames with concrete infills for the design of framed structures with infills. They have concluded that, the presence of infill not only improved the lateral strength and stiffness of the system, but also prevented the local buckling of the steel frames. Therefore, they have suggested infilling as a seismic rehabilitation method for locally buckled steel frames, as well. They have stated to calculate the lateral strength of the infilled system as the summation of ultimate load in steel frame and ultimate strength of the diagonal compression bars the effective width of which was suggested to be 5.4 times the thickness of the infill wall.

Govindan, Lakshmipathy and Santhakumar (1986) investigated the ductility of infilled frames on approximately quarter scale RC frame specimens. They have tested two, single-bay seven storey RC frame specimen as bare frame and brick infilled frame. Load controlled reversed cyclic lateral load was applied to the specimens up to lateral load capacity and beyond this point the test was conducted in a displacement controlled fashion up to the pre-defined ductility level. They have presented the results of their experimental study stating the positive contribution of infill on the lateral strength and stiffness of the RC frames.

Caccese and Harris (1990) have tested seven storey, 1:5 scale, concrete-wall frame building on shake table as a part of a bench mark study of earthquake simulation testing of small-scale RC structures. They have compared their test results with a 1:32 scaled model of precast concrete shear wall test specimen. The important conclusion being parallel to their research objective was so that, the small scale modelling can be an alternative to simulate the actual seismic behaviour of actual prototype concrete structures.

Armin, Mahrabi, Shing, Schuller, and Noland (1996) investigated the effect of masonry panels on the structural behaviour of RC frames scaled in 1:2. They have investigated the effect of panel aspect ratio, the lateral loading schemes as monolithic and cyclic loading, distribution of the vertical loads and the type of masonry on the behaviour of RC frames. They have also applied different analytical procedures to obtain the response analytically. The experimental results indicated that infill panels could significantly improve the performance of RC frames. However, specimens with strong frames and strong panels were observed to exhibit a better performance than those with weak frames and weak panels in terms of the load resistance and energy-dissipation capability. The lateral loads developed by the infilled frame specimens were measured to be always higher than that of the bare frame. This is even true for the least ductile specimen deforming up to a drift level of 2%.

Mosalam, White and Gegely (1997) investigated the static response of infilled frames by performing quasi-static experimentation. Their examination of the strain measurements along different locations on the diagonal of an infill wall confirmed that compressive stresses predominate along the diagonals, thus the infill panels can be truly idealized as compression-only struts. Furthermore, it was shown that high concentrations of stresses occur at the compressed corners. These strains and stresses decay rapidly towards the centre of the panel. Up to the cracking load of the infill panel, an almost linear relation exists between the strains and stresses along the diagonals of the infill walls, thus, validating the equivalent strut analogy for that stage of loading. However, they have concluded that the width of the strut tends to be larger towards the centre and has a variable effective cross-sectional area.

Dukunze (2000) investigated the behaviour of RC frames with brick infills. He has tested forty-nine one-bay one–storey, 1:3 scaled test frames together with two, 1:3 scaled three-storey three bay specimens to assess the effects of adjacent panels on the overall behaviour of infilled frame systems. The significant parameters affecting the system strength were divided into those which are quantifiable and those which are not. The first category includes variables such as geometry and strength of infills, relative infill to frame stiffness, plastic bending moment capacity of the frame members, strength and rigidity of joints, beam to column relative stiffness, infill reinforcement, geometry and location of openings, effects of adjacent bays and upper stories, type unreinforced infill material and the type of frame. The second category encompasses parameters including, among the others, workmanship, climatic effects, grout and mortar variations due to job conditions, work stoppage, random variation of materials and human error. It was basically pointed out that, results of the diagonal testing of single infill panels with a perimeter frame proved to be useful in the determination of the behaviour of multi-bay, multi-storey infilled frames subjected to shear applied horizontally at the floor levels.

Asteris (2003) investigated the influence of the masonry infill panel opening in the reduction of the infilled frames stiffness by means of a new finite element technique. The main parameters were the percentage and location of the opening with respect to the whole infill. The author has concluded that, the presence of an opening significantly reduced the stiffness and the strength of the infilled frames. A centrally located opening for frames causes a reduction in strength and stiffness values less than the openings located at either end of the loaded diagonal and size, shape and location of openings had a definite influence on frame hinges developing at failure.

Dönmez (2006) investigated the analytical modelling of infill walls and the effect of infills on the overall system behaviour of RC framed structures during the earthquake. A representative RC building damaged during August 17, 1999 Kocaeli earthquake was modelled and analyzed for different situations by using SAP2000 computer software package. Different acceleration-time histories recorded during the Kocaeli and Düzce earthquakes were applied to the building for the analysis.

Akın (2006) reported to create a simple method to analyze the seismic behaviour of RC infilled frames subjected to earthquake loadings by verifying the proposed procedure with the experimental studies carried out by **Benjamin and Williams (1958)** and **Fiorato, Sözen and Gamble (1970)**. It was reported to determine the seismic response on an infilled RC frame by modelling the system as a wall with stiffness properties expressed as a composite of the two materials of RC frame and infill wall. The object of the study was, therefore, stated to use the so calculated drift as an estimator of the possible damage of the infill and surrounding RC frame. Total of four buildings with identical floor plans which survived 2003, Bingöl earthquake with light damages were reported to be modelled in SAP2000 computer package considering the proposed model. It was concluded to accurately estimate the response of RC infilled structures to any given ground motion and by making simple deflection checks it was reported to reasonably estimate the damage state of the building of concern.

The studies related to understand and simulate the infilled frame behaviour lie in a wide range. Some of the studies that made important contributions on the topic are summarised in this part. The positive contribution of infills on the frame system behaviour is commonly reported by either prototype or scaled model tests. The reported analytical investigations concentrated around the equivalent diagonal concept practices. The strut parameters were stated to be one of the most commonly studied issues for the related specific frame-infill system. In addition, 1:3 scale of RC frame tests is commonly accepted as to reflect similar behaviour with that of the prototype.

2.3. Contribution of RC Infills on RC Frame Behaviour

As the contribution of infills on overall system behaviour was well understood, the possibility and feasibility of retrofitting or strengthening of the existing deficient RC framed systems with the infills appeared as an important research topic for the structural engineering. The studies published in the literature related to the research on the parameters of RC infilling commonly concluded that, the use of RC infills as monolithical construction or cast-in-place application, etc. considerably improves the behaviour of RC frames under lateral loads and therefore, this method has appeared as a commonly applied seismic retrofit method.

The research theme of this dissertation is pre-quake retrofit of deficient RC framed structures by PC panel method as an alternative to cast-in-place RC infill application. Therefore, the RC infilling method needed to be well understood. Some of the published, remarkable studies are summarized in this part as to provide information about the efficiency and development of retrofitting RC framed structures by utilizing RC infills.

Kahn (1976) and Kahn and Hanson (1979) conducted a comprehensive experimental program to investigate the contribution of RC walls for earthquake strengthening of RC frames in one-half scale. Three strengthening techniques were investigated; one wall cast within an existing frame, a second was precast as a single unit and mechanically connected within the frame and the third was precast in six individual sections that were mechanically connected to the frame and each other. In addition, a bare frame was also tested. They have designed the tests to give a qualitative understanding for how infilled RC walls interacted with an existing RC frame. They have concluded that all types of RC wall application considerably improved seismic behaviour of RC frames and the cast-in-place RC wall demonstrated nearly the same nominal shear stress as the monolithically cast wall. Moreover, the storey drift of the cast-in-place RC infill was determined as half of that of multiple panels precast one. In addition, it was concluded that the multiple precast panel filling technique provided the greatest promise for aseismic rehabilitation with successful panel-to-panel connections. One of the major

14

observations was reported to be as the quick degradation of load lateral carrying capacity after the infill failure due to the lack of confinement of the column core which resulted in severe shearing forces in columns. Such deteriorations of existing columns are reported possibly to be a problem for structures using infill walls for earthquake strengthening. To minimize this column shear problem, additional column confinement utilization was suggested.

Yüzügüllü (1979) investigated the application of multiple precast RC panels for seismic performance improvement of RC frames. Bolted and welded connections in between panels were experimentally evaluated on a number of test specimens, by the researcher. The use of multiple precast RC panels with welded connections was reported to be very effective in RC frame strengthening together with the consideration of the high amount of energy dissipation.

Yoichi, Taneo and Masamichi (1980) reported their study over the evaluation of seismic performance improvement of RC framed structures by addition of shear walls. They have tested 1:3 scaled one-storey one-bay RC frames with different types of infills as shear resisting elements. They have stated their philosophy behind the strengthening as to increase lateral strength of the system and the ductility of the frame for earthquake energy dissipation capacity by plastic deformations. Steel bracing, steel frame in frame, steel truss in frame, cast-in-place RC infill, precast concrete wall panels as infills with openings and precast concrete wall panels as panels were investigated as the strengthening methods. All strengthened specimens provided increase in lateral load carrying capacity while, the lateral strength of the all strengthened specimens were measured to be in between the lower and upper bounds; bare frame and monolithic RC wall infilled specimen, respectively. The findings by the analytical modelling studies were reported to be well coincided with the experimental data.

Bertero and Brokken (1983) studied the effects of unreinforced and reinforced masonry and reinforced lightweight concrete infills on RC moment resisting framed buildings experimentally and analytically. The experimental investigation consisted of a series of quasi-static cyclic and monotonic load tests on 1:3 scaled models of the

lower 3-1/2 stories of 11 storey-3 bay RC frame infilled in the outer two bays. They have concluded that RC frames could be effectively retrofitted for seismic resistance purposes by the addition of RC infills that were properly attached to the frame. The study provided the research interest to the changes in dynamic characteristics of the building which should also be taken into consideration during the retrofit or strengthening design. The increase in the mass by addition of RC infills was reported to be negligible when all transverse frames of the prototype building under consideration were infilled in the same manner. The decrease of the fundamental period was also discussed and reported to be realized by incorporation of RC infills together with increase in damping when compared to that of bare frame. The increase in the strength was defined to be larger than the demanded strength; thus referring to the point of strength gain, the addition of RC infills was stated to be beneficial.

Higashi, Endo and Shimizu (1984) conducted tests on three-storey, one-bay frames strengthened by various techniques. The specimens were tested under horizontal and vertical loads. The three-storey one-bay frames with poorly detailed column reinforcement were infilled with either precast concrete panels, with steel bracing, by introducing steel frame inside or post cast RC walls. It was concluded that the specimens with steel-frame, steel-brace and four precast concrete panels showed not only higher lateral strength but also provided improvement in ductility.

Altın (1990) carried out a comprehensive research on strengthening of RC frames with RC infills in M.E.T.U. Structural Mechanics Laboratory. The effect of type of infill reinforcement and connection details between frame and RC infill were evaluated over the fourteen 1:3 scaled one-bay two-storey RC frames subjected to reversed cyclic loading. The model specimen used in this research was also used as standard test frames of PC panel method research with few changes. The effect of flexural capacity of columns and column axial loads on lateral strength and overall behaviour of the system were the two other variables studied. The study concluded with the considerable seismic performance improvement of RC frames by use of cast-in-place RC infills. The RC infills were found to increase both strength and stiffness significantly under lateral loads, provided that infills were properly connected to the frame.

Altın, Ersoy and Tankut (1992) investigated the hysteretic response of RC frames which were strengthened by means of cast-in-place RC infills. They have tested one-bay two-storey infilled frames in 1:3 scale under reversed cyclic loading. The use of RC infills for strengthening of RC frames which were in need of retrofit was observed to be very effective. The importance of workmanship quality for RC infill construction was underlined. The RC infill-to-frame connections were reported to be very important otherwise; the infills were found to be ineffective under reversed cyclic loading. The significant changes in the dynamic characteristics of the building that were introduced to the system by addition of the RC infills were also pointed out. The increase in strength demand was suggested to be calculated and checked against the strength increase; in cases of RC infill application for seismic strengthening purposes. Using the test results, they have made a simple dynamic evaluation to predict the dynamic behaviour of infilled frames under seismic action.

Frosch (1999) suggested precast infill wall system as a strengthening technique for RC framed buildings. Starting from the point of that, the requirements of the connection of discrete concrete elements to each other, he has tested RC frames to evaluate the connection between adjacent precast wall panels and to determine minimum details for satisfactory connection performance under the cyclic shear loading across the connection interface. He has assembled precast concrete panels into an infill wall for the rehabilitation of an existing structure. The main variables investigated were reported to be the shear key configuration, shear key size, panel spacing, the amount of the vertical reinforcement in the closure strip, the strength of the closure strip grout and precast panel thickness. The study pointed out that, the relative strength between the grout and panel concrete influenced the joint behaviour. The lower strength material controlled the peak capacity and failure surface location however; the residual capacity was not affected. Moreover, the peak and residual capacities of the infill walls decreased directly with the wall thickness and increased directly by the increase in the amount of vertical reinforcement in the closure strip.

Canbay (2001) tested a 1:3 scale, three-bay, two-storey frame in a vertical position under reversed cyclic lateral loads to investigate the behaviour and strength of RC

frames with cast-in-place RC panels in M.E.T.U. Structural Mechanics Laboratory. Considerable amount of increase in energy dissipation capacity, initial stiffness and lateral load capacity when compare to that of bare frame have been stated as the main conclusions.

Anıl (2002) investigated the behaviour of the frames that were strengthened by RC infills with openings under lateral reversed cyclic loadings. The main parameters were the size and arrangement of the openings in the infill panel. For this purpose, he has tested one bay-one storey, 1:3 scaled RC frames after strengthening by RC infills with different opening configurations.

Sonuvar, Özcebe and Ersoy (2004) experimentally investigated the rehabilitation of RC frames with RC infills as a post-quake seismic performance improvement method. They have tested five test specimens which were in 1:3 scale, consisting of two one-bay two-storey frames having the commonly observed structural deficiencies in Turkey. The specimens were subjected to the reversed cyclic loading. The experimental program was reported to be followed in two stages. In the first step, the bare frames were subjected to the reversed cyclic loading to introduce moderate damage and then the damaged frames were rehabilitated by applying RC infills. They have applied also different local strengthening methods to the column bases in order to decrease the adverse effect of inadequate lap splice length of the column longitudinal bars. They have concluded that, infilling the frames by utilizing RC infills increased the energy dissipation capacity, considerably. Introducing partial steel jacketing at lap splice regions of the columns and introducing boundary columns in the infill to overcome the deficiency caused by lapped splices had favourable effects on energy dissipation capacity of the test specimens.

Kara (2006) reported to experimentally investigate strengthening of non-ductile RC frames by introducing partial RC infills, over nine test specimens subjected to reversed cyclic lateral loading. The one-bay two-storey RC frame specimens were expressed to reflect the commonly observed structural deficiencies. Effect of the infill aspect ratio, existence of edge member at the free end of the infill panel and location of the openings

over the infill surface were stated to be as the experimentally investigated parameters. Test results were stated to observe to improve in lateral load carrying capacity, stiffness and energy dissipation by introducing partial RC infills. The importance of proper beam and column connections in between the RC infill and surrounding frame was underlined by stating to reach the most successful performance improvement over the so strengthened specimen. Positive effect of existence of the edge members on the performance improvement by partial RC infill replacement and increasing lateral load carrying capacity and stiffness with respect to the increased aspect ratio were further concluded.

The literature survey related to seismic performance improvement by RC infill application as a retrofit and pre-quake strengthening method commonly pointed out some important issues. Monolithically cast RC infills are reported to provide the better performance than that of cast-in-place RC infills under lateral loads. However, with a qualitative workmanship the performance improvement is stated to may be getting closer to that of the monolithical construction. Connection in between frame and RC infill is underlined to be very important for a better performance improvement, especially for post-peak behaviour under lateral forces. In addition, 1:3 scaled models were similarly reported to well represent the prototype behaviour in case of RC frame strengthening studies.

2.4. Development of PC Panel Method

The seismic performance improvement need of existing vulnerable building stock with efficient and practical methods became evident by the experiences of the recent earthquakes such as Erzincan (1992), Dinar (1995), Kocaeli and Düzce (1999), etc. There still exists a huge volume of seismically deficient RC framed structures with traditional hollow brick infills; the majority of which is for the public residential. For these structures to survive the moderate and strong ground motions, the inadequate lateral strength and stiffness deficiencies should be overcome. Yet, most common solution to the problem was replacement of the existing hollow brick infill with cast-in-place RC infills to improve seismic performance of the building. The positive contribution of this method on seismic performance of RC framed structures is evident by even above stated scientific studies.

Cast-in-place RC infill application requires evacuation of the building for a while. This provides additional costs for evacuation and hiring during the construction together with the moral disturbance to the occupants. Besides, it is a time consuming procedure. Since the volume of the vulnerable building stock is high, cast-in-place RC infill application stands far away from being a feasible solution.

M.E.T.U. Structural Mechanics Laboratory dealt with this issue deeply, by conducting comprehensive research projects as to present new and practical seismic performance improvement alternatives. A number of practical seismic strengthening and rehabilitation methods being applicable to RC framed structures were experimentally evaluated and proposed. **Keskin (2002), Erduran (2002)**, **Mertol (2002), Erdem (2003)** and **Akin (2009)** experimentally studied on the application of CFRP sheets as cross strips over the infill diagonals. **Binici and Özcebe (2006)** proposed the analysis guidelines for FRP strengthened infill walls for use in seismic evaluation methods. **Sevil (2010)** experimentally investigated the seismic performance improvement of deficient RC frames by use of steel fibre reinforced mortars as a new layer over the existing infill plaster. The common point of these methods were so that, the existing infill was upgraded by the proper procedure, any infill replacement was realized.

Performance of the RC frame - infill system under lateral loads was observed to be considerably improved in both methods.

High strength PC panel application method was also first designed and experimentally evaluated in M.E.T.U. Structural Mechanics Laboratory within NATO-SFP 977231 project conducted by **Özcebe (2000)** as a practical pre-quake seismic strengthening method for RC framed structures with hollow brick infills. The previous studies of the researchers on the development of high strength PC panel technique are summarized as follows.

Duvarcı (2003) carried out the first tests to evaluate the performance of the hollow clay brick infilled RC frames strengthened by high strength PC panels. Total of five 1:3 scaled RC frames were prepared and tested. The model frame was first designed and used by **Altın (1980)** as well as the test setup. This model frame is termed as "standard frame" for the later studies. RC frames were constructed by incorporating the commonly observed structural deficiencies of the target buildings such as inadequate confinement, poor concrete quality, inadequate transverse reinforcement and strong beam-weak column, etc. The frames were then infilled with hollow clay tiles and strengthened with different types of precast concrete panels. Rectangular and strip shaped PC panels with shear keys were used. The panel-to-frame connections were provided by anchorage dowels, while the panel-to-panel connections were realized by welding the panel reinforcements on the edges and then infilling the gaps by epoxy mortar. Two frames were tested as pilot tests in order to observe the functionality of the setup and one was the reference specimen with hollow clay bricks.

The specimens were subjected to constant column axial force and reversed cycling loading in the lateral direction. Both types of PC panels with shear keys greatly improved the system behaviour under lateral loads when compared to that of hollow clay brick infilled reference specimen. Lateral strength, stiffness and energy dissipation characteristics were improved considerably, ~3 times of the reference specimen, in average. The study recommended investigating the elimination of shear keys and welded connections for panel-to-panel connections and the effect of inadequate lap-

splice length of the column longitudinal bars. Moreover, tests on the same type of frames with cast-in-place RC infill walls were suggested for comparison of the performance of the high strength PC panel type retrofitting with that of the classical RC infilling technique. It was also pointed out that the shape of the panels did not have a significant effect in PC panel strengthening in the investigation over the standard model frame specimens.

Süsoy (2004) expanded the PC panel method research by testing total of eight 1:3 scaled one-bay one-storey frame specimens. Panel geometry (full height strip or nearly square), panel to panel connections (shear keys, welding, only epoxy), panel to frame connections (welding, dowels at two or four sides), effect of inadequate lap-splice length of the column longitudinal bars and constant column axial load levels were the investigated parameters. The reference frames and strengthened specimens were tested in the common test setup of the laboratory, under constant column axial loads and reversed cyclic loading in the lateral direction PC panels considerably improved lateral strength of the system by ~2.5 times with respect to that of the reference specimen, whereas initial lateral stiffness increased about ~3.3 times.

The very important conclusion from the study was the proof of redundancy of shear keys and welded connections for panel-to-panel connections. Epoxy mortar was reported to be successful to provide necessary panel-to-panel connection strength and recommended for the further studies. Lower axial load and presence of lap-spliced reinforcement were observed to create a negative effect on the lateral strength together with bar slip problems in specimens with lap-spliced column reinforcement. One-bay one-storey test frames reported to provide the similar results and behaviour as that of one-bay two-storey RC frame specimens. Therefore, it was concluded that these specimens can be used to take the advantages of simplicity in specimen construction and testing procedure.

Baran (2005) stated the test results of total of fourteen one-bay two-storey 1:3 scaled RC frame specimens. Effect of column axial load level, lap-splice deficiency, inner or outer side applications of PC panel method, presence of shear keys and welded connections for panel-to-panel connections were the main parameters investigated. The

lateral strength, lateral stiffness and the amount of the dissipated energy considerably improved by PC panel application when compared to that of reference specimens. Redundancy of shear keys and welded connections were pointed out once again as **Süsoy (2004)** also concluded. The complete use of anchorage bars at four sides of the infill composite was stated to be essential at the few lower stories of the buildings in real practice. In case of analytical studies, equivalent diagonal strut method was preceded and this method was reported to estimate the initial stiffness levels of the strengthened specimens reasonably, while the lateral strength was slightly overestimated for the specimens with lap-splice deficiency. The cost and application advantages of the proposed PC panel method were also discussed by the researcher.

Okuyucu and Tankut (2009) reported the test results of five one-bay one-storey frame tests that were conducted to investigate the effects of PC panel concrete strength on the performance improvement of RC frames by PC panel method. The PC panel strength was initiated as ~40-45 MPa and this grade of concrete for PC panels were generally produced and utilized in the past studies. Rectangular and strip shaped PC panels ~30 MPa and ~45 MPa, without any shear keys and welded panel-to-panel connections were produced and used to strengthen the specimens. The strength of the PC panel was found to be more dominant on behaviour of RC frames strengthened by rectangular panels when compared to that of strip panels. Panel concrete strength was very effective on initial stiffness values of strengthened specimens together with number of anchorage dowels when compared to the other seismic performance indicators. The lower strength panel provided the lower lateral load capacity and initial stiffness improvement, but higher ductility and total energy dissipation when compared to that of higher strength PC panels. However, it was underlined that the total energy dissipation comparisons could not be assumed as a certain comment so that; energy dissipation was directly related to loading scheme.

The above mentioned researchers matured the experimental evaluation of high strength PC panel technique. The only lacks of the method investigation was designated to be the experimental evaluation on the effect of frame aspect ratio and comparison of the performance improvement with that of the upper bound reference as cast-in-place RC infilled specimens which became the research topics of the present dissertation.

CHAPTER 3

TEST SPECIMENS

3.1. General

Total of fifteen, 1:3 scaled RC tests specimens were prepared and tested under constant column axial load and reversed cyclic loading in the lateral direction in M.E.T.U. Structural Mechanics Laboratory. Other than the *standard specimen* group, *narrower* and *wider* geometry specimen series were considered in the aspect ratio evaluation. The bare frames of each specimen series were prepared in structurally deficient manner as to reflect the target buildings. The specimens of each series are as follows:

- Bare frame
- Hollow clay brick infilled frame: *lower bound reference*
- Rectangular shaped PC panel strengthened frame
- Strip shaped PC panel strengthened frame
- Cast-in-place RC infilled frame: *upper bound reference*

This chapter presents information about the quasi-static test specimen dimension and reinforcement properties together with the preparation details. The procedure of the PC panel application to strengthen the test specimens in the laboratory conditions is explained. Designation of the test specimens, dimensions and reinforcement of each series of frames, the material properties, construction stages, strengthening applications with either PC panels of cast-in-place RC infills are provided with the necessary details.

3.2. Designation of Test Specimens

The designation of test specimens was done primarily considering the aspect ratio of the specimen series, so that the first letter indicates the aspect ratio of the series and the remaining for the infill type. Aspect ratio is defined as the ratio of the beam span length to column height of the first storey; both of the dimensions which are measured as joint-to-joint centreline distances. Frame specimens of three different aspect ratio values were taken into consideration in the present research and these values for each series are tabulated in **Table 3.1**. Since, standard frame was considered as the model in the previous PC panel investigations, the designation was realized with referring the beam span length of standard specimen. The specimen series with narrower and wider beam spans compared to that of standard frame were termed as *narrower* and *wider* series. Test specimens are denominated as presented in **Table 3.2**. The abbreviation of **NB**, shortly represents the **b**are frame of **n**arrower specimen series, for instance.

Table 3.1. Aspect Ratio Values of Test Specimen Series

$\alpha = L/h_1$	N - Series	S - Series	W - Series
h_1, beam length (mm)	700	1400	2050
H, column height (mm)	975	825	825
Aspect ratio, α	0.72	1.70	2.48
Scaled Drawing			
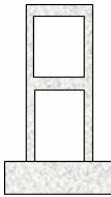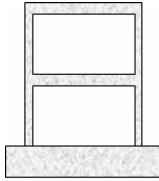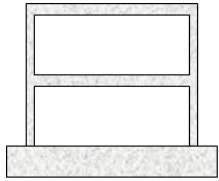
Table 3.2. Designation of Quasi-static Test Specimens

Series	Bare	Reference	Rectangular Panel Strengthened	Strip Panel Strengthened	Cast-in-place RC Infill Strengthened
Narrower ($\alpha = 0.72$)	NB	NR	NRP	NSP	NRC
Standard ($\alpha = 1.70$)	SB	SR	SRP	SSP	SRC
Wider ($\alpha = 2.48$)	WB	WR	WRP	WSP	WRC

3.3. Materials

The materials used in specimen productions and their mechanical properties are presented in this section, before presenting geometry, reinforcement and strengthening details of the individual test specimens.. It should be underlined that, all of the specimen productions were realized in M.E.T.U. Structural Mechanics Laboratory.

3.3.1 Concrete

It was a sensitive stage to product low strength frame concrete, which was of great importance of similitude, together with almost high strength PC panel concrete for the scaled test specimens. Standard aggregate and cement tests were initially performed in M.E.T.U. Materials of Construction Laboratory; small amount of test mixes were prepared and then the mix designs were optimized. Frame, panel and RC infill concrete were all produced in M.E.T.U. Structural Mechanics Laboratory. Target concrete strength was ~10 – 15 MPa for frames, ~45 MPa for PC panels and ~20 MPa for cast-in-place RC infills. Mix design of each concrete mixes are presented in following **Table 3.3**, **Table 3.4** and **Table 3.5** for frames, PC panels and cast-in-place RC infills, respectively. CEM 32.5 standard cement was used for both frame and RC infill concrete while CEM 42.5 cement was preferred for PC panel construction. Vibration was applied to frame concrete after pouring in formwork as shown in **Figure 3.1.**

Table 3.3. Mix Design of RC Frame Concrete (weight for $1m^3$ concrete)

	Weight (kg)	**Proportion by weight (%)**
Cement (CEM 32.5)	449	19
0 - 3 mm Aggregate	902	38
3 - 7 mm Aggregate	475	20
7 - 15 mm Aggregate	290	12
Water	264	11
Total	2380	100

Table 3.4. Mix Design of PC Panel Concrete (weight for 1m^3 concrete)

	Weight (kg)	**Proportion by weight (%)**
Cement（CEM 42.5)	875	38
0 - 3 mm Aggregate	760	33
3 - 7 mm Aggregate	445	19
Water	230	10
Admixture (Plasticizer)	9	0.4
Total	2310	100

Table 3.5. Mix Design of Cast-in-place RC Infill Concrete (weight for 1m^3 concrete)

	Weight (kg)	**Proportion by weight (%)**
Cement（CEM 32.5)	881	39
0 - 3 mm Aggregate	791	35
3 - 7 mm Aggregate	384	17
Water	203	9
Total	2260	100

Figure 3.1. Vibration of Frame Concrete in Formwork

Special attention was paid for PC panel concrete production since the target strength was higher. Rectangular and strip shaped PC panels without any shear keys were all 20 mm thick. Therefore, smaller size aggregates had to be used in a lower w/c ratio. In order to improve the workability of the PC panel concrete, superplasticizer (Sika Viscocrete 5W) was used. Vibration of PC panel concrete in slender moulds was also considerably avoided by superplasticizer utilisation. A few plastic hammer blows were generally enough for compacting of the PC panel concrete bewaring any damage to panel formwork.

Upper bound references of all frame series were cast-in-place RC infilled specimens. First bare frame was prepared, and then anchorage dowels and RC infill reinforcement were installed into the frame opening together with the wooden formwork construction. Finally, test specimen was horizontally settled and the infill concrete was poured as shown in **Figure 3.2**. Since the necessary amount of concrete for RC infill was less then the mixing capacity of the concrete mixer, one batch was enough with six cylinder specimens. Curing and cylinder specimen testing applications were all same as frame concrete.

Figure 3.2. Cast-in-place RC Infill Preparation for Specimen **NRC**

Considering the mixing capacity of ~500 kg for the concrete mixer, RC frame concrete for all specimens was prepared as batches. At least six standard cylinder specimens were taken from each batch following the standard procedures, in order to define the compressive strength of the frame concrete on the day of testing. Standard test cylinders were 150 mm in diameter and 300 mm in height. Concrete specimens were kept under the same curing conditions as the test frames. Curing of the concrete was of primary concern to gain the target strength. Frame specimen and its cylinder concrete specimens were coated by wet burlap, ~24 hours after casting. This application provided the necessary moisture and temperature conditions for chemical hydration. Same concrete sampling procedure was also applied for RC infill and PC panel concrete batches. Since the panels were cured in a heatable water tank, so the cylinder specimens were.

Concrete specimens were capped and tested under uniaxial compression on the day of testing under same loading rate as shown in **Figure 3.3**. Compressive strength values for all concrete and mortar of each test specimen are tabulated in **Table 3.6.**

Figure 3.3. Compressive Strength Test of Cylinder Concrete Specimens

Table 3.6. Compressive Strength Values of Concrete and Mortar for All Test Specimens

Specimen	Panel Type	Compressive Strength (MPa)		
		Frame Concrete	**Panel Concrete**	**Mortar / Plaster**
NB	-	7.9	-	-
NR	-	19.0	-	5.0
NRP	rectangular	14.5	48.0	5.0
NSP	strip	13.8	48.0	5.0
NRC	RC infill	16.0	16.0	-
SB	-	13.7	-	-
SR	-	12.2	-	5.5
SRP	rectangular	11.9	55.7	3.5
SSP	strip	16.1	58.0	5.8
SRC	RC infill	15.0	23.1	-
WB	-	14.9	-	-
WR	-	17.6	-	5.1
WRP	rectangular	16.2	55.8	5.4
WSP	strip	12.8	62.1	5.3
WRC	RC infill	13.6	16.4	-

3.3.2. Mortar / Plaster

Hollow clay brick infill walls of the model frames were similarly produced in the laboratory by ordinary workmanship. The mortar which was also used in plastering was prepared with the mix design given in **Table 3.7**. CEM 32.5 cement and lime was utilized in mortar mixes as binders to reflect the common application in the site. Before the frame tests, individual infill wall panels were also prepared and tested under diagonal compression in order to get information about the mechanical properties of the infill composites. The mortar and plaster of these wall panels were also prepared by the same mix design. At least six mortar samples were taken from each mortar mix. The cylinder mortar specimens were 100 mm in diameter and 200 mm in height. These samples were kept under the same conditions of infill and tested on the day of testing, in M.E.T.U. Materials of Construction Laboratory. Compressive strength values of mortar/plaster mixes for all specimens are presented in **Table 3.6**.

Table 3.7. Mix Design of Mortar/Plaster (weight for $1m^3$ mortar)

Material	Cement	Lime	Sand	Water	Total
Weight (%)	11.0	11.0	62.0	16.0	100

3.3.3. Hollow Clay Bricks

Hollow clay bricks are commonly used in Turkey for traditional infill wall construction. Since a true model representation of the prototype was tried as much as possible, 1:3 scaled hollow clay bricks were used in lower bound reference specimen production. The bricks were of special production in a factory of Turgutlu – Manisa city presented as in **Figure 3.4**.
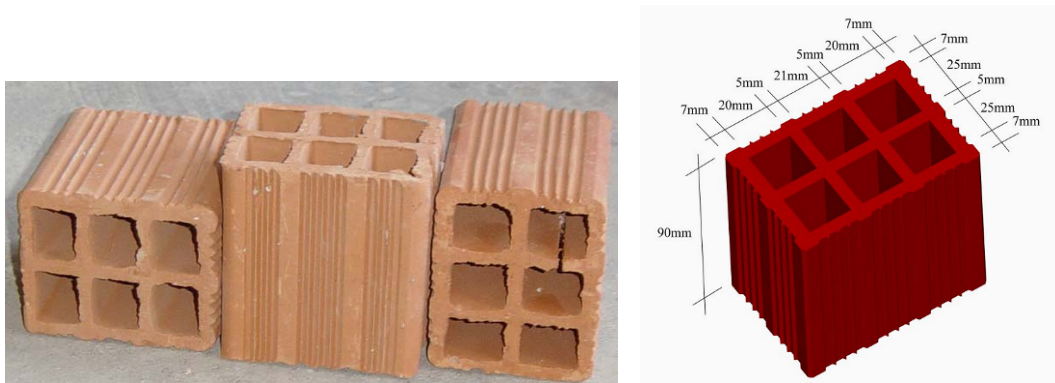
Figure 3.4. Hollow Clay Bricks

Randomly selected infill bricks were subjected to compression tests parallel to their holes. The brick was first capped on both upper and lower faces and then the load was applied. Compression test results of hollow clay bricks are presented in **Table 3.8**.

Infill wall preparations were all done by ordinary workmanship. First the bricks were jointed together by mortar and then the same mortar was utilized as ~10 mm thick plaster on both interior and exterior sides. The infill was plastered together with surrounding beam and column surfaces on the exterior sides.

Table 3.8. Compression Test Results of the Hollow Clay Bricks

Test No	Failure Load (kN)	Gross Compressive Strength (MPa)	Net Compressive Strength (MPa)
1	64.7	11.0	23.0
2	81.5	13.9	29.0
3	76.3	13.0	27.1
4	65.5	11.2	23.3
5	81.8	13.9	29.1
6	78.0	13.3	27.7
7	82.5	14.1	29.3
8	77.5	13.2	27.5
9	88.2	15.0	31.3
10	73.2	12.5	26.0
Average:	*76.9*	*13.1*	*27.3*
C.O.V. :	*0.092*	*0.097*	*0.097*

3.3.4. Steel

Plain bar utilization as longitudinal and transverse reinforcement in load bearing structural members was observed to be one of the most critical structural deficiencies of the target building stock that adversely affect the structural behaviour. Therefore, Φ8 and Φ4 plain bars were respectively used as longitudinal and transverse reinforcement of frame elements in accordance with scaling considerations. Reinforcement detailing of beam and column sections is presented in **Section 3.4.** Φ6 plain bars were used in cast-in-place RC infill mesh as two layers. Φ10 deformed bars were considered as anchorage dowels of PC panels. Welded wire fabric steel mesh of Φ3 plain bars was used as PC panel reinforcement only by a single layer. Φ8 and Φ16 deformed bars were used in frame foundations as transverse and longitudinal reinforcements.

At least three coupons were randomly taken for each steel batch and subjected to axial tension tests in order to define the yield and ultimate strength values. Φ4, Φ6 and Φ8 plain bars were subjected to axial tension test in a test set-up in M.E.T.U. Structural Mechanics Laboratory which was especially arranged for axial tension tests, as shown

in **Figure 3.5**. The remaining samples were tested in M.E.T.U. Materials of Construction Laboratory due to capacity and test sample diameter limitations of the above mentioned set-up. Summary of steel coupon test results are presented in **Table 3.9**, at the end of this section. Stress – strain relationships of Φ4, Φ6 and Φ8 could be obtained by valuing extensometer readings to calculate the strains. A 50 mm capacity of extensometer with 0.01 mm precision was used to measure elongations. Besides, a strain gage was placed on one of the steel sample of Φ8 and more accurate measurements were taken in the elastic range simultaneously with extensometer readings as also shown in **Figure 3.5**.

closer view of deformation
measuring instrumentation
(strain gage for Φ8 bars)
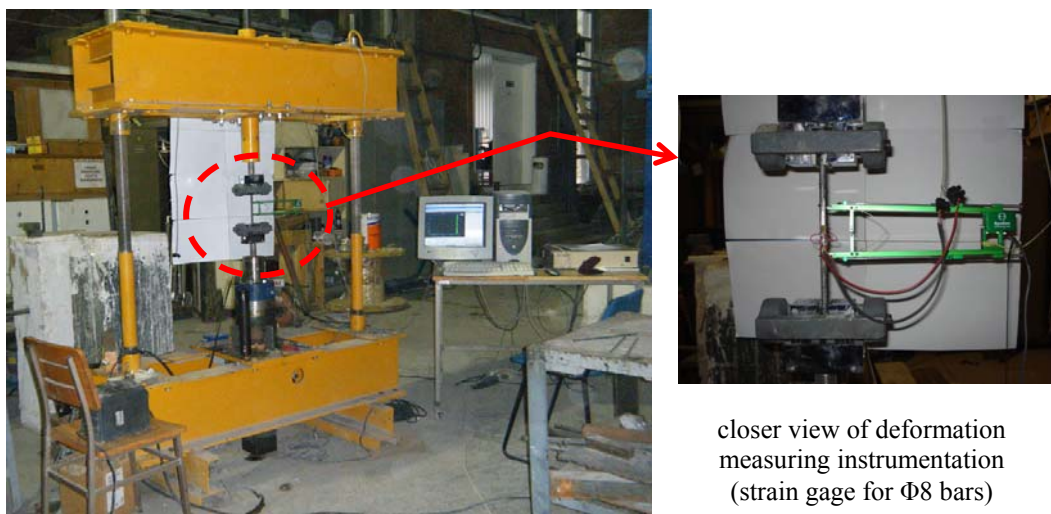
Figure 3.5. Test Set-up View for Steel Bar Tension Tests

Stress – strain relationships obtained by extensometer and load cell readings for Φ4, Φ6 and Φ8 plain bars are presented in **Figure 3.6** which also shows stress-strain relationships for Φ8 plain bar which were drawn by both strain gage and extensometer readings up to the yield point. Test data up to the ultimate strain could be obtained by extensometer, while strain gage could only provide data up to yield point. Therefore, only the extensometer readings were taken in the other coupon tests.
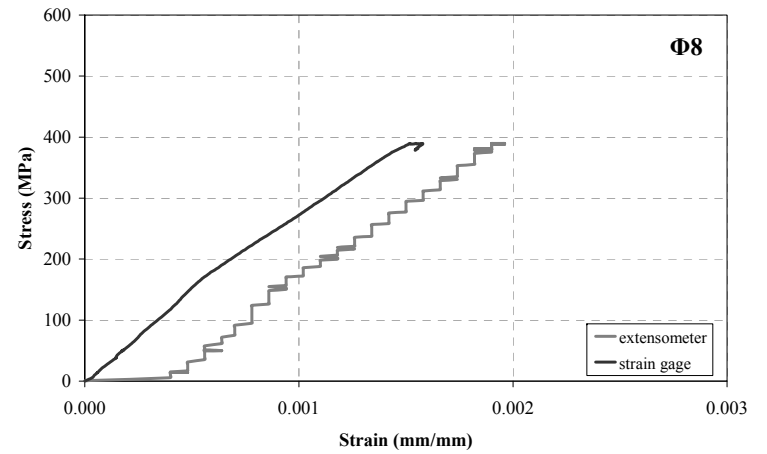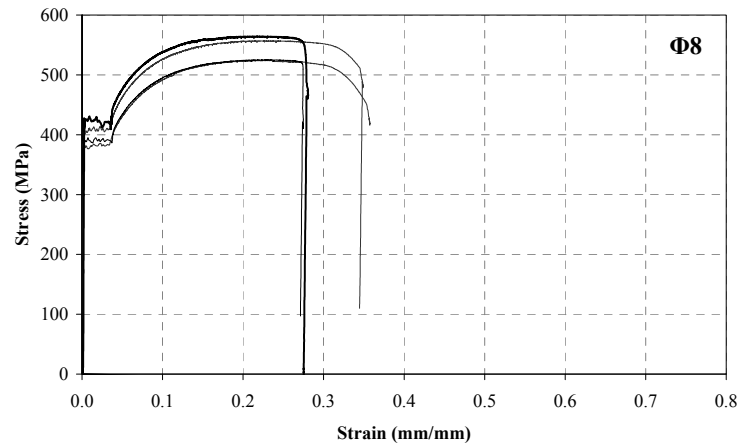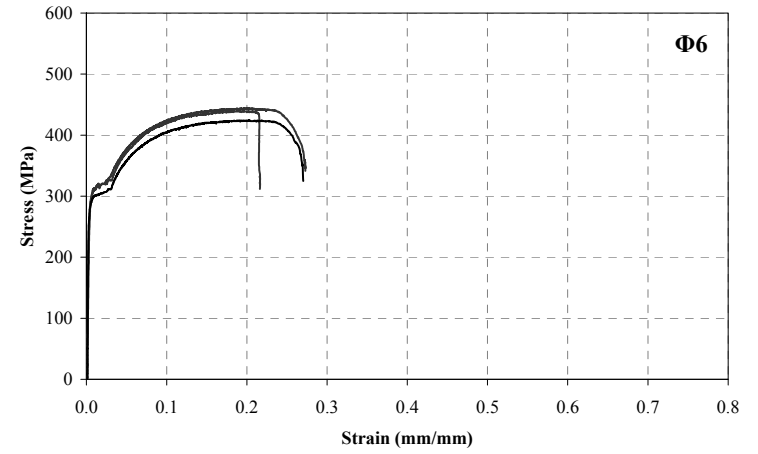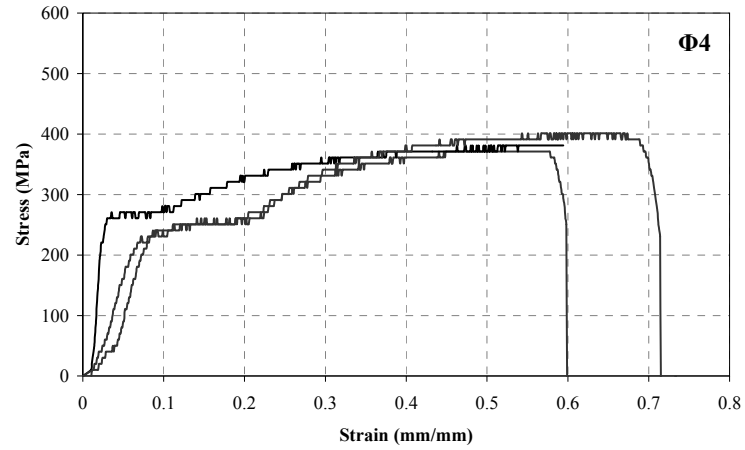
Figure 3.6. Stress – Strain Relationships for Steel Bars

Table 3.9. Mechanical Properties of Steel Bars

Φ (mm)	Property	Location	f_y (MPa)	f_u (MPa)
3	Plain	Mesh reinforcement for PC panels	-	680
4	Plain	Transverse reinforcement for frame beams and columns	268	395
6	Plain	Cast-in-place RC infill reinforcement	329	445
8	Plain	Longitudinal reinforcement for frame beams and columns	405	545
8	Deformed	Transverse reinforcement for frame foundation	432	615
10	Deformed	Anchorage dowels of PC panels and cast-in-place RC infills	518	-
16	Deformed	Longitudinal reinforcement of frame foundation	420	-

3.3.5. Epoxy Mortar

Epoxy mortar was utilized in PC panel application for two purposes. Anchorage dowels were placed in surrounding frame member by Spit Epcon, and PC panels were epoxy glued to infill by Sikadur-31 type gluing chemicals.

Spit Epcon is a kind of chemical embedment system for fixing of rebars in concrete. This product is made up of two components contained in a single cartridge with two identical cylinders. First cylinder contains 100% epoxy resin and the second one contains hardener. The epoxy is applied to the hole which all dust is totally removed. Materials in two cylinders are mixed in the special apparatus and the final mix is injected from the bottom of the hole, gradually filling it until 50% full. The anchorage rebar was inserted into the hole by hand with a twisting motion until the end of the hole was reached. The bar should also be cleaned and free from oil and grease. Final check for that hole to see if it was filled and it was waited for the resin to harden. It is reported

to wait ~24 hours for perfect strength and load application. Specific bond strength values of Spit Epcon epoxy for varying concrete grades and rebar diameters together with other detailed information are presented in the product catalogue. **(Spit-Epcon, 2005)**

Sikadur – 31 epoxy mortar was utilized to glue PC panels to the infill surface and to provide shear resistant panel-to-panel connections. By using this material, a successful transformation of non-structural infill into a load bearing structural member was realized; out of plane resistance against buckling of the PC panels was achieved through connecting them to the existing infill surface. The gaps in between panels and anchorage dowels were also filled by this chemical.

Sikadur-31 is a two-component solvent-free thixotropic epoxy adhesive mortar. Component A and B are mixed by a proportion of 3 (A) : 1 (B); by weight or volume. The mixing can be easily done by ordinary tools as illustrated in **Figure 3.7**. Some mechanical properties of this chemical are tabulated in **Table 3.10** as provided the product catalogue. The values are reported for the end of 10 days curing less than 20 ^{o}C curing temperature.

Figure 3.7. Sikadur – 31 Epoxy Mortar Preparations

The commercial product of Sikadur – 31 was preferred for the PC panel application among the others considering the following superiorities.

- Applicability to concrete, plaster, stone, wood, glass, etc. different surfaces

- Ease in mixing and provision of good workability properties

- Being a thixotropic material that is suitable for vertical application

- Applicability to both dry and moist surfaces

- High resistance to chemicals and water – resistance

- Hardening without shrinkage; no volume loss

- Only one material for gluing and filling work

- Suitable mechanical properties for PC panel application

Table 3.10. Some Important Mechanical Properties of Sikadur – 31 Epoxy Mortar

Property	Value (MPa)
Compressive strength	65
Flexural tensile strength	35
Direct tensile strength	17
Adhesion to concrete	> 4
Adhesion to steel	15
Modulus of elasticity	4300

Sikadur – 31 was placed on PC panels surfaces as a thin layer and then the panel was glued to the infill. Cleaning of the panel and infill surfaces were of great importance for perfect bond. Detailed information about this chemical is provided in product catalogue. **(Sikadur – 31, 2009)**

3.4. Geometry and Reinforcement Details of Specimens

General information about the bare frame dimension and reinforcement of each group specimens are provided in this section first, and detailed information about each of the RC frame specimens such as panel configuration, cast-in-place RC infill properties, etc. are given in the following sections. The data of each test was evaluated both within its series and among the specific test data of the other group specimens.

RC frames were designed and produced in M.E.T.U. Structural Mechanics Laboratory, considering the most commonly observed structural deficiencies observed in the target building stock. Test specimens reflected the typical characteristics and common weaknesses of the RC framed structures in Turkey as exampled follows:

- Low concrete strength and poor workmanship.
- Utilisation of plain bars as both longitudinal and transverse reinforcement.
- Poor confinement with 90 degree hooks of stirrups.
- Strong beams - weak column connections.

Presence of lap splices in column longitudinal bars was observed to be one of the most critical structural weaknesses which affected the infilled frame behaviour most adversely under the seismic excitations. **Sonuvar, Özcebe and Ersoy, (2004)** Effect of lap-spliced column reinforcement on seismic performance improvement by PC panel application was previously investigated. **Duvarcı, (2003), Süsoy, (2004)** Therefore, all longitudinal column bars were continuous and no lap-spliced column reinforcement was used in the present study.

Reinforcement of the test specimens was prepared in the laboratory with a special attention introducing the above mentioned structural deficiencies. Φ8 and Φ4 plain bars were used as longitudinal and transverse reinforcement, respectively. The spacing of the beam and column stirrups was the same as 100 mm. Section geometry and

reinforcement details of beam, column and foundation of the specimens were the same for all RC frame specimen series as presented in **Figure 3.8** and **Figure 3.9**.
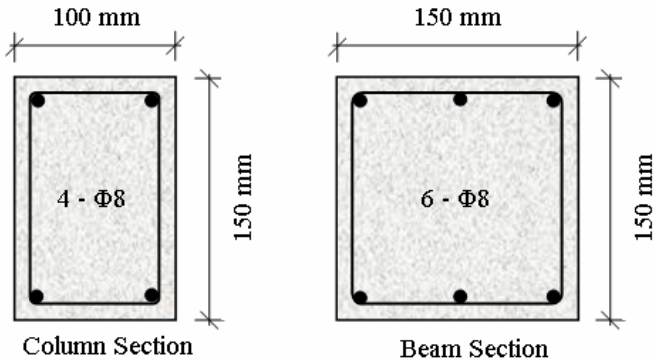
Figure 3.8. Dimension and Reinforcement of Column and Beam Sections
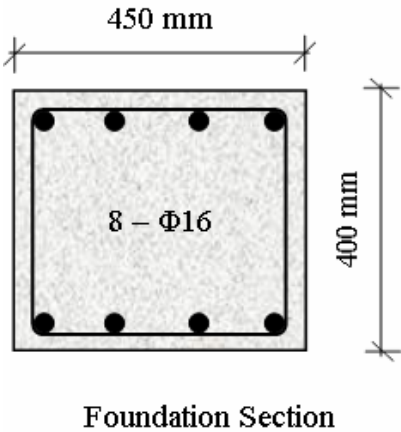
Figure 3.9. Dimension and Reinforcement of Foundation Sections

RC frame specimens of all series were constructed following the same procedure. Reinforcement cage was first prepared. Formwork of the frame was set onto the floor of the laboratory and its horizontal level was established. The mould was coated by a thin layer of grease and finally the reinforcement was properly installed. Clear cover distances were carefully arranged. The steel hole pipes of the foundation were all coated by grease and located. These pipes created the holes necessary for fixing the model foundation to the universal base. Finally, concrete was prepared and cast. Soon after the concrete hardened, the hole pipes were taken out and the specimen was

covered by a wet burlap. Demoulding was realized ~6-7 days after casting and curing procedure was carried out considering the temperature of the laboratory. None of the specimens was tested before 28 days of casting.

The formwork of RC models was manufactured from 2.0 mm thick steel plates that were assembled with bolts. The steel forms were accurately manufactured with an error of one-tenth of a millimetre. The steel plates, forming the parts of the formwork, were stiff enough to avoid any unexpected deformations during casting of the specimens. The stiffness of the steel plates was gained by bending both edges. The width and the length of the bent edges were 20 mm and 50 mm, respectively. The details of the formwork for the columns and beams and for the rigid foundation of narrower series of specimens are presented in **Figure 3.10** and **Figure 3.11**. Standard and wider series of specimens were prepared by using the same type of formwork sets that were prepared in suitable dimensions.

The specimen preparation was realized in the following order. Bare frames were first cast and subsequently modified according the specimen requirements such as infilling by the hollow brick infill, strengthening by PC panels or cast-in-place RC infill in the openings of both storeys. Dimensional and reinforcement details of each series of the RC bare frames are presented in the following sections.
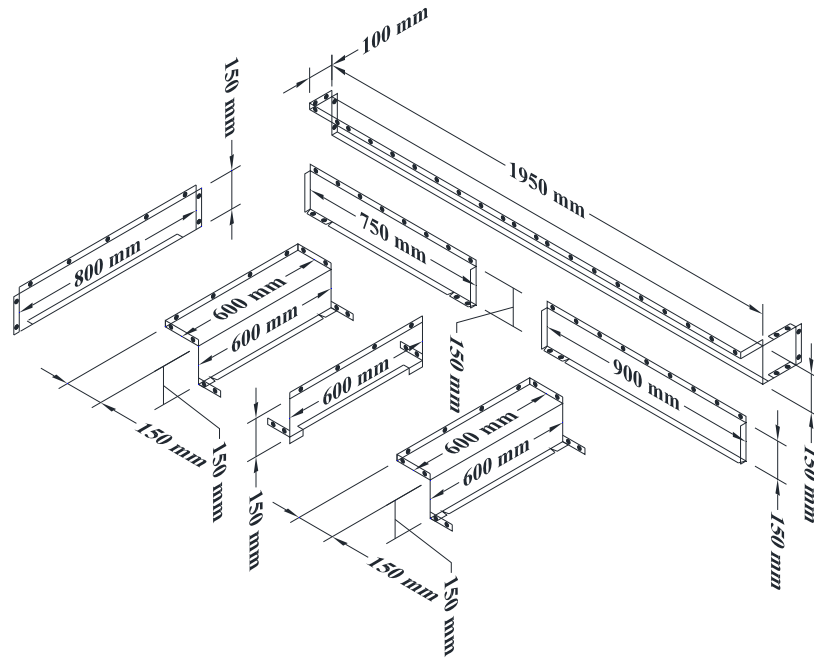
Figure 3.10. Details of the Formwork for the Beams and Columns of Narrower Series Specimens
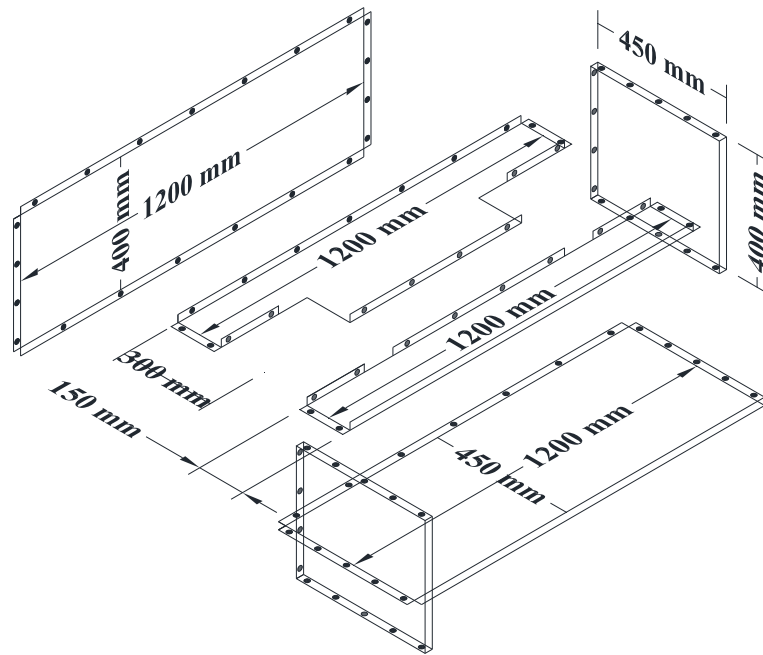
Figure 3.11. Details of the Formwork for the Rigid Foundation Beam of Narrower Series Specimens

3.4.1. Narrower Series of Specimens

First series of specimens was designed and constructed with an aspect ratio of; α =0.72. Since these specimens had the narrowest beam span when compared to standard specimen; they were shortly termed as *narrower series* of specimens. This geometry of specimens were tested in order to see the effectiveness of PC panel application on the frame systems on which the flexural effects are dominant. Designation of narrow series specimens and definition of aspect ratio are presented in **Section 3.2**. Dimensions of narrower series RC frame are presented in **Figure 3.12.** Reinforcement details of narrower series frames are shown in **Figure 3.13.** Narrower series specimens were cast horizontally by using steel formworks same as the other group specimens. **Figure 3.13** also provides a view of narrower series of RC frame formwork and reinforcement just before pouring.
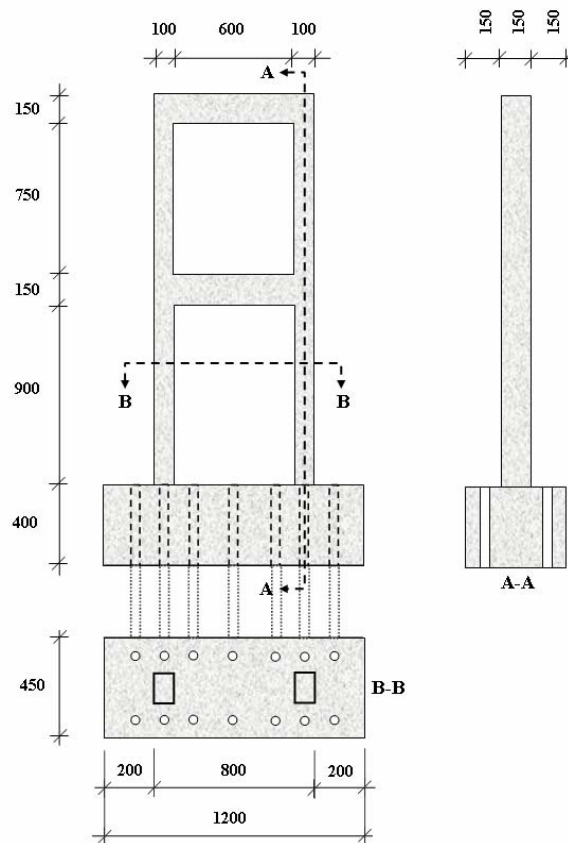
Figure 3.12. Dimensions of Narrower Series Specimens (dimensions in mm)
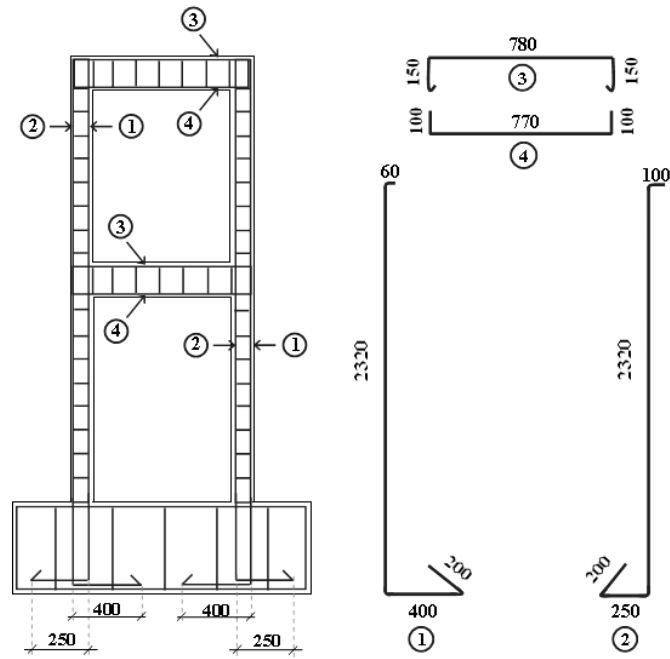
Figure 3.13. Reinforcement Details of Narrower Series Specimens (dimensions in mm)

3.4.2. Standard Series of Specimens

PC panel application was previously investigated on RC frames with an aspect ratio of; α = 1.70. **Duvarcı, (2003), Süsoy, (2005), Baran (2005)** This geometry of specimens were also prepared and tested for the aspect ratio effect evaluation and shortly termed *standard series* of specimens. Dimension and reinforcement details of the standard series bare frame are presented in **Figure 3.14** and **Figure 3.15. Figure 3.15** also provides a view of standard series of RC frame formwork and reinforcement just before pouring. The details of the standard series RC frame formwork for the columns, beams and for the rigid foundation beam and are similar to that of narrower series specimens presented in **Figure 3.10** and **Figure 3.11**.
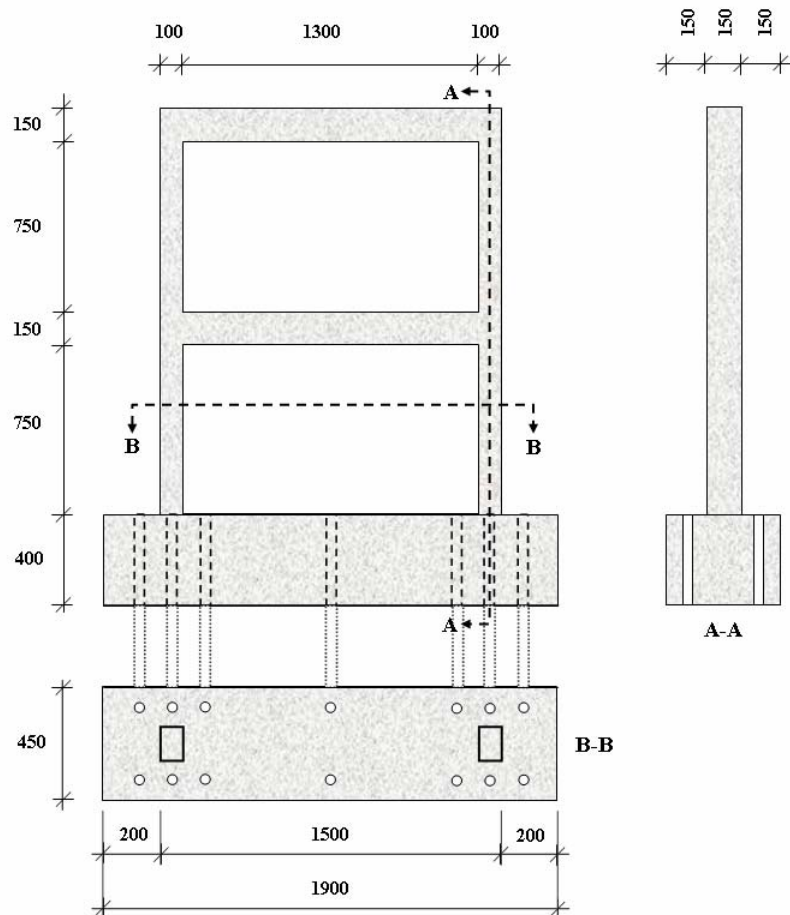
Figure 3.14. Dimensions of Standard Series Specimens (dimensions in mm)

44
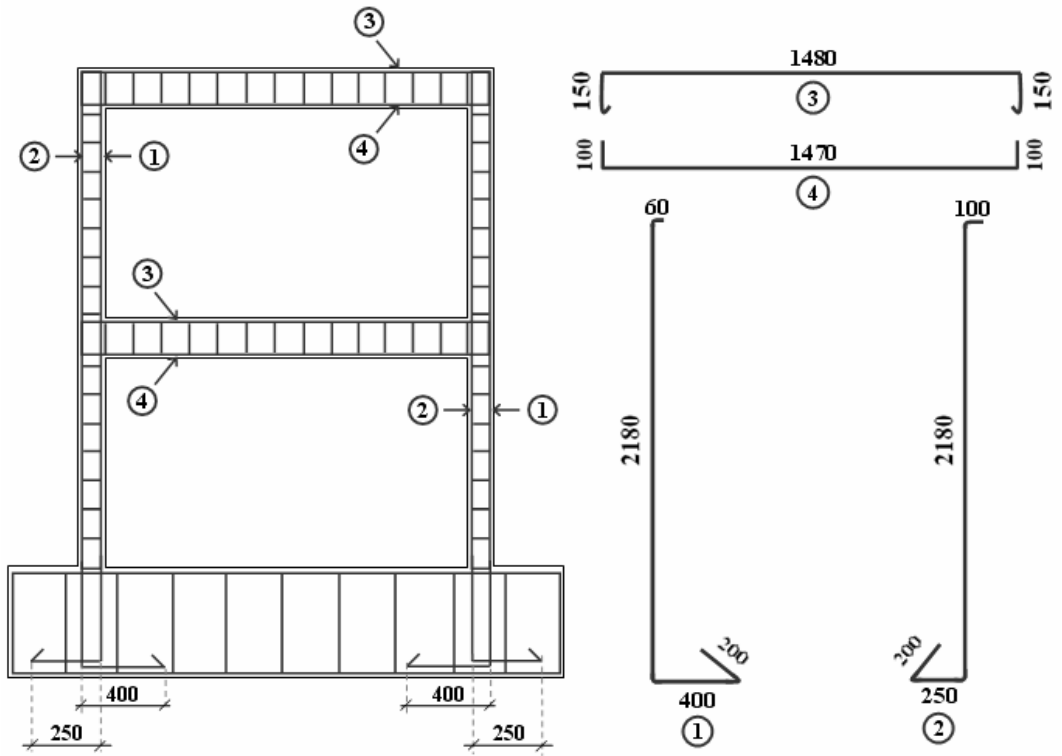
Figure 3.15. Reinforcement Details of Standard Series Specimens (dimensions in mm)

3.4.3. Wider Series of Specimens

Last group of specimens were designed and constructed with an aspect ratio of; α = 2.48 and shortly termed as *wider series* of specimens. This geometry of specimens were tested in order to see the effectiveness of PC panel application on the shear dominant frame system with a wider span. Dimension and reinforcement details of wider series bare frame are presented in **Figure 3.16** and **Figure 3.17**. **Figure 3.17** also provides a view of wider series of RC frame formwork and reinforcement just before pouring. Wider series of specimens were similarly prepared using a steel formwork similar to that of narrower and standard specimen moulds, as presented in **Figure 3.10** and **Figure 3.11**.
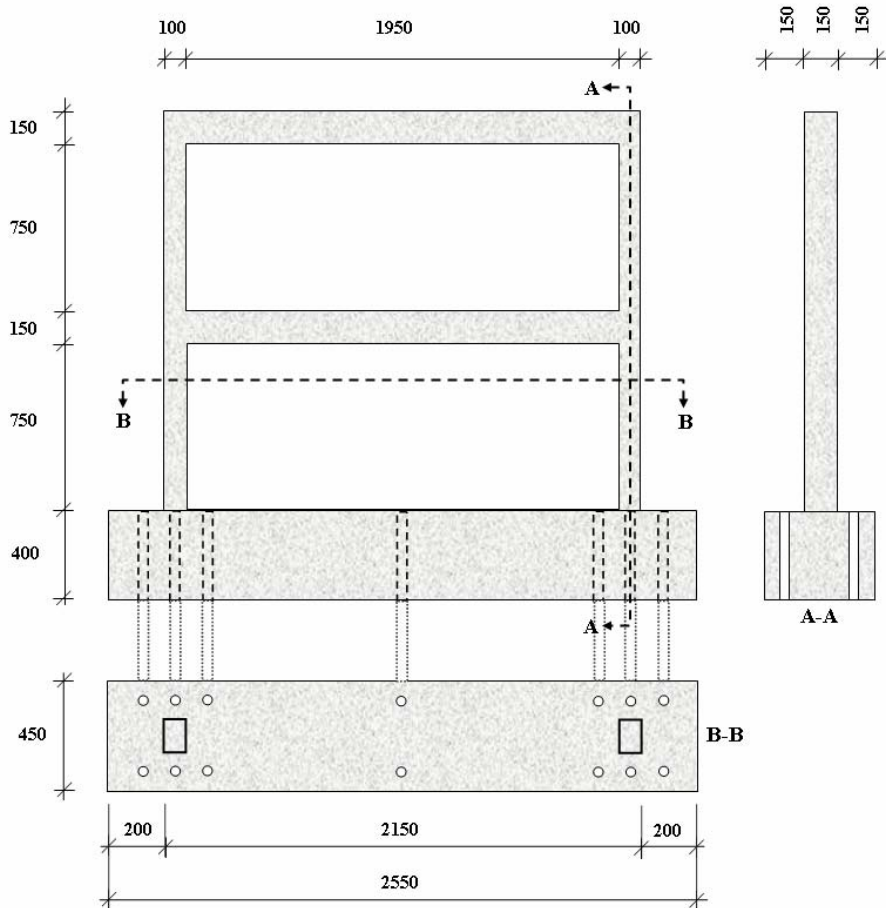
Figure 3.16. Dimensions of Wider Series Specimens (dimensions in mm)
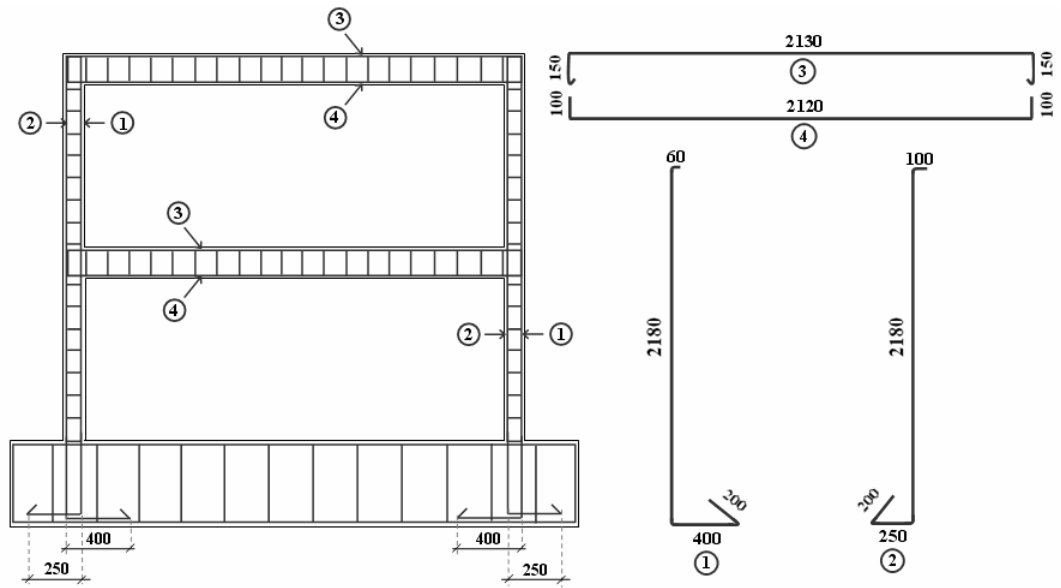
Figure 3.17. Reinforcement Details of Wider Series Specimens (dimensions in mm)

3.5. Procedure of PC Panel Strengthening for RC Frame Specimens

Total of five test specimens were planned to be tested in each specimen group. The bare frame was prepared first and then the necessary modifications were realized for each specimen. The application of PC panel method is to be presented first together with the used strip and rectangular shaped PC panel properties in this section. The preparation details of each specimen are presented in following sections such as hollow brick infilling work, the arrangement of PC panels and anchorage dowel locations, details of cast-in-place RC infill walls, etc.

PC panel method for improving seismic behaviour of RC framed structures was developed in M.E.T.U. as to provide an alternative to cast-in-place RC infill application. It is just a simple conversion of existing non-structural hollow brick infill wall into a load bearing structural member; not a kind of infill replacement. Manageable sized, rectangular and strip shaped almost high strength PC panels are epoxy glued to existing infill surface. Frame-to-panel connections are provided by proper anchorage dowel arrangements. The procedure is, as stated, very simple and occupant-friendly pre-quake retrofitting method for RC framed systems since; PC panel application does not require evacuation. This practical method is not time consuming which is also an important advantage. The disturbance to the occupant is no more than a simple painting work and ordinary workmanship is expected to be enough for the application so that ~60-70 kg of the each PC panel can be held and placed by two workers.

The properties of the PC panels used in the current research are presented first. The procedure that was followed to strengthen the specimens with PC panels is explained. This methodology is also estimated to be valid for real site applications in future.

3.5.1. Rectangular and Strip Shaped PC Panels

PC panels made of almost high strength concrete were used to convert existing non-structural infill wall into a load bearing structural member. Previous researchers investigated various panel types with shear keys or welding points as for panel-to-panel connections. **Duvarcı, (2003), Süsoy, (2005), Baran (2005)** Shear keys and welded connections were found to be unnecessary in panel-to-panel connections when compared to that of epoxy connections. This is an important simplification by panel production and PC panel application points of views. Therefore, this study was carried out only using simple geometry, strip and rectangular panels without any shear keys or welded connections as explained in detail in this section.

The dominating factor on panel design at the beginning was the weight of the panel for the real site applications. A PC panel of ~60-70 kg can be handled and placed onto the infill by two workers. Moreover, portable lifting mechanisms can also be used for and easier panel placement in the site. The thickness of the panels was also of great importance not only for weight optimisation but also for architectural needs. ~40–50 mm thick panels were considered to be proposed for real practice. Strip and rectangular shaped PC panels were designed and scaled for the PC panel research at the beginning by considering these facts. Numbers of rectangular and strip panels for each type of RC frame specimen are summarized in **Table 3.11**.

Table 3.11. Number of PC Panels Used to Strengthen Each Frame Specimen

	N - Series		**S** - Series		**W** - Series	
	Rectangular	**Strip**	**Rectangular**	**Strip**	**Rectangular**	**Strip**
First Storey	8	6	12	12	18	18
Second Storey	6	6	12	12	18	18

Rectangular Shaped PC Panels

Since the experimental study was carried out on 1:3 scaled test specimens, the rectangular panels were also designed and produced in 1:3 scale. No shear keys or welded connections were provided for panel-to-panel connections. These connections were only realized by a thin layer of epoxy mortar. Rectangular panels had the dimensions of 320 mm in vertical direction whereas it was 245 mm in horizontal direction. The panel thickness was 20 mm. One layer of Φ3 mm welded wire fabric steel mesh with 50 mm spacing was used as reinforcement for both types of PC panels. Reinforcement and dimensions of rectangular panels are given in **Figure 3.18.**

Rectangular PC panels were kept in their 1.5 mm thick forms at least for 24 hours and then placed in heatable water tank for curing together with its cylinder concrete specimens. The panels were left to open air in order to dry before strengthening application.
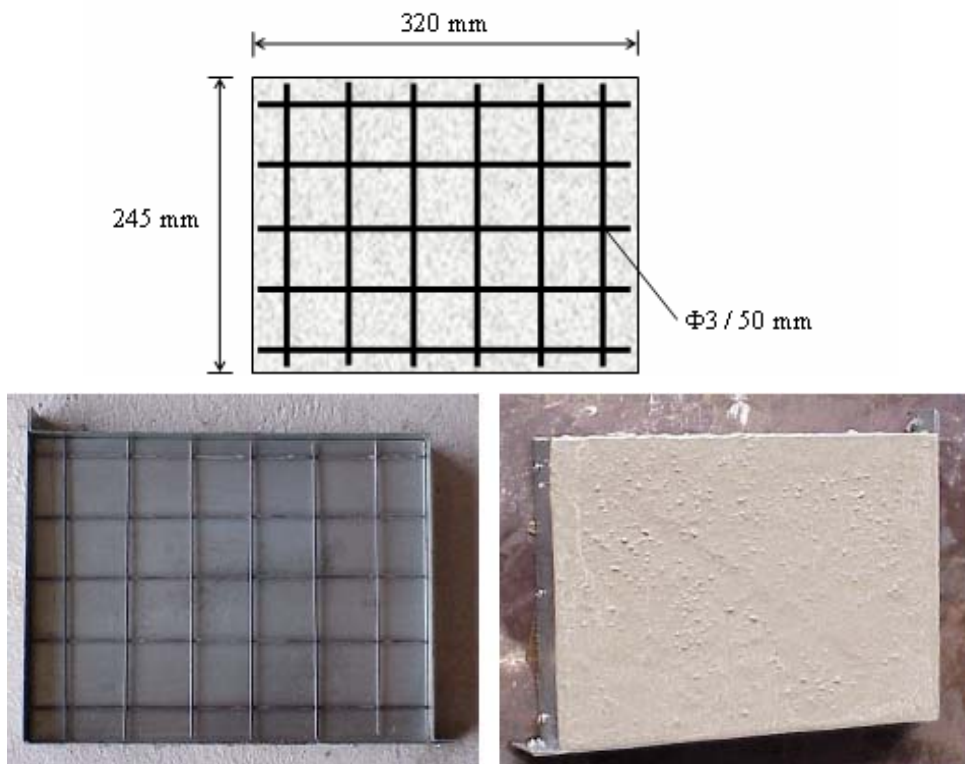
Figure 3.18. Dimensions and Moulding of Rectangular PC Panels

Panel-to-foundation connections were of great importance since the most critical load effects take place in this location. Panel-to-frame connections were also very important in order to provide a monolithic behaviour of the new load bearing wall with the surrounding frame. Therefore, anchorage dowels were provided in these connections. Detailed information about dowel configurations of both strip and rectangular panels for each RC test frame are presented in **Section 3.5.3** and **Section 3.5.4.** Rectangular panels were produced considering the necessary gap locations for the anchorage dowels like a kind of jigsaw puzzle, as illustrated in **Figure 3.19.**

middle panels   top/bottom panels   side panels   corner panels
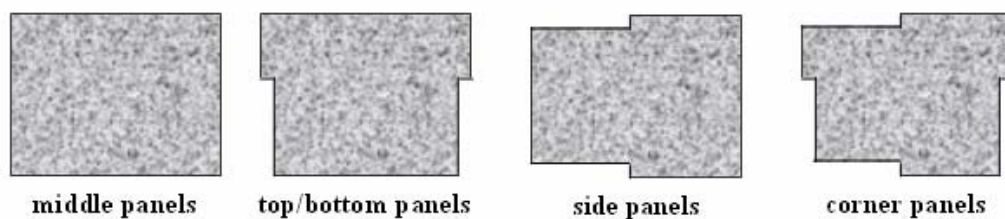
Figure 3.19. Rectangular PC Panels with Varying Dowel Gaps

Strip Shaped PC Panels

Strip panels are full height tall panels extending from the base to the lower face of the beam in each storey of the RC test frame. These panels were 740 mm in height and 105 mm in width, with a thickness of 20 mm, except for first storey of specimen **NSP**. The height of the strip panel for first storey of specimen **NSP** was 890 mm. These panels also did not have any shear keys and welded connections. A thin layer of epoxy mortar was utilized for panel-to-panel and panel-to-infill connections. Anchorage dowel gaps were provided on the strip panels for necessary locations as shown in **Figure 3.20**. Steel reinforcement, casting and curing procedures were all same as the rectangular panels. Dimensions and reinforcement details of strip panels are presented in **Figure 3.21.**

one side with anchorage dowels   two sides with anchorage dowels
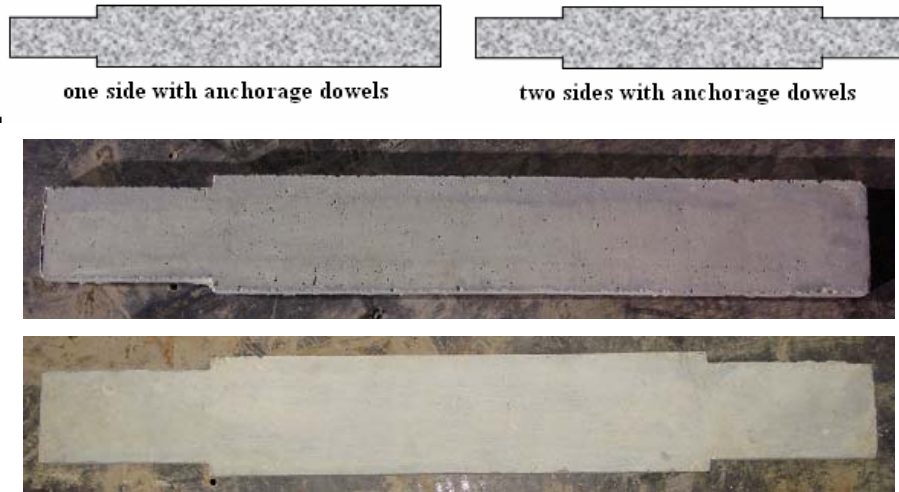
Figure 3.20. Strip PC Panels with Varying Dowel Gaps

740 mm

105 mm

Φ3 / 50 mm Mesh

890 mm

105 mm

First storey strip panel for specimen **NSP**

Φ3 / 50 mm
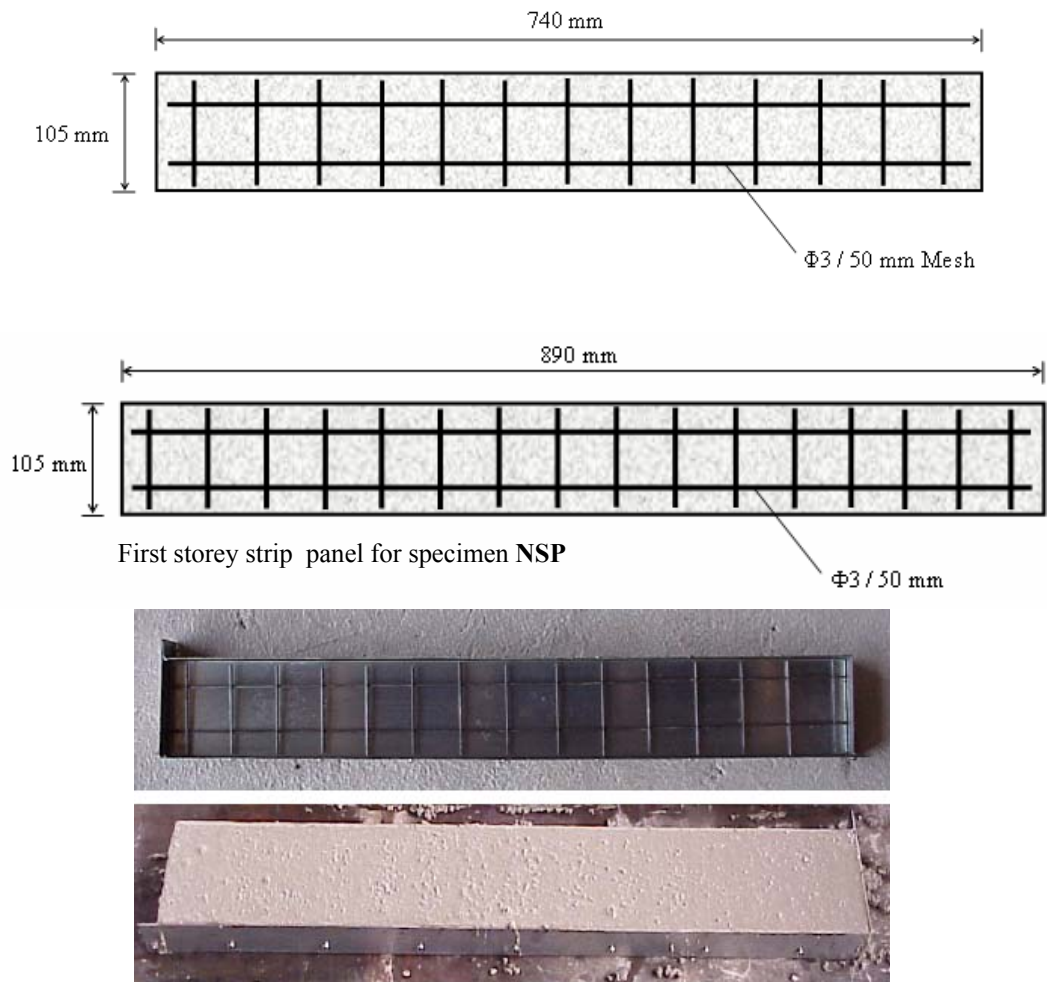
Figure 3.21. Dimensions and Moulding of Strip PC Panels

3.5.2. Application of PC Panel Technique

The PC panel strengthened test specimens were prepared following the application procedure explained in this section. It should be underlined that the real site application is expected not to differ than that of experimental study.

Strip and rectangular shaped PC panels were used to strengthen the specimens and no shear keys or welded connections were realized for panel-to-panel connections. These connections were provided by only a thin layer of epoxy mortar as illustrated in **Figure 3.22** and **Figure 3.23**. Panel-to-panel connections must have full contact and enough shear capacity in order to provide a successful conversion of hollow brick infill into a solid, load bearing wall. Sikadur-31 chemical product, properties of which were presented in **Section 3.3.5**, was used as epoxy mortar and special attention was paid for production of successful panel-to-panel connections.
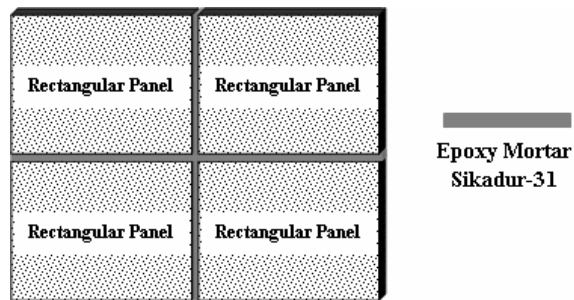
Figure 3.22. Panel – to – Panel Connections for Rectangular PC Panels
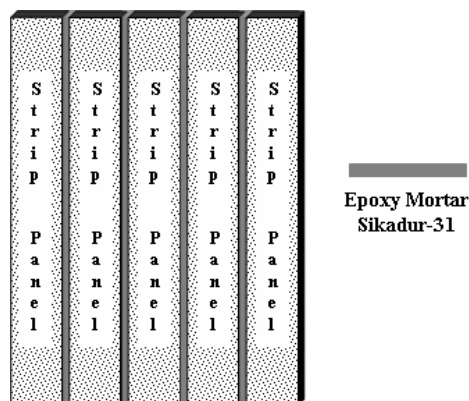
Figure 3.23. Panel – to – Panel Connections for Strip PC Panels

Rectangular and strip shaped PC panels were epoxy glued to the interior faces of infill walls in both stories. Anchorage dowels were used for frame-to-panel and foundation-to-panel connections, as the first step of PC panel application. Φ10 deformed bars were used as anchorage dowels for both frame and foundation connections. ~70 mm depth holes were drilled into inner faces of beams and columns with a diameter of 12 mm. (**Figure 3.24-a**) Anchorage dowel holes were then cleaned by first a metal brush and then compressed air. (**Figure 3.24–b, c**) Wet cloth was sometimes used for hole cleaning as well. Dust free, dry holes were filled by anchorage epoxy resin, the information about Spit Epcon epoxy product was provided in **Section 3.3.5**, and anchorage dowels were installed. (**Figure 3.24-d, e, f**) 24 hours of time was enough for complete hardening of anchorage epoxy and load application to rebar. An illustrative dowel application is shown in **Figure 3.24** as stated in anchorage epoxy product catalogue. **(Spit Epcon System, 2005)**
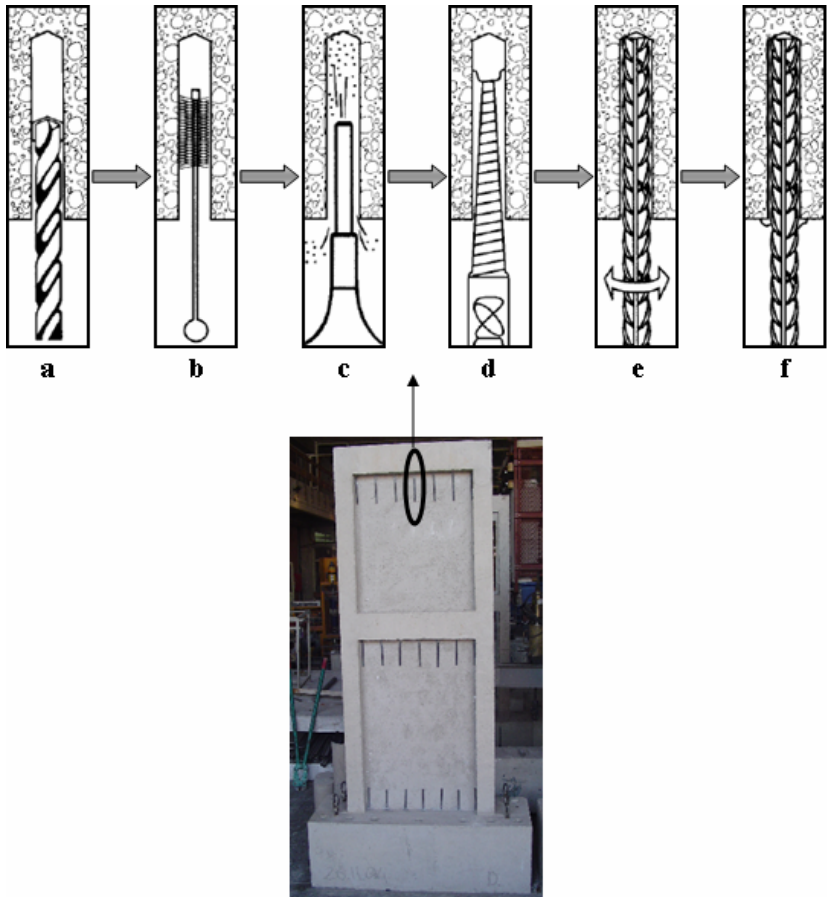
Figure 3.24. Method of Anchorage Dowel Installation

PC panels were epoxy glued to infill plaster soon after the anchorage dowels were properly placed and anchorage epoxy got its strength. The panels and infill surface should be dry, clean and dust-free before the application. The curing procedure of the PC panels was finalized at least 3 days before the application and the wet panels were left in open air to dry. A thin layer of epoxy mortar was coated on panel surface and then the panel was placed on plaster surface as exampled in **Figure 3.25.** The shear capacity of panel-to-panel connections is of major importance in order to develop full shear capacity of new load bearing structural member. Therefore, special attention was paid for panel-to-panel connections. A plastic hammer was used to provide full contact in between panel and plaster; and panel connection surfaces. This procedure was repeated up to all necessary plaster surfaces were PC panel glued. After panel placing, openings around anchorage dowels and possible gaps of connections were carefully filled by epoxy and the overall surface was finalized. ~24 hours was enough for panel epoxy to get its full strength and then the specimen was ready for test. Basic step views of PC panel gluing for specimen **NSP** are presented in **Figure 3.25.**
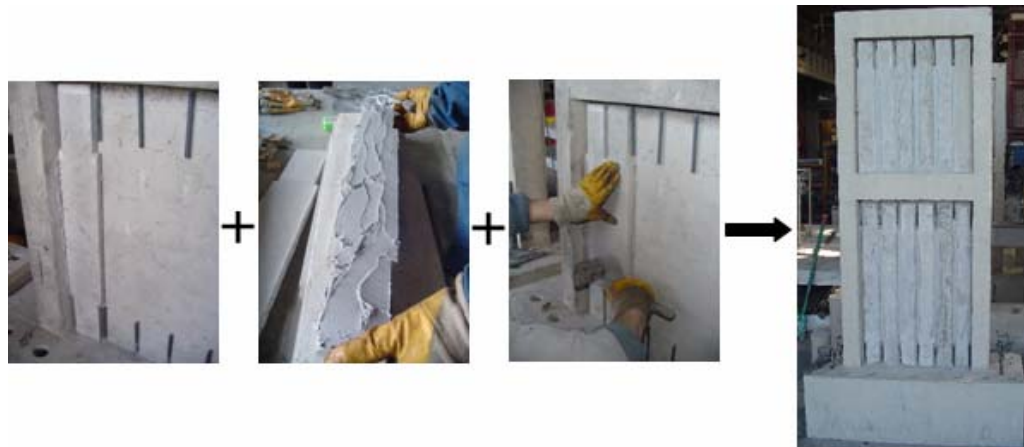
Figure 3.25. PC Panel Application for Specimen **NSP**

PC panels were produced in steel moulds which ended up with one smooth and one relatively rough surface. Panels were glued to the plaster from their rough sides. Therefore, smooth sides of panels formed the outer surface of new load bearing structural wall; so that a simple painting work can be enough for finalizing the application before regular occupancy. Each of the PC panel strengthened specimen was also lime washed before the test in order to observe all cracks.

3.6. Properties of Test Specimens

Total of fifteen RC frames were tested in the experimental investigation. General properties of all series of specimens are presented in this section.

3.6.1. Bare Frames; Specimens NB, SB and WB

Three bare frames of each aspect ratio were prepared and quasi-statically tested. Scaled drawings of each bare frame are presented in **Figure 3.26**. Photo views of the bare frames in the test setup are all provided in **Chapter 5**. Specimens **NB**, **SB** and **WB** were ordinary RC frames without any infill. No lap-splice connections were provided on column longitudinal bars.
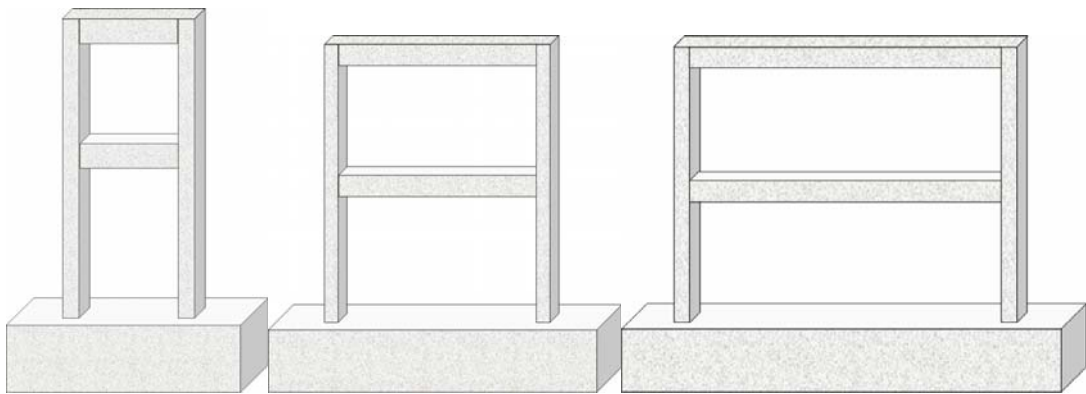
Figure 3.26. Scaled Drawing of Specimens in the Order of **NB**, **SB** and **WB**

3.6.2. Lower Bound Reference Frames; Specimens NR, SR and WR

Specimens **NR, SR** and **WR** were prepared and tested as the lower bound references of all groups since these specimens resembled the typical deficiency and construction characteristics the of target buildings. RC bare frames were first poured, then infilled by 1:3 scaled bricks and both surfaces of the infill were finalized by ~10 mm thick plaster by an ordinary workmanship as shown in **Figure 3.27**. No lap-splice connections were provided on column longitudinal bars. **NR, SR** and **WR** were tested under quasi-static

loads in the horizontal direction as the lower bound reference specimens for that of strengthened frames. Reinforcement and dimension details of these frames were previously presented in **Section 3.4.** Schematic drawing and vertical section views of specimen **NR** is only presented in **Figure 3.28**, since views of specimens **SR** and W**R** are similar. Before and after test views of these specimens are provided in **Chapter 5**.

Figure 3.27. Hollow Clay Brick Infill Wall Workmanship **(Duvarcı, 2003)**
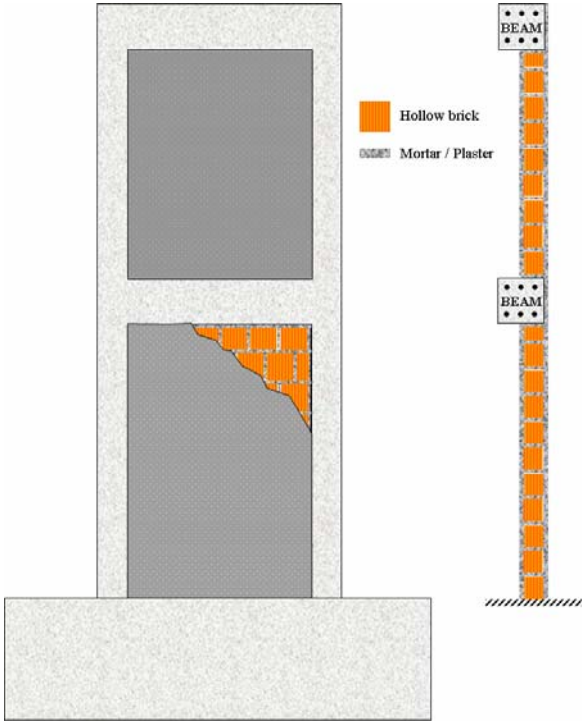
Figure 3.28. Detailing of Infill Wall in Vertical Section, Specimen **NR**

3.6.3. Rectangular PC Panel Strengthened Frames; Specimens NRP, SRP and WRP

The panel and anchorage dowel arrangement details of the test specimens strengthened with rectangular shaped PC panels are presented in this section. The PC panel application presented in **Section 3.5** was applied to these specimens as explained. The anchorage dowel configuration of specimens **NRP**, **SRP** and **WRP** are presented in **Figure 3.29** and views of specimens after PC panel application are provided in **Figure 3.30**.
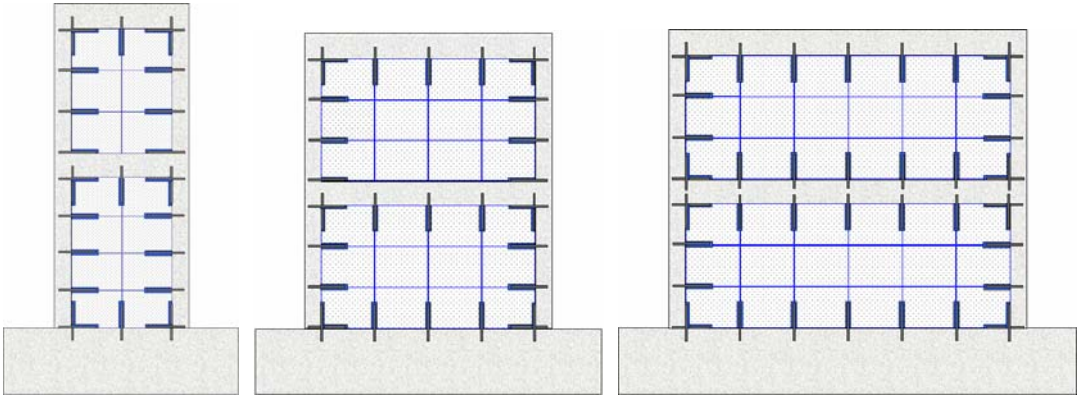
Figure 3.29. Anchorage Dowel Configurations for Specimens **NRP, SRP** and **WRP**

Figure 3.30. Views of Specimens **NRP**, **SRP** and **WRP** after PC Panel Application

Specimen NRP

Total of fourteen rectangular PC panels, eight for first storey and six for second storey, were used to strengthen specimen **NRP**. Anchorage dowels were provided in all four faces of the first floor; while no dowel was provided on the floor level beam of second storey as shown in **Figure 3.29**. Details of PC panel arrangement of specimen **NRP** in vertical section is presented in **Figure 3.31.** The vertical section details of specimens **SRP** and **WRP** are similar to that of specimen **NRP**.
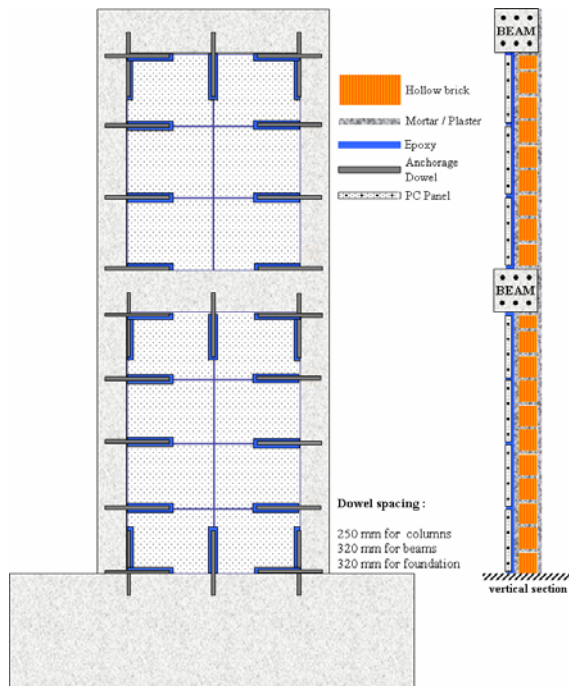
Figure 3.31. PC Panel Arrangement of Specimen **NRP** in Vertical Section

Specimen SRP

Total of twenty-four rectangular PC panels were used to strengthen specimen **SRP**; twelve panels for each storey. The dowel arrangement was in same fashion as specimen **NRP**; no anchorage dowel was provided on the floor level of second storey as viewed in **Figure 3.29**. The PC panel arrangement in vertical section details of specimens **SRP** is similar to that of specimen **NRP** as presented in **Figure 3.31**.

Specimen WRP

Specimen **WRP** was strengthened by total of thirty-six rectangular PC panels; as with the equal numbers of panels in each storey. Apart from specimen **NRP** and **SRP**, anchorage dowels were also provided along the second storey floor level together with the other infill surrounding frame elements. Provision of anchorage dowels in the second storey floor level was decided and applied in both specimens **WRP** and **WSP**, after a premature failure of a wider series of specimen strengthened with strip PC panels. This specimen failed by a sliding shear failure of second storey infill composite along the second storey basement level beam due to absence of anchorage dowels. Therefore, the anchorage dowels were also provided in the upcoming PC panel strengthened specimens of wider series in this level. Anchorage dowel arrangement of specimen **WRP** is presented in **Figure 3.29**. The PC panel arrangement in vertical section details of specimens **WRP** is similar to that of specimen **NRP** as presented in **Figure 3.31**. General view of specimen **WRP** after PC panel application is depicted in **Figure 3.30.**

3.6.4. Strip PC Panel Strengthened Frames; Specimens NSP, SSP and WSP

The panel and anchorage dowel arrangement details of the test specimens strengthened with strip shaped PC panels are presented in this section. The PC panel application presented in **Section 3.5** was applied to these specimens as explained. The anchorage dowel configuration of specimens **NSP**, **SSP** and **WSP** are presented in **Figure 3.32** and views of specimens after PC panel application are provided in **Figure 3.33.**
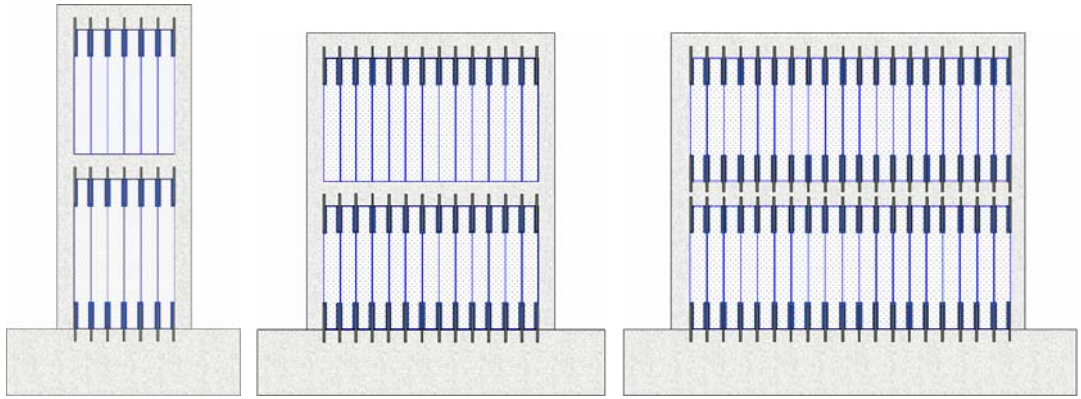
Figure 3.32. Anchorage Dowel Configurations for Specimens **NSP, SSP** and **WSP**

Figure 3.33. Views of Specimens **NSP**, **SSP** and **WSP** after PC Panel Application

Specimen NSP

Total of six strip panels were used to strengthen each floor of the specimen **NSP**. Since the floor heights of each storey were different, PC panels were prepared considering the infill height of each storey. Strip PC panel-to-frame connections were only realized on beam and foundation levels of first storey and to the beam on the top of the second storey. No anchorage dowel was placed on the floor level of the second storey for specimen **NSP**. Details of PC panel arrangement of specimen **NSP** in vertical section is presented in **Figure 3.34.** The vertical section details of specimens **SSP** and **WSP** are similar to that of specimen **NSP**.
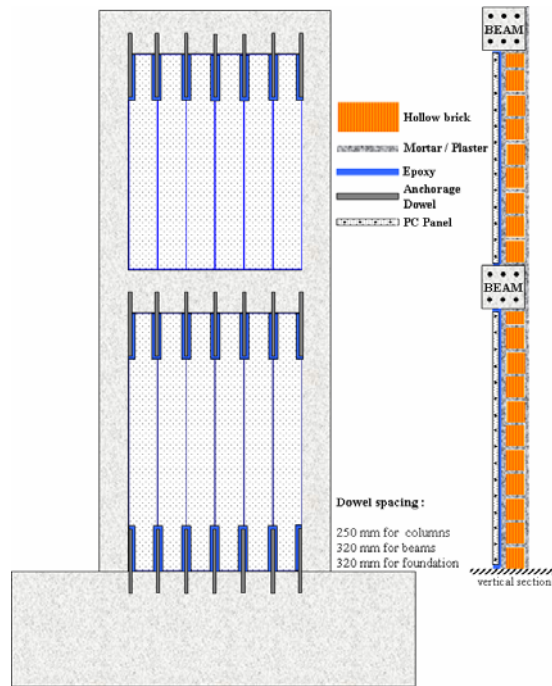
Figure 3.34. PC Panel Arrangement of Specimen **NSP** in Vertical Section

Specimen SSP

Total of twenty-four PC strip panels, placed by equal numbers in both storeys, were used to strengthen specimen **SSP** following the PC panel application procedure. No anchorage dowel was provided on the floor level of second storey. Anchorage dowel configuration of specimen **SSP** is provided in **Figure 3.32** and view of this specimen after strengthening is provided in **Figure 3.33**.

Specimen WSP

Specimen **WSP** was strengthened by total of eighteen strip shaped PC panels for each storey. Anchorage dowels were placed on the floor level of second storey in order to prevent a premature shear failure along the second floor infill-panel rigid block interaction zone referring to the experiment mentioned in **Section 3.8.** Anchorage dowel configuration of specimen **SSP** is provided in **Figure 3.32** and view of this specimen after strengthening is provided as in **Figure 3.33**.

3.6.5. Upper Bound Reference Frames; Specimens NRC, SRC and WRC

PC panel technique was developed to be an alternative to cast-in-place RC infill application with the compensating advantages like ease in application, no-necessity of evacuation and considerable amount of seismic performance improvement. In order to compare the seismic performance improvement gained by PC panel application with that of cast-in-place RC infill method; one RC frame specimen of each aspect ratio series was strengthened by cast-in-place RC infill and tested as the upper bound references; specimens **NRC**, **SRC** and **WRC**.

Common practice of reinforcement detailing and concrete pouring was followed during the preparation of cast-in-place RC infills. RC frames were first cast and cured properly. Deformed bars were used as anchorage dowels and located to surrounding beam, column and foundation elements of all specimens as Φ10/250 mm. The anchorage dowel configuration of specimens **NRC**, **SRC** and **WRC** are presented in **Figure 3.35**. Φ6 plain bars were used to produce steel mesh of 150 mm spacing by a mechanical connection with steel wires, in the laboratory. Two layers of the steel mesh were connected to the dowels and 60 mm thick infill concrete was cast. Wooden formwork was used for infill production and concrete pouring was realized by positioning the RC frame on the horizontal direction. RC infill panel and construction details of strengthened specimens **NRC**, **SRC** and **WRC** are presented in this section.
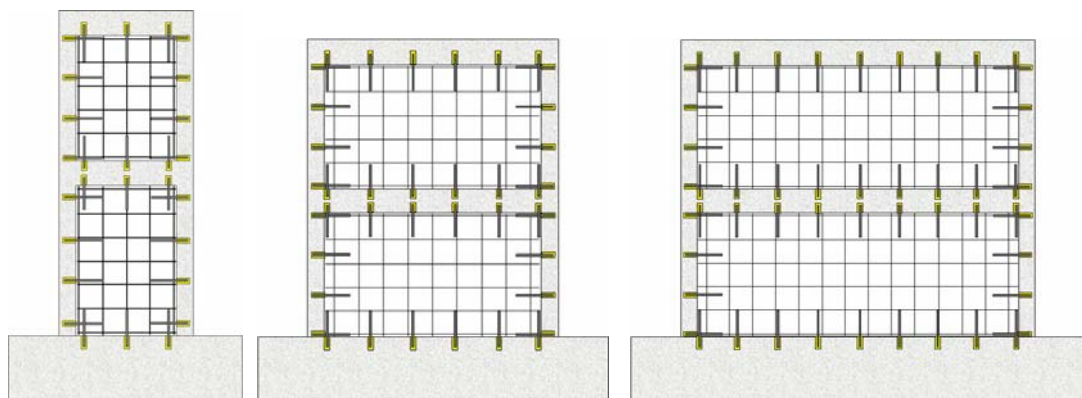
Figure 3.35. Anchorage Dowel Configurations for Specimens **NRC, SRC** and **WRC**

Specimen NRC

Specimen NRC was prepared and tested as the upper bound reference of narrower specimen series. Since the first and second storeys were different in height, steel mesh dimensions were also varied as illustrated in **Figure 3.36**. Views from production stages of this specimen are further depicted in **Figure 3.37**. Schematic view of dowel locations, mesh reinforcement and vertical section detail of specimen **NRC** is presented in F**igure 3.38**. The vertical section details of specimens **SRC** and **WRC** are similar to that of specimen **NRC**.
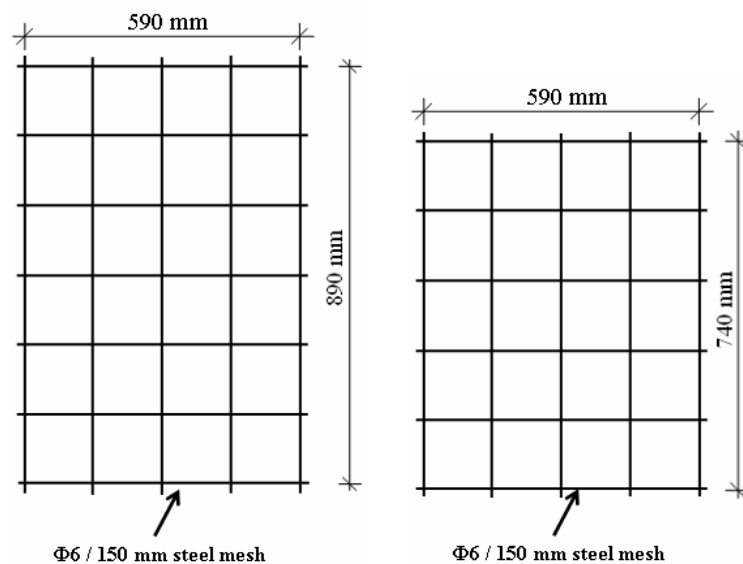
Figure 3.36. Mesh Reinforcement of Specimen **NRC** for First and Second Storey

Figure 3.37. Views from Production Stages of Specimen **NRC**

64
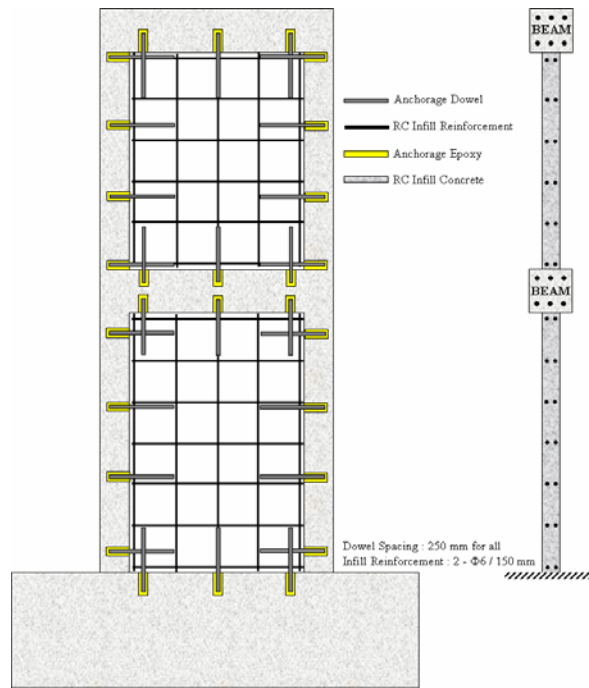
Figure 3.38. Dowel Arrangement and Vertical Section of Specimen **NRC**

Specimen SRC

Specimen **SRC** was prepared and tested as the upper bound reference of standard specimen series. Steel mesh dimensions of first and second storey infill of this specimen are illustrated in **Figure 3.39**. Views from production stages of specimen **SRC** are depicted in **Figure 3.40**.
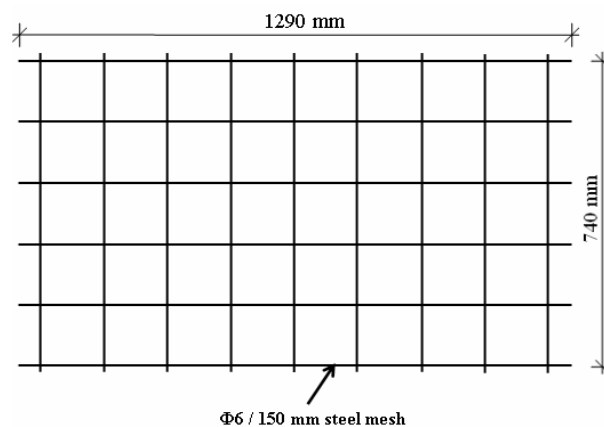
Figure 3.39. Mesh Reinforcement of Specimen **SRC** for First and Second Storey

Figure 3.40. Views from Production Stages of Specimen **SRC**

Specimen WRC

Specimen **WRC** was prepared and tested as the upper bound reference of wide specimen series. Steel mesh dimensions of first and second storey infill of this specimen are illustrated in **Figure 3.41**. Photo views of the upper bound reference frames in the test setup are all provided in **Chapter 5**.
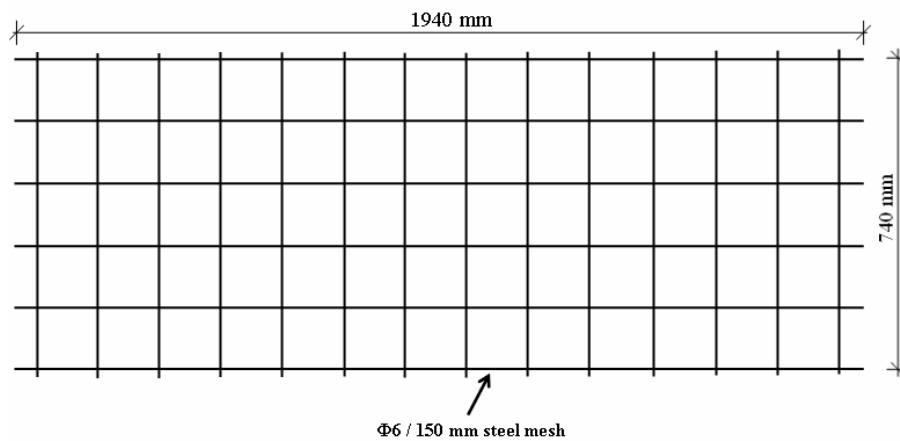
Figure 3.41. Mesh Reinforcement of Specimen **WRC** for First and Second Storey

CHAPTER 4

TEST SETUP AND PROCEDURE

4.1. General

RC frame tests have been carried out in M.E.T.U. Structural Mechanics Laboratory for several years either to evaluate the infilled frame behavior or to investigate performance improvement by various methods. Early tests were performed on twin specimens located horizontally; then the loading and measurement systems were improved for horizontally located test setup. **(Altın, 1990), (Ersoy and Uzsoy, 1971), (Canbay, 2001), (Sonuvar, Özcebe and Ersoy, 2004)** The experimental system which was used for the present study was developed and used by previous researchers of PC panel method investigation either for one-bay one-storey or one-bay two-storey standard specimens. **(Duvarcı, 2003), (Süsoy, 2004), (Baran, 2005)** Since the current research topic was to investigate the effect of the frame aspect ratio on PC panel strengthening, the setup and some loading apparatus were all modified or re-constructed for the new geometry of the narrower and wider RC frames.

Experimental study was carried out on 1:3 scaled specimens as mentioned. This scale limitation was directly due to the loading capacity of the test setup and the other physical conditions of the laboratory such as capacity of the crane, laboratory surface area, etc. Specimen scaling and dimensional analysis studies have been performed considering the reported proper scales for RC test specimens and 1:3 was chosen to be the experimental research scale. **(Altın, 1990), (See Appendix-A)**

Proper instrumentation and precise data collection were of greater importance for the reliability of the test results. Axial load on columns, lateral load applied to the frame on

beam levels and corresponding displacements, deflections were all measured and recorded by a modern data acquisition system. The details of test setup used for 2D quasi-static RC frame experiments and test procedure will be explained in this chapter.

4.2. Test Setup

RC frame tests under quasi-static loadings were carried out in M.E.T.U. Structural Mechanics Laboratory. General view of the test setup and laboratory are presented in **Figure 4.1**. Test setup basically consisted of a universal base, loading system, reaction wall, test specimen and a rigid guide frame made of steel around the specimen to control the out-of-plane displacements as illustrated in **Figure 4.2**. Instrumentation and data acquisition system were also the remaining components. Whole system was built in-situ with all its parts attached to the strong floor of the laboratory. This strong floor basement had 600 mm thickness with several 150 mm diameter holes which were used to prestress universal base and some other test components to the floor. The distance in between two holes is 1000 mm in a row. Lateral load was applied by the proper mechanism placed on the reaction wall. Vertical loading was realized by another loading system. Elements of the test setup are below presented in detail.

Figure 4.1. General View of the Laboratory and Test Setup after Specimen **SR** Test

Cross Beam

Spreader Beams

Prestressing
Cable

Load Cell

Ram

Pins

Ram

Strong Wall

Universal Base
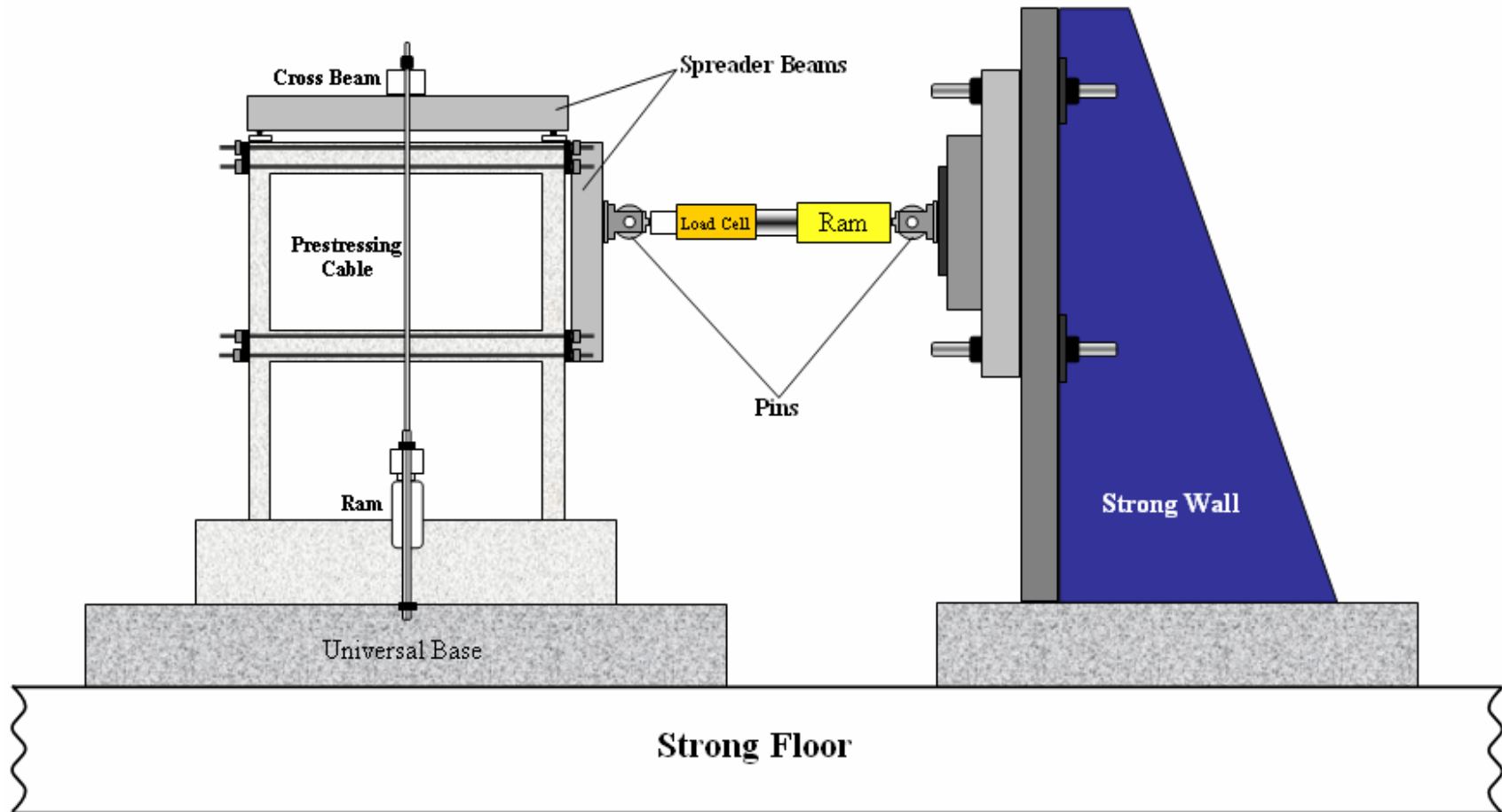
Strong Floor

Figure 4.2. Test Setup

4.2.1. Reaction Wall

The reaction wall in 4.5 meters height had been previously constructed on the strong floor of the laboratory for lateral load applications as can be seen in **Figure 4.1** and **Figure 4.2** as painted in blue. This wall was prestressed to the strong floor by high strength steel bolts. There existed a number of regularly placed holes on the vertical face of the reaction wall for lateral loading mechanisms. This flexibility enabled to apply lateral loading to all narrow, medium and wide sized specimens of this research other than the previous research RC frame specimens with varying number of storeys.

4.2.2. Universal Base

Test frames should be fixed at the foundation level and would not be allowed to move in any direction; since the specimens were tested vertically. Strong floor of the M.E.T.U. Structural Mechanics Laboratory had holes for specimen fixing, the between distance of which was 1000 mm. This hole meshing did not let to fix 1:3 scaled RC frame specimens in front of the reaction wall, properly. Closer holes were needed for this fixity. In order to solve this problem, a universal base which provided conditions for testing of specimens in varying aspect ratios, was designed and produced in the laboratory. Plan details of 400 mm height universal base is presented in **Figure 4.3**. The universal base was fixed to the strong floor by total of six 50 mm diameter high-strength steel bolts. The foundation of the test specimen was also fixed to the universal base by fourteen 45 mm diameter steel bolts.
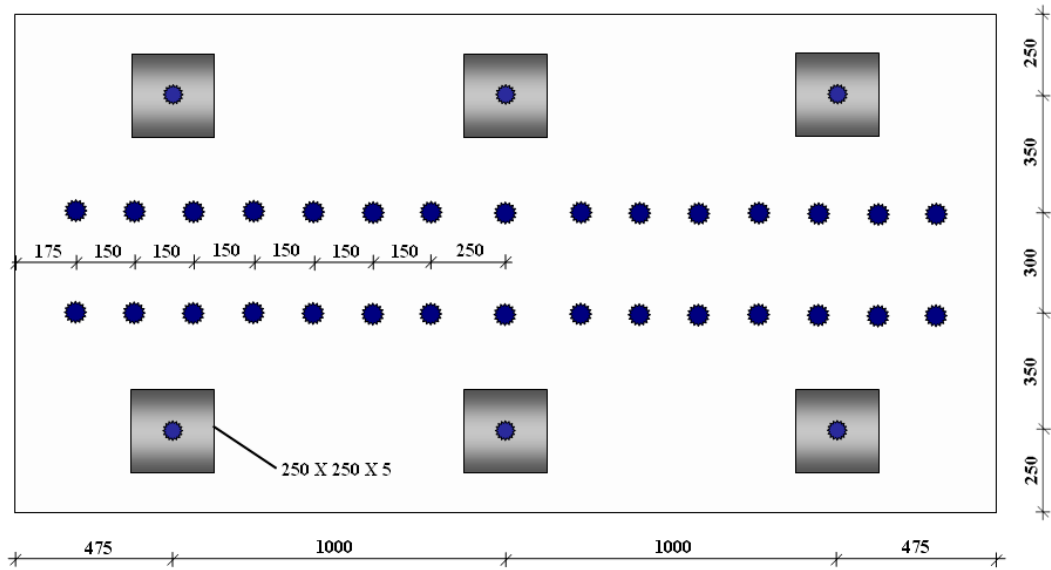
Figure 4.3. Plan View of the Universal Base

Universal base is a reinforced concrete product. Φ18 deformed bars were used as longitudinal reinforcement at both top and botton layers in the longer direction, in a uniform distribution. Φ14 deformed bars were used at both top and bottom layers in the transverse direction. Φ14 deformed bars were welded to top and bottom longitudinal reinforcements. ~2 m^3 ready mix concrete from a concrete manufacturing company was poured for this element. Existing steel molds of the laboratory were modified and used for this pouring.

Total of six, 60-mm diameter holes were placed for fixity of the universal base to the strong floor of the laboratory, by embeddment of steel pipes into the concrete with special attention. Thirty four M37 nuts were also carefully placed in the universal base for fixing of the test specimens with varying aspect ratios as illustrated in **Figure 4.3**. Detailed information about universal base production was previously reported. **(Duvarcı, 2003), (Baran, 2005)**

4.2.3. Guide Frame

Test setup was first used by **(Duvarcı, 2003), (Baran, 2005)** and was modified for the present work. Two preliminary tests have been performed for proper functioning of the test set-up. **(Duvarcı, 2003), (Baran, 2005)** Out-of plane deformations caused premature failure of one of the pilot test specimens by deforming laterally due to unsymmetrical infill placement and application of load in plane of symmetry. Masonry infill and PC panels were placed on the back side of the specimen, and this resulted in some eccentricity with respect to the loading axis. In order to prevent this kind of premature failures, it was decided to improve the test setup by construction of a guide frame around the test specimen with lateral supports on the top beam level.

An external steel guide frame was constructed on the universal base by providing lateral support to the beam with rollers that were called *"ball transfer units"*. This rather rigid guide frame surrounded the test specimen and consisted of four columns made of built-up box sections. Columns were post-tensioned to the universal base by using high-strength steel bolts and were connected by another built-up box section of L shaped steel profiles in both long and short directions. Connection beams of longer direction were movable by bolted type of joints, while the beams of the shorter directions were fixed to the column upper joints by welding. This mobility of the longer connection beam was realized for varying height of test specimens. General view of guide frame is given in **Figure 4.4**.

Ball bearings of 2.5 kN axial load capacity were attached to the box section of the connection beam as shown in **Figure 4.5**. For each test specimen of the research, total of four rollers were placed to the box sections locating two on each side. Rollers gently touched the test frame beam, controlling the out-of-plane displacements and smoothly allowing in-plane displacement.
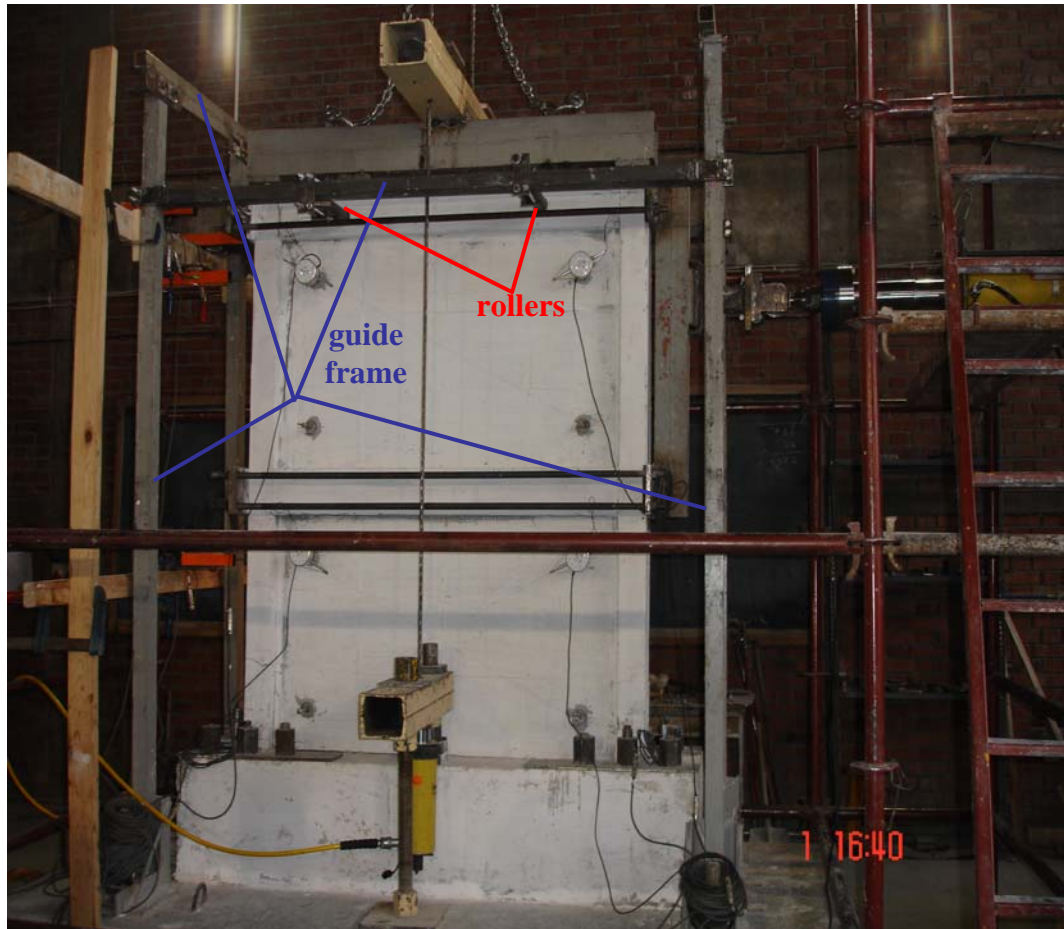
Figure 4.4. General View of Guide Frame

Figure 4.5. Ball Transfer Units

73

4.2.4. Loading System

RC specimens were first fixed to the universal base by total of fourteen 45 mm diameter steel bolts, the instrumentation was placed and then the test was carried out. Constant column axial load was applied by *vertical loading system* and kept constant during the test. Reversed cyclic loading of earthquake simulation was applied in lateral direction by *lateral loading system*. Details of both vertical and lateral loading systems are explained in this section.

Vertical Loading System

Column axial load was applied to all frame specimens and kept constant during the experiment, by vertical loading system shown in **Figure 4.6**. Axial load level for each specimen is tabulated in **Chapter 6** within the test results.

Figure 4.6. Vertical Loading System

Axial load was applied by hydraulic jacks on both front and rear sides of the specimen and transferred to the cross beam by prestressing cables. The cross beam was connected to spreader beam. Spreader beam was simply supported over the second floor beam and thus, the load was equally distributed to both columns by this mechanism. Both of the cross and spreader beams of the system were made of steel box sections. Applied axial load was measured by a pressure gage and controlled during the test.

Lateral Loading System

Reversed cyclic lateral loading was applied to all specimens as to simulate the ground motion effect under the laboratory conditions. Lateral loading system mainly consisted of an adjustable steel frame attached to the reaction wall, a load cell, a hydraulic pump and pin connections at either ends of the loading column consisting of the jack and load cell. An illustration of the horizontal loading system is presented in **Figure 4.7**.
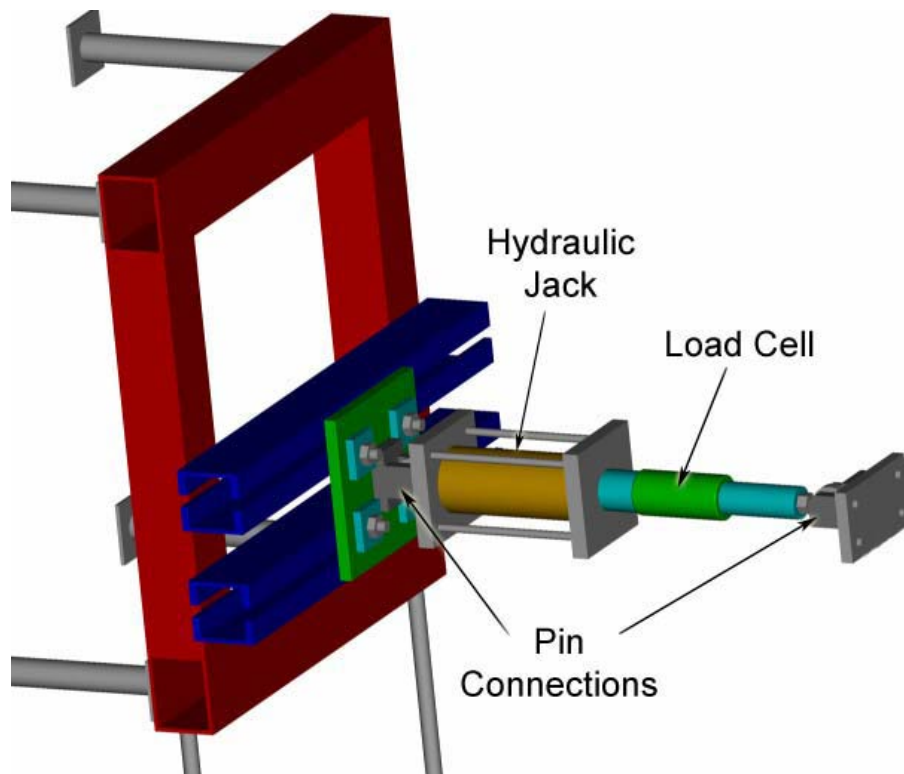
Figure 4.7. Components of Lateral Loading System **(Süsoy, 2004)**

Loading was applied by the assemblage of a hydraulic jack and a load cell with pin connections at both ends which provided the system to create axial stress only. The hydraulic jack had a capacity of 600 kN under tension and 450 kN under compression. The load cell was able to measure up to 600 kN force and its all callibration checks were done regularly before the tests. General view of lateral loading system and pin connections are presented in **Figure 4.8** and **Figure 4.9**, respectively.
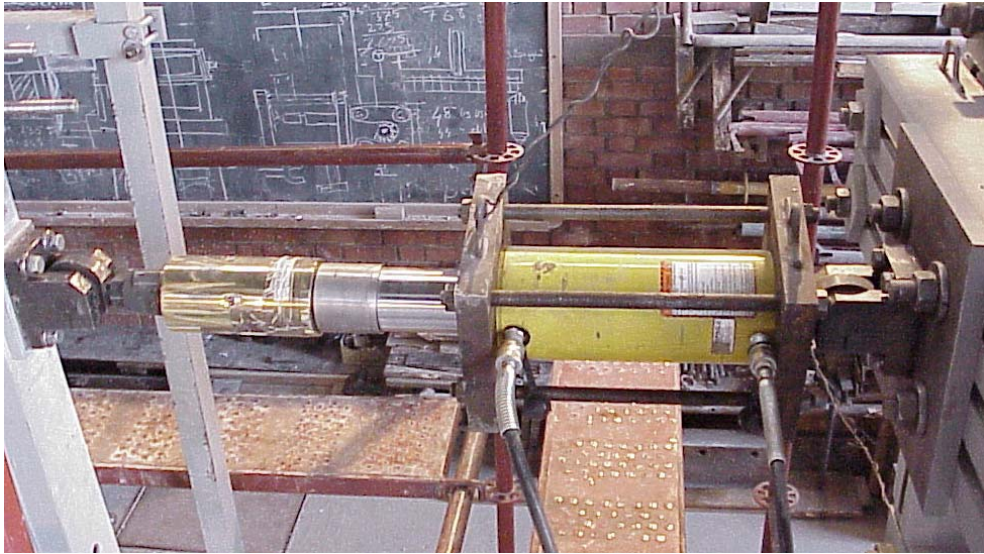
Figure 4.8. Lateral Loading System
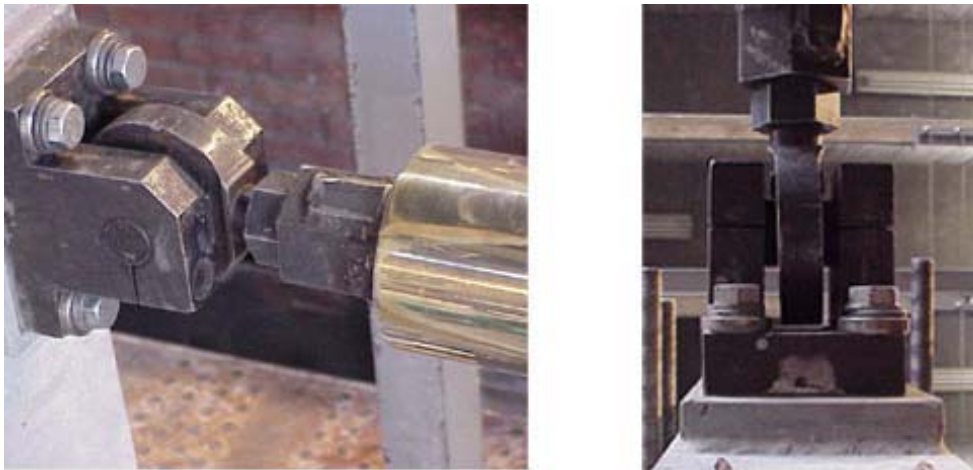
Figure 4.9. Close View of Pin Connections

Lateral load was applied to the frame through a spreader beam and load was shared between two storey beams as sketched in **Figure 4.10**. Load was applied at one-third of the span of spreader beam. Lateral load applied at second floor level always remained twice the one at first floor level; creating a triangular lateral load distribution in elevation.
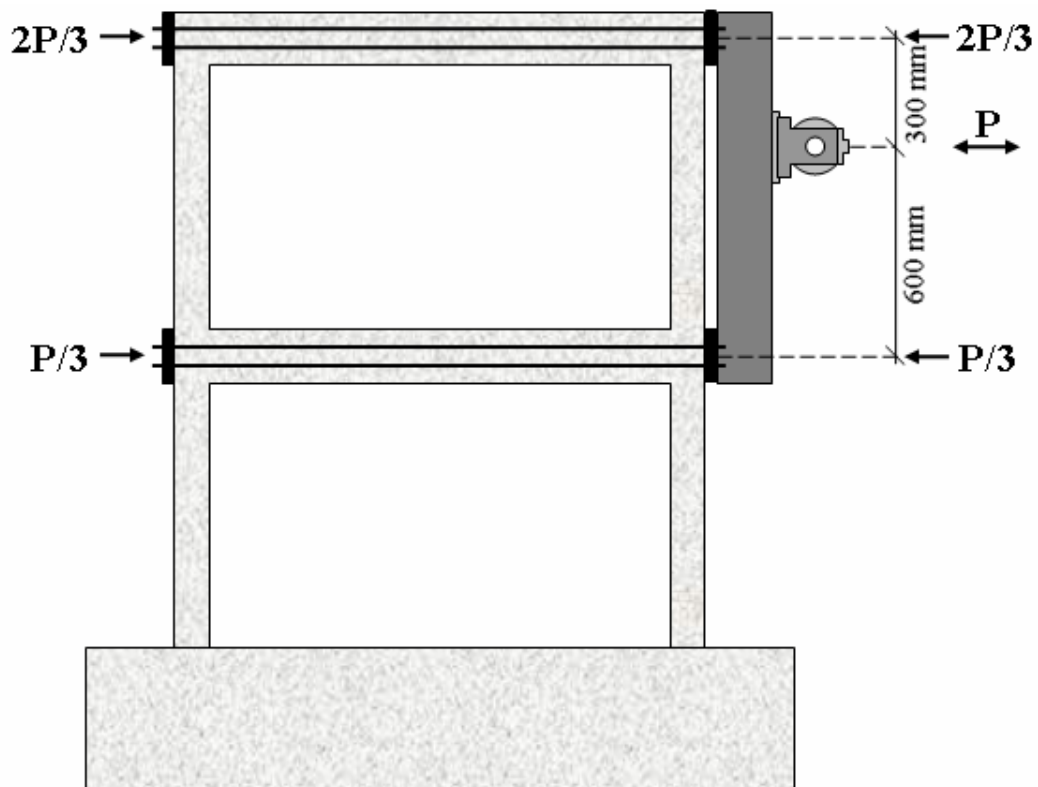
Figure 4.10. Lateral Load Shearing for All Specimens

Lateral load was applied to the specimen in a hysteretic manner. This was accomplished through a double acting hydraulic jack loading the plates located at both ends of the beams which were welded to the spreader beam at both floor levels. The clamps made of four steel bars connected to two loading plates at both ends of each beam were loosely attached to the test frame, at floor levels. The steel bars of Φ30 connecting the plates were loosely clamped not to cause a confining effect (external prestress) and these clamps were carefully checked before each test.

Test specimens were all designed and constructed following the common practice. Therefore, the hollow brick infill wall was located eccentically on the exterior side of the beam in all appropriate specimens. Thus, the contribution of the infill made the frame behaviour somewhat unsymmetrical but the placement of the PC panels on the infill wall reduced eccentricity. Therefore, the lateral load was applied to the specimen in the plane of symmetry of the column. In the experiments of the reference and PC panel strengthened specimens, it was observed that the ball bearings gently touched the specimens meaning that there was no significant eccentricity introduced to the specimen. Since cast-in-place RC infill was concentrically located in the plane of symmetry of the column, no eccentricity existed together with the bare frames and the lateral load was also applied to these specimens in the plane of symmetry of the column. The application of lateral load on to all specimens are illustared in **Figure 4.11**, **Figure 4.12**, **Figure 4.13**, **Figure 4.14**.
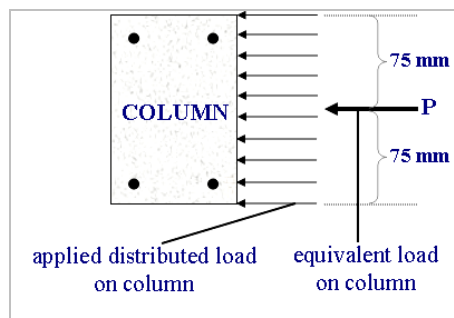
Figure 4.11. Lateral Load Application through the Bare Frame Specimens
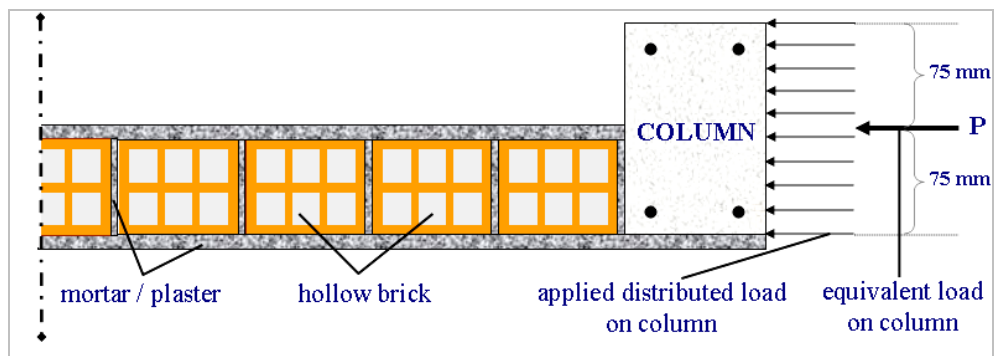
Figure 4.12. Lateral Load Application through the Reference Specimens
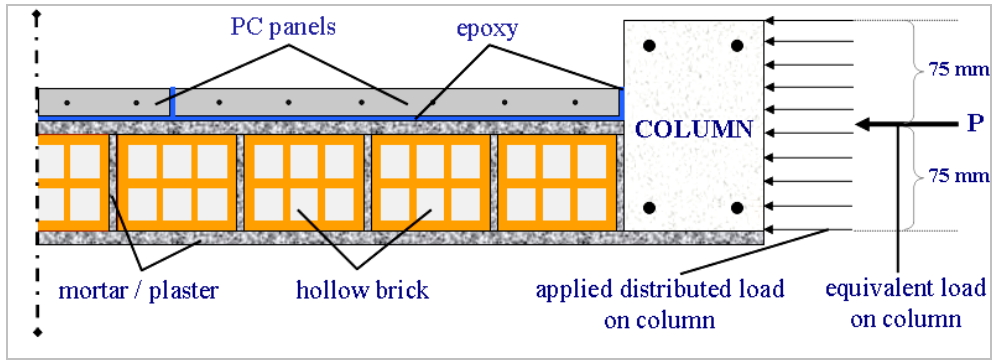
Figure 4.13. Lateral Load Application through the PC Panel Strengthened Specimens
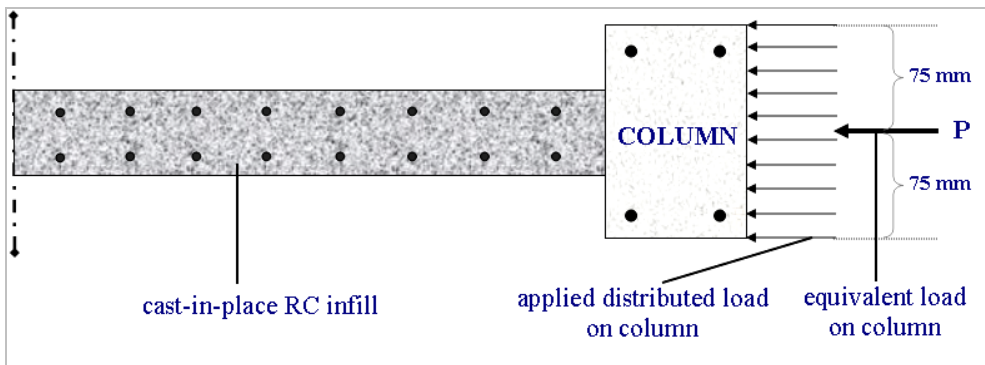
Figure 4.14. Lateral Load Application through the Cast-in-place RC Infilled Specimens

4.3. Instrumentation and Data Collection

Deformations and applied vertical and lateral loads were continuously recorded throughout the test. Experimental data was also monitored during the test both in numerically and graphically. The base shear versus top displacement was used for managing the load reversals. Load and deformation measuring devices were arranged on the specimens as shown in **Figure 4.15**. Calibration of all instruments was regularly checked in M.E.T.U. Structural Mechanics Laboratory.
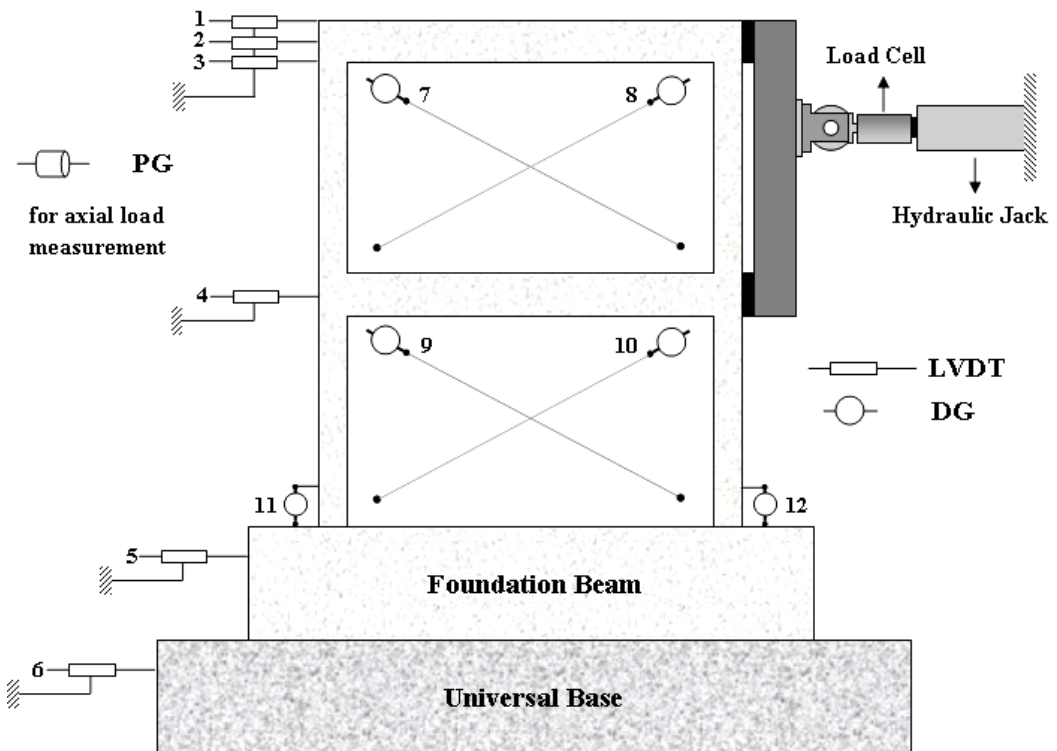
Figure 4.15. General Instrumentation

Axial force on the columns was measured by a pressure gage (PG) and controlled to be constant during the experiment. Lateral load was measured by a load cell as shown in **Figure 4.16**. The load cell had measuring capacity of 600 kN with a precision of ± 0.01 kN.
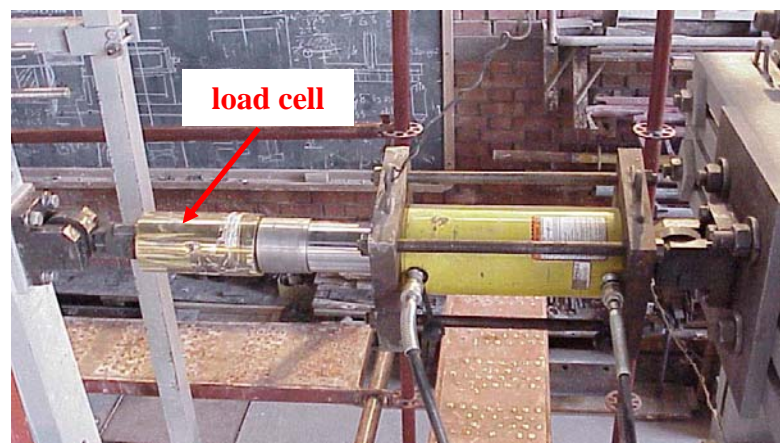
Figure 4.16. Lateral Load Measuring Load Cell

Linear Variable Displacement Transducers (LVDT) and electrical Dial Gages (DG) were installed for deformation measurements. Top displacement was measured by LVDT1, LVDT2 and LVDT3. Strokes of these gages were centrally aligned at the beginning of the test so that displacement data of both pulling and pushing half-cycles could be measured and recorded. These gages had the stroke of 200 mm with a precision of ± 0.01 mm. Average of LVDT1 and LVDT2 readings was taken as top displacement and LVDT3 reading was used to control this data. Besides, these readings were individually analyzed in order to check the existence out-of-plane deformations.

LVDT4 was placed for measuring first storey displacement to calculate both storey drifts. It had a stroke capacity of 100 mm with a precision of ± 0.01 mm. Stroke of this transducer was also centrally located to measure displacement of each reversed cycle. All LVDT devices were fixed to the timber frame neighboring the specimen as shown in **Figure 4.17.**

Figure 4.17. LVDT's Fixed to the Timber Frame **(Süsoy, 2004)**

LVDT5 and LVDT6 were located to monitor rigid body displacements of the specimen foundation and universal base. Each of them was a transducer with 50 mm measurement capacity with ± 0.01 mm precision. These LVDT's were fixed to individual steel frames and strokes were also centrally aligned. Considerably large deformations were never recorded in any of the test, which showed proper fixity of both specimen to the universal base and universal base to the strong floor and therefore no splitting.

DG7, DG8, DG9 and DG10 were electrical dial gauges with a capacity of 50 mm with the precision of ± 0.01 mm and used to measure shear deformations of the infill. It is obvious that, these gages were not used for bare frame tests. These gages were placed 130 mm away from both beam and column surfaces. The reason for this placing was to protect the gage from the localized effects like corner crushing. Sikadur-31 epoxy mortar was utilized to fix gage base onto the infill surface. This base had a nut at its center the diameter and shape of which perfectly coincided with the dial gage holder. Data measured by DG9 and DG10 were used to calculate shear deformations of the first storey infill while the data of DG8 and DG9 were used for the second storey. Shear deformation calculation is detailed in **Appendix-B**. These gages were not assembled for bare frames, naturally.

DG11 and DG12 were mounted at the bottom of both north and south columns in vertical position to measure the displacement values at the bottom of the column. Both gages had the measurement capacity of 20 mm with a precision of ± 0.01 mm. Gages were located onto the plane of symmetry of the column, 80 mm away from the column base. Sikadur-31 epoxy mortar and proper basement with a centered nut was mounted to the point and the gage was connected as shown in **Figure 4.18**. These gage readings were to get an idea about the variations in the column base-rotations, crushing of the concrete under compression and cracking of concrete and yielding of steel under tension.

Figure 4.18. Views of DG10 and DG11

Deformation and load measuring devices were subsequently cable connected to the data acquisition system, shown in **Figure 4.19**. A computer software package supplied together with the data acquisition system, called StrainSmart, was operated for data acquisition. **(StrainSmart System5000, 2000)** Base shear – top displacement diagram was continuously displayed to manage the experiment on the screen of the computer during the experiments by this software as well. The data was exported at the end of the test and then processed

Figure 4.19. General view of Instrumentation and Data Acquisition System

4.4. Test Procedure

When the specimen was ready for test after the curing period, it was located on the universal base and fixed by fourteen 45-mm bolts. The specimen was carefully lime washed in order to follow the cracks easier during the test. Steel plates of the lateral loading were clamped to the frame at the beam levels and connected by four steel bars to the spreader beam of lateral loading system. Narrower, standard and wider widths of specimens with varying aspect ratios were tested in this research. Therefore, lateral load application system was oriented for each specimen by moving the steel frame away from the reaction wall and the vertical alignment was also done. Hydraulic jack and pump connection was realized and the hose was checked for perfect oil transmission. Stroke of the hydraulic cylinder was centrally aligned for pull and push force applications of the loading.

Soon after the lateral loading system was located, supports of the vertical loading system were placed on the top each column and then the spreader beam was simply supported. The supports were centrally oriented as to apply equal load to each column, centrically as possible. Prestressing cable and hydraulic jack installation of axial loading system was done after the instrumentation was located. Ball transfer units were connected as the last stage of system implementation.

Since the specimen was properly placed in the setup, the instrumentation was located and a number of initial controls were done. Detailed information about instrumentation is provided in **Section 4.3**. Basic stages of the pre-test checks and preparations can be stated as follows.

- Working security around the test setup was carefully checked.
- The vertical loading system was connected to the crane through a steel chain as a precaution for any kind of out-of-control setup split, etc. Lateral loading adjustment had also similar kind of security connection to the reaction wall, it was also checked.

- Dial gages mounted in the infill corners to measure the shear deformations were broadly tied to the lateral load transmitting steel bars over the beam surfaces in order to protect the gages by hanging at the time of any sudden separation.
- Cameras located to record the experiment.
- Additional light was provided, if necessary, for better crack detection.
- Material strength for concrete and mortar were defined just before the test.
- Previous experiment results were kept handy for comparisons during the test.
- Test specimen was carefully visualized for any kind of pre-test crack. If there was any kind of crack like this, it was noted.
- Grounding was checked to avoid any kind of noise during data recording.
- The data logging computer system was connected to an uninterruptible power supply against the risk of data loss due to any kind of electricity cuts.
- Vertical load (30 kN for each column) was applied and then the test was performed.

Reversed cyclic lateral loading was applied to all specimens. Loading history of each specimen is presented in **Chapter 5**. The test was started by load controlled cycles and when the lateral load capacity was reached, then the test was continued by displacement controlled loading. Load was applied by hydraulic pump and experiment was managed through the graphical data. The test was terminated controlling stiffness degradation from the experimental data.

Crack check was carefully done after each cycle. Cracks were drawn by red pencil and visualization was provided by white lime wash. Every crack, crushing, separation, spillage was photo – recorded and all observations were noted. Each experiment was also recorded by camera. When the experiment was terminated, the experimental data was exported and recorded; necessary photos were quickly taken; the instrumentation and loading systems were picked up; finally the specimen was carried from the setup. Tested specimens were kept in the laboratory for a while; they existed in the laboratory at least during the appertaining tests of the same aspect ratio.

CHAPTER 5

TEST RESULTS AND OBSERVED BEHAVIOUR

5.1. General

Quasi-static 2D frame test results of RC frame specimens and the test observations are presented in this chapter, in the order of narrower, standard and wider series. The loading history, hysteretic lateral load-displacement curves of both storey levels, lateral load-first storey infill shear displacement curve are presented. Lateral load-column base vertical displacement curves for both north and south columns and lateral load-second storey infill shear displacement curve are presented in **Appendix-C** for each specimen. The test observations are stated in detail for each loading cycle. In addition, crack patterns of each specimen are also drawn and presented. The terminology used in the chapter is given in **Figure 5.1.** Finally, brief information about dynamic shake table tests and evaluation of these test results are presented.
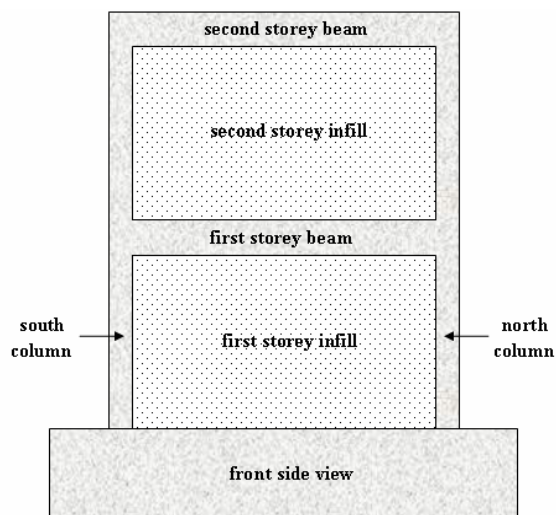
Figure 5.1. Terminology Used in Test Observation Explanations

5.2. Narrower Series Specimens

5.2.1. Specimen NB

Specimen **NB** is the bare frame of the narrower specimen series with no infill. The test was performed to obtain experimental data for verification of the analytical modeling studies of infilled/strengthened frames of narrower series. In addition, the bond-slip effect was also analytically investigated on the basis of the bare frame test results.

Specimen **NB** was subjected to lateral loading history presented in **Figure 5.2**, on which the numbers in parenthesis represent the corresponding second storey level top displacement in mm. Maximum forward and backward lateral loads were measured to be **8.4 kN** and **7.6 kN**, respectively. Hysteretic total lateral load – displacement curves of second and first storey are presented in **Figure 5.3** and **Figure 5.4**.
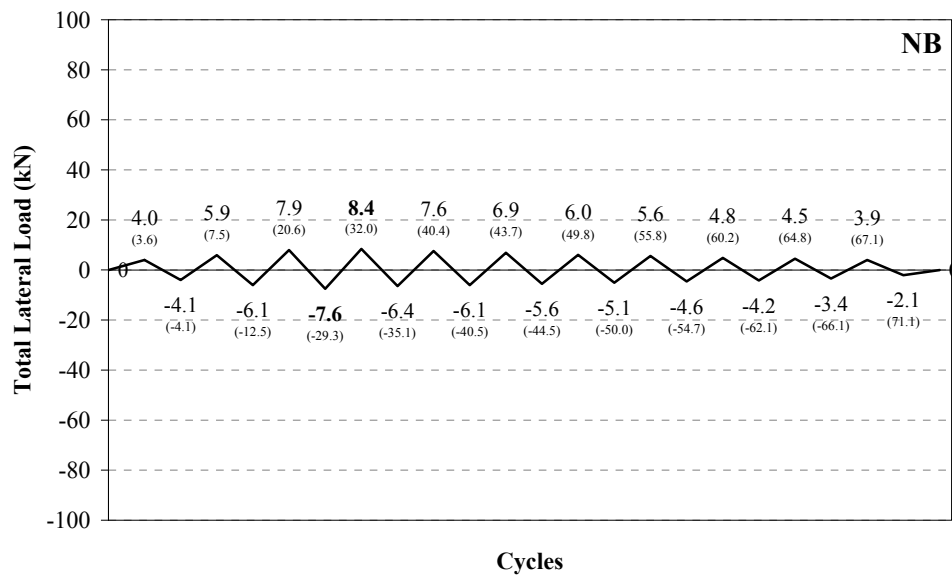
Figure 5.2. Loading History of Specimen **NB**

The initial stiffness of specimen **NB** was calculated to be **1.1 kN/mm**; as one of the major conclusions drawn from the total lateral load-top displacement curve**.** The initial stiffness of the specimen was defined as the initial slope of the total lateral load-second

storey level displacement curve in the first forward half cycle. At the instant of forward maximum loading, the interstorey drift ratios for the first and second stories were **0.0189** and **0.0151**, respectively whereas these values were **0.0189** and **0.0134** at the instant of backward maximum loading, respectively.
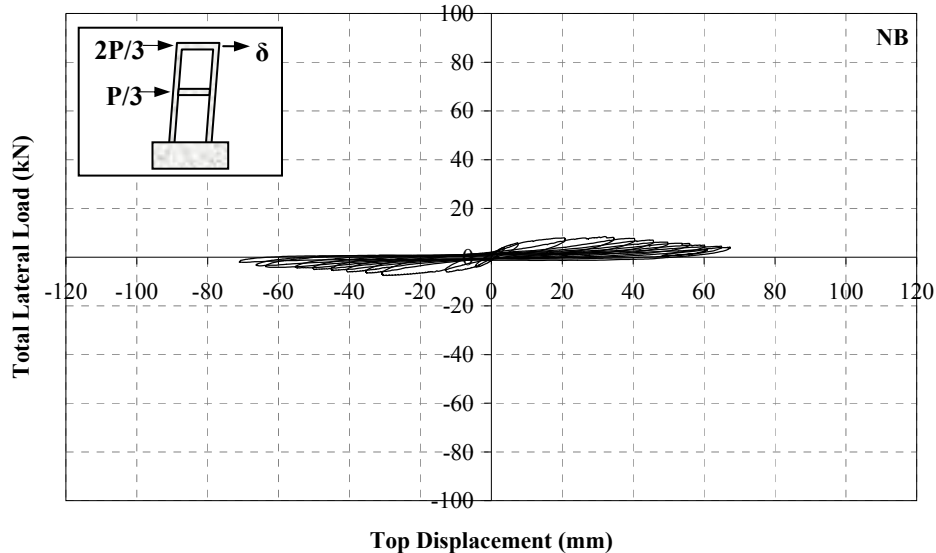
Figure 5.3. Total Lateral Load – Second Storey Level Displacement Curve, Specimen **NB**
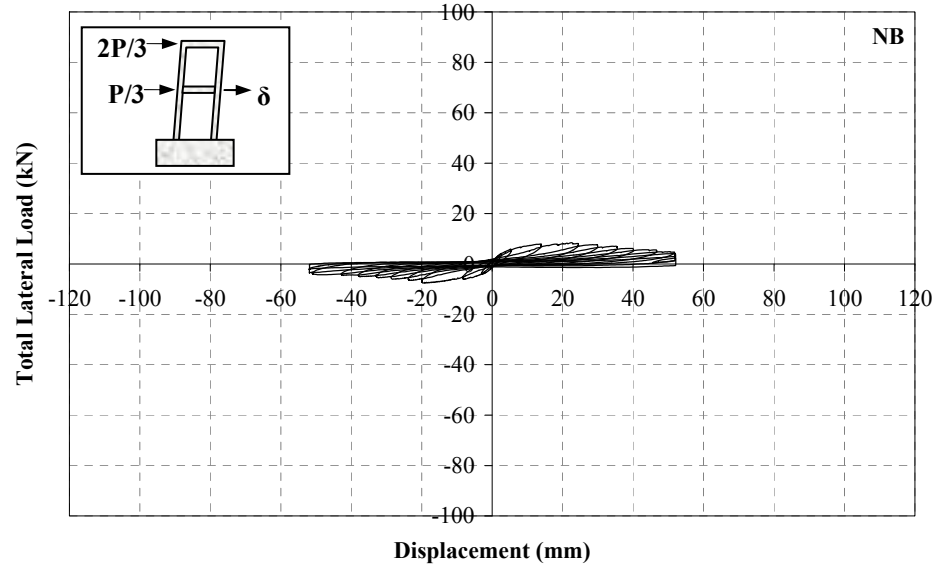
Figure 5.4. Total Lateral Load – First Storey Level Displacement Curve, Specimen **NB**

The major test observations of specimen **NB** are summarised below:

- In the first forward and backward half cycles, specimen **NB** was laterally loaded to +4.0 kN and -4.1 kN, respectively. A flexural crack was observed at the south column base in backward half cycle, while no crack occured in first forward half cycle.

- In the second forward half cycle, a seperation at the north column base-foundation joint was observed together with a crack at the inside of north column – beam joint of the first storey. Another crack was monitorised on the first storey beam – south column joint in the second backward half cycle, being symmetrical to that of the second forward half cycle.

- In the third forward half cycle, new flexural cracks occured at the north column base and over north column heigth approximately ~30 mm below the first storey beam-north column joint. Besides, a new diagonal crack on north column – first storey beam joint was also visible. The specimen reached its lateral loading capacity in the backward direction by **7.6 kN.** Symmetrical new cracks on south column occured in the third backward half cycle, both on column base and over column height. Moreover, another crack occured on the second storey base level of south column. Previous cracks on both columns and first storey beam – column joints widened in the third load reversal.

- The specimen reached its loading capacity in the forward direction, in the fourth forward half cycle by **8.4 kN.** In the fourth cycle, existing cracks widened and seperations on column bases became more visible. Two new cracks of first storey north column approximately ~50 mm and ~100 mm under the first storey beam-north column joint occured in the fourth forward half cycle. In the fourth backward half cycle, a flexural crack approximately ~70 mm below the first storey beam-south column joint occured on south column of first storey. New diagonal cracks on first storey beam-column joints also appeared.

- Beginning with the fifth forward half cycle, the experiment started to be carried out in displacement controlled fashion. In the fifth forward half cycle, a new crack occured on the south column base. Both forward and backward half

cycles resulted in new diagonal joint cracks on first storey beam – column joints which widened from joint corners to first storey column webs. Early concrete crushings started to appear on first storey beam-column joints.

- In the sixth forward half cycle, no new cracks occured. Besides, concrete crushings at column bases and first storey beam-column joints started. New cracks north first storey column approximately ~60 mm and ~120 mm under the joint occured in the sixth forward half cycle together with new diagonal joint crack on first storey beam – north column joint. Existing cracks propagated in both load reversals.

- In the seventh forward half cycle, two new cracks on first storey south column approximately ~70 mm and ~140 mm under the joint occured, being symmetrical with the north column cracks.Concrete crushings on joint regions became quiet visible.

- No additional cracks were observed in the remaining cycles, other than concrete crushings on column bases and first storey beam – column joints. The test was finalized after eleventh lateral load cycle, by reaching closely 70 mm of top displacement in both forward and backward loadings.

Views of specimen **NB,** before and during the experiment, are presented in **Figure 5.5**, and crack profiles of front and rear sides are presented in **Figure 5.6**.

Figure 5.5. Views of Specimen **NB**, Before and During the Experiment
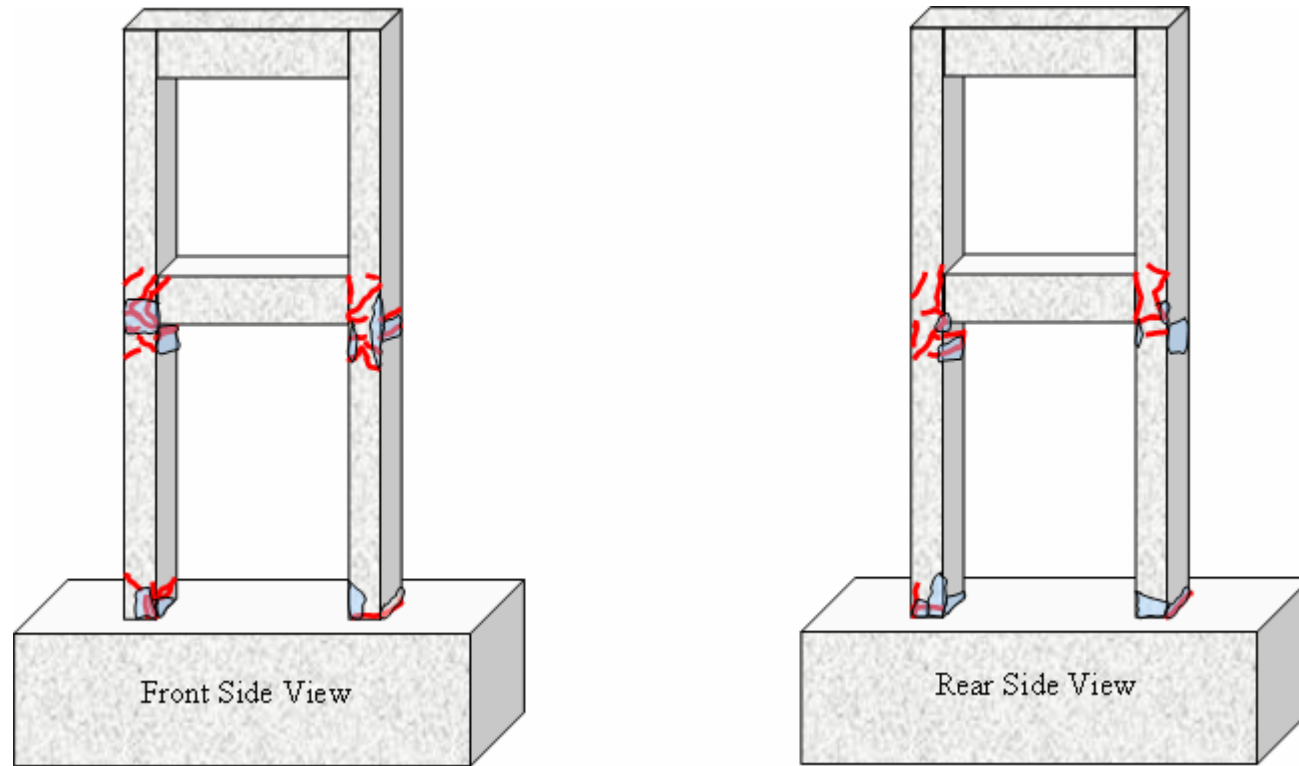
Figure 5.6. Front and Rear Side Crack Profiles of Specimen **NB**

5.2.2. Specimen NR

Specimen **NR** is the lower bound reference specimen of narrower frame series which represents the present state of typical existing building. It was infilled by hollow clay bricks plastered on both sides. The test results of this specimen would serve as a lower bound reference for the behaviour and capacity improvement evaluation of the narrower RC frame specimens strengthened by PC panels.

Specimen **NR** was subjected to lateral loading history presented in **Figure 5.7**, on which the numbers in parenthesis represent the corresponding second storey level top displacement in mm. Maximum forward and backward loads were measured to be **34.5 kN** and **35.1 kN**, respectively. Hysteretic total lateral load–displacement curves of second and first storey are presented in **Figure 5.8** and **Figure 5.9**. Total lateral load-shear displacement curves of first storey infill panel is presented in **Figure 5.10**
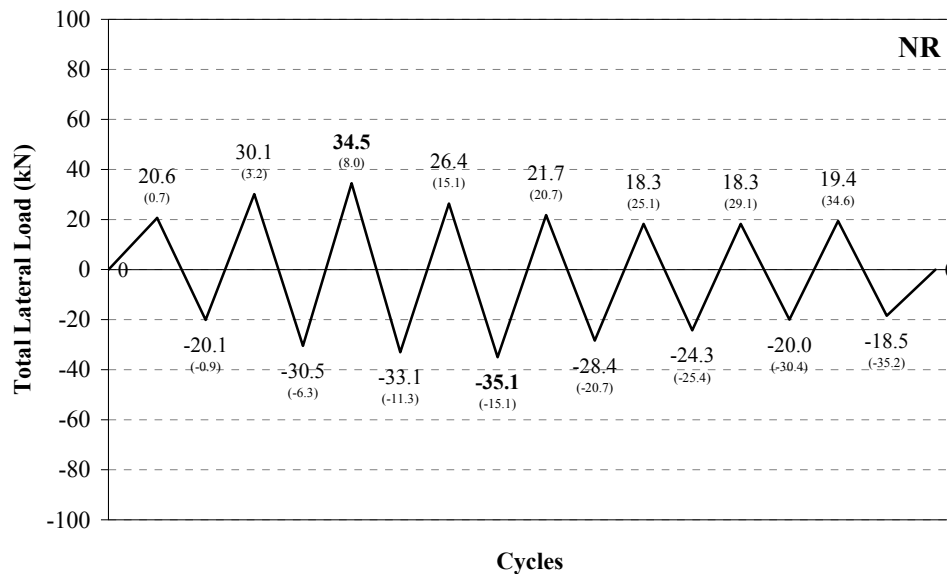
Figure 5.7. Loading History of Specimen **NR**

The initial stiffness of the specimen was calculated to be **10.9 kN/mm** as one of the major conclusions drawn from the total lateral load-top displacement curve**.** At the

instant of forward maximum loading, the interstorey drift ratios for the first and second stories were **0.0032** and **0.0055**, respectively whereas these values were **0.0088** and **0.0073** at the instant of backward maximum loading, respectively.
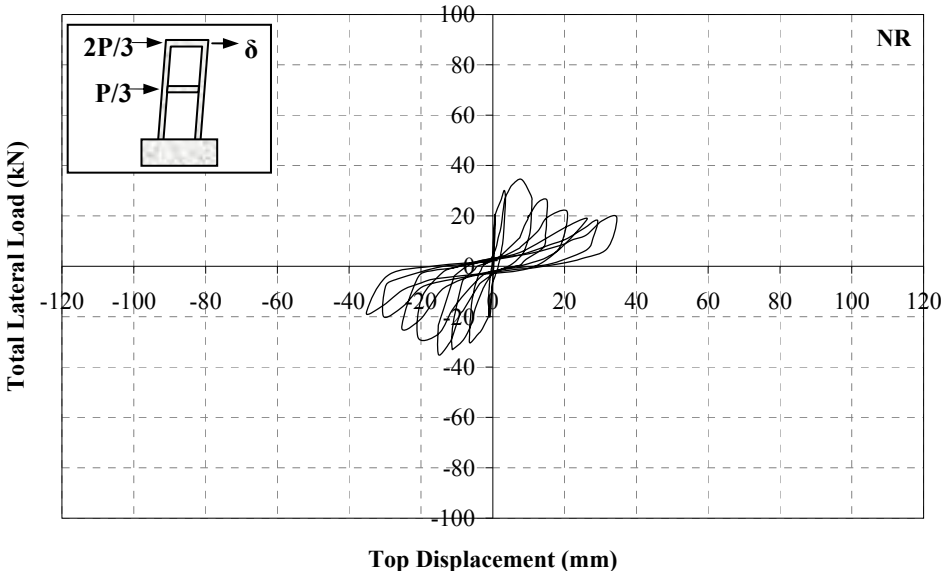
Figure 5.8. Total Lateral Load – Second Storey Level Displacement Curve, Specimen **NR**
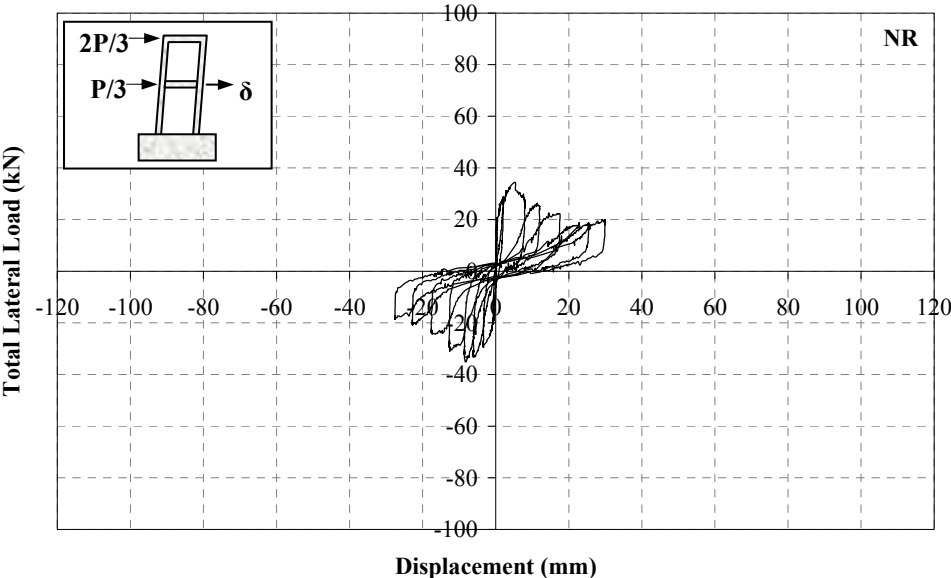
Figure 5.9. Total Lateral Load – First Storey Level Displacement Curve, Specimen **NR**
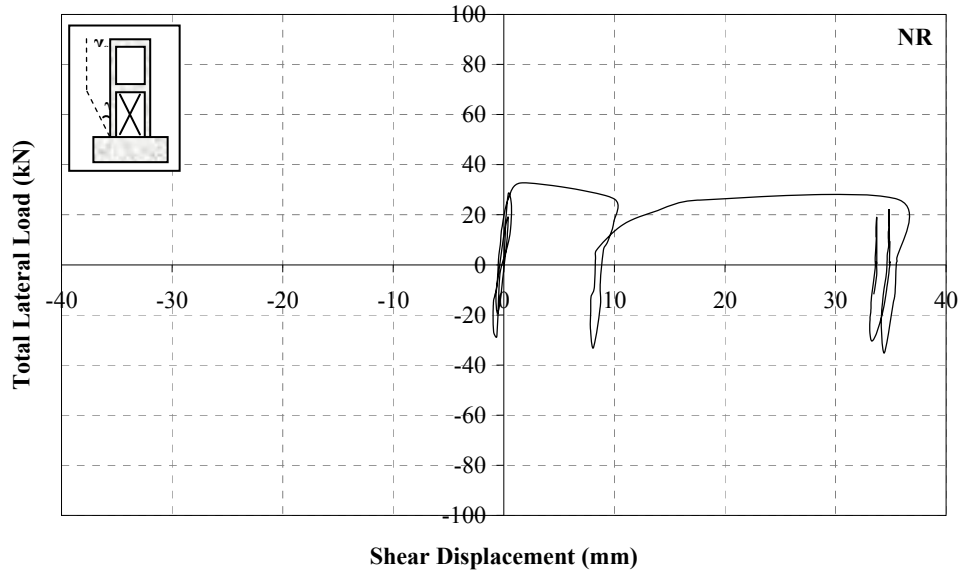
Figure 5.10. Total Lateral Load – First Storey Infill Shear Displacement Curve, Specimen **NR**

The major test observations of specimen **NR** are summarised below:

- In the first forward and backward half cycles, specimen **NR** was laterally loaded to + 20.6 kN and – 20.1 kN, respectively. Two hairline cracks on north column, approximately ~200 mm and ~400 mm above the base, occured on first forward half cycle. In the backward half cycle of this reversal, a hairline crack approximately ~200 mm above the south colum base appeared together with the first plaster crack on the tension zone of the infill at the basement level of the rear side.

- In the second forward half cycle, seperation of infill from the basement level occured together with a new crack on north column base. Three new cracks at approximate heights of ~250 mm, ~500 mm and ~700 mm of north column occured together with three diagonal shear cracks on first storey beam-north column joint and a crack on tension zone of rear side plaster. Three new cracks at approximate heights of ~150 mm, ~400 mm and ~600 mm of south column occured together with a new diagonal shear crack on first storey beam-south column joint together with a new crack on the south column base in the second

94

backward half cycle. Existing plaster crack width of the rear side increased and a new crack also occured on the tension zone of rear side plaster.

- In the third forward half cycle, specimen **NR** reached its lateral loading capacity in the forward loading direction by **34.5 kN**. No new column or beam crack occured. However, the plaster of the rear side wounded by a number of cracks at first storey beam level and new cracks on the second storey plaster being parallel to both columns appeared. The rear side plaster at the corner of north column on the base was also seperated. In the third backward half cycle, two new cracks below the south column – first storey beam joint occured. Symmetrical plaster cracks at the rear side on first storey beam level appeared. Existing infill crack on the tension side widened to ~5 mm. Front side plaster on the upper corner of north column - first storey beam was crushed and seperated.

- The fourth loading reversal was controlled by the top displacement of second storey and the specimen **NR** reached its capacity of backward loading at this stage by **-35.1 kN.** A new plaster crack on the front side of infill has occured along the north column – infill interface of first storey in the fourth forward half cycle. Besides, the plaster around the corner of first storey north column – beam joint was seperated and the corner dial gage was out of recording as can be seen in **Figure 5.17**. The same damage has occured on the symmetrical corner by crushing of the hollow clay brick in the corresponding backward half cycle. A number of plaster cracks appeared on the rear side around and above the first storey beam level. Existing cracks considerably widened together with a new crack on first storey beam- north column joint; the rear side corner plaster of south column seperated.

- In the fifth forward half cycle, the seperation of infill from the basement level was ~5 mm wide. New diagonal shear cracks appeared on both first storey beam-column joints, together with a new crack around the mid-span of first storey beam, the plaster of the rear side around the first storey beam also seperated from the frame. In the fifth backward half cycle, the number of cracks along the span of first storey beam increased and the hollow clay brick under the first storey beam were crushed.

- In the sixth cycle, the existing cracks widened and clay bricks of the first storey under the beam level were highly damaged, the plaster of the rear side around the first storey beam level was totally seperated. The test was finalized at the end of the eigth full cycle, while the stiffness was almost zero. 97

Views of specimen **NR,** before and after the experiment, are presented in **Figure 5.11**, and crack profiles of front and rear sides are presented in **Figure 5.12**.

Figure 5.11. Before and After Test Views of Specimen **NR**
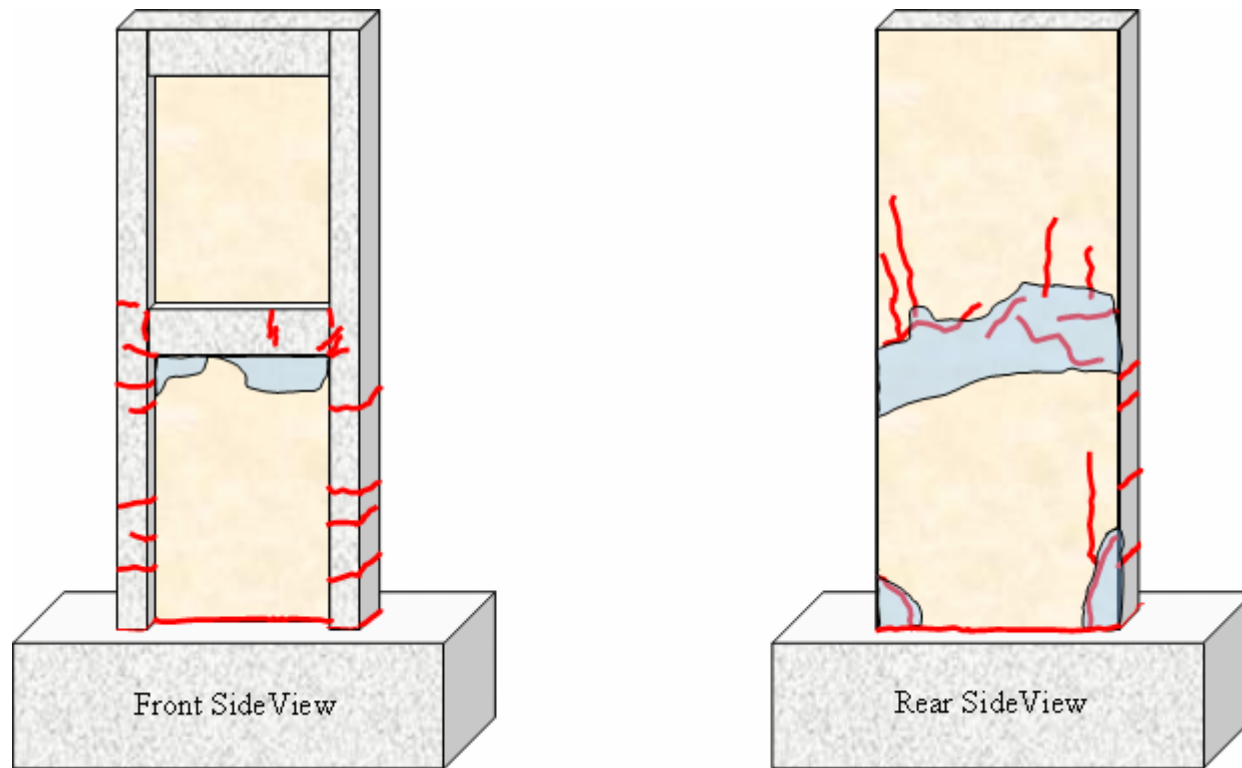
Figure 5.12. Front and Rear Side Crack Profiles of Specimen **NR**

5.2.3. Specimen NRP

Specimen **NRP** was the frame strengthened by rectangular shaped PC panels. The test results of this specimen were used to investigate the efficiency of PC panel method on seismic performance improvement of similar geometry frames. The test results were basically compared with the upper bound reference specimen **NRC** and and then lower bound specimen **NR**.

Specimen **NRP** was subjected to lateral loading history presented in **Figure 5.13,** on which the numbers in parenthesis represent the corresponding second storey level top displacement in mm. Maximum forward and backward loads were measured to be **66.4 kN** and **64.0 kN,** respectively. Hysteretic total lateral load – displacement curves of second and first storey are presented in **Figure 5.14** and **Figure 5.15**. Total lateral load-shear displacement curve of first storey infill panel is presented in **Figure 5.16**
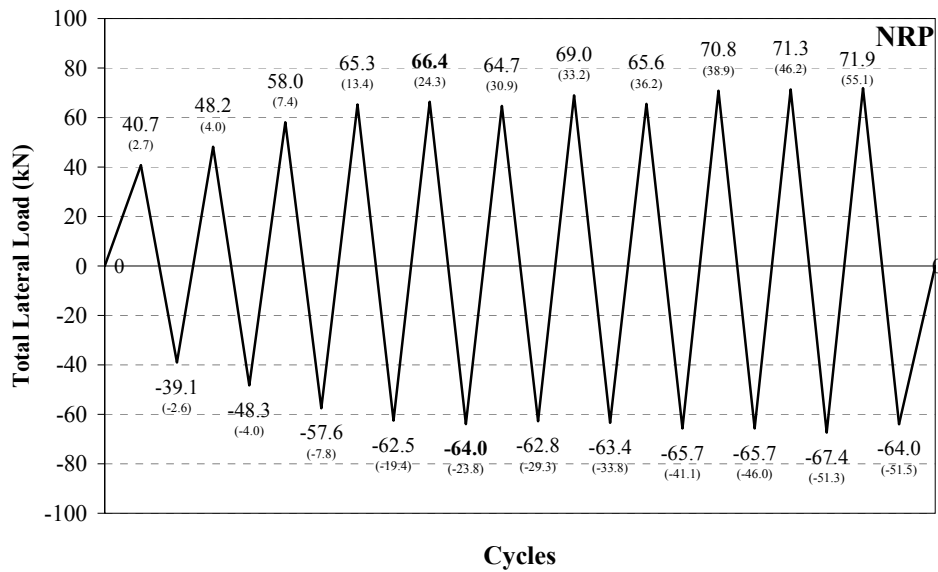
Figure 5.13. Loading History of Specimen **NRP**

The initial stiffness of the specimen was calculated to be **15.2 kN/mm**; as one of the major conclusions drawn from the lateral load-displacement curves**.** The initial stiffness of the specimen was defined as the initial slope of the lateral load-second storey level

displacement curve in the first forward half cycle. At the instant of forward maximum loading, the interstorey drift ratios for the first and second stories were **0.0098** and **0.0164**, respectively whereas these values were **0.0092** and **0.0164** at the instant of backward maximum loading, respectively.
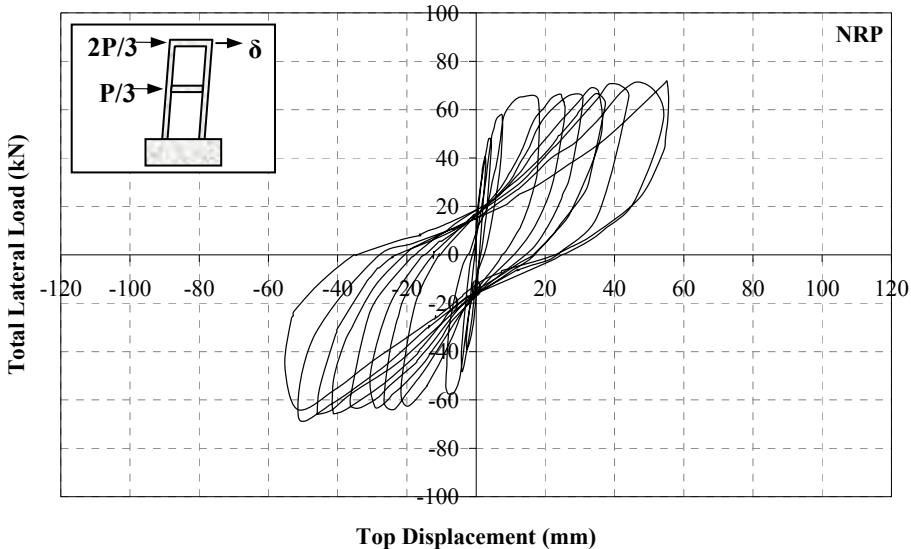
Figure 5.14. Total Lateral Load – Second Storey Level Displacement Curve, Specimen **NRP**
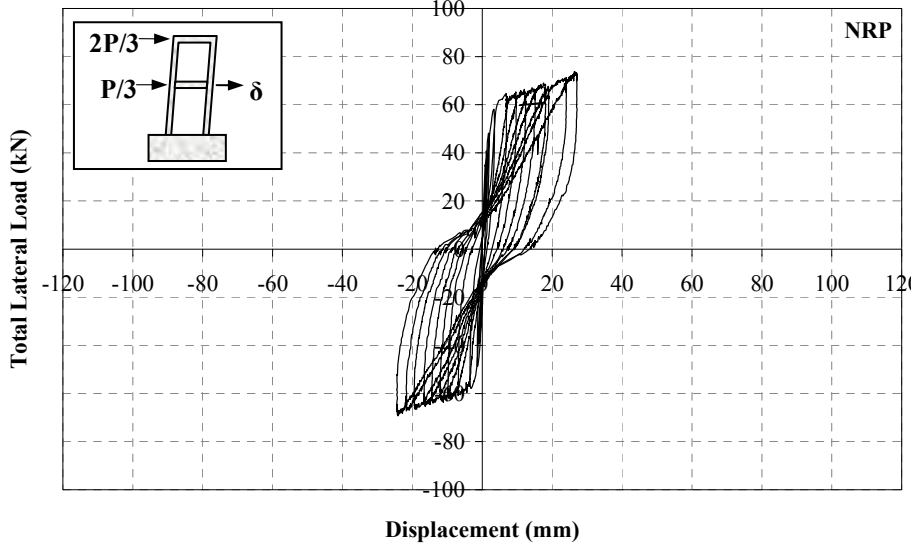
Figure 5.15. Total Lateral Load – First Storey Level Displacement Curve, Specimen **NRP**
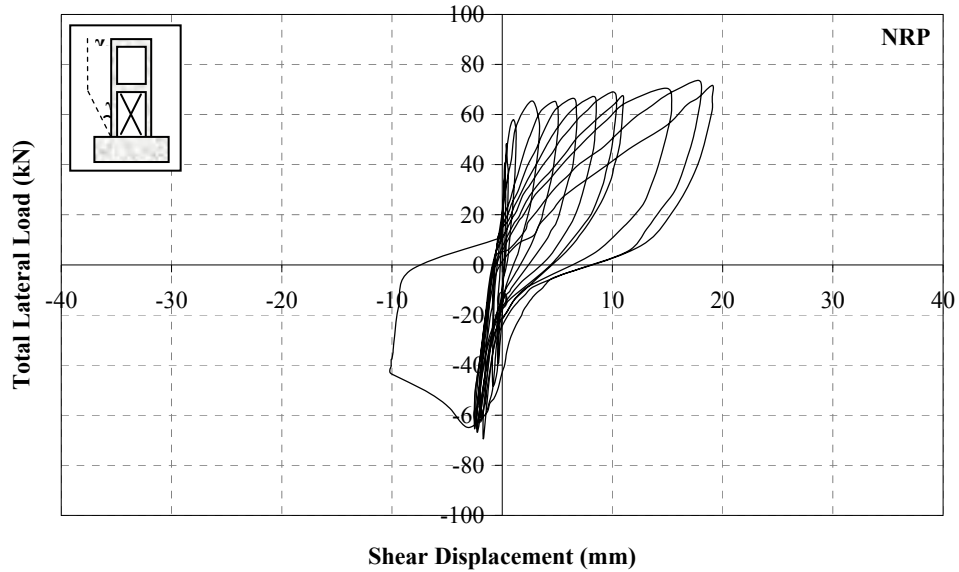
Figure 5.16. Total Lateral Load – First Storey Infill Shear Displacement Curve, Specimen **NRP**

The major test observations of specimen **NRP** are summarised below:

- In the first forward and backward half cycles, specimen **NRP** was laterally loaded to + 40.7 kN and – 39.1 kN, respectively. In the first forward half cycle, total of five bending cracks occured on the north column; first being on the column base and the others were oriented ~100 mm from each other. The symmetrical cracks appeared on the south column in the first backward half cycle, together with a diagonal panel crack on the south column – foundation corner.

- Existing cracks on the north column were propagated through the front side of the column in the second forward half cycle; two new bending cracks occured above the existing cracks aligning ~90 mm distance in average, symmetrical panel crack on the north column – foundation corner occured together with a seperation along the infill – foundation connection being closer to the north column base. In the second backward half cycle, existing cracks on south column were propagated through the front side of the column. Two new bending cracks were appeared; one on the first storey beam north column

connection and the other ~90 mm below this one. Corner panel on north column –foundation connection, experinced cracks on the epoxy zone over the dowel locations. A plaster crack; starting from the third crack from the base arised to the foundation level occured on the rear side.

- In the third forward half cycle, two new bending cracks occured on the north column. The first one appeared ~80 mm away from the basement on the column dial gage level and the second was on the front side of the column being ~200 mm from the base. Seperation along the north column – infill panel surface was observed along the column height of the first storey, together with two additional cracks around second and fourth dowels from the base, to the column surface. Morever, first diagonal shear crack on the first storey beam – north column connection was realized. A plaster crack arising from ~200 mm below the beam level to the foundation following the column surface path occured on the rear side. Symmetrical shear crack on the first storey beam-south column connection occured in the third backward half cycle; seperation along the south column – infill panel surface was observed along the column height of the first storey, existing column cracks propagated through the front side and diagonal cracks occured on the plaster around the basement.

- In the fourth forward half cycle, ~3-4 mm wide cracks observed on the panel-to-panel and panel-to-foundation connections of first panel layer of the first storey together with widening of the existing column cracks. Horizontal cracks below the first storey beam appeared on the plaster together with a new horizontal crack aligned on the first and second panel connection line. Seperation of plaster from the column surface started. In the fourth backward half cycle, the bending crack ~150 mm away from the south column base widened up to ~5-6 mm being same as the seperation of the panel-infill composite from the foundation level. The plaster was seperated from the column surface. Following the crack path as drawn in **Figure 5.19**, and symetrical plaster cracks below the first storey beam appeared.

- The specimen reached the maximum forward and backward load levels in the fifth forward and backward half cycle with **66.4 kN** and **64.0 kN**, respectively. Displacement controlled loading was also started in this cycle. The dial gage measuring the north column base seperated from its location; cracks on north

column and openings in the panel connections were widened in fifth forward half cycle. In the fifth backward half cycle, seperation of infill-panel composite from the foundation level increased together with the same effect along the existing panel-to-panel connection cracks.

- In the sixth forward half cycle a diagonal crack occured on the corner panel of south column-foundation connection, some new plaster cracks occured on the first storey plaster surface. The existing cracks on the south column opened up to ~5-6 mm and and the seperation of infill from the foundation level was increased.

- In the seventh and eighth full cycles, existing cracks opened up and the lateral load applied to the specimen did not decrase with the incrasing displacement levels by showing a quiet ductile behaviour. Besides, the longitudinal reinforcement of the north column buckled at the foundation level in the eighth backward half cycle as shown in **Figure 5.17.**

- The longitudinal reinforcement of the south column also buckled on the foundation level in the ninth forward half cycle by reaching 38.5 mm top displacement as also shown in **Figure 5.17**. Crushing of the PC panel located on the corner of first storey beam-north column connection was observed in the ninth backward half cycle. The buckling of the north column longitudinal reinforcement on the basement level increased and the plaster over the north column surface on the first storey was fully seperated from the specimen.

Figure 5.17. Buckling of Longitudinal Reinforcement at South and North Column Bases, Specimen **NRP**

- In the tenth and eleventh cycles, buckling of the first storey column longitudinal reinforcement together with an increase in applied lateral load were observed. The test was terminated at the end of the eleventh cycle.

Views of specimen **NRP,** before and after the experiment, are presented in **Figure 5.18**, and crack profiles of front and rear sides are presented in **Figure 5.19**.

Figure 5.18. Before and After Test Views of Specimen **NRP**
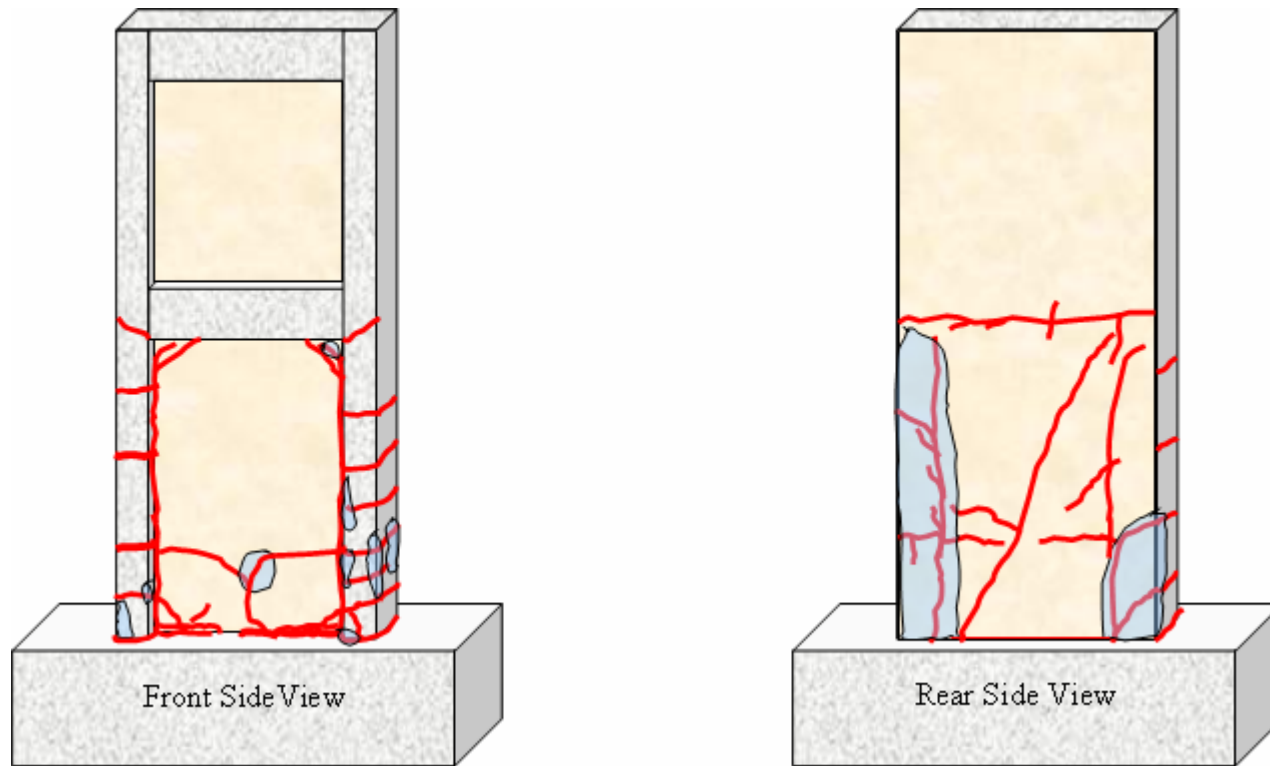
Figure 5.19. Front and Rear Side Crack Profiles of Specimen **NRP**

5.2.4. Specimen NSP

Specimen **NSP** was the frame strengthened by strip shaped PC panels. The test results of this specimen were used to investigate the efficiency of PC panel method on seismic performance improvement of similar geometry frames. The test results were basically compared with the upper bound reference specimen **NRC** and and then lower bound specimen **NR**. In addition, the performance improvement comparisons were also done for specimen **NRP**.

Specimen **NSP** was subjected to lateral loading history presented in **Figure 5.20,** on which the numbers in parenthesis represent the corresponding second storey level top displacement in mm. Maximum forward and backward loads were measured to be **64.3 kN** and **62.0 kN**, respectively. Hysteretic total lateral load – displacement curves of second and first storey are presented in **Figure 5.21** and **Figure 5.22**. Total lateral load - shear displacement curve of first storey infill panel is presented in **Figure 5.23**.
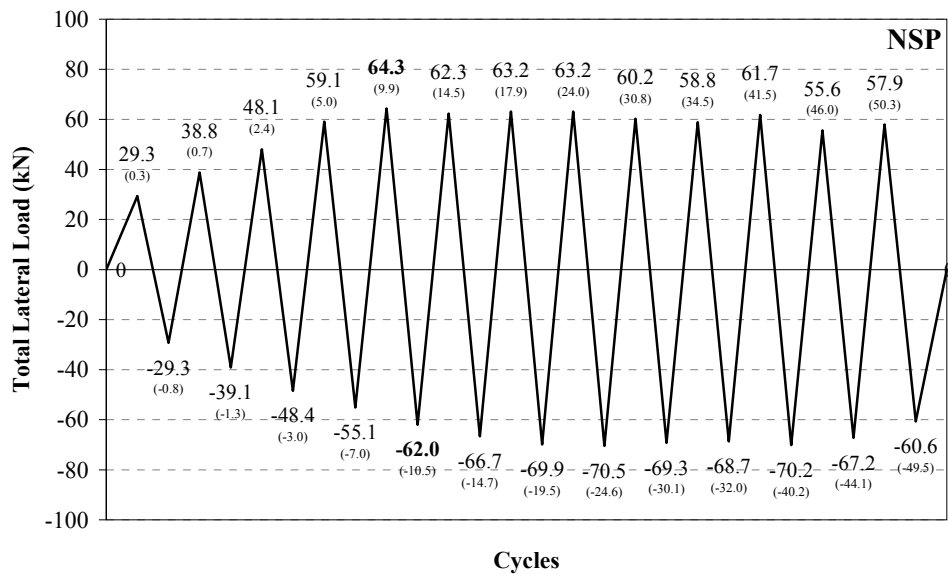
Figure 5.20. Loading History of Specimen **NSP**

The initial stiffness of the specimen was calculated to be **64.3 kN/mm** as one of the major conclusions drawn from the lateral load-displacement curves**.** At the instant of

forward maximum loading, the interstorey drift ratios for the first and second stories were **0.0045** and **0.0061**, respectively whereas these values were **0.0045** and **0.0068** at the instant of backward maximum loading, respectively.
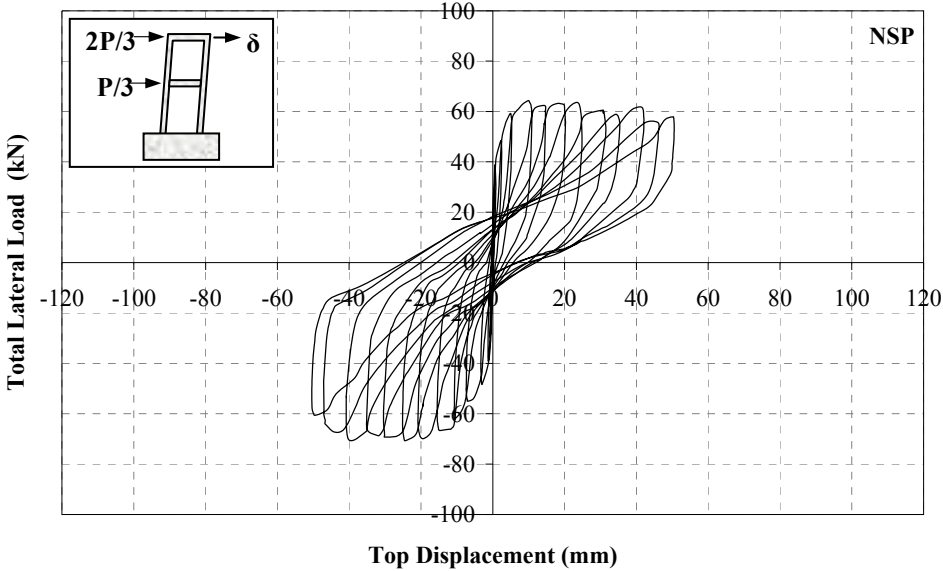
Figure 5.21. Total Lateral Load – Second Storey Level Displacement Curve, Specimen **NSP**
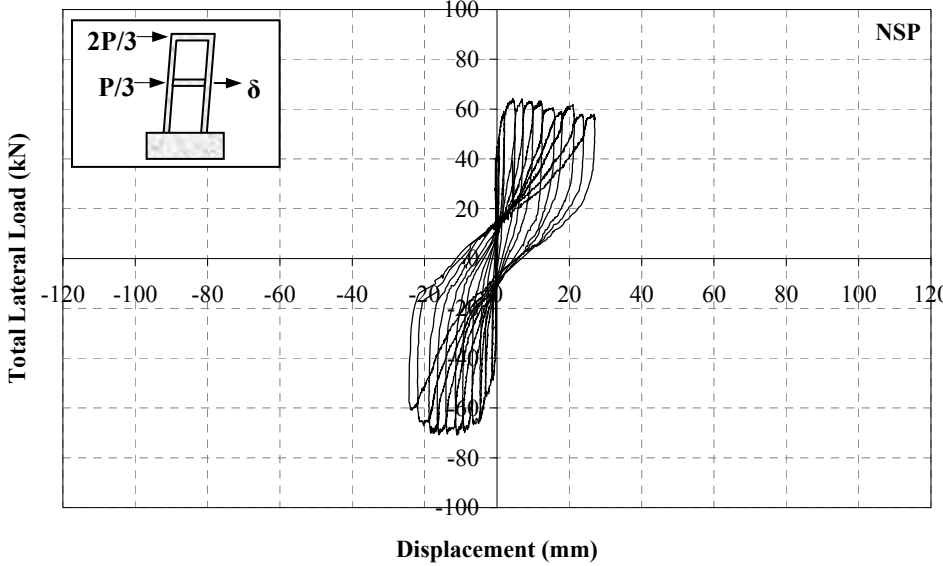
Figure 5.22. Total Lateral Load – First Storey Level Displacement Curve, Specimen **NSP**
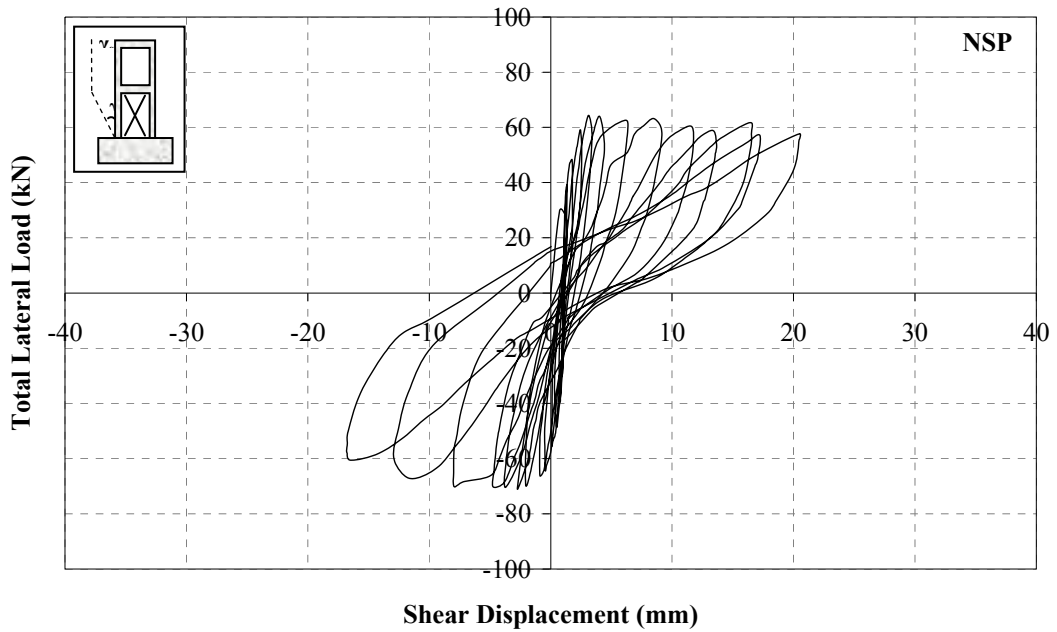
Figure 5.23. Total Lateral Load – First Storey Infill Shear Displacement Curve, Specimen **NSP**

The major test observations of specimen **NSP** are summarised below:

- In the first forward and backward half cycles, specimen **NSP** was laterally loaded to + 29.3 kN and – 29.3 kN, respectively. A crack on the south column base appeared in the first backward half cycle, while no cracks occured in the first forward half cycle.

- In the second forward half cycle, total of three bending cracks occured on the north column first being on the basement and the remaining were aligned up to the mid-height. A plaster crack following the column-infill interaction surface apperaead from mid-height to the basement. Two new bending cracks appeared on the first storey north column, up to the mid-height being symmetrical as south column in the second backward half cycle. The cracks on the plaster, following the interaction line of infill – south column were also appeared as drawn in **Figure 5.26.**

- Seperation of infill-panel composite from the north column surface was realized in the third forward half cycle together with the first panel crack. The panel

107

crack appeared in a bending crack format on the corner side of north column-foundation connection, ~200 mm above the basement. Existing bending cracks on north column aroused through the front side and two new cracks appeared over the mid-height. The plaster cracks on the rear side occured on the same level with column cracks and plaster crack aligning the infill-north column surface propagated through the first storey beam level. The similar seperation in between panel-infill composite and south column surface occured in the first storey the third forward half cycle, together with the plaster cracks of the rear side on the same line of the seperation. The first shear crack on the south column-first storey beam connection also occured in this cycle.

- In the fourth forward half cycle, a new bending crack occured on the north column ~100 mm below the first storey beam level. The first diagonal shear crack also appeared on the connection of first storey beam and north column. Seperation in between panel and foundation was realized. The panel crack was propagated through the foundation level as illustrated in **Figure 5.26**. The plaster crack on the same line with the panel crack was propagated together with some new narrow cracks on the line of infill-panel connection with the north column of the first storey. Two new bending cracks occured in the fourth backward half cycle just below the mid-height of the south column. The plaster seperation on the rear side along the interaction line of panel-infill composite with the south column widened and new plaster cracks occured on the same level with the column bending cracks.

- The specimen reached its lateral loading capacity in the fifth cycle by **64.3 kN** and **62.0 kN** in the forward and backward directions, respectively. The experiment was conducted by displacement control after this cycle. The panel and plaster cracks around the north column – foundation connection propagated and widened as shown in **Figure 5.24**. A new bending crack occured on the north column just below the first storey beam connection. In the fifth backward half cycle, the specimen experienced two new flexural cracks on the south column just below the first storey beam connection together with new plaster cracks of the rear side on the same level with the existing cracks of the south column.

Figure 5.24. Panel and Plaster Cracks after Fifth Forward half cycle, Specimen **NSP**

- In the sixth forward half cycle, the specimen experienced flexural cracks on the first storey beam, being closer to north and south column connections together with widening of the existing shear crack on the first storey beam-south column connection. Seperation of the infill- PC panel composite from the north column surface in the first storey and widening of the plaster cracks on the rear side was more pronounced in this cycle also. In the sixth backward half cycle, the existing cracks on the south column widened and a new diagonal panel crack occured on the corner of south column-foundation connection.

- In the seventh forward half cycle, the existing panel and plaster cracks were widened and a new plaster crack occured on the second storey, at the south column – infill composite interaction. In the seventh backward half cycle, a new plaster crack occured on the second storey, at the north column – infill composite interaction, being symmetrical as the one with south column. Crushing of the concrete on the north column base was first observed in this cycle.

- In the eighth forward half cycle, the existing panel cracks widened up to ~5-6 mm and some cracks on the north column propagated through the front side. Existing cracks on south column widened in the eighth backward half cycle.

- In the nineth forward half cycle, the existing shear crack on the first storey beam-north column connection widened up to ~3-4 mm together with a new diagonal shear crack on the first storey beam closer to the mentioned beam-column joint. Besides, crushing of the concrete at the second storey beam-north column connection was observed together with a hairline flexural crack around the mid-height of the second storey north column In the nineth backward half

cycle, seperation of infill-PC panel connection from the south column interacton surface was realized in the second storey.

- In the tenth forward half cycle, seperation of the second storey infill-PC panel composite from the first storey beam level was observed. Diagonal panel cracks of the first storey occured in the tenth backward half cycle. Longitudinal reinforcement buckled on the first storey beam-north column connection together with crushing and spalling of the concrete.

- In the eleventh and twelfth cycles, the existing cracks widened and crushing and spalling of the concrete and plaster were realized as illustrated in **Figure 5.26**. The test was terminated at the end of the twelfth cycle.

Views of specimen **NSP,** before and after the experiment, presented in Figure **5.25,** and crack profiles of front and rear sides are presented in Figure **5.26**.

Figure 5.25. Before and After Test Views of Specimen **NSP**

Front Side View

Rear Side View
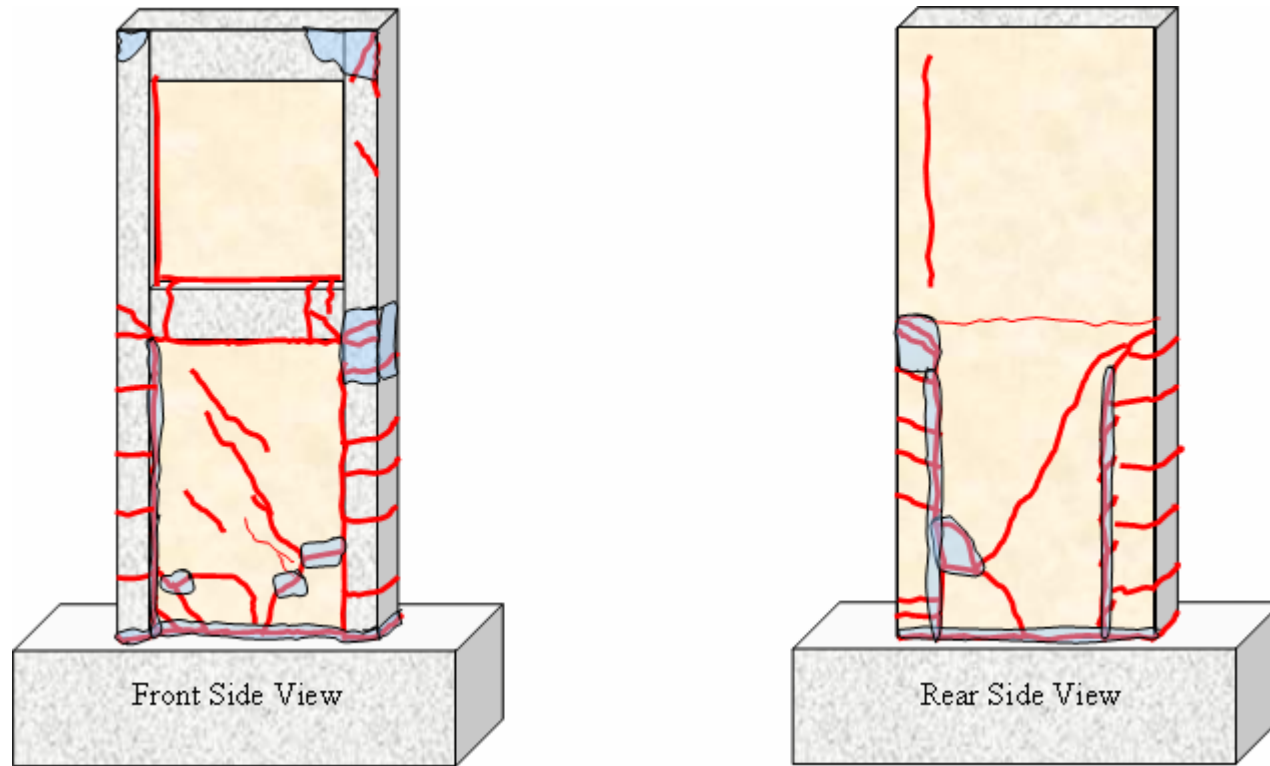
Figure 5.26. Front and Rear Side Crack Profiles of Specimen **NSP**

5.2.5. Specimen NRC

Specimen **NRC** was tested as the upper bound reference with cast-in-place RC infills. The test results of this specimen were compared with the performance improvement by PC panel application for both strip and rectangular panels.

Specimen **NRC** was subjected to lateral loading history presented in **Figure 5.27**, on which the numbers in parenthesis represent the corresponding second storey level top displacement in mm. Maximum forward and backward loads were measured to be **68.4 kN** and **70.1 kN**, respectively. Hysteretic total lateral load − displacement curves of second and first storey are presented in **Figure 5.28** and **Figure 5.29**. Total lateral load-shear displacement curve of first storey infill panel is presented in **Figure 5.30.**
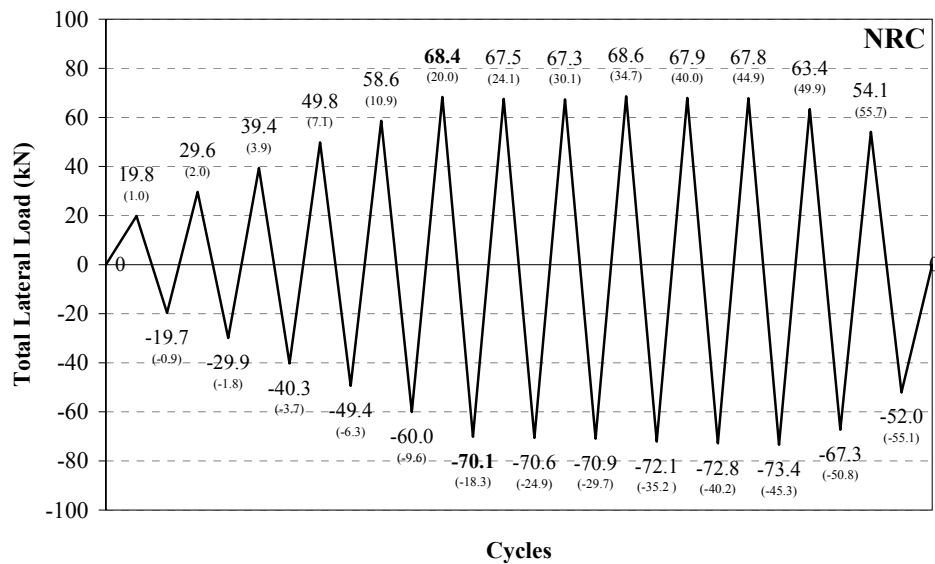
Figure 5.27. Loading History of Specimen **NRC**

The initial stiffness of the specimen was calculated to be **21.7 kN/mm** as one of the major conclusions drawn from the lateral load-displacement curves**.** The initial stiffness of the specimen was defined as the initial slope of the lateral load-second storey level displacement curve in the first forward half cycle. At the instant of forward maximum loading, the interstorey drift ratios for the first and second stories were **0.0106** and

112

0.0108, respectively whereas these values were **0.0104** and **0.0091** at the instant of backward maximum loading, respectively.
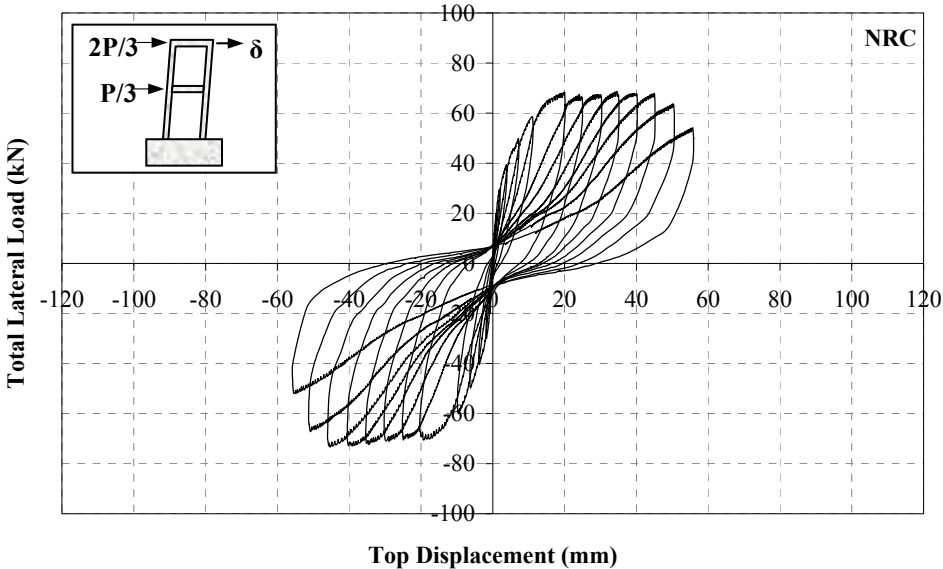
Figure 5.28. Total Lateral Load – Second Storey Level Displacement Curve, Specimen **NRC**
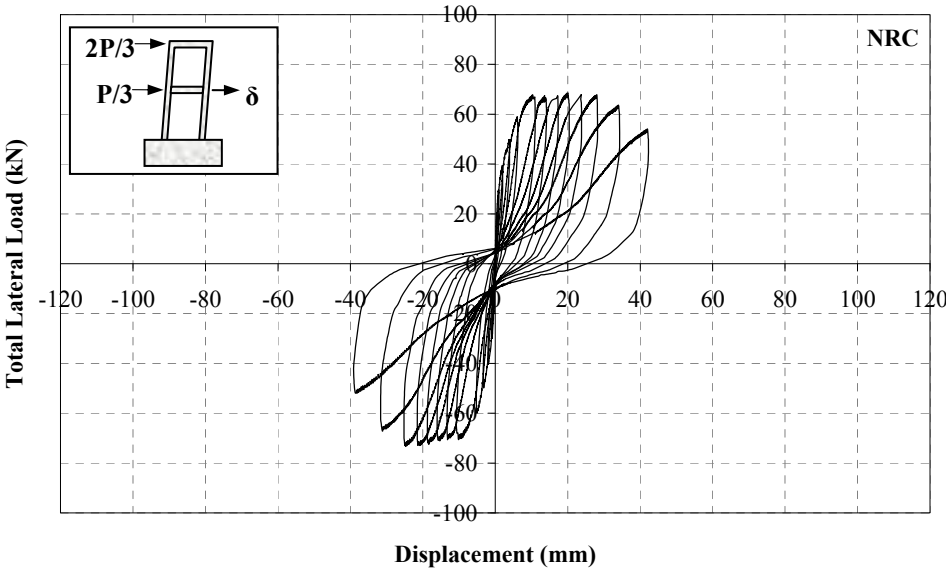
Figure 5.29. Total Lateral Load – First Storey Level Displacement Curve, Specimen **NRC**
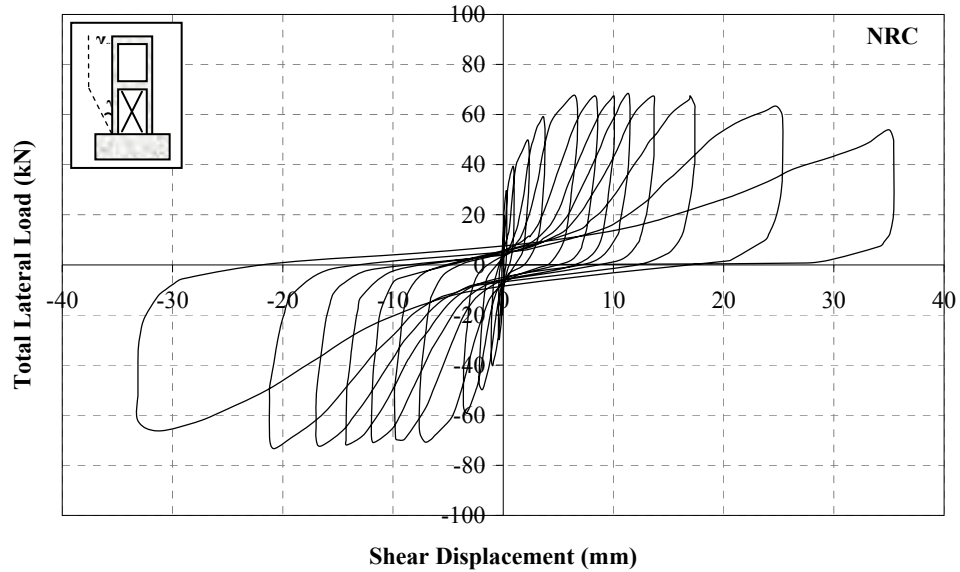
Figure 5.30. Total Lateral Load – First Storey Infill Shear Displacement Curve, Specimen **NRC**

The major test observations of specimen **NRC** are summarised below:

- In the first forward and backward half cycles, specimen **NRC** was laterally loaded to + 19.8 kN and – 19.7 kN, respectively. No cracks were observed in the first half cycles.

- A hairline flexural crack occured on the north column base and two other appeared on the first storey north column ~200 mm away from the base and each other, in the second forward half cycle. Symmetrical column cracks occured in the second backward half cycle on the south column in the first storey.

- In the third forward half cycle, the existing hairline crack on the north column base became more visible and two new flexural cracks; one being ~150 mm below the first storey beam-north column connection appeared on the north column. In the third backward half cycle, a flexural crack occured in first storey beam-south column connection. A new crack occured around the midheight of south column in the first storey together with propagation of the existing ones through the front side.

114

- In the fourth forward half cycle, the specimen experienced first diagonal cracks in the first storey RC infill. A flexural crack, which is symmetrical with the one occured in the third backward half cycle, aroused on the first storey beam – north column connection as well. In the fourth backward half cycle, existing cracks on the south column widened through the front side of the column together with new bending cracks on the south column. Diagonal shear cracks occured in this half cycle, as well. Horizontal cracks on the various locations appeared on the same line with the horizontal steel mesh reinforcement.

- In the fifth forward half cycle, a number of new diagonal cracks were added to the first storey RC infill. Existing cracks on the north column widened and propagated through the front side and some new cracks also occured on the north column of first storey. In the fifth backward half cycle, new diagonal cracks occured on the first storey RC infill and crack on the south column base widened.

- In the sixth forward and backward half cycles, the specimen reached its lateral loading capacity by **68.4 kN** and 7**0.1 kN**, respectively. In the sixth forward half cycle, a number of new diagonal cracks occured and existing ones widened on the first storey RC infill. North column cracks propagated through the infill in the first storey and column cracks widened. In the sixth backward half cycle, shear cracks on the first storey RC panel increased in the opposite direction and existing ones widened.

- In the seventh and eighth load reversals, new diagonal shear cracks occured on the first storey RC infill and existing diagonal panel cracks and column cracks widened. Besides, displacement controlled loading was started at seventh forward half cycle.

- In the nineth forward half cycle, the crack on the north column base widened. Existing cracks opened and localized concrete crushing that follows the cracks path on the first storey RC infill became visible as also illustrated in **Figure 5.32**.

- The test was terminated at the end of thirteenth load reversal. The specimen experienced apperance of new diagonal shear cracks on the first storey RC infill, widening of existing infill and column cracks together with concrete

crushing illustrated in **Figure 5.32** which provides crack pattern of specimen **NRC** at the end of the test.

Views of specimen **NRC,** before and after the experiment, presented in **Figure 5.31**, and crack profiles of front and rear sides are presented in **Figure 5.32**.

Figure 5.31. Before and After Test Views of Specimen **NRC**

Front Side View

Rear Side View
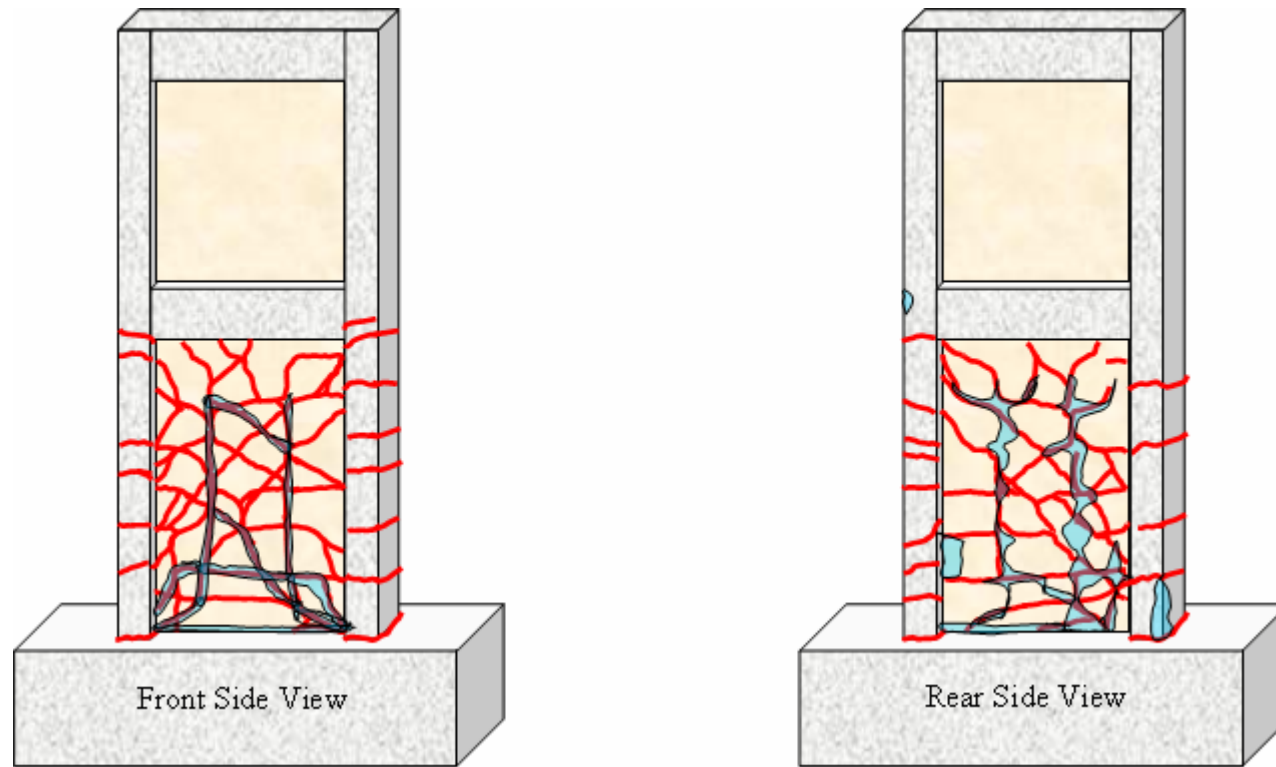
Figure 5.32. Front and Rear Side Crack Profiles of Specimen **NRC**

5.3. Standard Series Specimens

5.3.1. Specimen SB

Specimen **SB** was the bare frame with no infill. The test was performed to obtain experimental data for verification of the analytical modeling studies of infilled / strengthened frames of standard series. In addition, the bond-slip effect was also analytically investigated on the basis bare frame test results.

Specimen **SB** was subjected to lateral loading history presented in **Figure 5.33**, on which the numbers in parenthesis represent the corresponding second storey level top displacement in mm. Maximum forward and backward loads were measured to be **13.6 kN** and **13.4 kN**, respectively. Hysteretic total lateral load – displacement curves of second and first storey are presented in **Figure 5.34** and **Figure 5.35**.
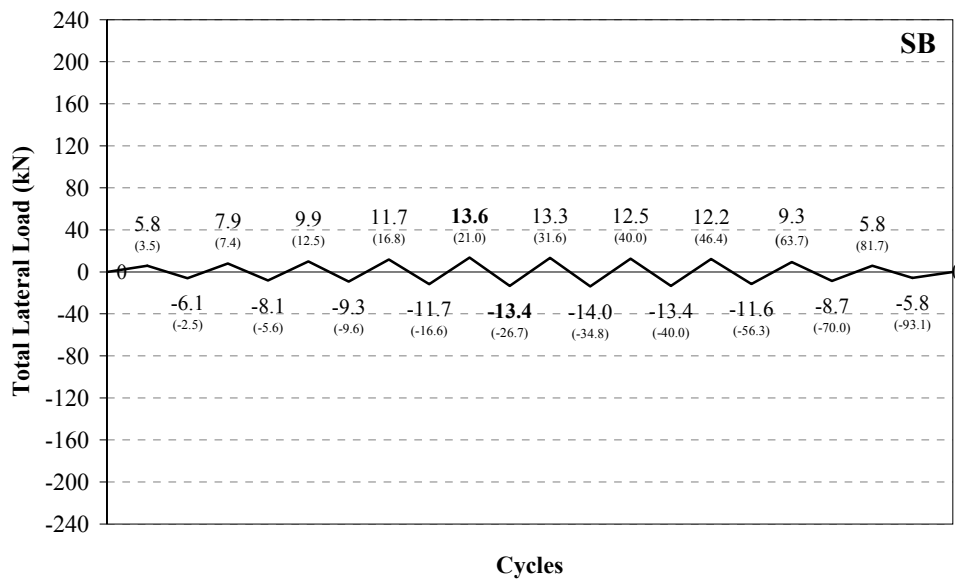
Figure 5.33. Loading History of Specimen **SB**

The initial stiffness of the specimen was calculated to be **1.2 kN/mm**; as one of the major conclusions drawn from the lateral load-displacement curves. The initial stiffness of the specimen was defined as the initial slope of the lateral load-second storey level

displacement curve in the first forward half cycle. At the instant of forward maximum loading, the interstorey drift ratios for the first and second stories were **0.0130** and **0.0115**, respectively whereas these values were **0.0173** and **0.0138** at the instant of backward maximum loading, respectively.
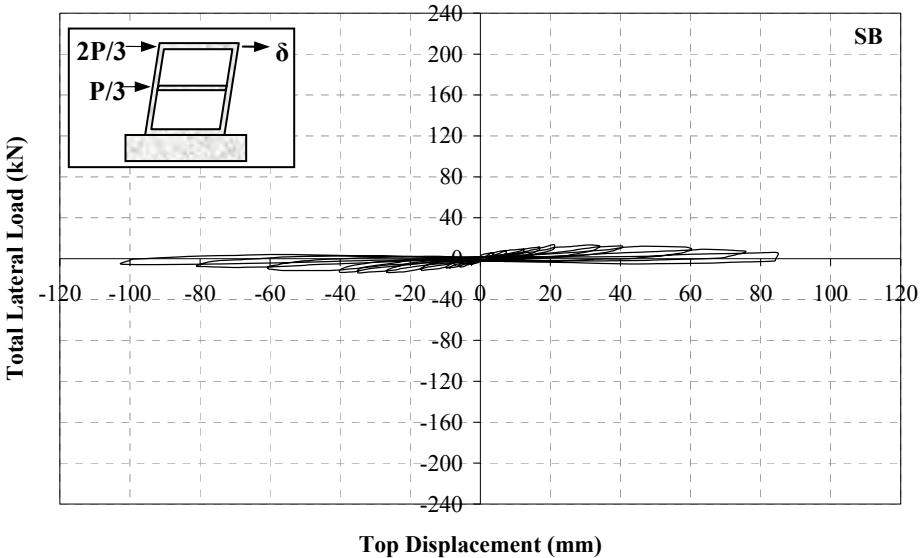
Figure 5.34. Total Lateral Load – Second Storey Level Displacement Curve, Specimen **SB**
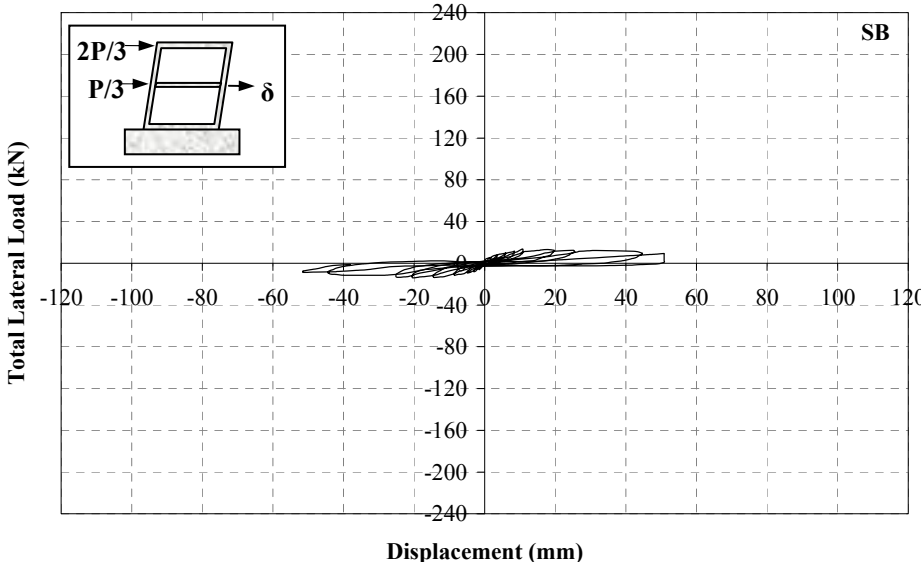
Figure 5.35. Total Lateral Load – First Storey Level Displacement Curve, Specimen **SB**

119

The major test observations of specimen **SB** are summarised below:

- In the first forward and backward half cycles, specimen **SB** was laterally loaded to +5.8 kN and -6.1 kN, respectively. In the first forward half cycle, a crack was observed at the base and another one at ~100 mm above the base level of north column. A crack that surrounded the beam perimeter on the first storey beam – south column joint appeared in the first backward half cycle.

- In the second forward half cycle, a new crack around the beam perimeter on the first storey beam – north column joint occured and the previous symmetrical crack propagated to the front side of the frame. A new hairline crack at the south column ~100 mm above the base occured and beam cracks around the perimeter formed a closed - continuous shape.

- In the third forward half cycle, existings cracks on north column base propagated through the front side. A new vertical crack occured on the front side of second storey beam – north column joint together with a flexural crack on first storey beam – north column joint. Symmetrical crack occured on the second storey beam – south column joint in the third half backward half cycle together with a new crack at ~100 mm above the south column base.

- In the fourth forward half cycle, existing crack witdhs increased and cracks propagated. Moreover, a new flexural crack just below the second storey beam - north column joint was observed. A new crack at ~50 mm above the south column base appeared together width widening of exisng cracks around in the fourth backward loading. Quiet symmetrical cracks also appeared on the second storey beam – south column joint as well. Besides, a new flexural crack on the span of the beam, ~200 mm from the first storey beam north column joint, also occured in this load reversal.

- Specimen **SB** reached its forward and backward lateral load capacities in the fifth loading cycle by **13.6 kN** and **13.4 kN,** respectively. In the fifth forward half cycle, two new cracks occured over the first storey beam span, approximately ~250 mm and ~500 mm away from the south column – first storey beam joint. In the fifth backward half cycle, a new crack ~80 mm above

the south column base apperared. A new crack at the north column-first storey beam joint surface and ~100 mm below the joint occured.

- The experiment was conducted in displacement controlled fashion starting from the sixth cycle. In the sixth forward half cycle new joint cracks on south column which are symmetrical with the ones that occured in fifth backward half cycle on the north column generated. Moreover, a vertical crack on north column – first storey beam joint also occured. In the sixth backward half cycle, a new crack on the north column base occured, another vertical crack on the south column – first storey beam joint also appeared. Existing cracks widened in this reversal.

- The test was no longer controlled by lateral displacement of second storey in the seventh cycle. Frame was loaded to 40.04 mm in both forward and backward directions. Existing cracks widened, no new crack was observed.

- In the eighth forward half cycle, the dial gauge that measured deflection of north column seperated from the frame and was out of recording no longer. Concrete crushings in both ends of first storey columns was visible. In the eigth backward half cycle, concrete crushings on the first storey column ends continued.

- In the ninth forward half cycle cover concrete of first storey beam – south column joint seperated from the frame and the reinforcement became visible. In the ninth backward half cycle, exitsting cracks widened and crushings increased.

- The test was finalized in the tenth load reversal by reaching 81.7 mm and 93.0 mm top displacements of second storey in both forward and backward half cycles, respectively.

Views of specimen **SB,** before and after the experiment, are presented in **Figure 5.36**, and crack profiles of front and rear sides are presented in **Figure 5.37**.
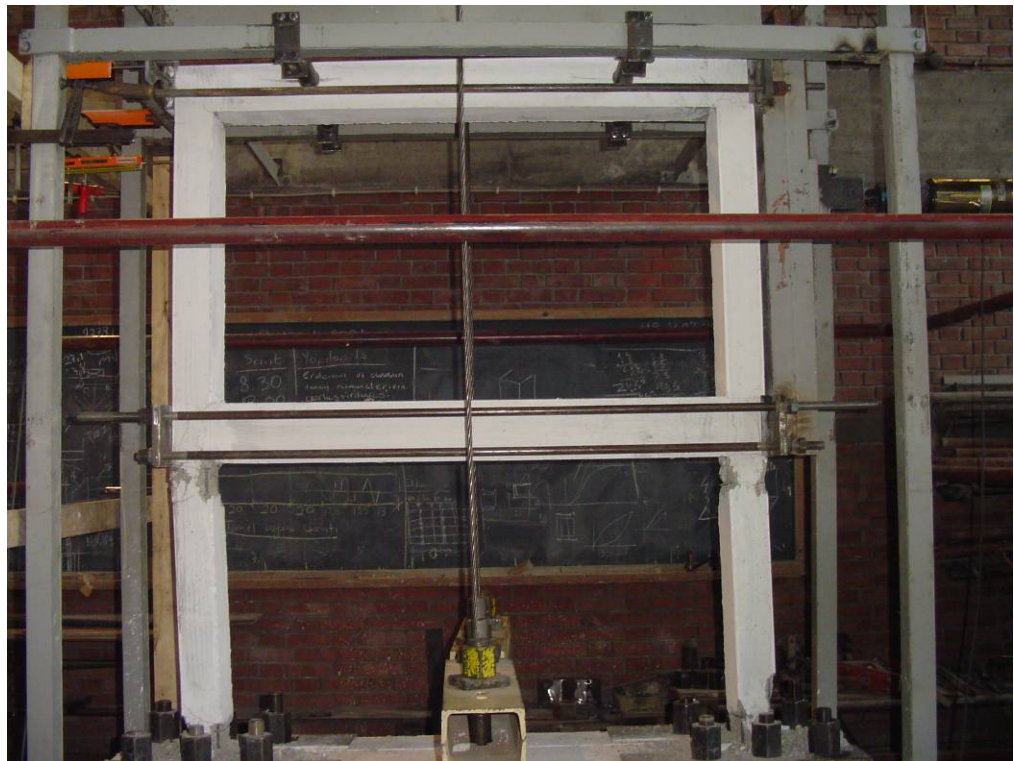
Figure 5.36. Before and After Test Views of Specimen **SB**

Front Side View

Rear Side View
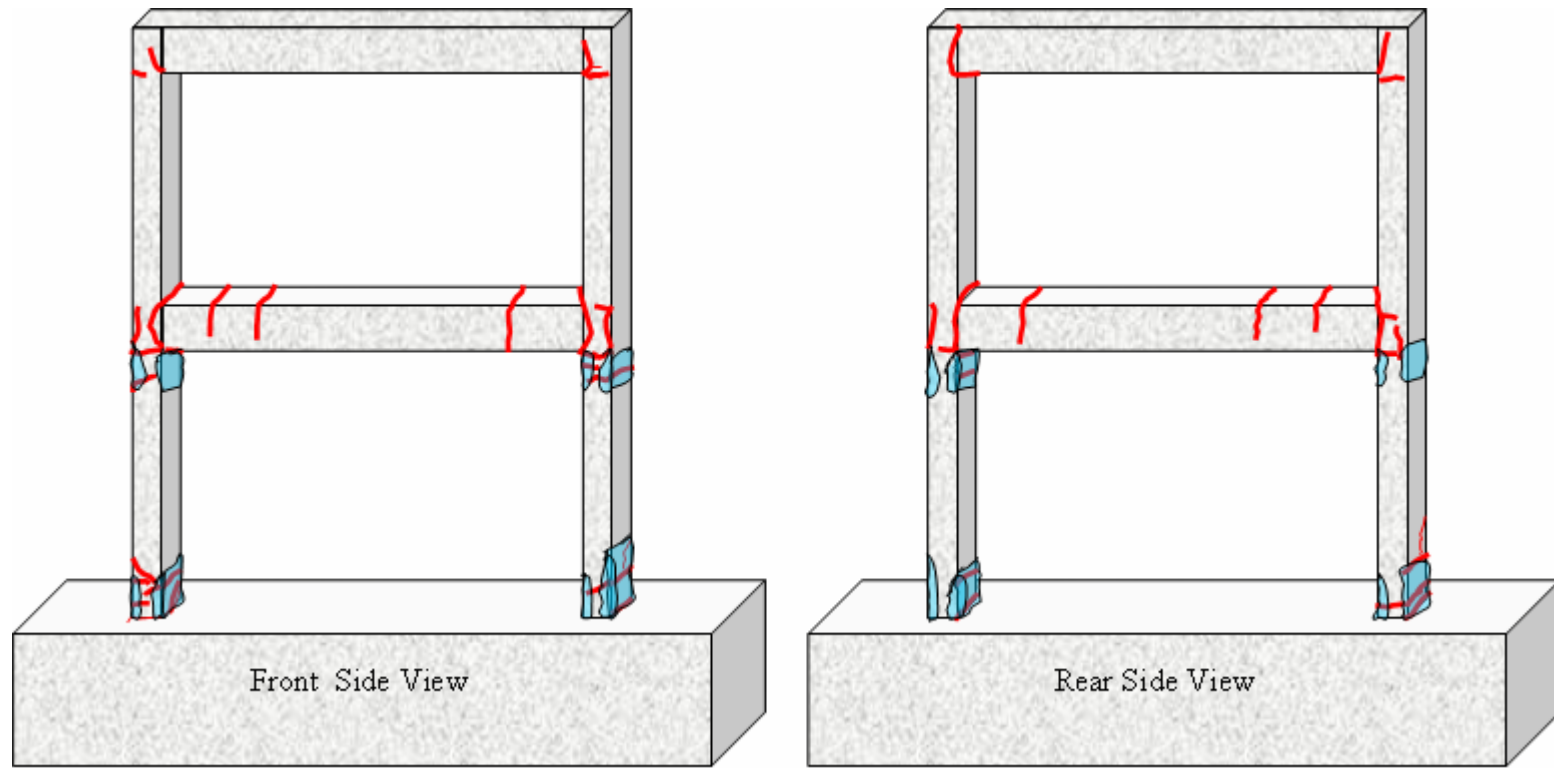
Figure 5.37. Front and Rear Side Crack Profiles of Specimen **SB**

5.3.2. Specimen SR

Specimen **SR** was lower bound the reference specimen of standard frame series which represents the present state of typical existing building. It was infilled by hollow clay bricks plastered on both sides. The test results of this specimen would serve as a lower bound reference for the behaviour and capacity improvement of the standard RC frame specimens strengthened by PC panels.

Specimen **SR** was subjected to lateral loading history presented in **Figure 5.38,** on which the numbers in parenthesis represent the corresponding second storey level top displacement in mm. Maximum forward and backward loads were measured to be **78.3 kN** and **75.5 kN**, respectively. Hysteretic lateral load – displacement curves of second and first storey are presented in **Figure 5.39** and **Figure 5.40**. Total lateral load-shear displacement curve of first storey infill panel presented is presented in **Figure 5.41.**
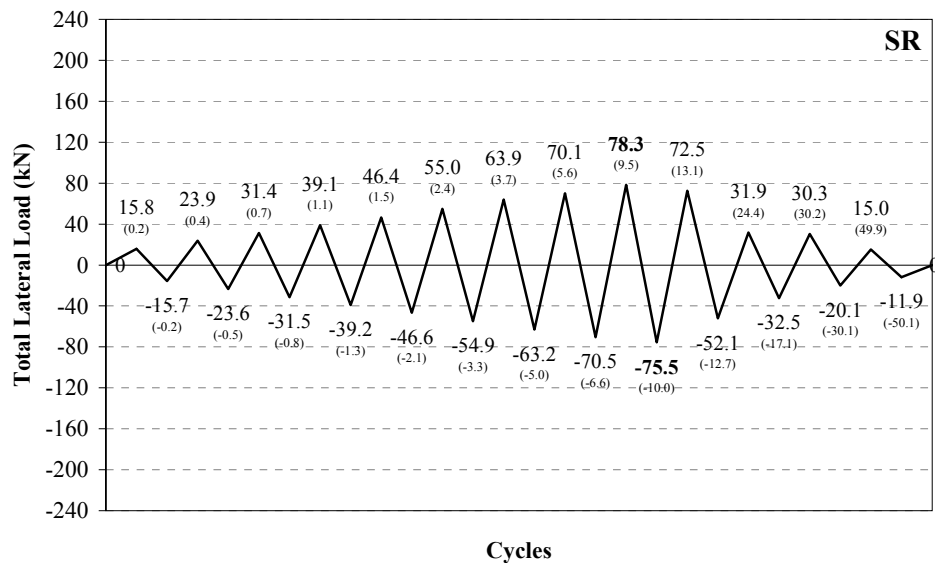
Figure 5.38. Loading History of Specimen **SR**

The initial stiffness of the specimen was calculated to be **57.5 kN/mm**; as one of the major conclusions drawn from the lateral load-displacement curves**.** The initial stiffness of the specimen was defined as the initial slope of the lateral load-second storey level

displacement curve in the first forward half cycle. At the instant of forward maximum loading, the interstorey drift ratios for the first and second stories were **0.0076** and **0.0035**, respectively whereas these values were **0.0056** and **0.0059** at the instant of backward maximum loading, respectively.
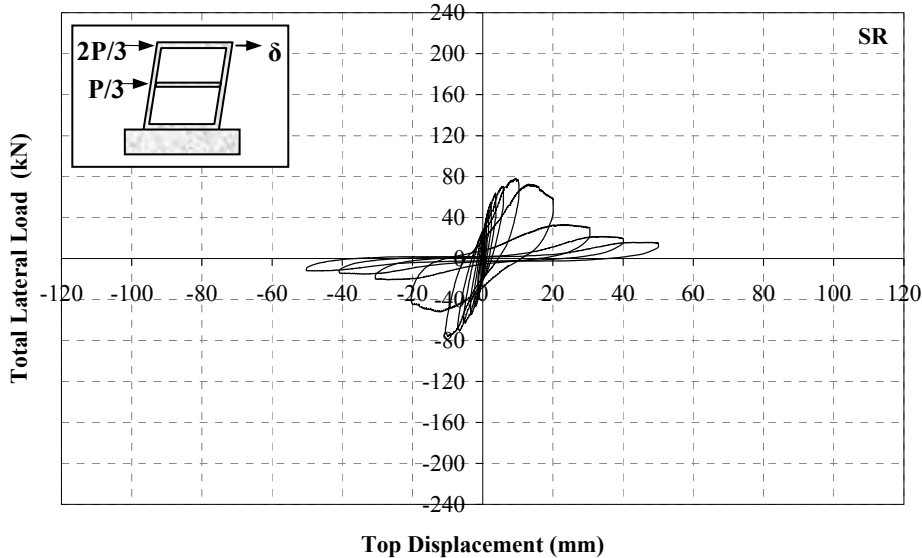
Figure 5. 39. Total Lateral Load – Second Storey Level Displacement Curve, Specimen **SR**
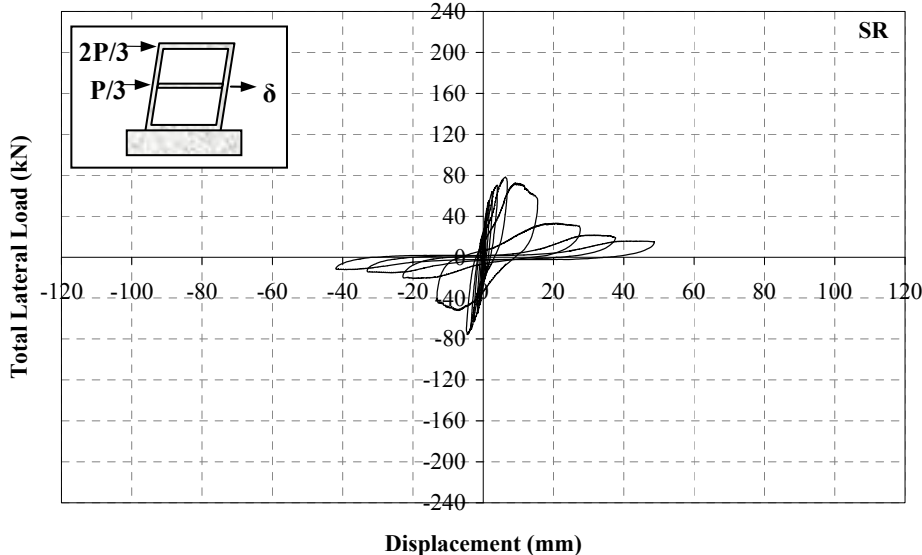
Figure 5.40. Total Lateral Load – First Storey Level Displacement Curve, Specimen **SR**
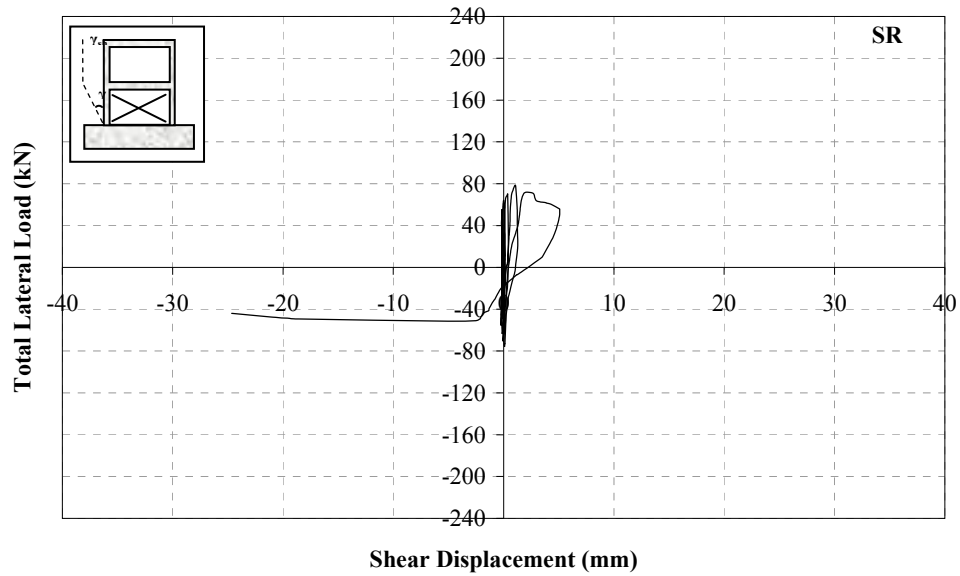
Figure 5.41. Total Lateral Load – First Storey Infill Shear Displacement Curve, Specimen **SR**

The major test observations of specimen **SR** are summarised as follows:

- In the first forward and backward half cycles, specimen **SR** was laterally loaded to 15.8 kN and 15.7 kN, respectively. In the first forward half cycle, a hairline flexural crack occured on the north column, ~150 mm above the base. The vertical plaster cracks occured on the rear side on both first and second storey north column zones, the symmetrical of which were also occured on the south column zone in the first backward half cycle. In addition, a flexural crack appeared on the south column, ~200 mm above the base level at the end of first backward half cycle.

- In the second forward half cycle, the previous flexural crack on north column propagated through the front side and the plaster cracks around the north column zone propagated in downward direction in both storeys. In the second backward half cycle, no new cracks occured on the column. However, new diagonal plaster crack occured on the rear side above the first storey beam-south column joint.

- In the third forward half cycle, the seperation of first storey infill from the north column was observed, approximately from the base to the mid-height of the column, ~350 mm – 400 mm. In the third backward half cycle, no new column crack was observed other than the new vertical plaster crack on the second storey south column-infill connection zone.

- In the fourth forward half cycle, the flexural cracks on the north column propagated through the front side and the existing plaster cracks on the rear side propagated together with addition of new hairline ones. In the fourth backward half cycle, the plaster cracks on the rear side of first storey widened and new ones occured especially concentrating on the south column base zone.

- In the fifth forward half cycle, a diagonal shear crack occured on the first storey beam-north column joint, and new plaster cracks occured on the rear side just below the first storey beam-north column joint and the symmetrical of these plaster cracks occured in the fifth backward half cycle below the first storey beam-south column joint, as well. In addition, a new flexural crack just around the mid-height of the south column occured in the fifth backward half cycle.

- In the sixth forward half cycle, a long diagonal shear crack occured on the first storey infill, together with relatively shorter ones. A flexural crack occured on the north column base and existing plaster cracks on the rear side widened. In the sixth backward half cycle, the seperation of first storey infill from the south column was started from the base and continued up to the mid-height of the column with a vertical crack. On the rear side, a new plaster crack occured above the south column base and the others appeared over the infill plaster surface.

- In the seventh forward half cycle, another big diagonal shear crack occured on the first storey infill and this crack was also oberved on the rear side plaster. In addition, another diagonal plaster crack aroused on the second storey, below the second storey beam-north column joint. In the seventh backward half cycle, the symmetical diagonal shear crack occured on the first storey infill which was also visible on the rear side. Besides, the flexural crack occured on the south column in the fifth backward half cycle, propagated through the rear side.

- In the eighth forward half cycle, new diagonal plaster cracks occured on the first storey infill being visible in both front and rear sides. Furthermore, new

diagonal plaster cracks also appeared on the first storey infill on the rear side. The existing plaster cracks of first storey widened and a new diagonal plaster crack also occured on the rear side, below the second storey beam-north column joint. In the eighth backward half cycle, the existing plaster cracks widened and new ones appeared on both sides. In addition, a diagonal shear crack occured on the first storey beam-south column joint the flexural crack occured in the first backward half cycle propagated and widened through the front side.

- In the ninth load reversal, the specimen reached its lateral loading capacity by 78.34 kN and 75.53 kN in forward and backward loading directions, respectively. The test was no longer carried out in displacement controlled fashion. In the ninth forward half cycle, a group of new diagonal shear cracks occured on the second storey infill surface as illustrated in **Figure 5.43.** The existing shear crack on first storey beam-north column joint widened up to ~2-3 mm. A long diagonal shear crack occured on the second storey infill plaster on the rear side. In addition, a diagonal shear crack occured on the second storey beam-south column joint as also illustrated in **Figure 5.43**. In the ninth backward half cycle, another shear crack occured on the first storey beam-south column joint and a number of new diagonal shear cracks appeared on the infill surface of both front and rear sides.

- In the tenth forward half cycle, the existing shear crack on the first storey beam-north column joint widened up to ~4 mm and the width of the some of first storey infill diagonal cracks increased up to ~10 mm. In the tenth backward half cycle, the plaster on both front and rear side started to spill and the bricks under the spilled plaster zones crushed. Both of the dial gages measuring the first storey infill shear deformations were out of record since the plaster of the dial gage placements.

- Three more displacement controlled loading cycles were applied and the test was terminated at the end of thirteenth cycle. A sudden decrease in lateral load was observed in the eleventh load reversal, while the infill panel of the first storey highly damaged. In twelfth and thirteenth cycles, the plaster on the rear side spilled out as illustrated in Figure 5.62. Relatively, Slight concrete crushing on both column bases occured together with the ones over the first storey beam-column joint shear cracks.

Views of specimen **SR**, before and after the experiment, are presented in **Figure 5.42** and crack profiles of front and rear sides are presented in **Figure 5.43.**

Figure 5.42. Before and After Test Views of Specimen **SR**

Front Side View

Rear Side View
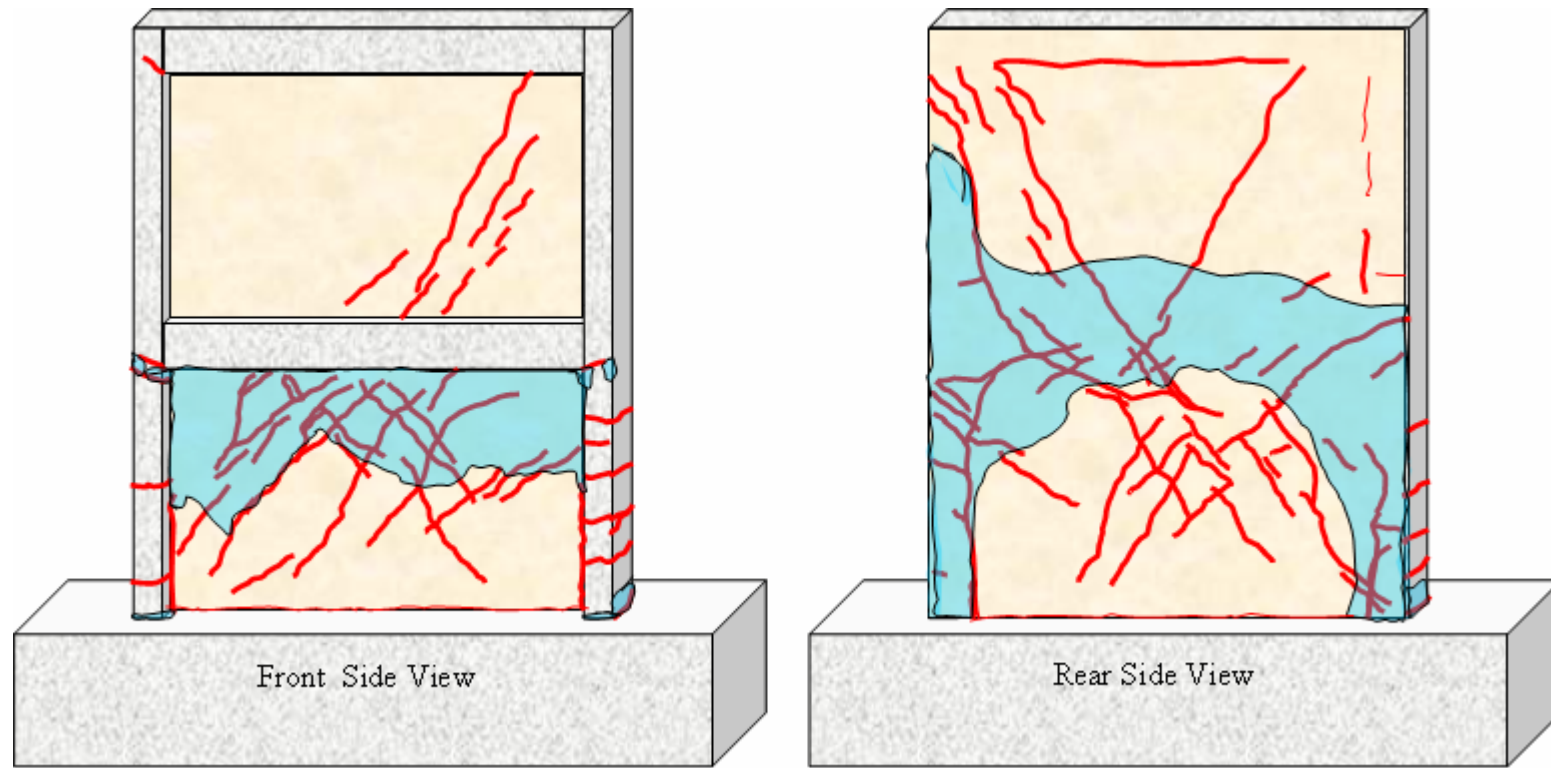
Figure 5.43. Front and Rear Side Crack Profiles of Specimen **SR**

5.3.3. Specimen SRP

Specimen **SRP** was the frame strengthened by rectangular shaped PC panels. The test results of this specimen were used to investigate the efficiency of PC panel method on seismic performance improvement. The test results were basically compared with the upper bound reference specimen **SRC** and and then lower bound specimen **SR**.

Specimen **SRP** was subjected to lateral loading history presented in **Figure 5.44,** on which the numbers in parenthesis represent the corresponding second storey level top displacement in mm. Maximum forward and backward loads were measured to be **187.5 kN** and **177.4 kN**, respectively. Hysteretic lateral load – displacement curves of second and first storey are presented in **Figure 5.45** and **Figure 5.46.** Total lateral load-shear displacement curve of first storey infill panel is presented in **Figure 5.47**
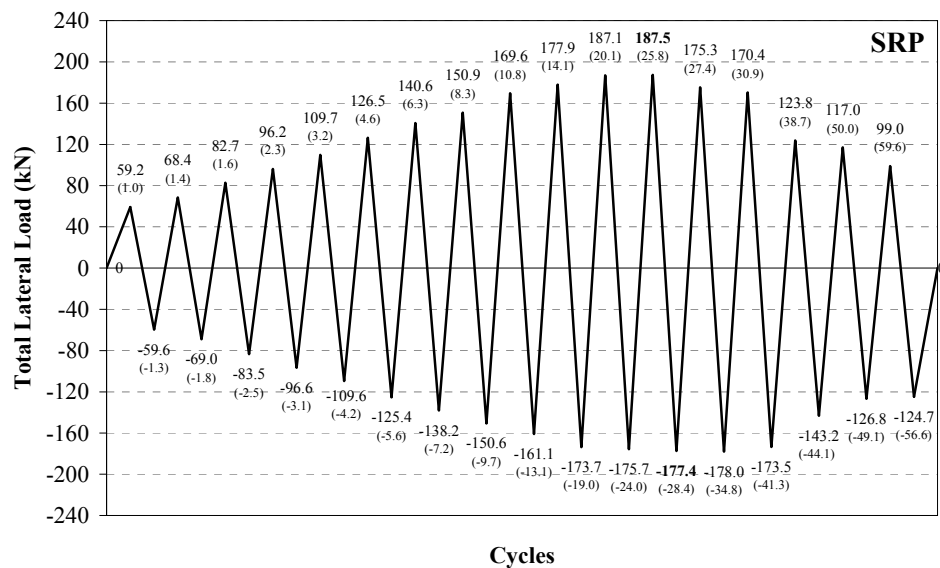
Figure 5.44. Loading History of Specimen **SRP**

The initial stiffness of the specimen was calculated to be **128.9 kN/mm**; as one of the major conclusions drawn from the lateral load-displacement curves**.** The initial stiffness of the specimen was defined as the initial slope of the lateral load-second storey level displacement curve in the first forward half cycle. At the instant of forward maximum

loading, the interstorey drift ratios for the first and second stories were **0.0151** and **0.0149**, respectively whereas these values were **0.0164** and **0.0165** at the instant of backward maximum loading, respectively.
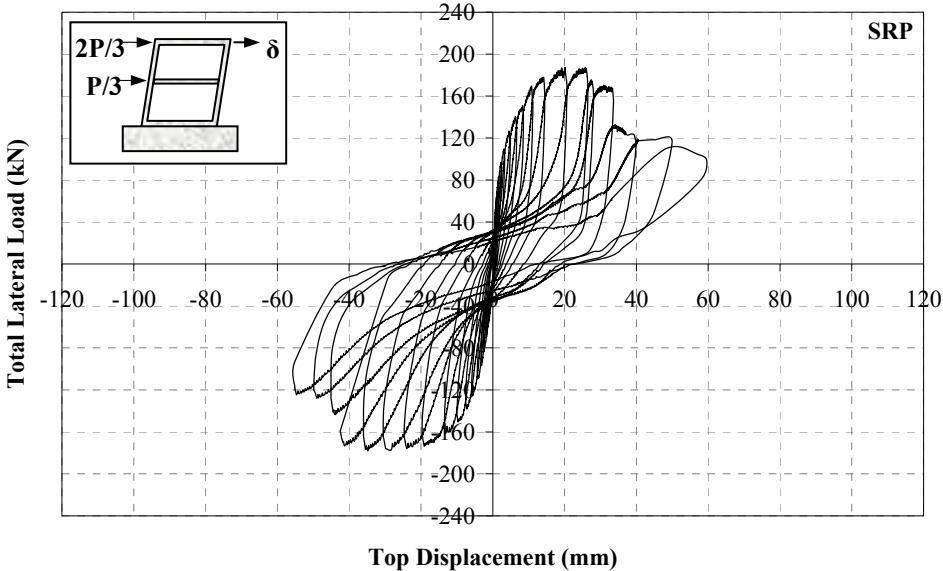
Figure 5.45. Total Lateral Load – Second Storey Level Displacement Curve, Specimen **SRP**
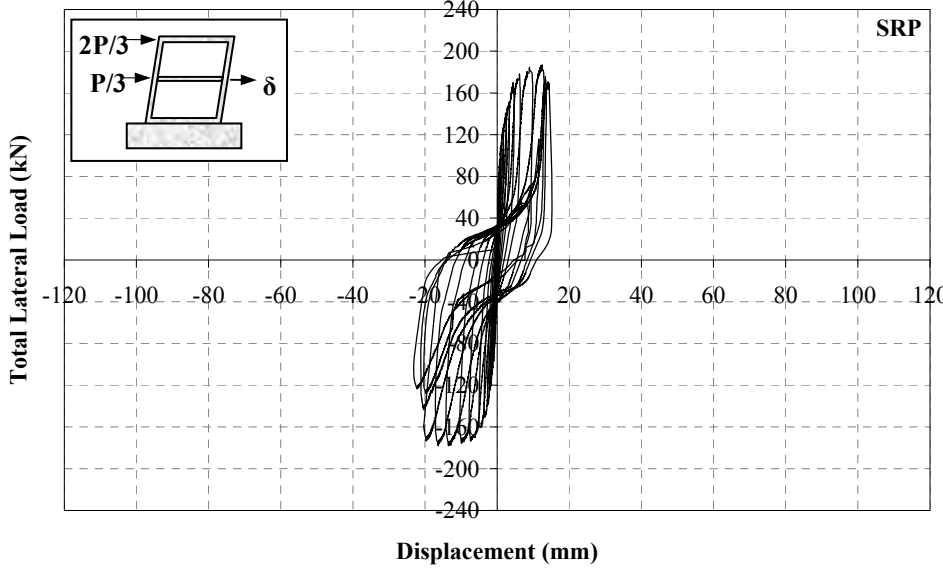
Figure 5.46. Total Lateral Load – First Storey Level Displacement Curve, Specimen **SRP**
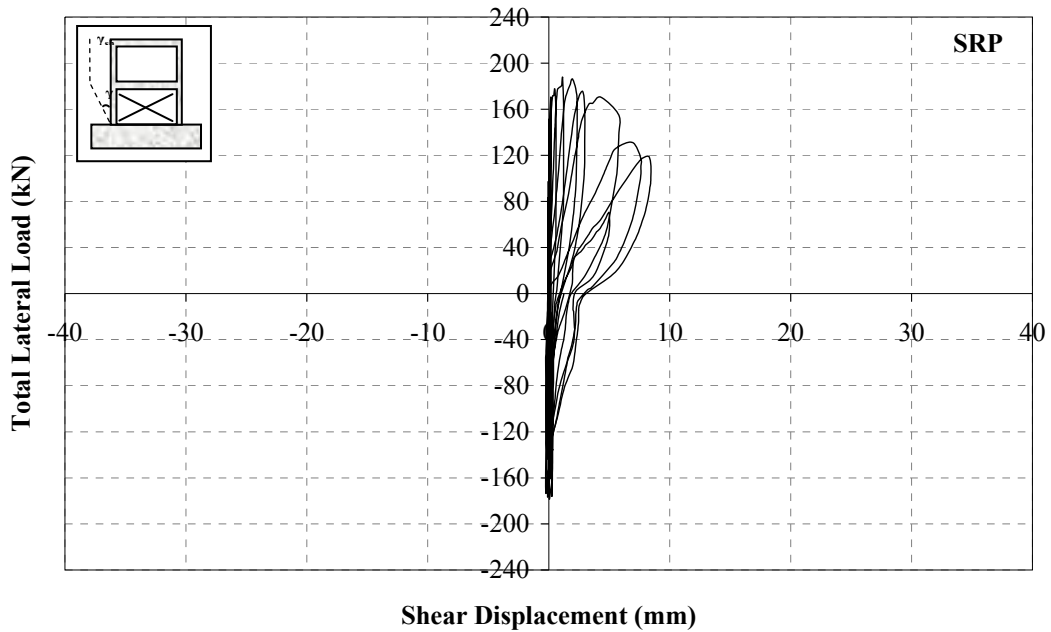
Figure 5.47. Total Lateral Load – First Storey Infill Shear Displacement Curve, Specimen **SRP**

The major test observations of specimen **SRP** are summarised as follows:

- In the first forward and backward half cycles, specimen **SRP** was laterally loaded to 59.2 kN and 59.6 kN, respectively. Hairline cracks were detected on both north and south column bases at the beginning of the test. No other cracks were observed in the first forward half cycle, while a new flexural crack occured on the south column base, in the first backward half cycle.

- In the second forward half cycle, a flexural crack occured on the north column, ~200 mm away from the base and two plaster cracks observed on the rear side around the north column base. In the second backward half cycle, two flexural cracks occured on the south column, just below the mid-height.

- In the third forward half cycle, a flexural crack occured on the north column, just below the first storey beam-north column joint. In the third backward half cycle, a flexural crack occured on the first storey south column, being very closer to the first storey beam-south column joint.

133

- In the fourth forward half cycle, another flexural crack occured on the first storey north column which was very closer to the one occured in the second forward half cycle. In addition, a new plaster crack occured on the rear side just over the north column. In the fourth backward half cycle, the flexural crack around the mid-height of the first storey south column propagated through the infill. A plaster crack aroused on the rear side being closer to the south column base. Moreover, seperation of infill from north column-foundation joint through the mid-span of the foundation was observed.

- In the fifth forward half cycle, a flexural crack occured on the north column base. Seperation of first storey infill from the north column surface was observed by a crack occurance from the north column base through the mid-height of the column. In the fifth backward half cycle, a new flexural column crack occured on the south column, ~150 mm above the base. The symmetrical infill seperation from the south column was observed. On the rear side, the seperation of infill from the foundation was observed by a crack aligning from south column base to the mid-span of the foundation. Moreover, plaster cracks above the south column mid-height level and along the first storey infill-south column connection zone were observed.

- In the sixth forward half cycle, the existing infill seperation from the foundation propagated and was quiet visible from the front side. A new flexural column crack occured just above the mid-height of the north column and new plaster cracks aroused around the north column base. In the sixth backward half cycle, a diagonal shear crack occured on the first storey beam-south column joint and a new flexural crack occured on the south column, above the mid-height. New plaster cracks appeared on the rear side and the seperation of first storey infill from the foundation was also started from the south column base side through the mid-span of the foundation.

- In the seventh forward half cycle, two new cracks occured on the first storey beam-north column joint as illustrated in **Figure 5.50**. The existing crack on the north column base and the vertical crack on of first storey infill-north column connection widened. New diagonal plaster cracks occured on the rear side over the first storey infill surface, one being on the second storey beam-south column joint region. In the seventh backward half cycle, another shear crack

occured on the first storey beam-south column joint. The existing south column crack, just above the base, propagated through the rear side. New plaster cracks occured on the first storey infill surface on the rear side and the seperation of infill from the foundation widened. In addition, on both column-foundation corners, new panel cracks occured symmetrically, lying over the anchorage dowel locations.

- In the eighth forward half cycle, ~2-3 mm openeing was observed on the north column base. Another flexural crack occured on the north column, ~20 mm above the base. A number of new diagonal cracks occured on the rear side over the first storey infill surface. In the eighth backward half cycle, existing plaster cracks widened and the plaster over the north column base started to crush. The seperation of infill from the foundation reached almost ~2-3 mm width.

- In the ninth forward half cycle, a hairline diagonal panel crack was observed on the front side. Existing plaster cracks widened and some new ones also aroused on the rear side. The panel concrete on the north column-foundation corner started to crush. In the ninth backward half cycle, the panel concrete on the south column-foundation corner started to crush. On the rear side, the plaster around the cracks started to spill out. Moreover, the concrete around the both column bases also started to crush and spill out.

- In the tenth forward half cycle, a diagonal shear crack occured on the second storey beam-north column joint. The existing north column crack, the one above the mid-height, propagated through the rear side. A number of new plaster cracks occured on the rear side first storey infill surface. In the tenth backward half cycle, a new shear crack occured on the first storey beam-south column joint, just coinciding with the existing one. The seperation of first storey infill from the foundation became quiet visible.

- In the eleventh load reversal, the specimen reached its lateral loading capacity in forward and backward directions by **187.5 kN** and **177.4 kN**, respectively. In the eleventh forward half cycle, the second storey infill started to seperate from the north column, by a vertical crack over the infill-north column connection surface. Concrete over the south column base crushed; the reinforcement on the south column base buckled and existing plaster cracks on the rear side widened. The gage measuring the vertical south column base displacement was out of

135

recording. In the eleventh backward half cycle, the concrete on the north column base crushed and the reinforcement became visible. Existing plaster cracks widened.

- In the twelfth forward half cycle, new cracks on the second storey beam, being very closer the second storey beam-north column joint occurred. On the rear side, a new plaster crack occured on the same joint location of second storey. In the twelfth backward half cycle, the plaster over the north column surface spilled out and the reinforcement on the north column base buckled.

- Beyond the thirteenth cycle, the test was conducted in displacement controlled fashion. The test was terminated at the end of seventeenth cycle. The plaster on the rear side spilled out from the regions illustrated on **Figure 5.50**. The concrete on column bases crushed as well as the panel concrete on both column-foundation corners. The gage on the north column base measuring the vertical column base displacements was out of recording at the end of sixteenth cycle as also shown in **Figure 5.48**.

Figure 5.48. Views of Both Column Bases at the End of Sixteenth Load Reversal, Specimen **SRP**

Views of specimen **SRP**, before and after the experiment, are presented in **Figure 5.49** and crack profiles of front and rear sides are presented in **Figure 5.50.**

Figure 5.49. Before and After Test Views of Specimen **SRP**

Front Side View

Rear Side View
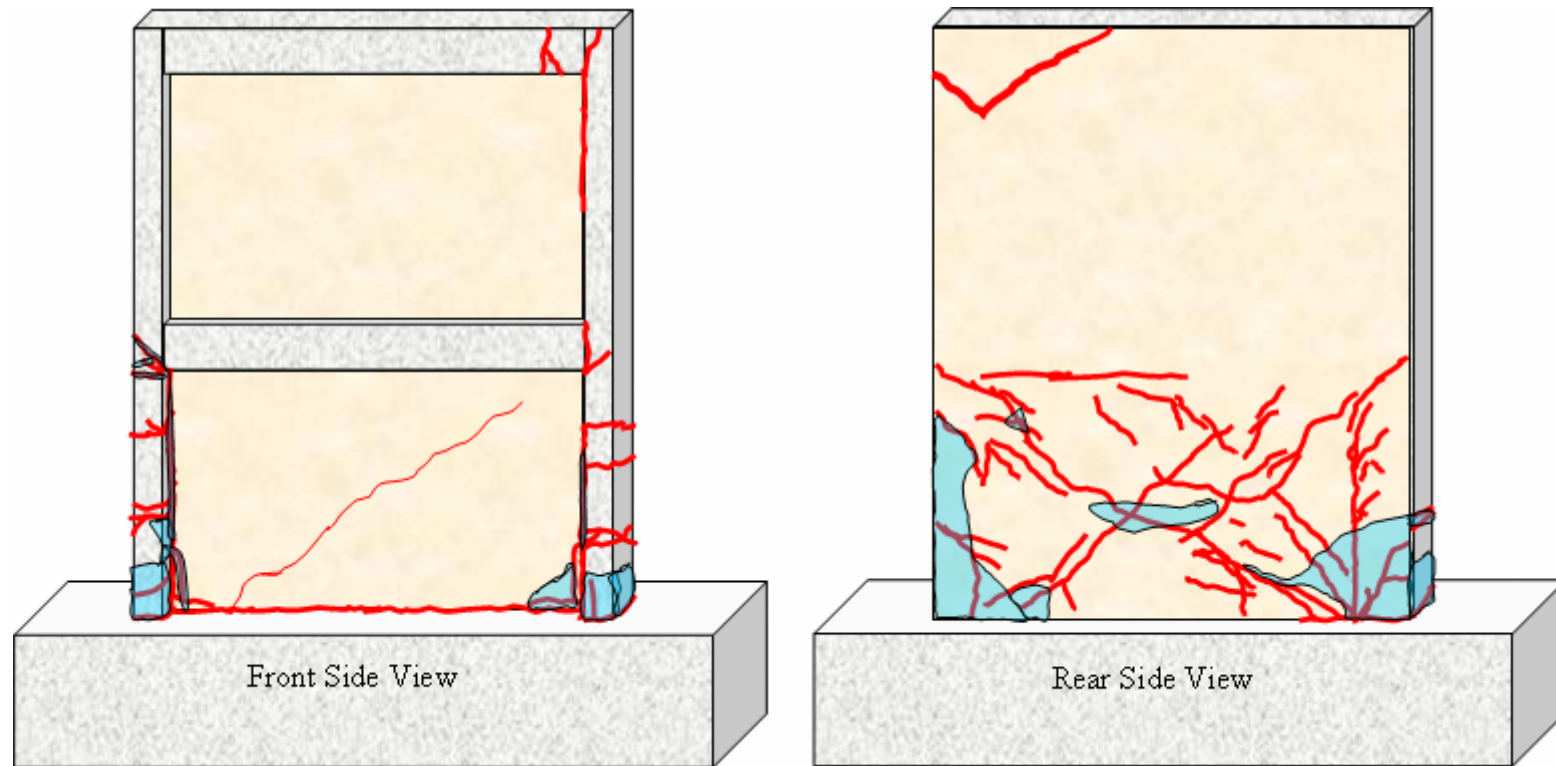
Figure 5.50. Front and Rear Side Crack Profiles of Specimen **SRP**

5.3.4. Specimen SSP

Specimen **SSP** was the frame strengthened by strip shaped PC panels. The test results of this specimen were used to investigate the efficiency of PC panel method on seismic performance improvement. The test results were basically compared with the upper bound reference specimen **SRC** and and then lower bound specimen **SR**. In addition, the performance improvement comparisons were also done for specimen **SRP**.

Specimen **SSP** was subjected to lateral loading history presented in **Figure 5.51,** on which the numbers in parenthesis represent the corresponding second storey level top displacement in mm.Maximum forward and backward loads were measured to be **172.0 kN** and **175.4 kN**, respectively. Hysteretic total lateral load – displacement curves of second and first storey are presented in **Figure 5.52** and **Figure 5.53**. Total lateral load-shear displacement curve of first storey infill panel is presented in **Figure 5.54**.
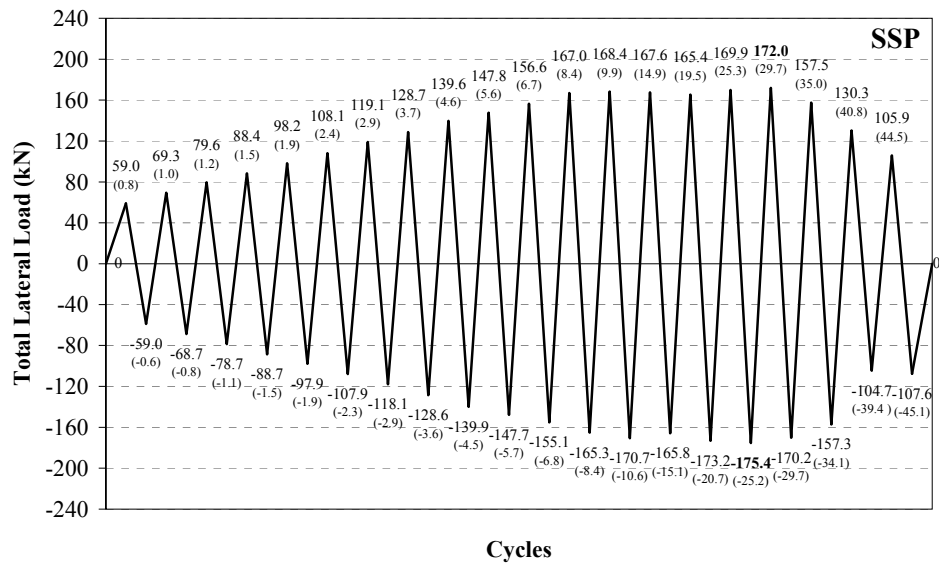
Figure 5.51. Loading History of Specimen **SSP**

The initial stiffness of the specimen was calculated to be **137.4 kN/mm** as one of the major conclusions drawn from the lateral load-displacement curves**.** The initial stiffness of the specimen was defined as the initial slope of the lateral load-second storey level

displacement curve in the first forward half cycle. At the instant of forward maximum loading, the interstorey drift ratios for the first and second stories were **0.0178** and **0.0167**, respectively whereas these values were **0.0148** and **0.0194** at the instant of backward maximum loading, respectively.
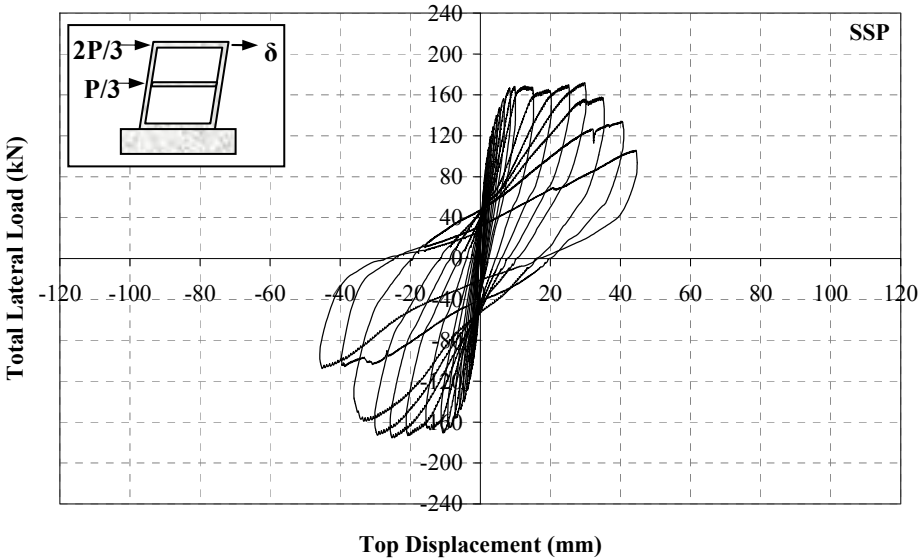
Figure 5.52. Total Lateral Load – Second Storey Level Displacement Curve, Specimen **SSP**
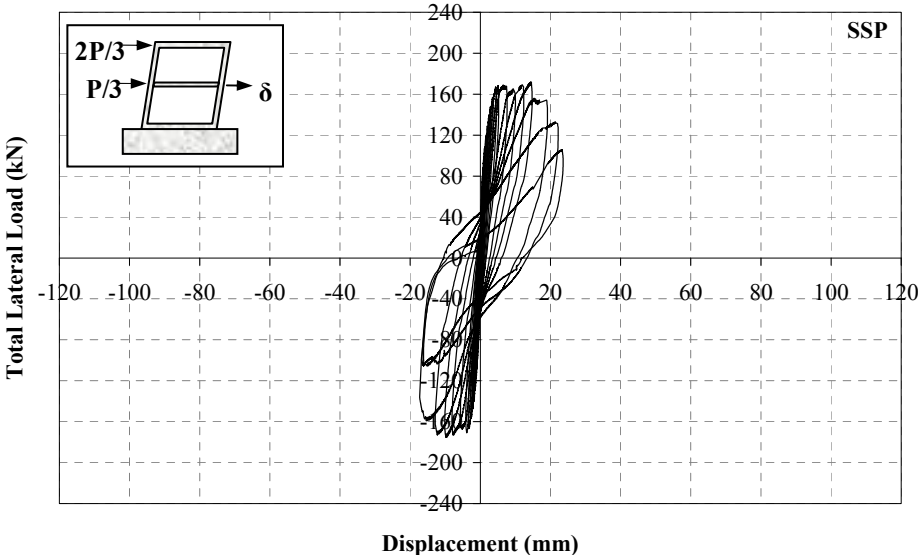
Figure 5.53. Total Lateral Load – First Storey Level Displacement Curve, Specimen **SSP**
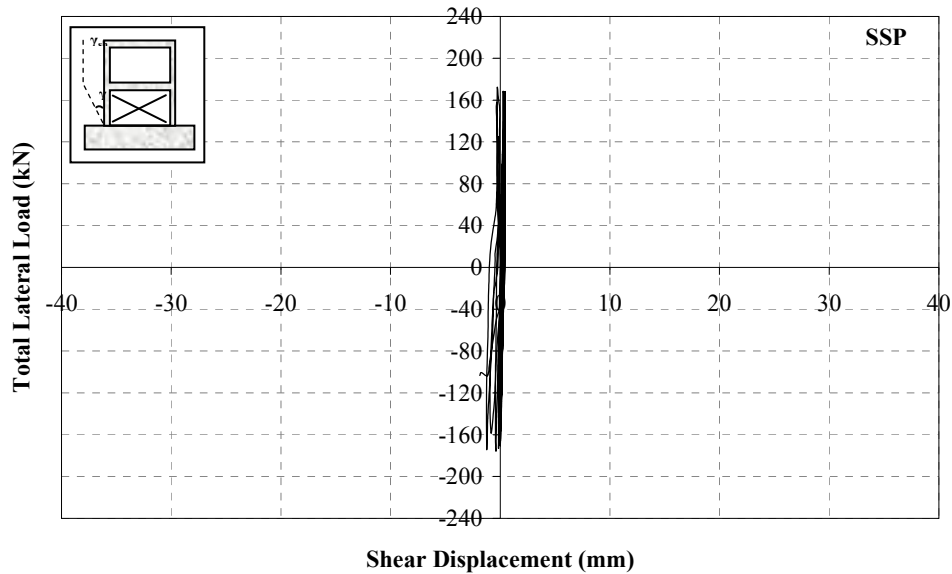
Figure 5.54. Total Lateral Load – First Storey Infill Shear Displacement Curve, Specimen **SSP**

The major test observations of specimen **SSP** are summarised below:

- In the first forward and backward half cycles, specimen **SSP** was laterally loaded to 59.0 kN and 59.0 kN, respectively. A hair line flexural crack was detected on south column, ~450 mm above the base, before the experiment. No cracks were observed at the end of first load reversal.

- In the second forward half cycle, no cracks occured on the specimen. In the second backward half cycle, the hairline flexural crack on the south column propagated through the front side. A diagonal shear crack occured on the first storey beam-south column joint. On the rear side, plaster crack occured approximately starting from the south column felxural crack level and aligning through the base over the infill-south column connection zone.

- In the third forward half cycle, two flexural cracks occured on the north column; one at the base and the other ~200 mm above the base. Hairline crack observed on the first storey infill-foundation connection line starting from the north column base. Plaster cracks occured on the rear side along the north column-first storey infill connection. In the third backward half cycle, the

141

symmetrical hairline crack on the first storey infill-foundation connection line starting from the south column base was detected. In addition, plaster crack around the south column base was also observed.

- In the fourth forward half cycle, the existing plaster crack on north column base widened and propagated through the front side. In the fourth backward half cycle, a flexural crack occured on south column, ~30-40 mm above the base and the rear side plaster cracks propagated.

- In the fifth forward half cycle, the existing cracks on north column and rear side plaster widened, no new one was detected. In the fifth backward half cycle, similarly the existng cracks widened and no new one was observed. However, the plaster on the rear side started to seperate over the first storey column zones.

- In the sixth forward half cycle, a flexural crack appeared on the north column, ~450 mm above the base. In the sixth backward half cycle, a new flexural crack occured on the south column front side, ~200 mm above the base.

- In the seventh forward half cycle, a diagonal shear crack occured on the first storey beam-north column joint and the flexural crack occured on the north column in the sixth forward half cycle propagated through the front side. In addition, a new flexural crack occured on the first storey north column, ~650 mm away from the base. The plaster cracks on the rear side around the first storey north column zone widened. In the seventh backward half cycle, a new plaster crack occured just below the first storey beam-south column joint and the existing plaster cracks widened.

- In the eighth forward half cycle, a new shear crack occured on the first storey beam-north column joint and existing flexure cracks on the north column widened. New plaster cracks occured on the second storey north column zone, above the mid-height. In the eighth backward half cycle, the shear crack on first storey beam-south column joint occured in second backward half cycle propagated and widened. In addition, the seperation of first storey infill from the south column surface and foundation became visible.

- In the ninth forward half cycle, the seperation of first storey infill from the north column surface was observed and the existing flexural cracks on north column propagated through the infill. On the rear side, the seperation of the plaster over the first storey north column from the frame increased. In the ninth

142

backward half cycle, a new shear crak occured on the first storey beam-south column joint. In addition a new flexural crack occured on the south column, ~650 mm above the base and the existing flexural cracks on the south column widened.

- In the tenth forward half cycle, the flexural crack on the north column base widened up to ~2 mm width and the seperation of first storey infill from the foundation increased. In the tenth backward half cycle, the existing flexural cracks on south column widened and the seperation of first storey infill from the south column surface increased.

- In the eleventh forward half cycle, a flexural crack occured on the second storey north column, ~150 mm above the first storey beam-north column joint. On the rear side, the plaster over the north column spilled out. In the eleventh backward half cycle, no new crack was observed, only the existing ones widened on both south column ans rear side plaster.

- In the twelfth forward half cycle, the north column flexural crack which appeared in the seventh forward half cycle propagated through the front side. On the rear side, the plaster spilled out from the first storey beam-north column joint and the shear crack became visible on the joint concrete surface. In addition, the plaster cracks on the rear side increased. In the twelfth backward half cycle, a hairline diagonal crack occured on the first storey infill surface which was also detectable on the rear side plaster. The plaster over the south column surface spilled out.

- In the thirteenth forward half cycle, a diagonal shear crack occured on the second storey beam-north column joint which further connected with the rear side plaster crack. In the thirteenth backward half cycle, panel cracks on the south column-foundation corner were realized over the anchorage dowel regions. All existing flexural and shear cracks widened.

- In the fourteenth cycle, the experiment was started to be carried out in displacement controlled fashion. The width of the flexural crack on the north column base reached up to ~5 mm and the other flexural cracks on north column widened. In the fourteenth backward half cycle, the existing shear cracks on first storey beam – south column joint widened and the seperation of infill from the first storey south column and foundation reached ~10 mm.

Moreover, more plaster pieces spilled out from the first storey south column top region.

- In the fifteenth forward half cycle, the concrete cover over the first storey beam-north column joint front side spilled out and the reinforcement became visible as shown in **Figure 5.55**. In the fifteenth backward half cycle, all flexural cracks over the first storey south column were visible on the rear side, since the plaster spilled out before.

Figure 5.55. Front and Rear Side Views of First Storey Beam-North Column Joint at the End of Fifteenth Cycle, Specimen **SSP**

- In the sixteenth load reversal, the seperation of first storey infill from the column and foundation surfaces increased up to ~20-30 cm width as shown in **Figure 5.56**.

Figure 5.56. Front and Rear Side Views of Infill Panel Separation after Sixteenth Cycle, Specimen **SSP**

- In the seventeenth load reversal, the specimen reached its lateral loading capacity on both forward and backward directions by **172.0 kN** and **175.4 kN**, respectively. In the seventeenth load reversal, the seperation of first storey infill from the column and foundation surfaces increasingly continued. In addition, the concrete on column bases crushed and on the rear side some plaster pieces further spilled out from the infill.

- In the eigthteenth load forward half cycle, the panel concrete locating on the north column-foundation corner crushed and the longitudinal reinforcement buckled on the south column base as shown in **Figure 5.57.** In the eigtheenth backward half cycle, and the reinforcement on the north column base was visible due to increased concrete crushing of this area.

Figure 5.57. Buckling of the Longitudinal Column Reinforcement on the South Column Base at the End of Eighteenth Cycle, Specimen **SSP**

- In the nineteenth load reversal, both of the gages measuring the vertical column base displacements were out of recording. Similarly the longitudinal reinforcement also buckled on the north column base and the brick crushed on the north column-foundation corner.

Views of specimen **SSP**, before and after the experiment, are presented in **Figure 5.58** and crack profiles of front and rear sides are presented in **Figure 5.59.**

Figure 5.58. Before and After Test Views of Specimen **SSP**

Front Side View

Rear Side View
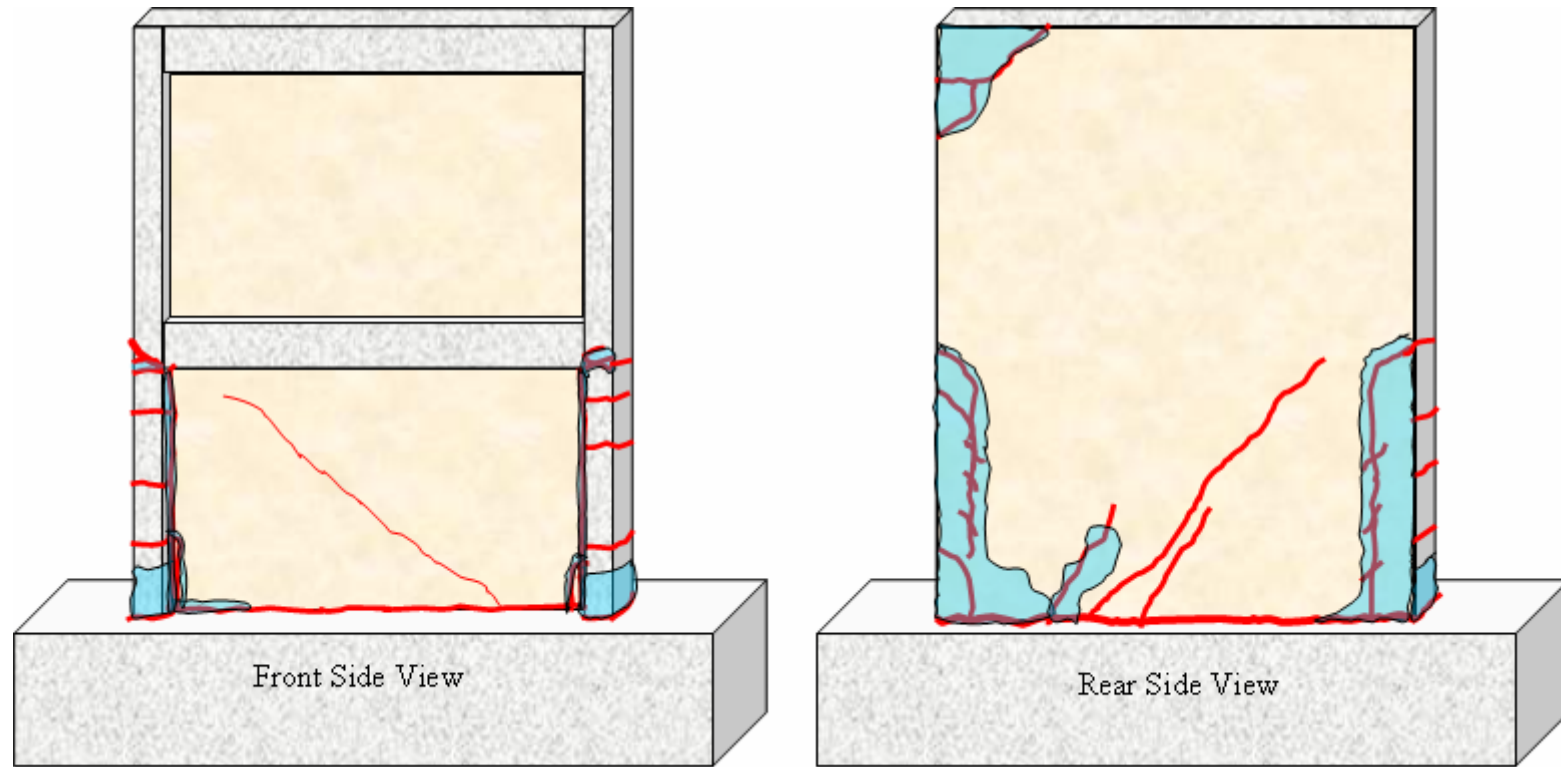
Figure 5.59. Front and Rear Side Crack Profiles of Specimen **SSP**

5.3.5. Specimen SRC

Specimen **SRC** was tested as the upper bound reference with cast-in-place RC infills for standard series specimens. The test results of this specimen were compared with the performance improvement in standard series of specimens by PC panel application for both strip and rectangular panels.

Specimen **SRC** was subjected to lateral loading history presented in **Figure 5.60**, on which the numbers in parenthesis represent the corresponding second storey level top displacement in mm. Maximum forward and backward loads were measured to be **189.7 kN** and **189.4 kN**, respectively. Hysteretic total lateral load – displacement curves of second and first storey are presented in **Figure 5.61** and **Figure 5.62**. Total lateral load - shear displacement curve of first storey infill panel is presented in **Figure 5.63**.
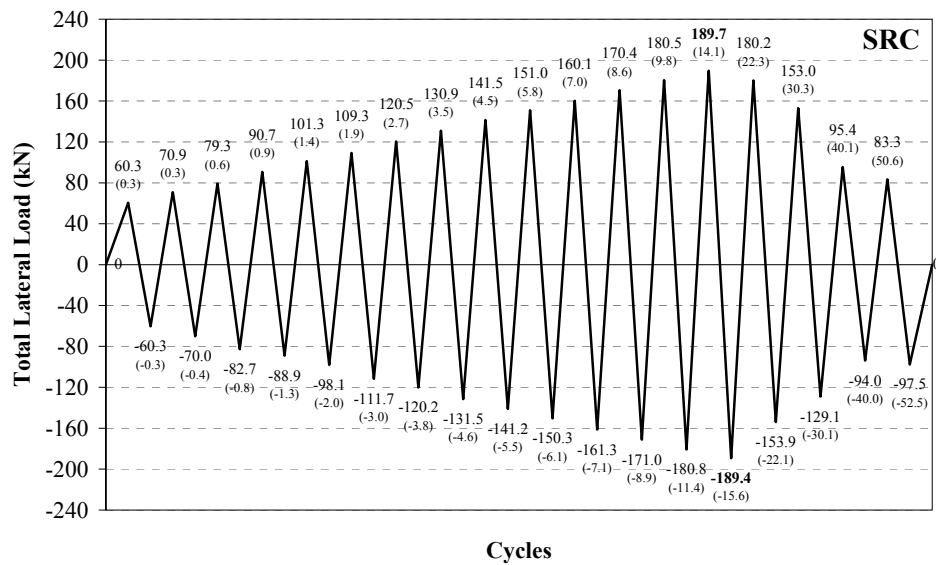
Figure 5.60. Loading History of Specimen **SRC**

The initial stiffness of the specimen was calculated to be **232.9 kN/mm**; as one of the major conclusions drawn from the lateral load-displacement curves**.** At the instant of forward maximum loading, the interstorey drift ratios for the first and second stories

148

were **0.0096** and **0.0068**, respectively whereas these values were **0.0087** and **0.0093** at the instant of backward maximum loading, respectively.
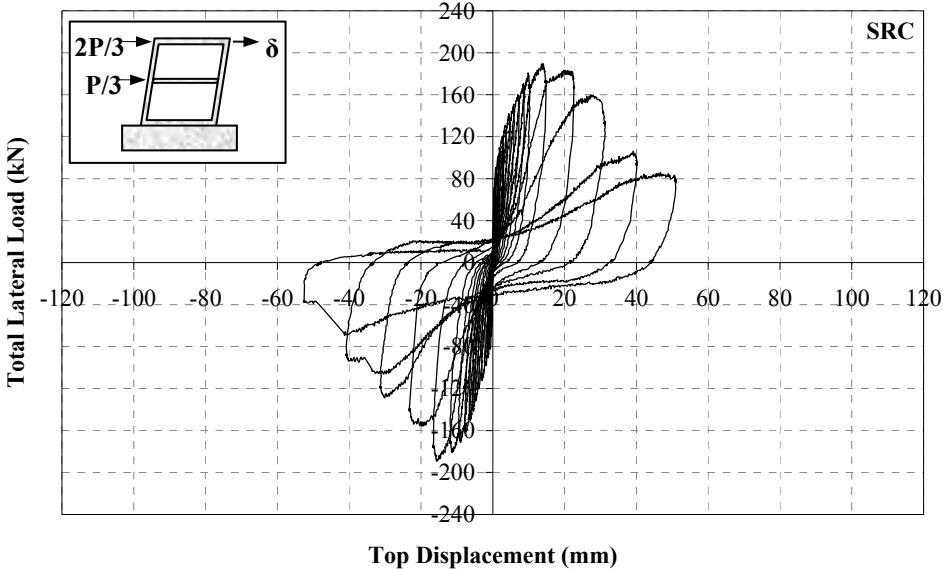
Figure 5.61. Total Lateral Load – Second Storey Level Displacement Curve, Specimen **SRC**
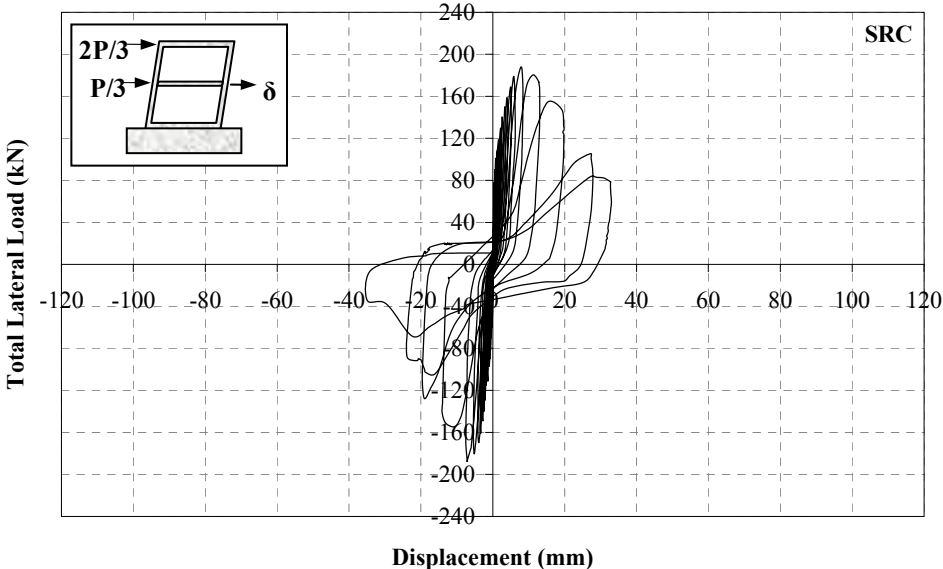
Figure 5.62. Total Lateral Load – First Storey Level Displacement Curve, Specimen **SRC**
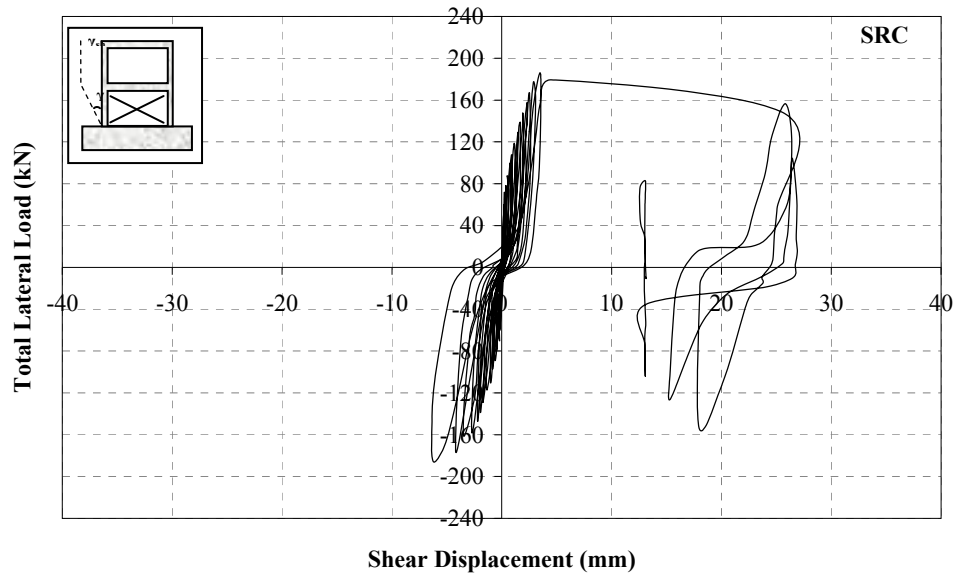
Figure 5.63. Total Lateral Load – First Storey Infill Shear Displacement Curve, Specimen **SRC**

The major test observations of specimen **SRC** are summarised below:

- In the first forward and backward half cycles, specimen **SRC** was laterally loaded to 60.3 kN and 60.3 kN, respectively. No cracks were observed in the first load reversal.

- Specimen experinced the first hairline crack on the first storey RC infill in the second backward half cycle being closer to first storey beam-north column joint. No cracks appeared in the second forward half cycle.

- In the third load reversal, hairline cracks on the steel mesh reinforcement locations of the RC infill started to be appearing in the first storey. In the third forward half cycle, a diagonal crack occured on the first storey RC infill just ~40 mm below the first storey beam and being started from the first storey beam-north column joint. In the third backward half cycle, a seperation crack of ~40 mm occured on the first storey beam – second storey south column corner.

- In the fourth forward half cycle, two cracks occured on the north column; one on the column base and the other being ~300 mm away from the basement. A seperation crack appeared on the first storey RC infill – foundation interface

150

approximately by the midlength of the RC infill starting from the north column base. Two symmetrical cracks occured on the south column in the fourth backward half cycle.

- In the fifth forward half cycle, existing crack on first storey north column propagated through the front side with the propagation of the seperation line in between first storey RC infill and the foundation. A seperation was observed in between first storey RC panel and north column interaction surface, along the midheight of the column. New diagonal cracks appeared on the first storey RC infill, together with a new crack on the corner of first storey beam – second storey north column. Diagonal cracks of the first storey RC infill increased in the fifth backward half cycle together with addition of two new bending cracks on the first storey south column

- The specimen experienced more new cracks, in the sixth forward half cycle, on the second storey RC panel as well as new cracks on the first storey RC panel. In the sixth backward half cycle, a new bending crack appeared on the first storey south column ~450 mm away from the basement together with addition of new cracks on RC panel of both storeys.

- In the seventh forward half cycle, a new crack arised on the second storey north column, and another one occured on the rear side of first storey beam-north column connection. A number of new diagonal cracks and cracks which follows the reinforcement path of the both storey RC infills occured. In the seventh backward half cycle, first storey north column damaged by new cracks. Existing cracks propagated throug the rear side. Similar panel cracks of the seventh forward half cycle were also realized.

- In the eighth forward half cycle, the first storey north column cracks being closer to the first storey beam-north column joint propagated through the rear side. New cracks on RC infill of the first storey occured in both forward and backward half cycle of the eighth load reversal.

- In the nineth forward half cycle, a new crack occured on the north column just below the first storey beam-north column joint. New panel cracks arised on the first storey RC infill. Besides, the seperation of the first storey RC infill from the foundation became more visible on the rear side. In the nineth backward half cycle, the existing crack on the south column base propagated through the

rear side, new cracks occured on the RC panel of both storeys. A diagonal beam crack occured on the rear side of the first storey beam, being closer to the north column joint.

- In the tenth load reversal, new cracks occured on the RC infills of both storeys. Besides, seperation of the RC infill from the first storey beam level was realized. In the tenth backward half cycle, two of the existing cracks on first storey south column propagated through the rear side

- In the eleventh forward half cycle, two new cracks occured on the rear side of the second storey north column. Existing column cracks being closer to the north column basement widened and propagated through the rear side of the frame. New RC infill panel cracks occured on both storeys. The seperation of first storey RC infill from the foundation became wider in the eleventh backward half cycle, together with additional RC infill cracks on the second storey.

- In the twelfth forward half cycle, new panel cracks occured on both storey RC infills. A new flexural crack occured on the second storey south column just ~100 mm above the first storey beam-north column joint. Some new panel cracks also appeared on the first storey RC infill.

- In the thirteenth forward half cycle, a new crack occured on approximately midheight of the second storey north column together with some new cracks on RC infills of both storeys. Slight concrete crushing of RC panel on the first storey beam-north column connection was observed. The cracks around the north column base propagated through the RC infill, on the front side. In the thirteenth backward half cycle, some new cracks occured on the first storey RC infill. Besides, on some crack locations slight crushing of the concrete was observed. Two new cracks on first storey beam, being closer to the north column joint occured on the rear side as illustrated in **Figure 5.66.**

- In the fourteenth load reversal, the specimen reached its lateral loading capacity by **189.7 kN** and **189.4 kN** in forward and backward half cycles, respectively. Cracks on both north and south column bases widened up to ~5 mm. Besides, slight crushing of the concrete around the crack lines located through middle area on the first storey RC infill was realized.

- The test was conducted by displacement control beyond fifteenth load reversal. In the fifteenth forward half cycle, RC infill was seperated from the foundation level and the crack on the north column base opened up to ~6 mm. Yielding of the longitudinal reinforcement of the north column was realized. Besides, the shear deformation measuring gage located closer to the first storey beam-north column joint on the first storey RC infill became out of recording. In the fifteenth backward half cycle, concrete crushing on north column base and RC infill corner of south column-foundation connection was observed.

- In the sixteenth load reversal, the crushing of the concrete on both column bases of the first storey and RC infill through the foundation connection was observed. The buckling of the longitudinal reinforcement on both north and south column was also observable. Besides, the dial gage measuring north column base vertical displacement became out of recording.

- In the seventeenth load reversal, the lateral load was approximately half of the lateral loading capacity in both forward and backward half cycles. Crushing and spalling of the concrete on column bases provided clear views of bar bucklings as also shown in **Figure 5.64**.

Figure 5.64. Buckling of the Longitudinal Reinforcement on Both North and South Column Bases at the End of Seventeenth Load Reversal, Specimen **SRC**

- The test was terminated at the end of the eighteenth load reversal considering stiffness degradation.

153

Views of specimen **SRC**, before and after the experiment, are presented in **Figure 5.65** and crack profiles of front and rear sides are presented in **Figure 5.66.**
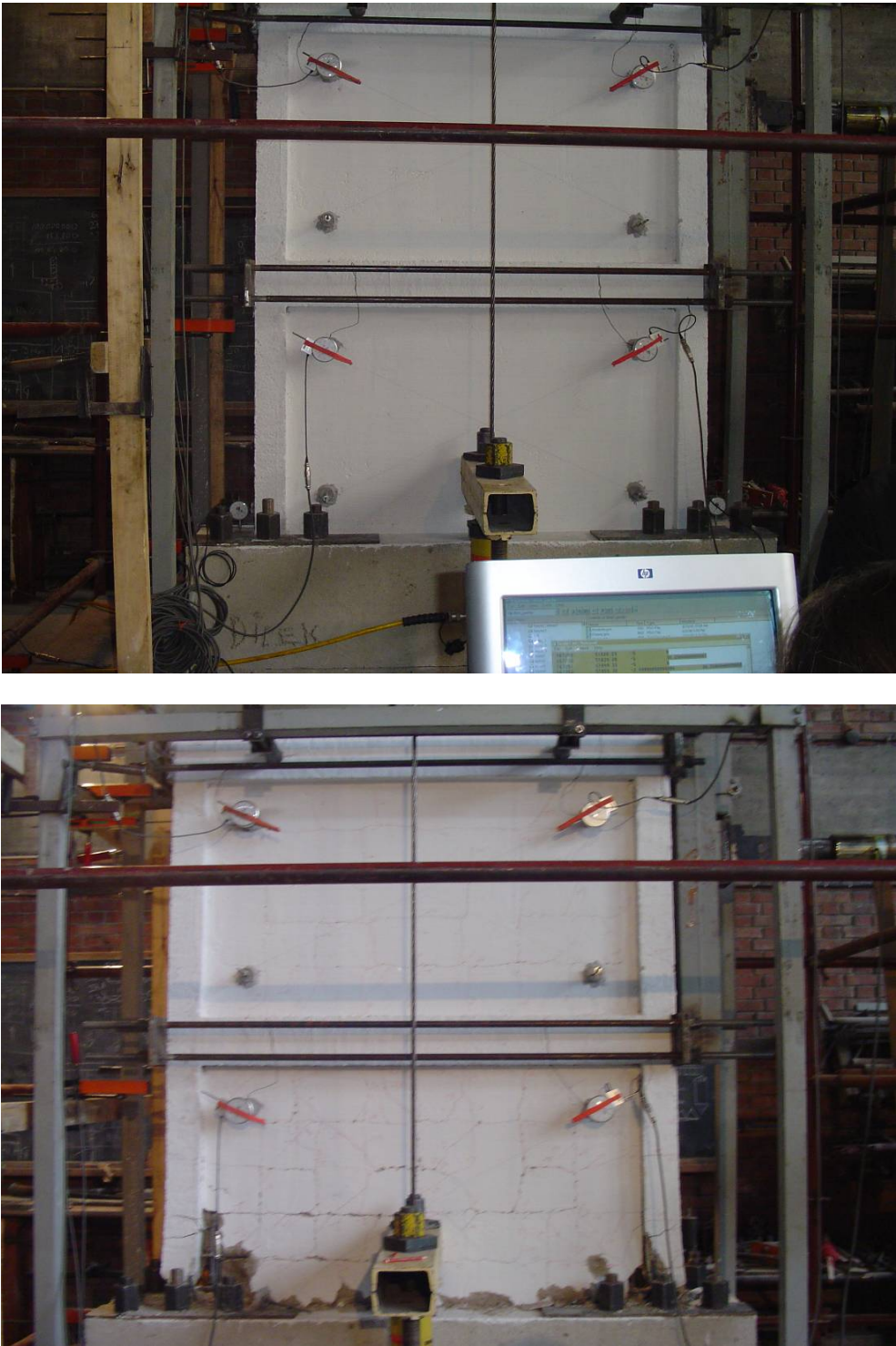
Figure 5.65. Before and After Test Views of Specimen **SRC**
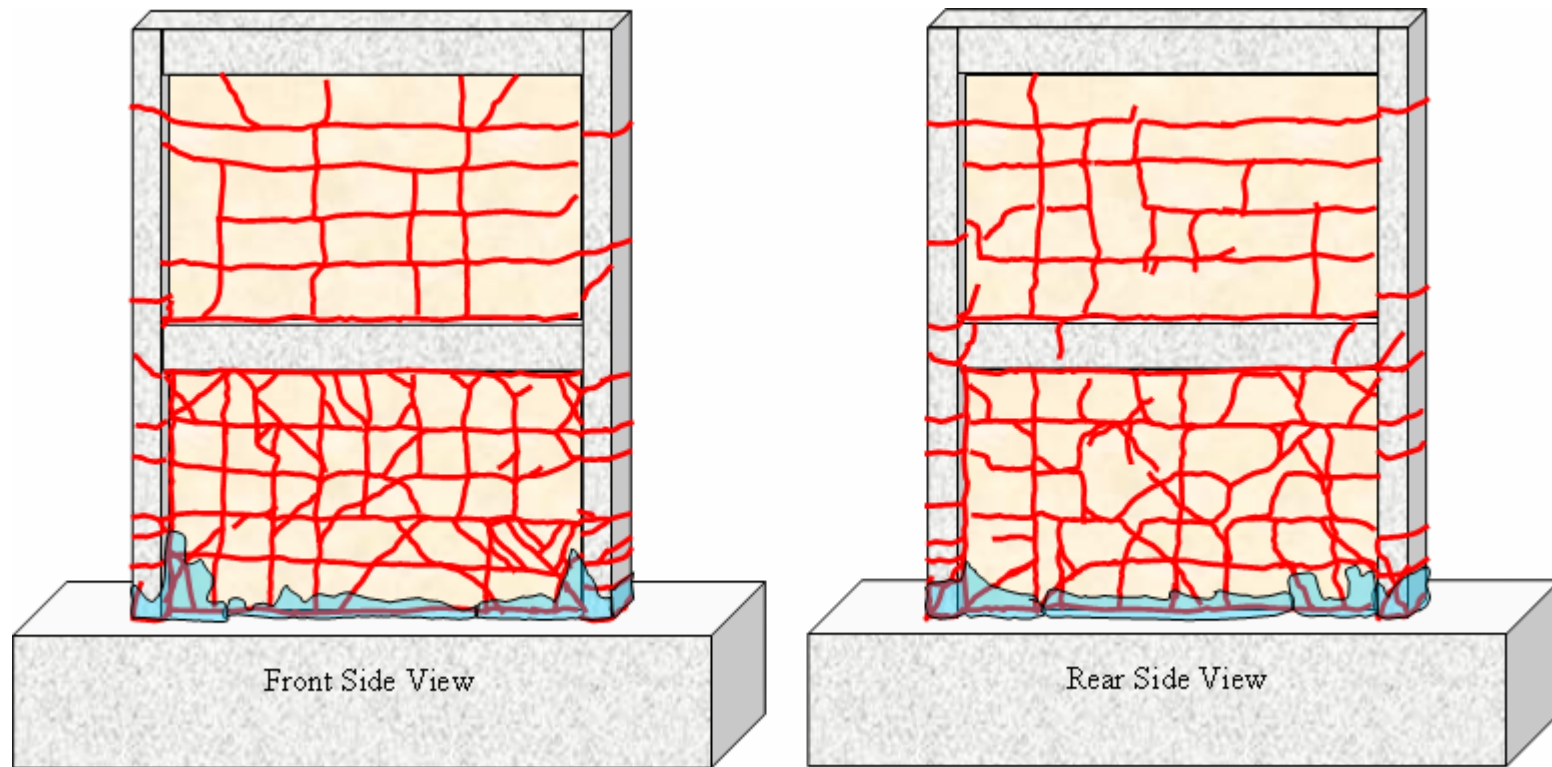
Figure 5.66. Front and Rear Side Crack Profiles of Specimen **SRC**

5.4. Wider Series Specimens

5.4.1. Specimen WB

Specimen **WB** is the bare frame of the narrower specimen series with no infill. The test was performed to obtain experimental data for verification of the analytical modeling studies of infilled/strengthened frames of wider series. In addition, the bond-slip effect was also analytically investigated on the basis of the bare frame test results.

Specimen **WB** was subjected to lateral loading history presented in **Figure 5.67,** on which the numbers in parenthesis represent the corresponding second storey level top displacement in mm. Maximum forward and backward loads were measured to be **15.4 kN** and **13.8 kN**, respectively. Hysteretic total lateral load − displacement curves of second and first storey are presented in **Figure 5.68** and **Figure 5.69**.
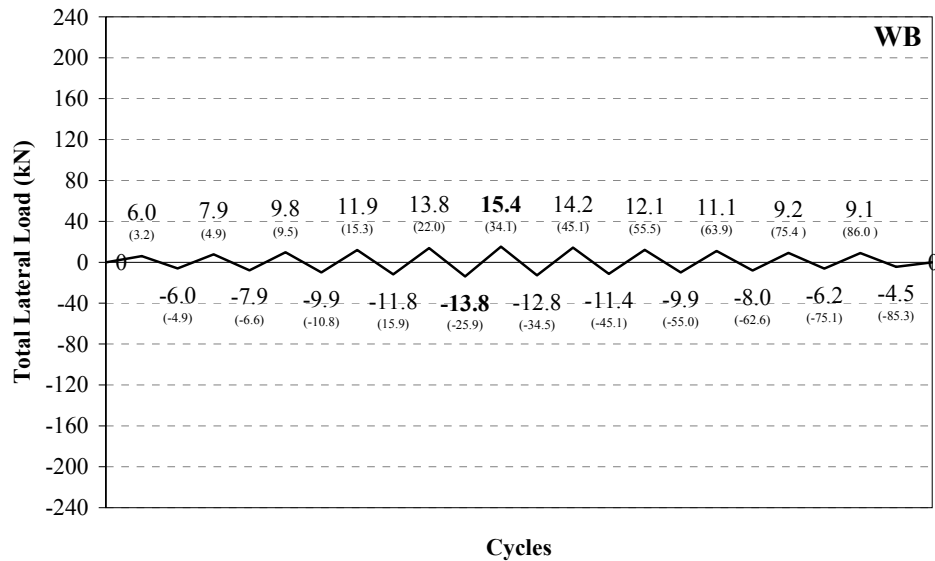
Figure 5.67. Loading History of Specimen **WB**

The initial stiffness of the specimen was calculated to be **1.4 kN/mm** as one of the major conclusions drawn from the lateral load-displacement curves**.** At the instant of forward maximum loading, the interstorey drift ratios for the first and second stories

156

were **0.0295** and **0.0109** respectively whereas these values were **0.0221** and **0.0085** at the instant of backward maximum loading, respectively.
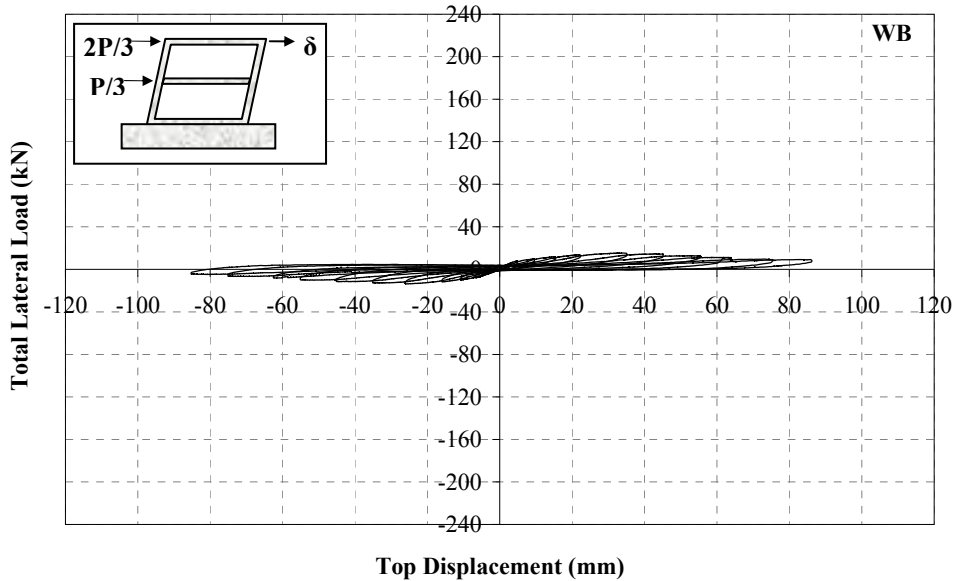
Figure 5.68. Total Lateral Load – Second Storey Level Displacement Curve, Specimen **WB**
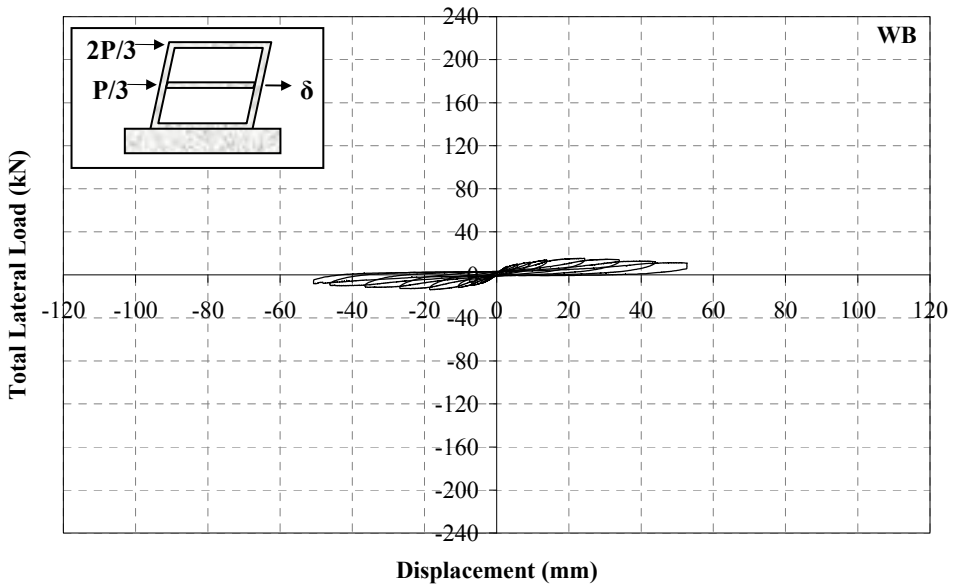
Figure 5.69. Total Lateral Load – First Storey Level Displacement Curve, Specimen **WB**

The major test observations of specimen **WB** are summarised below:

- In the first forward and backward half cycles, specimen **WB** was laterally loaded to +4.0 kN and -4.1 kN, respectively. A crack ~20 mm above the base occured on north column in the first forward half cycle together with another one which is ~100 mm below the first storey beam-north column joint. Moreover, a crack also occured on first storey beam – south column joint inner surface. In the first backward half cycle, a crack at the south column base appered, existing north column base crack spreaded to inner side. Besides, a digaonal shear crack occured on the first storey beam-north column joint.

- In the second forward half cycle, existing diagonal crack on the first storey beam-north column joint propagated from front to rear side through the inner surface of the joint. A new column crack ~150 mm away from the base occured on the inner surface of the north column, in the second backward half cycle. Another cracks appeared on the first storey beam-south column joint along the column perimeter.

- In the third forward half cycle, existing crack on south column base propagatet to rear side through the inner surface of the column. Existing crack on the first storey beam-north column joint propagated throuh the first storey north column with slight concrete crushing. Two new cracks appered on the inner surfaces both columns ~130 mm below the first storey beam-column joints. Existing cracks on first storey beam-south column joint propagated throug the rear side in the thir backward half cycle.

- In the fourth forward half cycle, the cracks on the first storey beam-north column joint widened and a new one apperaed on the front side along the beam perimeter. The crack existing at the north column base widened up to ~2 mm. Another crack arised at the second storey south column base on the inner surface. Slight crushing of the concrete was observed on the first storey beam-north column joint at the same line with the existing cracks and lateral load application point. In the fourth backward half cycle, a new flexural crack occured ~80 mm away from the north column base and propagated through the

rear side Besides, another crack arised on the front side of the first storey beam-south column joint through the beam perimeter.

- In the fifth forward half cycle, existing diagonal cracks on first storey beam-north column joint widened and the crack on the column base reached up to ~3 mm width. The existing crack on the first storey beam-south column joint propagated through the beam perimeter on the rear side. The south column crack above the base also propagated along the column perimeter. In the fifth backward half cycle, the existing cracks widened and slight concrete crushing on the north column joints was appeared and the specimen reached its lateral loading capacity in the backward direction by **13.8 kN.**

- In the sixth forward half cycle, the specimen reached the lateral loading capacity in the forward direction by **15.4 kN** and the test was started to be carried out by displacement control. A new column crack occured ~40 mm away from the north column base and the opening on the previous base crack became wider. In the sixth backward half cycle, concrete crushing on the inner sides of the first storey beam-south column and south column-foundation joints was observed. The crack on the north column base inner surface opened. Both of the column base vertical displacement measuring gages were out of recording at the end of sixth load reversal.

- In the seventh forward half cycle, concrete crushing on the south column base and inner side of the north column base was observed. The strirrup at the north column base was visible dur to spalling of the concrete in that region. Some new cracks arised on the first storey beam-north column joint rear side together with widening of the existing ones. Also, a new crack occured on the second storey north column just ~100 mm away from the base. The stirrup on the lower end of the south column was visible from the inner side. Besides the longitudinal reinforcement of both column bases were also visible from the inner side due spalling of the concrete.

- In the eighth and nineth load reversals, widening of the existing cracks were observed together with crushing and spalling of the concrete mainly on column bases and first storey beam-column joints. At the end of the nineth forward half cycle, the LVDT measuring the first storey displacement was out of recording since; its stroke reached the measuring limit.

- In the tenth forward half cycle, the stirrup on the north column base opened. Crushing and spalling of the concrete in the foundation and first storey joints continued. No considerable buckling of the column longitudinal reinforcement was observed for this specimen.

- The test was terminated at the end of eleventh load reversal so that the lateral stiffness was almost zero.

Views of specimen **WB**, before and after the experiment, are presented in **Figure 5.70** and crack profiles of front and rear sides are presented in **Figure 5.71.**

Figure 5.70. Views of Specimen **WB** During and After Test
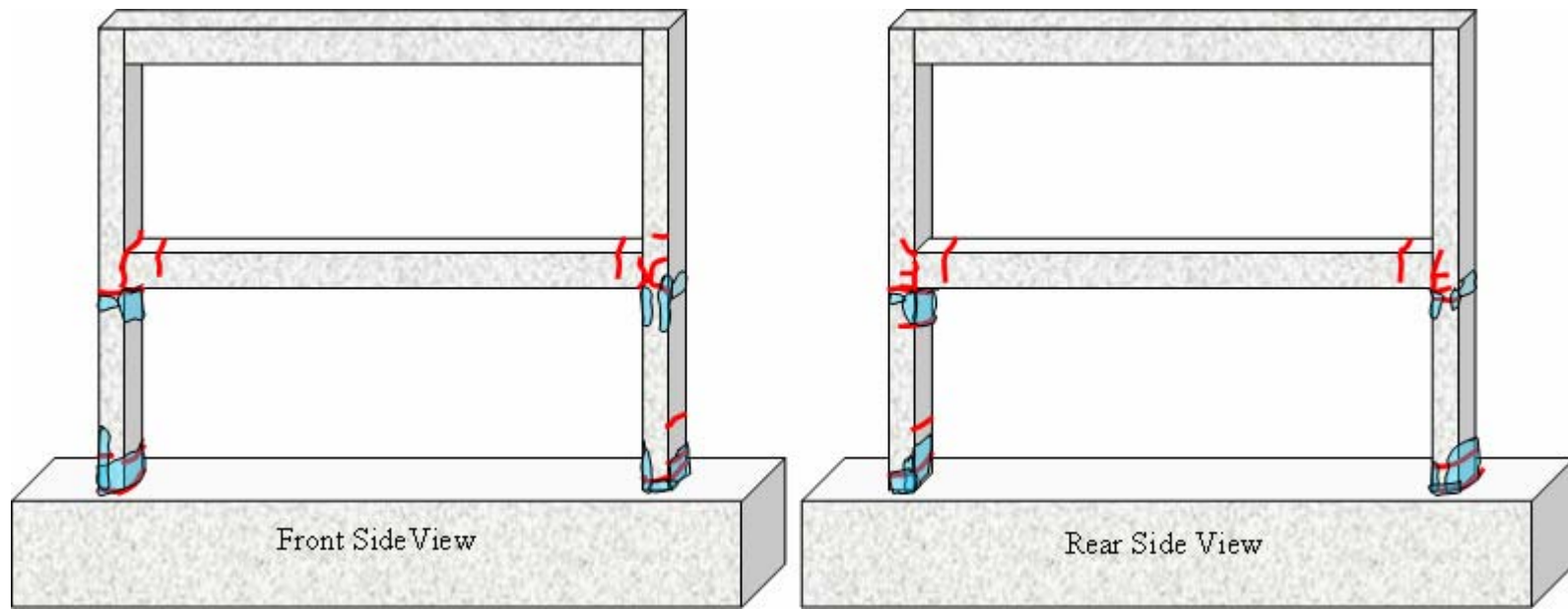
Figure 5.71. Front and Rear Side Crack Profiles of Specimen **WB**

5.4.2. Specimen WR

Specimen **WR** was the lower bound reference specimen of wider frame series which represents the present state of typical existing building. It was infilled by hollow clay bricks plastered on both sides. The test results of this specimen would serve as a lower bound reference for the behaviour and capacity improvement of the wider RC frame specimens strengthened by PC panels.

Specimen **WR** was subjected to lateral loading history presented in **Figure 5.72**, on which the numbers in parenthesis represent the corresponding second storey level top displacement in mm. Maximum forward and backward loads were measured to be **87.8 kN** and **82.3 kN**, respectively. Hysteretic total lateral load – displacement curves of second and first storey are presented in **Figure 5.73** and **Figure 5.74.** Total lateral load-shear displacement curve of first storey infill panel is presented in Figure **5.75.**
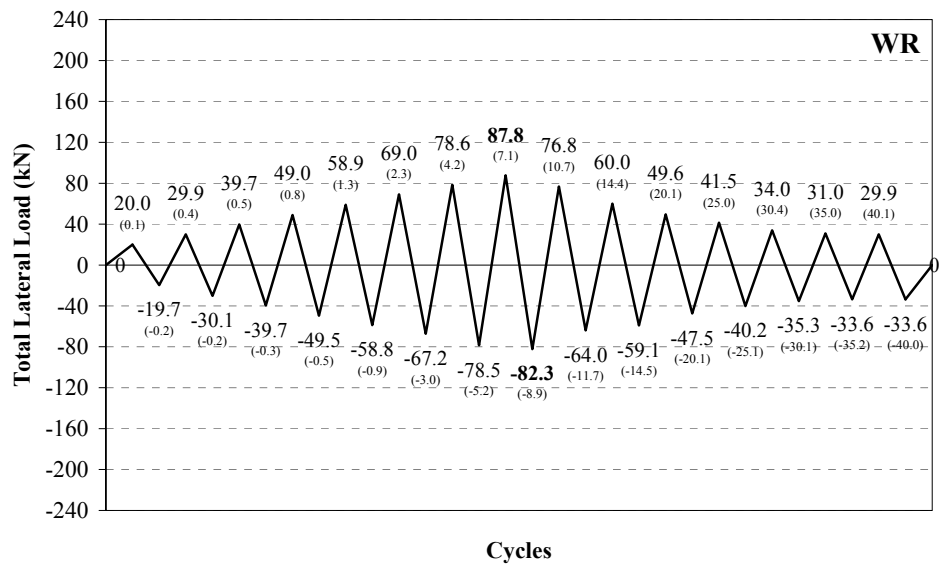
Figure 5.72. Loading History of Specimen **WR**

The initial stiffness of the specimen was calculated to be **122.3 kN/mm** as one of the major conclusions drawn from the lateral load-displacement curves**.** At the instant of forward maximum loading, the interstorey drift ratios for the first and second stories

were **0.0048** and **0.0034**, respectively whereas these values were **0.0047** and **0.0055** at the instant of backward maximum loading, respectively.
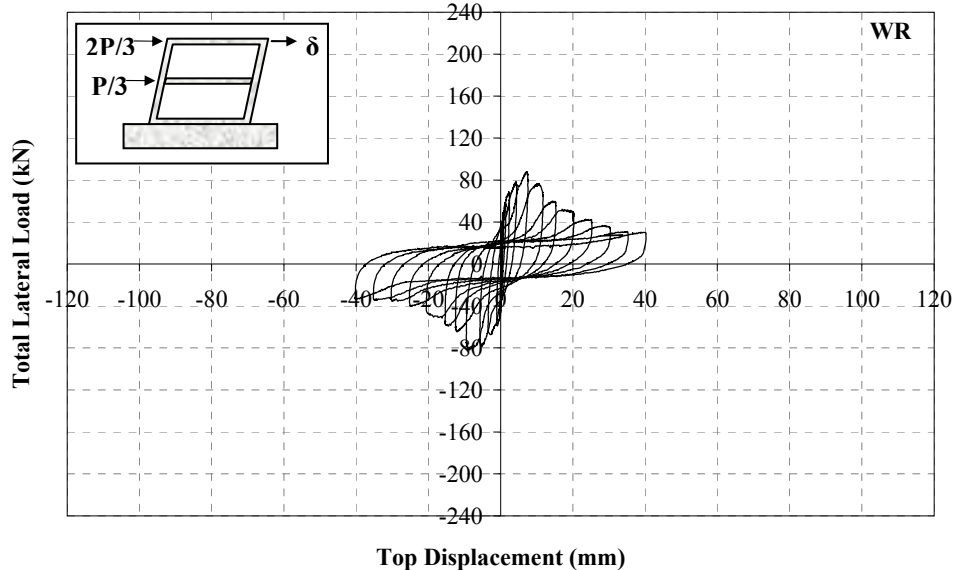
Figure 5.73. Total Lateral Load – Second Storey Level Displacement Curve, Specimen **WR**
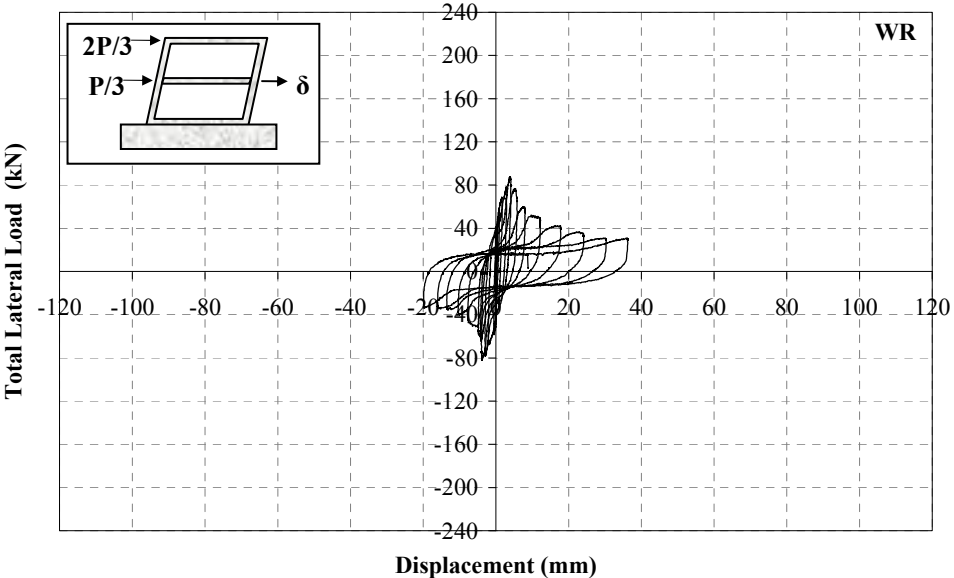
Figure 5.74. Total Lateral Load – First Storey Level Displacement Curve, Specimen **WR**
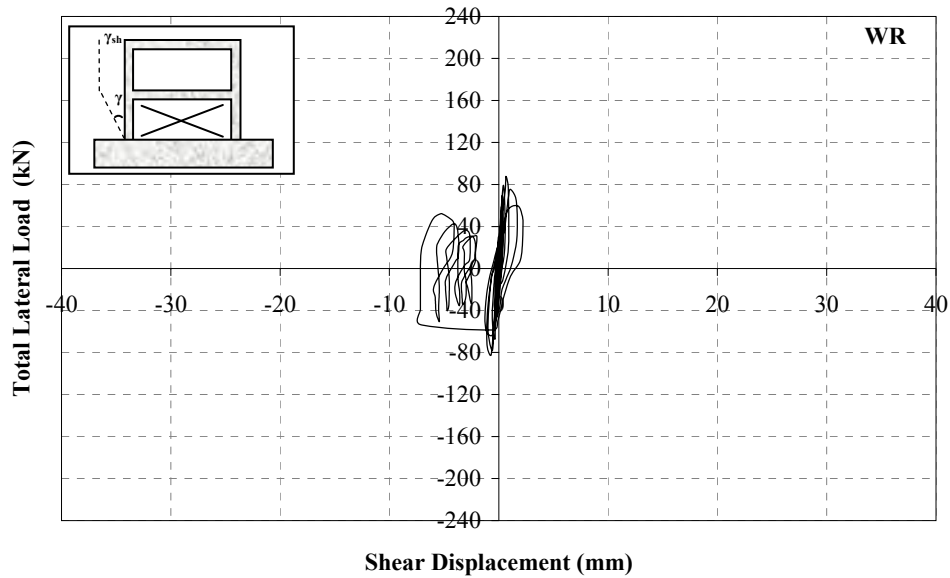
Figure 5.75. Total Lateral Load – First Storey Infill Shear Displacement Curve, Specimen **WR**

The major test observations of specimen **WR** are summarised below:

- In the first forward and backward half cycles, specimen **WR** was laterally loaded to 20.0 kN and 19.7 kN, respectively. No cracks and damages were observed.

- In the second forward half cycle, five cracks occured on first storey north column. The cracks were at the base, ~150mm, ~350mm and ~550 mm away from the foundation level and one just below the first storey beam-north column joint. A hairline horizontal crack on the plaster over the north column ~350 mm away from the basement and a vertical one from the base to the horizontal crack along the north column-infill interaction were observed on the rear side. In the second backward half cycle, four new cracks also occured on first storey south column. The cracks were at the base, ~300 mm and ~450 mm away from the foundation level and one at the first storey beam-south column joint.

- In the third forward half cycle, the north column crack ~150 mm away from the base propagated through the front side. A seperation was observed on the rear

165

side in between infill plaster and foundation. Moreover, another plaster crack occured being closer to the existing ones from previous forward half cycle. In the third backward half cycle, a hairline crack along the north column-first storey infill interaction was connected to the existing crack on the joint. On the other side, relatively short plaster cracks on both storey south column zone occured.

- In the fourth forward half cycle, a number of plaster cracks were introduced on the specimen especially on the second storey. The cracks were mainly localized on the first storey beam-second storey infill corner above the beam level and along the second storey north column-infill interaction zone. Also, the seperation in between infill plaster and foundation on the rear side became visible from the front side as well. Nearly symmetrical plaster cracks appeared along the second storey infill-south column interaction, in the fourth backward half cycle. Besides, hairline plaster cracks were also witnessed over the first storey plaster in the fourth load reversal.

- In the fifth forward half cycle, existing crack on the first storey beam-north column joint propagated. A diagonal plaster crack around the midspan occured on the first storey beam level on the rar side. In the fifth backward half cycle, the seperation in between first storey infill and foundation increased. Moreover, horziontal new cracks arised along second storey plaster-first storey beam interaction and new cracks along the first storey infill-south column interaction appeared on the rear side.

- In the sixth forward half cycle, diagonal cracks occured on the infill being visible on both front and rear sides. The seperation of first storey infill from north column propagated and widened. The seperation of infill from the foundation propagated through the midspan of the foundation and was aslo visible on the rear side at the end of sixth backward half cycle. New plaster cracks were observed around the second storey beam level as also illustarted in Figure xx, in the sixth backward half cycle. New diagonal cracks also appeared on the front side of the first storey infill.

- In the seventh forward half cycle, the flexural cracks on the north column and plaster around of the rear side widened, the seperation of first storey infill from the north column increased. Plaster cracks appeared on the rear side along the

second storey infill-south column interaction. In the seventh backward half cycle, a new crack occured on the first storey beam-south column joint, seperation of first storey infill from the south column increased, new diagonal cracks were introduced on the first storey infill. Moreover, a crack arised on the front side along the interaction line of second storey infill-second storey beam. Some diagonal plaster cracks were also visible on the same location at the rear side.

- In the eighth load reversal, the specimen reached its laterale loading capacity by **87.8 kN** in forward direction and **82.3 kN** in the backward direction. Occurance of a diagonal shear crack on the second storey beam-north column joint was of the primary observation in the eighth forward half cycle. The diagonal shear cracks on the first storey infill increased just below the first storey beam level. A vertical plaster crack occured on the rear side second storey beam level. In the eighth backward half cycle, a number of diagonal cracks occured on the plaster around the first storey beam on the rear side.

- The test was continued by displacement control in nineth load reversal. In the nineth forward half cycle, new diagonal cracks appeared on first storey infill. The plaster was cracked along the second storey infill - first storey beam interaction. In the nineth backward half cycle, first storey infill seperation from the south column was ~3 mm, together with widening of the cracks on first storey beam-south column joint. The plaster cracks on the rear increased and existing ones widened up to ~2-3 mm.

- In the tenth forward half cycle, crushing of the plaster on the first storey beam-nort column corner started. In the tenth backward half cycle, the plaster around the first storey beam-north column joint was spilled and the dial gage located on the first storey beam-south column corner to measure shear deformations was out of recording.

- In the eleventh forward half cycle, crushing of the plaster on the first storey beam-north column corner continued. Opening of the crack along the first storey infill and south column interaction reached ~4 mm and plaster cracks on the rear side widened and increased. Existing cracks on first storey north column surface spreaded through the front side. In the eleventh backward half cycle, crushing of the plaster started on the first storey beam-south column

corner. Besides, relatively wide cracks occured on the opposite corner of the first storey infill just beyond the shear deformation measuring dial gage.

- In the twelfth forward half cycle, cracked zoneS of the plaster on the rear side started to spill and existing plaster cracks widened. The plaster spilled out and the hollow bricks started to crush on both corners of first storey beam-column joints. Besides, diagonal cracks occured on the bottom end of the first storey south column.

- In the thirteenth forward half cycle, new diagonal cracks were observed on the first storey beam-south column joint together with crushing and spilling of the concrete. In the thirteenth backward half cycle, new diagonal cracks were observed on the first storey beam-north column joint. The longitudinal column reinforcement was visible on this joint, from the rear side. Plaster spilling from the rear side of the specimen mainly occured in thirteenth load reversal

- In the fourteenth load reversal, hollow clay bricks on both top corners of first storey infill crushed and spilled out. Due to crushing of the concrete on both first storey beam-column joints, the longitudinal reinforcement was visible.

- The test was terminated at the end of the fifteenth load reversal.

Views of specimen **WR**, before and after the experiment, are presented in **Figure 5.76** and crack profiles of front and rear sides are presented in **Figure 5.77.**
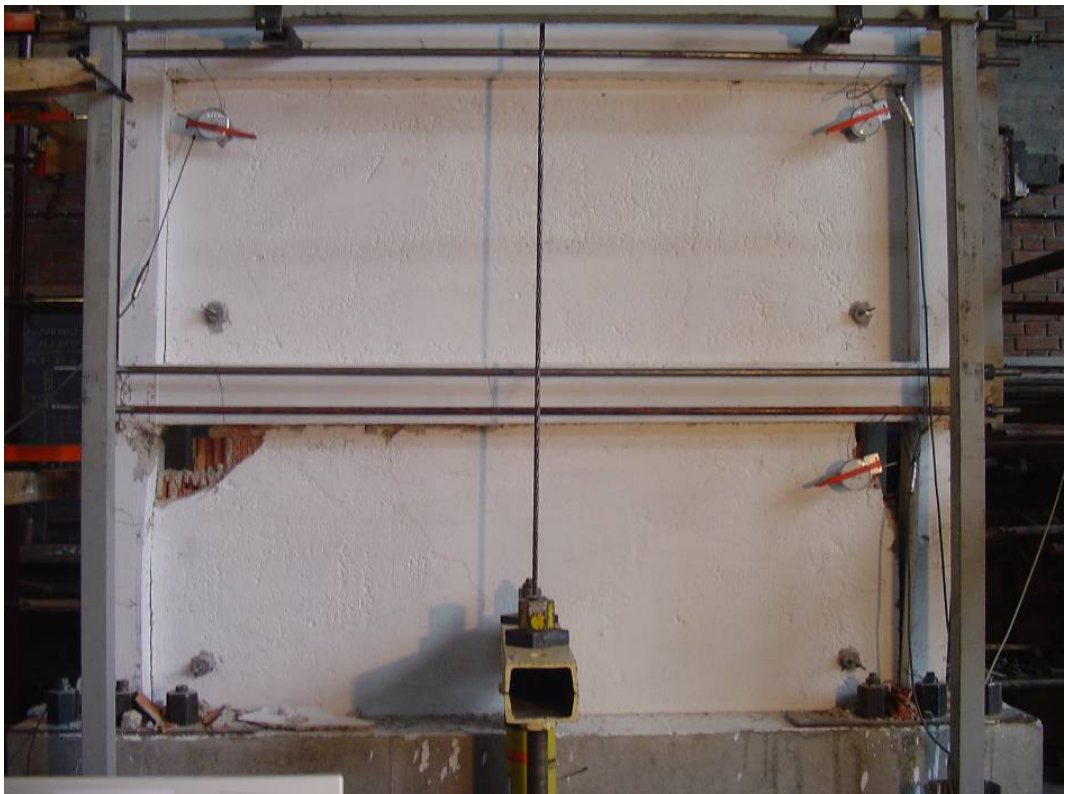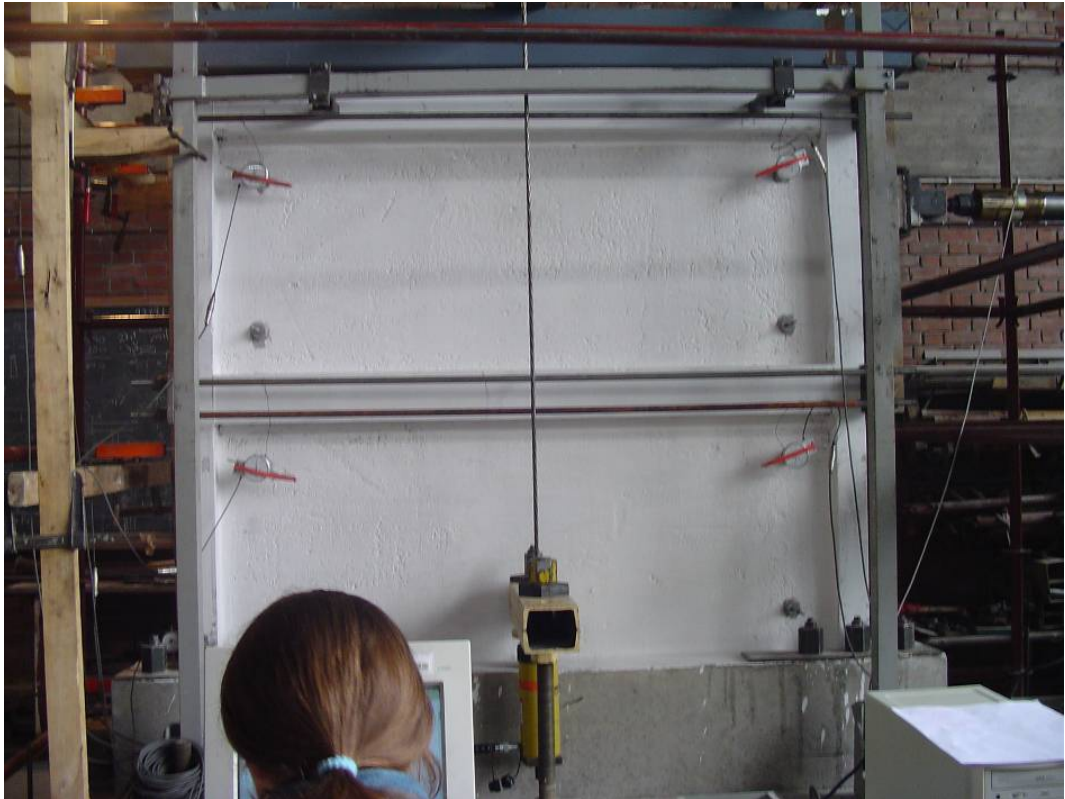
Figure 5.76. Before and After Test Views of Specimen **WR**
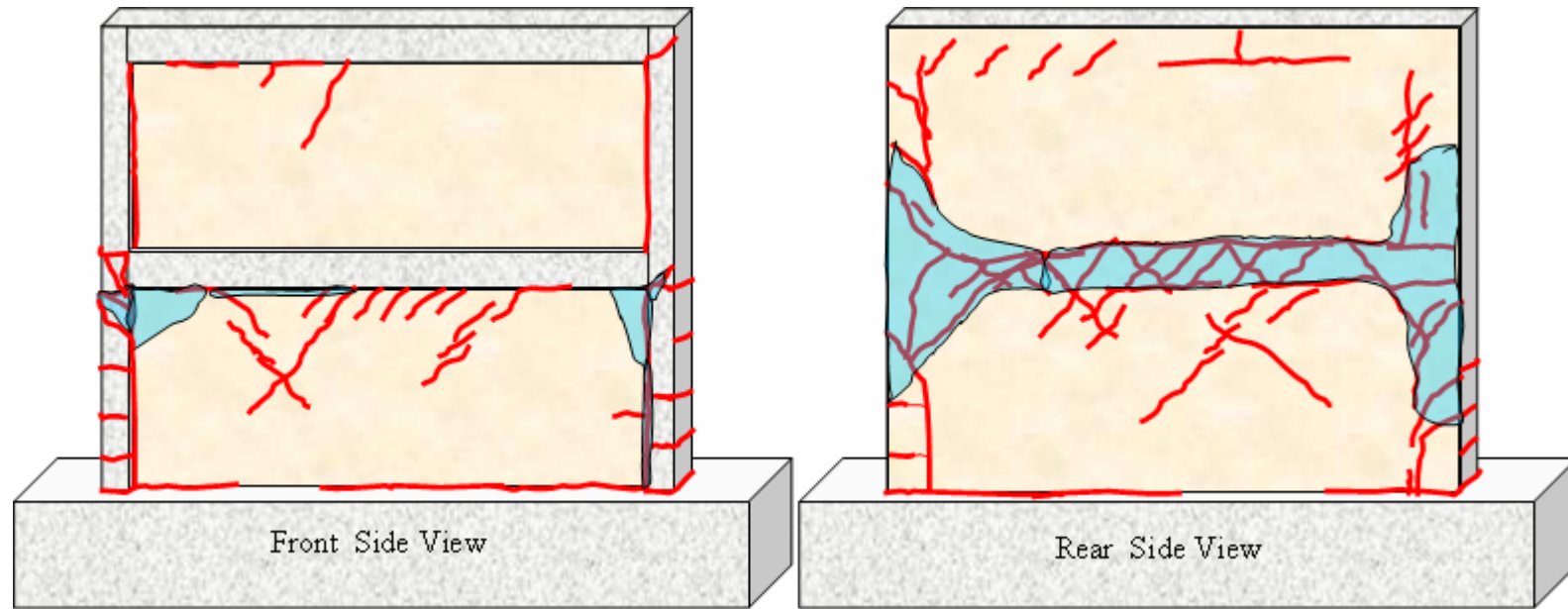
Figure 5.77. Front and Rear Side Crack Profiles of Specimen **WR**

5.4.3. Specimen WRP

Specimen **WRP** was the frame strengthened by rectangular shaped PC panels. The test results of this specimen were used to investigate the efficiency of PC panel method on seismic performance improvement. The test results were basically compared with the upper bound reference specimen **WRC** and and then lower bound specimen **WR**.

Specimen **WRP** was subjected to lateral loading history presented in **Figure 5.78**, on which the numbers in parenthesis represent the corresponding second storey level top displacement in mm. Maximum forward and backward loads were measured to be **166.6 kN** and **160.1 kN**, respectively. Hysteretic lateral load – displacement curves of second and first storey are presented in **Figure 5.79** and **Figure 5.80**. Total lateral load-shear displacement curve of first storey infill panel is presented in **Figure 5.81.**
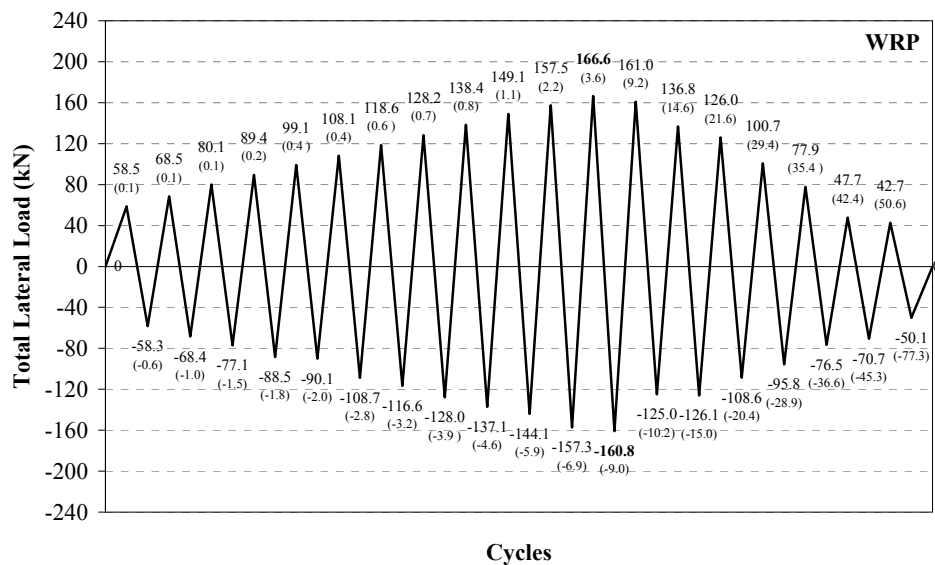
Figure 5.78. Loading History of Specimen **WRP**

The initial stiffness of the specimen was calculated to be **188.2 kN/mm**; as one of the major conclusions drawn from the lateral load-displacement curves**.** The initial stiffness of the specimen was defined as the initial slope of the lateral load-second storey level displacement curve in the first forward half cycle. At the instant of forward maximum

loading, the interstorey drift ratios for the first and second stories were **0.0046** and **0.0004**, respectively whereas these values were **0.0046** and **0.0057** at the instant of backward maximum loading, respectively.
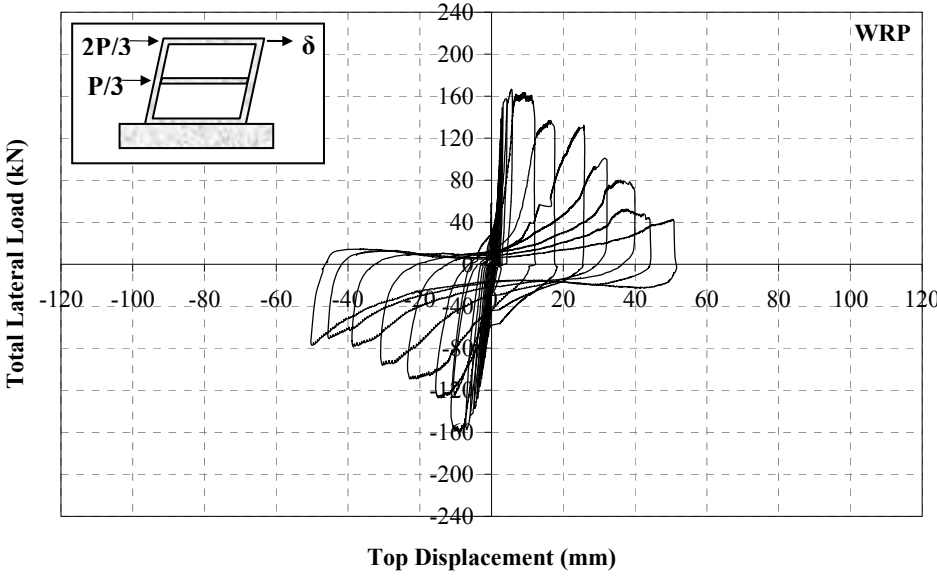
Figure 5.79. Total Lateral Load – Second Storey Level Displacement Curve, Specimen **WRP**
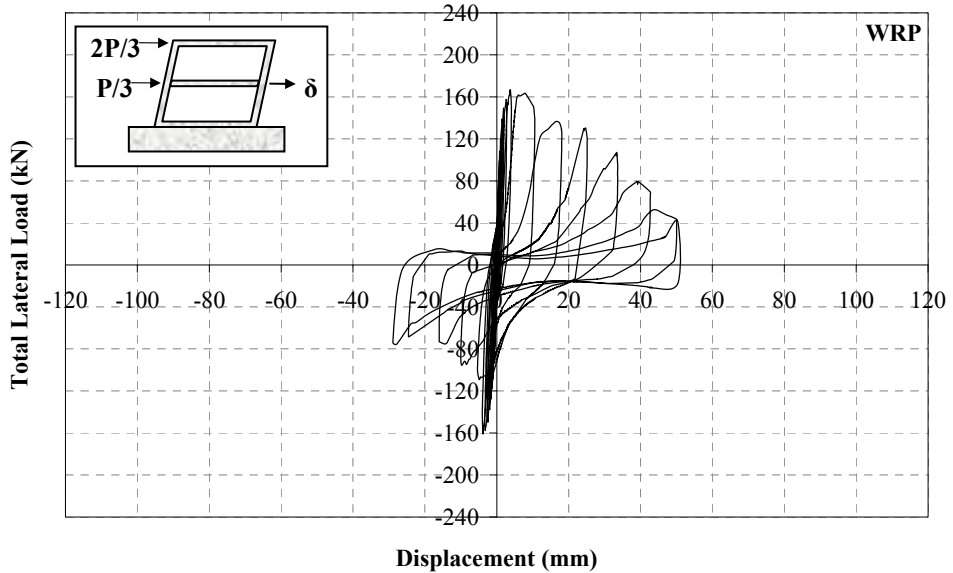
Figure 5.80. Total Lateral Load – First Storey Level Displacement Curve, Specimen **WRP**
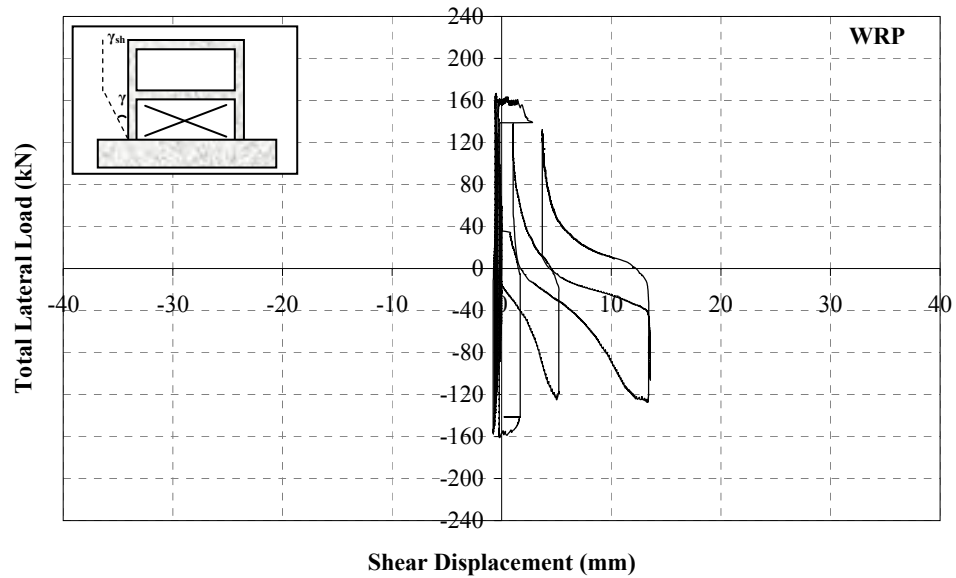
Figure 5.81. Total Lateral Load – First Storey Infill Shear Displacement Curve, Specimen **WRP**

The major test observations of specimen **WRP** are summarised below:

- In the first forward and backward half cycles, specimen **WRP** was laterally loaded to 58.5 kN and 58.3 kN, respectively. In the first forward half cycle, two flexural cracks occured on the north column, ~200 mm and ~500mm away from the basement. In the first backward half cycle, new cracks appeared on the south column; one being at the base, the other ~200 mm away from the basement and the last one just below the first storey beam-south column joint.

- In the second forward half cycle, a new crack occured on the north column base and plaster cracks aroused on the rear side around the first storey north column. In the second backward half cycle, a new flexural crack occures on the south column, ~250 mm away from the base and no plaster cracks occured.

- In the third forward half cycle, a shear crack occured on the first storey beam-north column joint. In the third backward half cycle, two new cracks occured on the south column, ~450 mm and ~600 mm away from the base. On the rear

173

side, a vertical crack occured along the first storey infill – south column connection.

- In the fourth forward half cycle, new flexural cracks appeared on the north column, ~250 mm and ~600 mm away from the base. On the rear side, a vertical plaster crack occured on the rear side along the first storey infill – north column connection. In the fourth backward half cycle, a diagonal shear crack occured on the first storey beam-south column joint and existing flexural cracks on south column widened.

- In the fifth forward half cycle, new flexural cracks aroused on the front side of the north column while no other cracks appeared in the backward half cycle of this reversal.

- In the sixth forward half cycle, the existing north column flexural cracks widened and seperation of first storey infill from the foundation started from the north column-foundation joint through rhe mid-span of the foundation. Besides, the first panel crack occured on the first storey. In the sixth backward half cycle, the seperation of first storey infill from the foundation was similarly observed from south column-foundation joint through the mid-span of the foundation.

- In the seventh forward half cycle, the flexural cracks on the north column which were occured in the first forward half cycle, propagated through the front side. A vertical panel crack appeared on the first storey infill-north column joint region aligning closer to anchorage dowel location. In the seventh backward half cycle, the existing north column crack just above the mid-height, propgated through the infill surface on the front side. The seperation of first storey infill from the south column surface also started by a vertical crack.

- In the eighth load reversal, the existing cracks widened in general. In addition, a horizontal plaster crack lying along the first storey beam bottom level was observed at the end of eighth backward half cycle.

- In the ninth forward half cycle, a vertical joint crack occure on the first storey beam-north column joint. New flexural cracks also occured on north column, below this joint. In the ninth backward half cycle, new flexural cracks appeared below the first storey beam-south column joint. Besides, a horizontal crack occured on the rear side along the plaster-foundation connection.

174

- In the tenth forward half cycle, a flexural crack occured on the first storey north column just below the mid-height. The seperation of first storey infill from the north column surface was observed by occurace of a vertical crack on this zone. In addition, a horizontal crack was observed on the first storey panel just under the first storey beam bottom level. In the tenth backward half cycle, the first flexural on the second storey south column, ~150 mm above the mid height as shown in **Figure 5.82**, and the existing plaster cracks on the rear side widened.

Figure 5.82. Crack on Second Storey South Column at the End of Tenth Cycle, Specimen **WRP**

- In the eleventh forward half cycle, the second storey north column experienced flexural cracks, ~350 mm and ~500 mm away from the first storey beam-north column joint. A diagonal shear crack occured on the second storey beam-north column joint and another horizontal crack was also occured on the second storey beam-infill connection. In the eleventh backward half cycle, new horizontal cracks occured on the first storey PC panels, being closer to the south column zone and ~450 mm and ~500 mm above the foundation level.
- In the twelfth load reversal, the specimen reached its lateral loading capacity by **166.6 kN** and **160.8 kN** in forward and backward directions, respectively. A number of new cracks occured on first storey PC panel and wider diagonal plaster cracks also appeared on the rear side as illustrated in **Figure 5.85**.

- In the thirteenth forward half cycle, the test was started to be carried out in load controlled fashion. New panel cracks appeared on both storey infill panels and rear side plaster. The second storey infill panel – first storey beam connection experienced a horizontal crack. Plaster over the first storey beam-north column joint started to seperate from the frame. In the thirteenth backward half cycle, new shear cracks occured on the first storey beam-north column joint and the previously occured panel cracks of thefirst storey infill widened up to ~8-9 mm.

- In the fourteenth forward half cycle, new shear cracks occured on the first storey beam-south column joint. The cover concrete over the first storey beam-north column joint spilled out and the transverse reinforcement became visible. Existing panel cracks widened and new ones also occured. In the fourteenth backward half cycle, the existing panel cracks widened up to ~20-25 mm. The first storey beam-north column joint was highly damaged as shown in **Figure 5.83**.

Figure 5.83. View of First Storey Beam-North Column Joint at the End of Fourteenth Cycle, Specimen **WRP**

- The specimen was loaded to five cycles more and the test was terminated at the end of nineteenth cycle. Up to the end of the test, the plaster at rear side was seperated over the crack zones as illustrated in **Figure 5.85**. The panel cracks widened up to ~30 mm - ~40 mm during the loadings. As the stiffness reached almost zero, the test was finalized at the end of nineteenth cycle.

Views of specimen **WRP**, before and after the experiment, are presented in **Figure 5.84** and crack profiles of front and rear sides are presented in **Figure 5.85**.
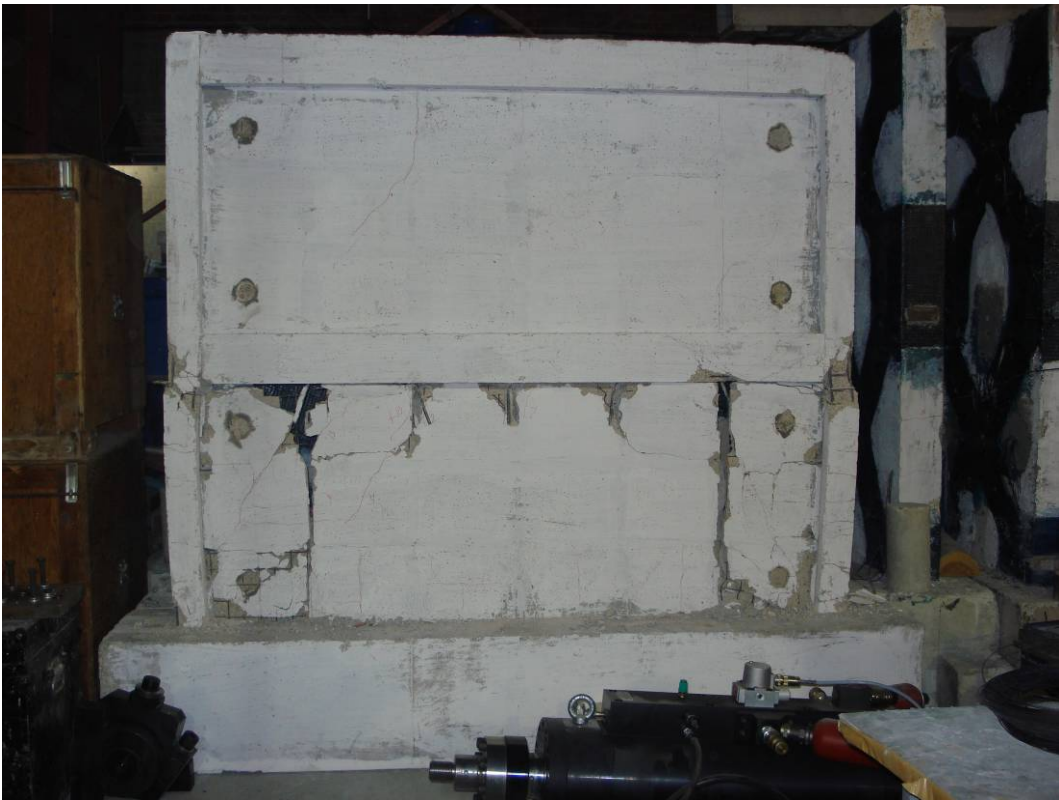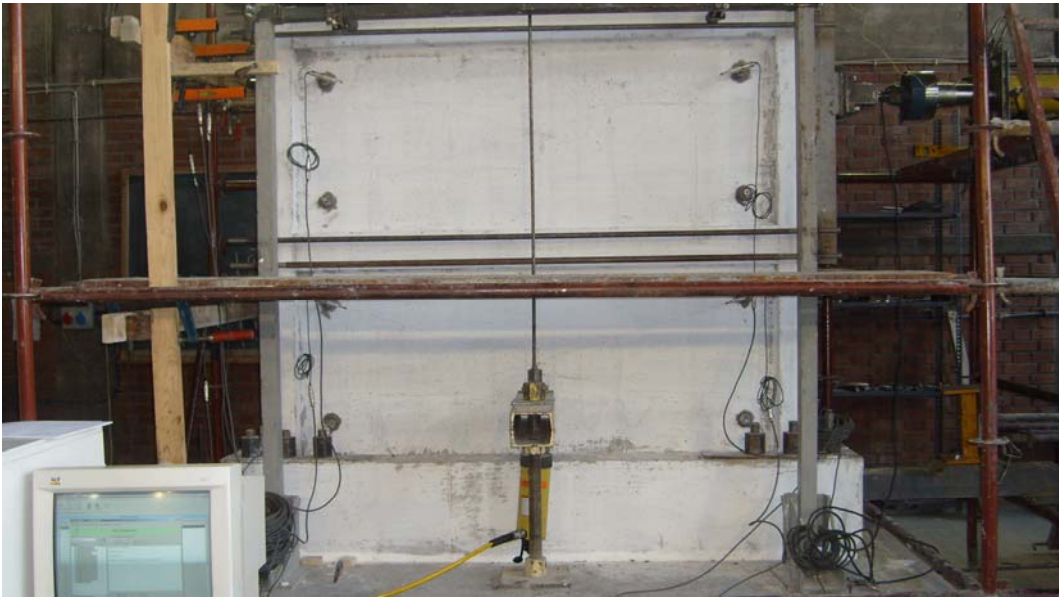
Figure 5.84. Before and After Test Views of Specimen **WRP**

Front Side View

Rear Side View
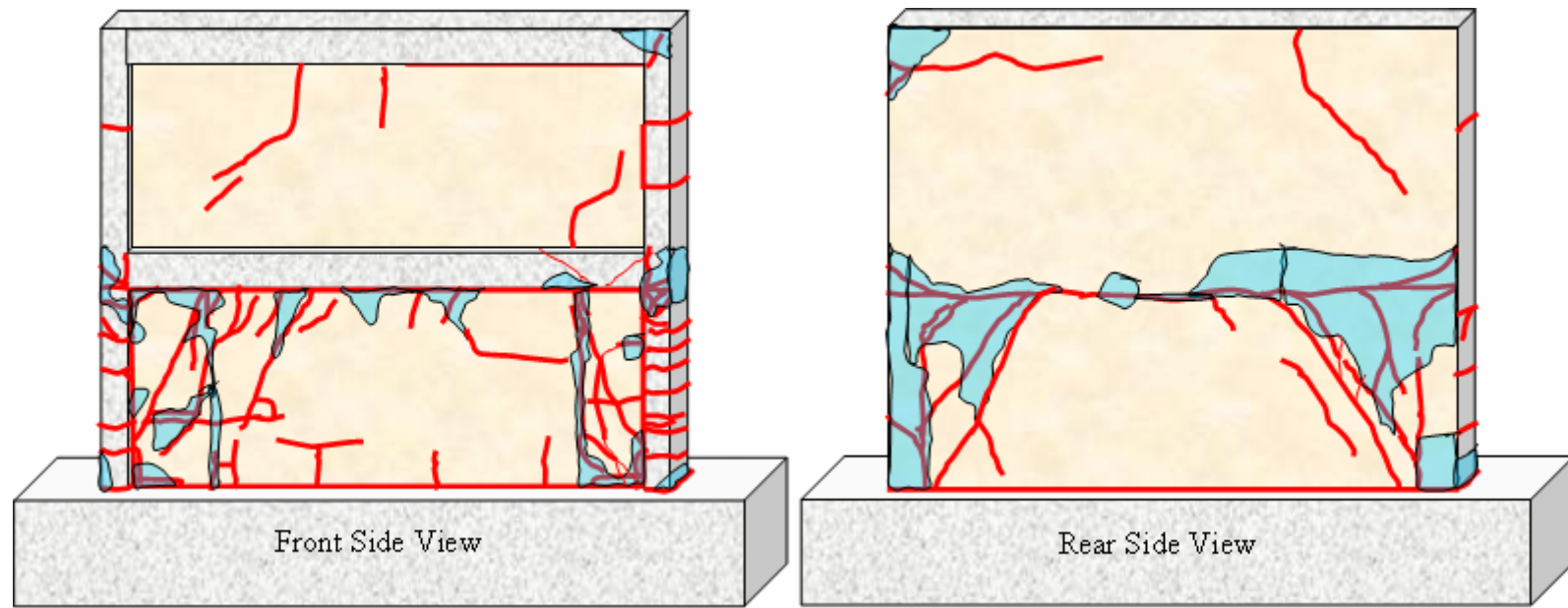
Figure 5.85. Front and Rear Side Crack Profiles of Specimen **WRP**

5.4.4. Specimen WSP

Specimen **WSP** was the frame strengthened by strip shaped PC panels. The test results were basically compared with the upper bound reference specimen **WRC** and and then lower bound specimen **WR**. In addition, the performance improvement comparisons were also done for specimen **WRP**.

Specimen **WSP** was subjected to lateral loading history presented in **Figure 5.86**, on which the numbers in parenthesis represent the corresponding second storey level top displacement in mm.Maximum forward and backward loads were measured to be **178.1 kN** and **164.7 kN**, respectively. Hysteretic total lateral load – displacement curves of second and first storey are presented in **Figure 5.87** and **Figure 5.88**. Total lateral load-shear displacement curve of first storey infill panel is presented in **Figure 5.89.**
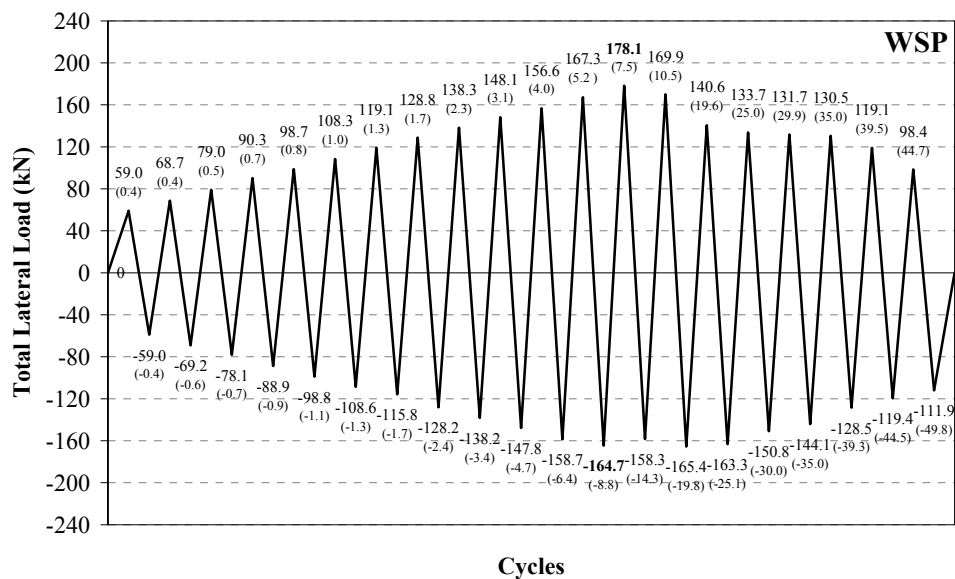
Figure 5.86. Loading History of Specimen **WSP**

The initial stiffness of the specimen was calculated to be **240.2 kN/mm** as one of the major conclusions drawn from the lateral load-displacement curves**.** At the instant of forward maximum loading, the interstorey drift ratios for the first and second stories

were **0.0048** and **0.0039**, respectively whereas these values were **0.0036** and **0.0064** at the instant of backward maximum loading, respectively.
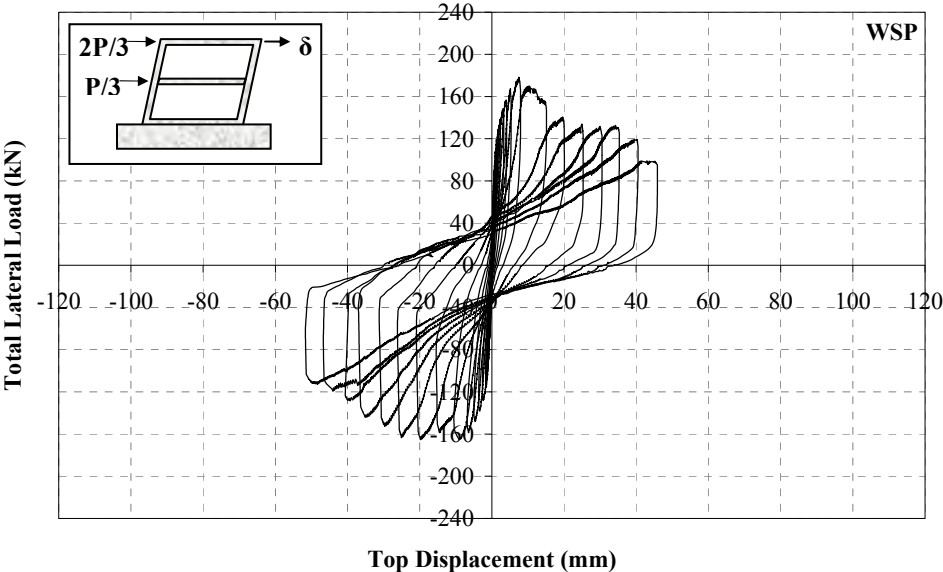
Figure 5.87. Total Lateral Load – Second Storey Level Displacement Curve, Specimen **WSP**
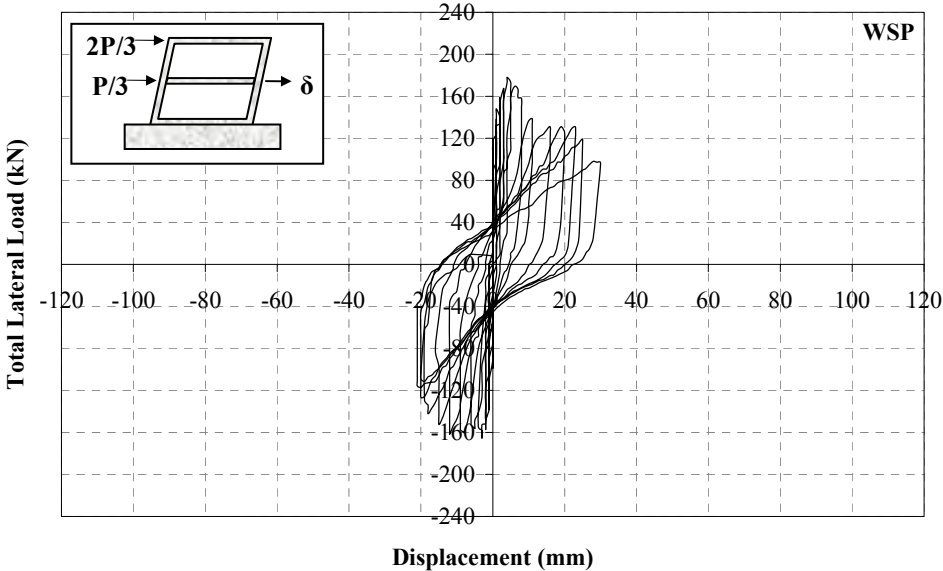
Figure 5.88. Total Lateral Load – First Storey Level Displacement Curve, Specimen **WSP**
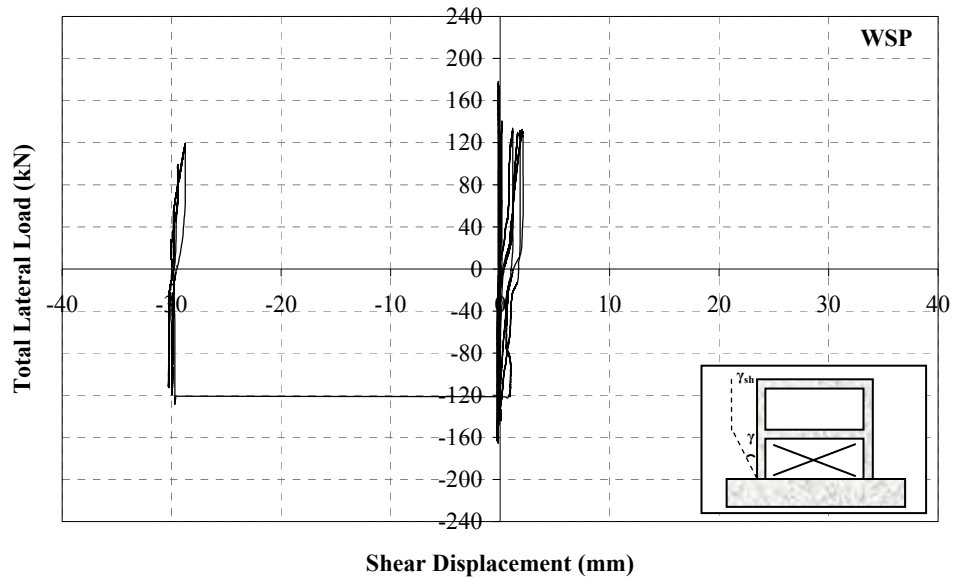
Figure 5.89. Total Lateral Load – First Storey Infill Shear Displacement Curve, Specimen **WSP**

The major test observations of specimen **WSP** are summarised as follows:

- In the first forward and backward half cycles, specimen **WSP** was laterally loaded to 59.0 kN and 59.0 kN, respectively. No cracks were observed in the first load reversal.

- In the second and third cycles, no cracks were observed.

- In the fourth forward half cycle, a flexural crack occured on the north column base. Similarly, another flexural column crack also occured on the south column base, in the fourth backward half cycle.

- No cracks occured in the fifth and sixth loading reversals.

- In the seventh forward half cycle, no cracks were observed, while a flexural crack appeared on the south column, ~300 mm above the basement level, in the seventh backward half cycle.

- In the eighth forward half cycle, new plaster cracks occured on the rear side above the first storey north column base. In the eighth backward half cycle, new flexural cracks occured just above the first storey south column mid-height. Besides, the seperation of first storey infill from the foundation level, starting

181

from the south column base and aligning through the mid-span of the foundation, was observed. Vertical plaster cracks on the same level of first storey infill-north column interaction were observed on the rear side.

- In the ninth forward half cycle, new flexural cracks appeared on the north column, aligning ~200mm, ~300mm and ~400mm above the base level and plaster crack was observed on the rear side, being closer to the north column base. In the ninth backward half cycle, the first shear crack occured on the first storey beam-south column joint and the existing crack just below this joint propagated through the front side. A new plaster crack aroused on the rear side, below the first storey beam – north column joint.

- In the tenth forward half cycle, a new flexural crack occured on the first storey north column, ~150mm away from the base. In addition, a shear crack occured on the first storey beam-north column joint. The existing plaster cracks widened and a new one occured below the first storey beam-north column joint. In the tenth backward half cycle, a new crack appeared on the first storey beam-south column joint aligning through the PC panel layer and the south column cracks propagated through the infill on the front side.

- In the eleventh forward half cycle, new flexural cracks occured on the north column, ~450 mm away from the basement. A crack appeared on the first storey infill-foundation connection, starting from the north column base aligning through the mid-span of the foundation. A long, vertical crack also appeared on the first storey infill-north column connection surface. In the eleventh backward half cycle, symmetrical seperations of ~2-3 mm width were observed for first storey infill similar as the ones in the forward half cycle of this reversal. A new shear crack occured on the first storey beam-south column joint.

- In the twelfth forward half cycle, the joint crack occured in first storey beam-north column joint at the end of the tenth load reversal propagated through the rear side and existing cracks widened; especially the plaster cracks together with a hairline PC panel crack on the first storey. In addition, a vertical plaster crack appeared on the second storey aligning parallel to second storey infill-north column connection surface. In the twelfth backward half cycle, the specimen reached its lateral loading capacity in tha backward direction by **164.3**

kN. In this half cycle, a panel crack occured on the south column-foundation corner zone being closer to anchorage dowel locations and the seperation of first storey infill from the foundation reached ~3-4 mm width. On the rear side, the existing plaster cracks widened together with addition of new, short cracks around the south column base.

- In the thirteenth load reversal, the specimen reached its lateral loading capacity in the forward direction by **178.1 kN.** New shear cracks occured in first storey beam-column joints, in this reversal as shown in **Figure 5.90**. The seperations in between the first storey infill-north column connection and the infill-foundation connection reached ~4 mm width. In the thirteenth backward half cycle, the loading was started to be performed in displacement controlled fashion. A diagonal shear crack occured on the second storey beam-south column connection as illustrated in **Figure 5.93**.

Figure 5.90. Views of First Storey Beam-Column Joints at the End of Thirteenth Load Reversal, Specimen **WSP**

- In the fourteenth load reversal, the existing shear cracks in first storey beam-column joints widened up to ~8-10 mm and the first storey infill seperations both from columns and foundation also widened. In addition, a new shear crack appeared on the first storey beam-south column joint.
- In the fifteenth forward half cycle, the damage localized in the first storey beam-north column joint by widening of the existing shear crack. No new

cracks occured in the fifteenth backward half cycle, other than widening of the existing ones.

- No new cracks occured in the sixteenth cycle. The existing cracks widened.

- Localized concrete crushings were observed in the seventeenth load reversal. Concrete on first storey beam–column joints crushed, as well as the concrete in column bases crushed and the longitudinal reinforcement became visible for both columns. A diagonal shear crack occured on the second storey beam-north column joint together with localized concrete crushing. The first storey infill seperation from the foundation and surrounding columns widened up to ~20-30 mm.

- In the eighteenth load reversal, the existing cracks widened and the crushing of the concrete in joint regions increased as shown in **Figure 5.91**. The longitudinal reinforcement became visible on the column base.

Figure 5.91. Rear Side Views at the End of Eighteenth Load Reversal, Specimen **WSP**

- The test was terminated at the end of the nineteenth cycle. The dial gage placed on the first storey infill at the first storey beam–south column joint seperated from the infill and became out of recording, during the nineteenth load reversal.

Views of specimen **WSP**, before and after the experiment, are presented in **Figure 5.92** and crack profiles of front and rear sides are presented in **Figure 5.93**.

Figure 5.92. Before and After Test Views of Specimen **WSP**
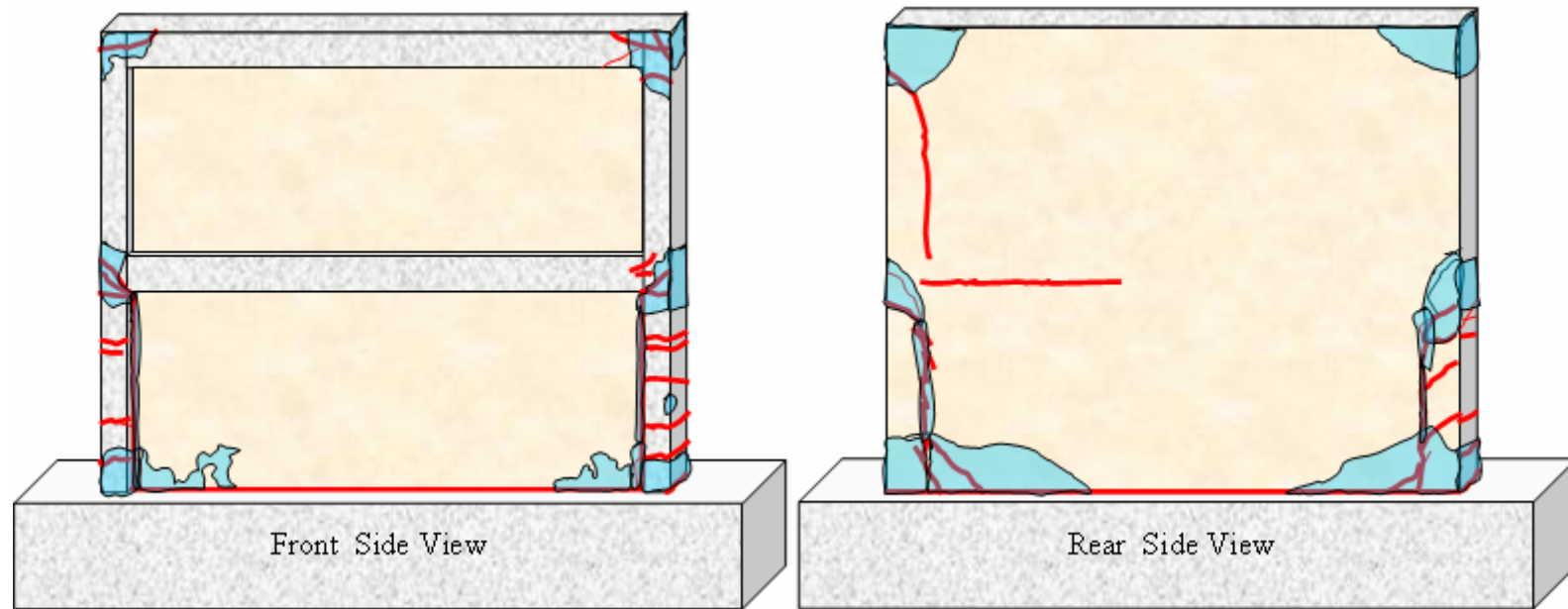
Figure 5.93. Front and Rear Side Crack Profiles of Specimen **WSP**

5.4.5. Specimen WRC

Specimen W**RC** was tested as the upper bound reference for wider series of specimens with cast-in-place RC infills. The test results of this specimen were compared with the performance improvement by PC panel application for both strip and rectangular panels.

Specimen **WRC** was subjected to lateral loading history presented in **Figure 5.94**, on which the numbers in parenthesis represent the corresponding second storey level top displacement in mm. Maximum forward and backward loads were measured to be **186.8 kN** and **163.1 kN**, respectively. Hysteretic total lateral load – displacement curves of second and first storey are presented in **Figure 5.95** and **Figure 5.96**. Total lateral load-shear displacement curve of first storey infill is presented in **Figure 5.97**.
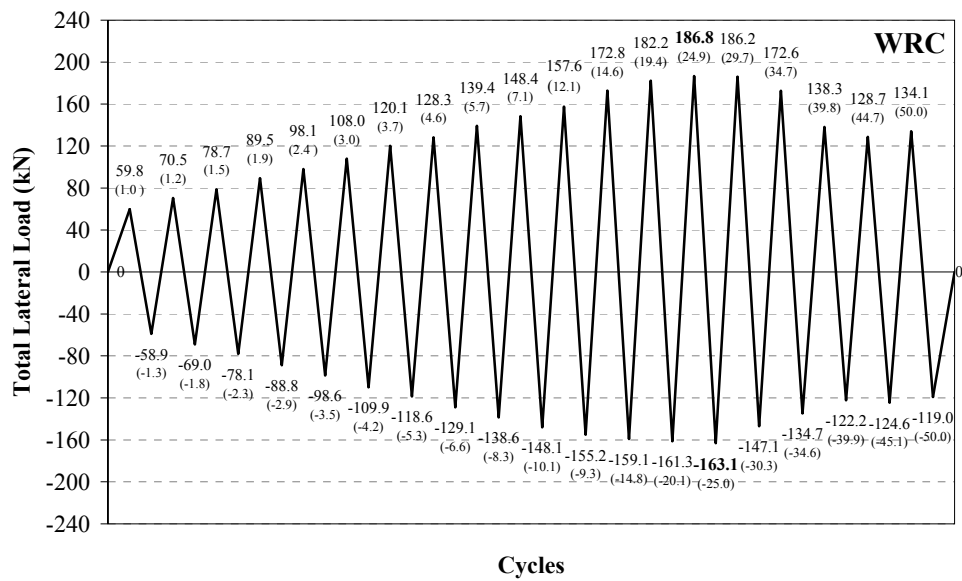
Figure 5.94. Loading History of Specimen **WRC**

The initial stiffness of the specimen was calculated to be **267.8 kN/mm** as one of the major conclusions drawn from the lateral load-displacement curves**.** At the instant of forward maximum loading, the interstorey drift ratios for the first and second stories

187

were **0.0164** and **0.0126**, respectively whereas these values were **0.0171** and **0.0121** at the instant of backward maximum loading, respectively.
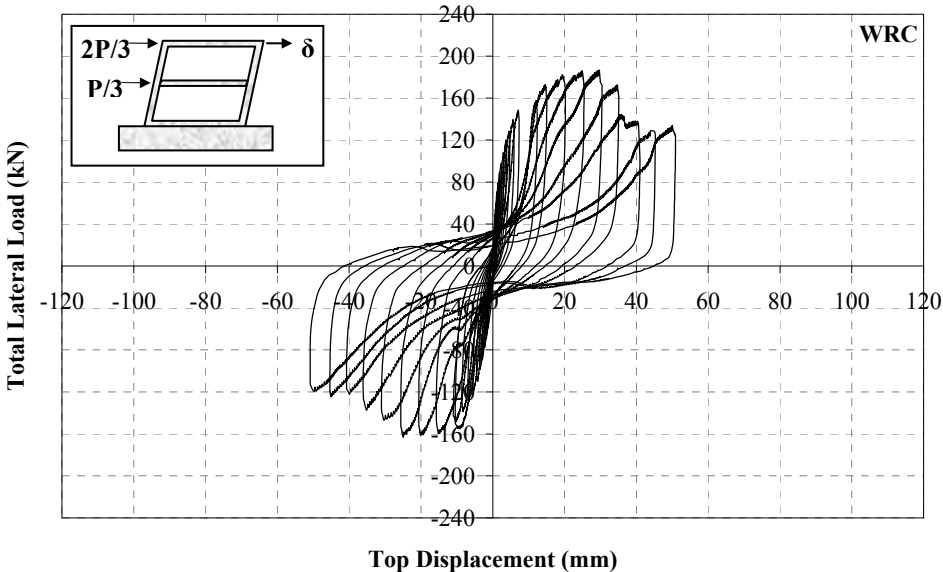
Figure 5.95. Total Lateral Load – Second Storey Level Displacement Curve, Specimen **WRC**
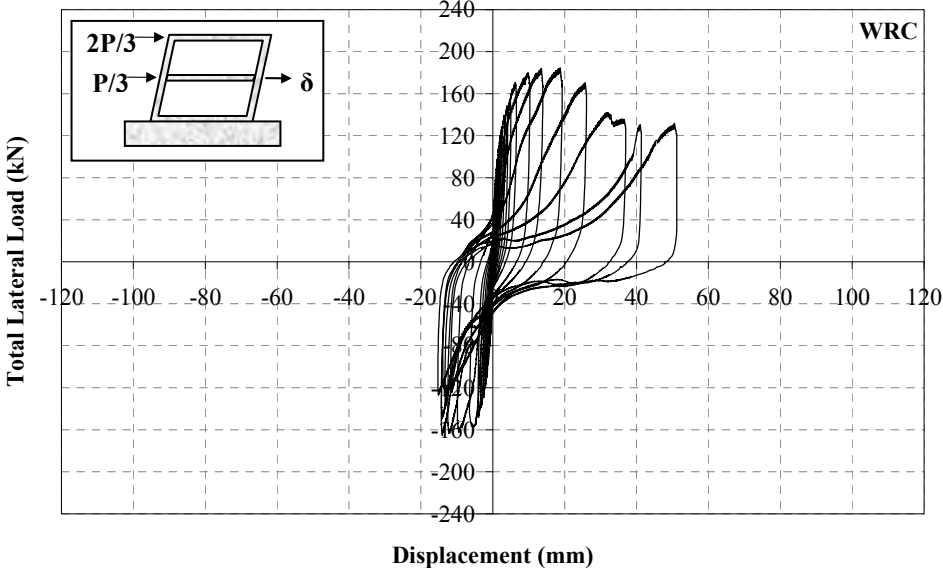
Figure 5.96. Total Lateral Load – First Storey Level Displacement Curve, Specimen **WRC**
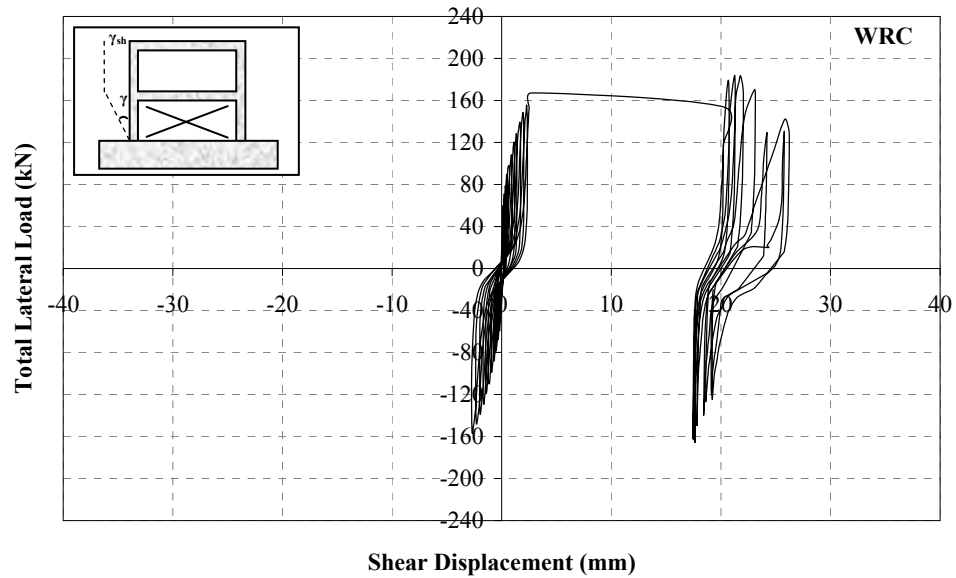
Figure 5.97. Total Lateral Load – First Storey Infill Shear Displacement Curve, Specimen **WRC**

The major test observations of specimen **WRC** are summarised below:

- In the first forward and backward half cycles, specimen **WRC** was laterally loaded to 59.8 kN and 58.9 kN, respectively. Cracks occured on both north and south column bases together with symmetrical hairline cracks approximately at midheight of both first storey columns.

- In the second forward half cycle, the previously occured midheight crack on first storey north column propgated through the front side, while a new flexural crack appeared on south column just below the first storey beam-south column joint in the second backward half cycle.

- In the third forward half cycle, the previous midheight hairline crack on north column propagated through the front side, a new crack arised ~150 mm above the north column base. Besides, new flexural crack appeared on north column just below the first storey beam-north column joint. The crack on the south column base widened in the thrid backward half cycle, while the previous

midheight hairline crack on south column also propagated through the front side.

- The specimen experinced the first diagonal shear cracks on first storey infill panel in the fourth load reversal. Moreover, another diagonal shear crack on the first storey beam-south column joint also appreared in the fourth forward half cycle together with a new flexural crack on the first storey north column just ~100 mm above the midheight.

- In the fifth load reversal, the first cracks were observed on the second storey infill panel, while new ones also arised on the first storey RC infill. The crack on the south column base propagated and a seperation of RC infill from the foundation level starting from the south column base was visible on both front and rear sides.

- In the sixth forward half cycle, as diagonal shear crack appeared on first storey beam-north column joint. Seperation of RC infill from the foundation level starting from the north column base started in this half cycle. Another flexural crack occured on the first storey south column ~150 mm below the first storey beam-north column joint. The seperation of infill from the foundation propagated through the midspan of the foundation. New cracks also appeared on first and second storey infills, at the end of the sixth load reversal.

- In the seventh forward half cycle, the seperation of second storey RC infill from the first storey beam level started from the north column side, while a new crack arised on the first storey beam-south column joint in the backward half cycle of the reversal. At the end of seventh load reversal, new cracks following the first storey RC infill mesh reinforcement appeared in both forward and backward half cycles together with new hairline diagonal ones.

- In the eighth forward half cycle, a diagonal crack appeared on the north column just ~100 mm below the first storey beam-north column joint and a new flexural crack was observed below the mentioned shear crack. Another seperation was also appeared in between first storey RC infill and north column interaction. In the eigtht backward half cycle, a new crack arised at the top of the on the beam and the seperation of RC infill from the foundation spreaded through the midspan of the foundation. New panel cracks appeared on both storey RC infill panels at the end of eighth load reversal.

- In the nineth forward half cycle, a seperation was observed at the top of the second storey RC infill from the second storey beam level, while the existing seperation of first storey infill panel from the north column surface was further developed. Existing cracks on north column surface propagated through the rear side and new cracks on both storey RC infills developed at the end of the full nineth load reversal. The seperation of RC infill from the foundation increased and cracks on south column widened in the nineth backward half cycle.

- In the tenth forward half cycle, a new diagonal crack occured at the top of the first storey north column as shown in **Figure 5.98**. The seperation of first storey RC infill from foundation and south column increased as well as the seperation of second storey infill from the second storey beam level. Apperance of new cracks on RC infills was also observed at the end of tenth load reversal.

Figure 5.98. Diagonal Shear Crack on First Storey North Column at the End of Tenth Load Reversal, Specimen **WRC**

- In the eleventh forward half cycle, existing cracks opened and a number of new cracks occured on both storey RC infills. The seperation of first storey RC infill from north column surface developed more and was easily visible from the rear side, also. The same damage was also observed in the eleventh backward half

191

cycle in between south column and first storey RC infill. New panel cracks appeared on both storeys. The crack at the south column base opened up to ~3 mm. New diagonal shear cracks occured on both joints of south column to first and second storey beams and a new flexural crack occured on the second storey south column as shown in **Figure 5.99.**
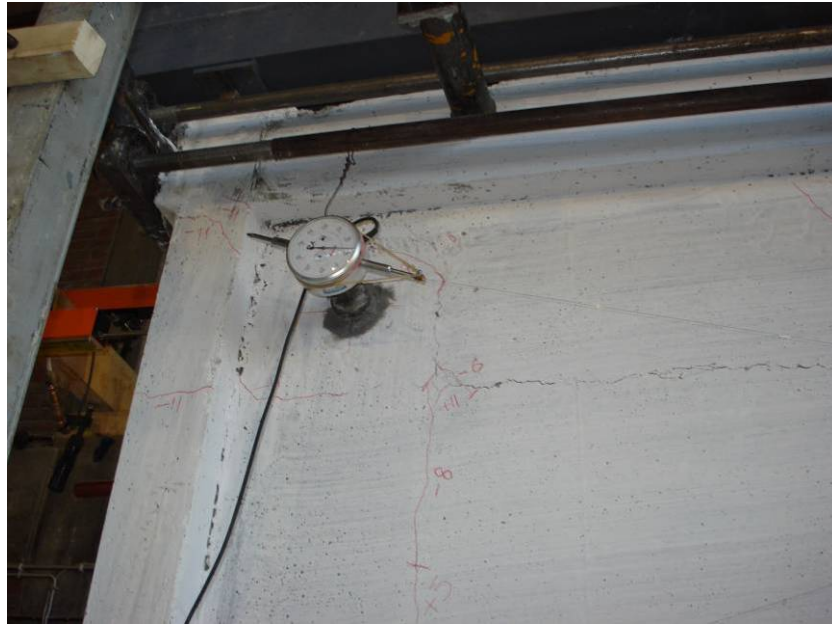
Figure 5.99. View of Second Storey South Column at the End of Eleventh Load Reversal, Specimen **WRC**

- In the twelfth forward half cycle, the width of existing panel cracks increased and new cracks also appeared on both storey RC infills. The cracks on first storey beam-south column joint widened and the seperation of RC infill from the foundation progressed along the infill width at the twelfth backward half cycle. New shear cracks on both south column-beam joints also appeared together with the increasing number of both storey RC infill panel cracks.

- In the thirteenth forward half cycle, existing cracks widened on RC infills and north column. The seperation of first storey RC infill from the foundation increased, at the end of thirteenth backward half cycle. Besides, the number of the diagonal cracks on first storey beam-south column joint much increased

being more visible on the rear side as illustrated in **Figure 5.102**. Additional cracks on RC infills were observed at the end of thirteenth load reversal.

- The specimen reached its lateral loading capacity at fourteenth load reversal, in both forward and backward directions by **186.8 kN** and **163.1 kN**, respectively. The number of the panel cracks and width of the existing ones considerably increased in the fourteenth forward half cycle. New diagonal cracks appeared on the first storey beam joints, on the rear side and crushing and spilling of the infill concrete on the north column-foundation joint zone was realized.

- The experiment was further carried out by displacement controlled loading starting from the fifteenth load reversal. In the fifteenth forward half cycle, the number of the panel cracks increased on both storey infills as well as the widths of the existing ones. The crushing and spilling of the RC concrete infill concrete around the first storey beam level was visible especially on rear side. In the fifteenth backward half cycle, the concrete crushed around the first storey beam-south column joint.

- In the sixteenth load reversal, the existing cracks widened. Crushing and spilling of concrete mainly occured on first storey RC infill corners and arund the first storey beam level.

- In the seventeenth load reversal, the concrete on both column bases crushed and spllied causing a drastic reduction in lateral load carrying level from 172.6 kN to 138.3 kN, in the forward direction and similarly from 134.7 kN to 122.2 kN in the backward direction. Joints of the first storey beam were also further damaged by crushing of the concrete.

- Crushing and spilling of both RC infill and frame concrete increased at the end of the eigtheenth load reversal. Closer views of first storey beam-column joints are provided in **Figure 5.100**.

Figure 5.100. Views of First Storey Beam-Column Joints at the End of Eighteenth Load Reversal, Specimen **WRC**

- The test was terminated at the end of nineteenth load reversal by reaching ~50 mm top displacements on both forward and backward directions.

Views of specimen **WRC,** before and after the experiment, are presented in **Figure 5.101** and crack profiles of front and rear sides are presented in **Figure 5.102**.

Figure 5.101. Before and After Test Views of Specimen **WRC**
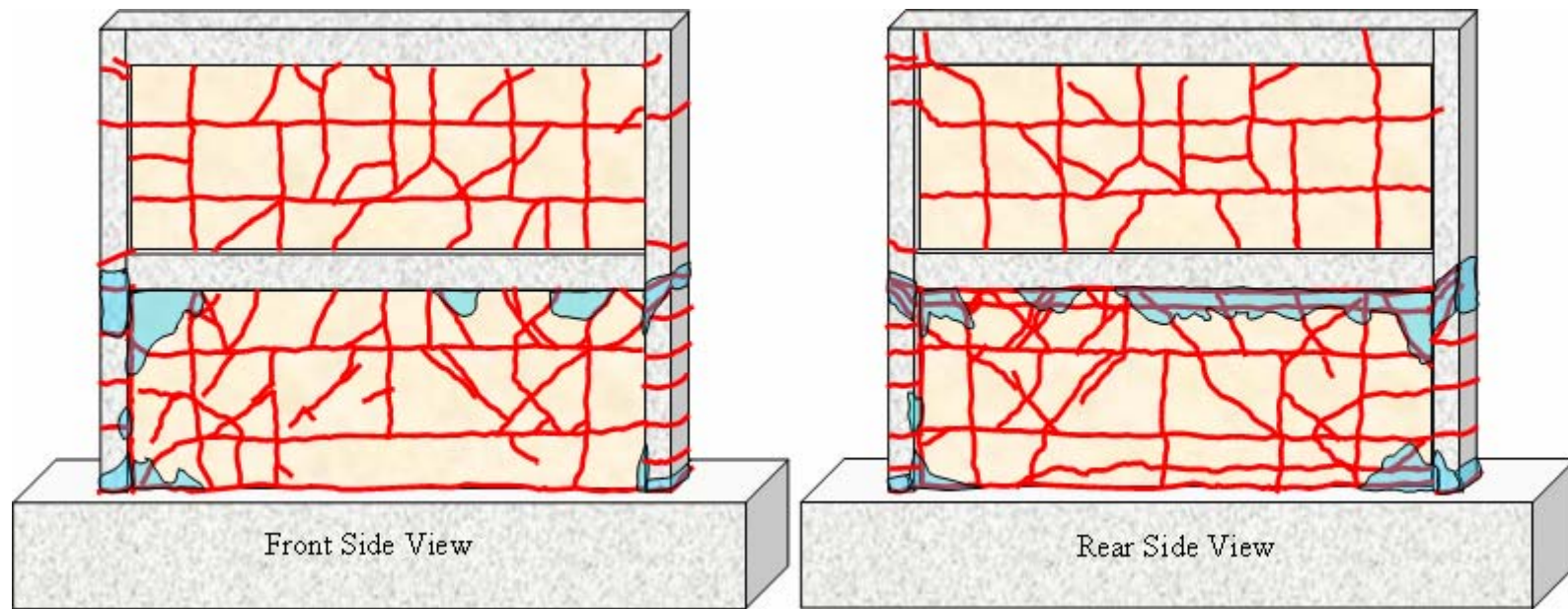
Figure 5.102. Front and Rear Side Crack Profiles of Specimen **WRC**

5.5. 3D Shake Table Tests

In addition to quasi-static RC frame tests on 2D specimens in M.E.T.U. Structural Mechanics Laboratory, dynamic shake table tests were also performed on 3D RC frame specimens in IZIIS, Skopje-Republic of Macedonia within the NATO Science for Peace Project, S*f*P 977231. (**Özcebe, G. et. Al, 2000**) These tests were realized in oder to verify the effectviness of PC panel application under dynamic loading conditions. Total of two, 3D RC frame specimen tests were conducted in this research; one being the reference specimen with hollow brick infills and the other as rectangular PC panel strengthened specimen. The specimens were similarly constructed in a seismically deficient fashion as 2D RC frame specimens, also having lap-splice deficiency on the column longitudinal reinforcement. Series of dynamic loadings were applied to the specimens on the shake table. In these tests, acceleration and displacements measurements over different locations were recorded and evaluated. Dynamic shake table tests also confirmed the considerable seismic performance improvement of RC frames by PC panel application. Brief information about shake table test specimens, dynamic loading and test results are presented in this section.

5.5.1. 3D Test Specimens

Total of two, 1:3 scale 3D frame specimens were subjected to dynamic shake table testing. The dimensional details of 3D specimens are provided in **Figure 5.103**. The first specimen was the reference specimen **SR**, mid-bay of which was infilled by hollow clay bricks and previously tested within the project studies. (**Garevski et.al, 2004**) The second specimen was the rectangular PC panel strengthened frame, **SS**. However, strengthened specimen **SS** was modified by two times and subjected to various loadings by the names of **SS-LR** and **SS-LRM** as explained in **Table 5.1**. Commonly observed structural deficiencies were introduced into both 3D specimens being identical to 2D specimens of the present research. In addition, lap-splice deficiencies of longitudinal column reinforcement were also introduced to the models. The column reinforcement was spliced at floor levels with a lap-splice length of 160 mm (20Φ) and the lap-splice length of the column longitudinal bars at foundation level

197

was 320 mm (40Φ). Hollow clay bricks were provided from M.E.T.U. Structural Mechnaics Laboratory selected from the same batch as the ones used in 2D frame specimens. Mechanical properties of steel reinforcement used in the 3D model preparations were almost the same as the ones used in 2D frame specimens. Reinforcement diamaters and detailing were also identical to the 2D frame specimens. Compressive strength of frame elements, slabs, PC panel concrete and mortar were 15.0 MPa, 30.2 MPa, 45.6 MPa and 5.2 MPa, respectively. Detailed information about the 3D model design, properties of the test specimens, dynamic loading system and procedure are presented by (**Garevski et.al, 2004**).
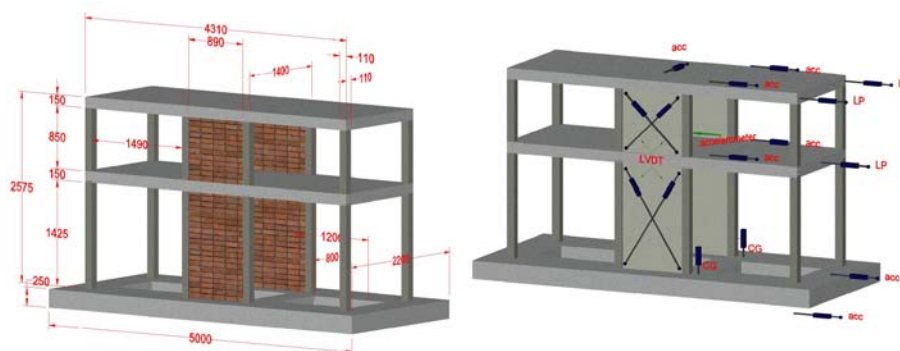
Figure 5.103. Geometric Dimensions (in mm) and Instrumentation of 3D Model

Only the central-bay of the 3D specimen on the longitudinal frame was infilled by hollow clay bricks and strengthened by rectangular shaped PC panels. The PC panel application procedure presented in **Section 3.5.2** was followed using the same kinds of epoxy mortars and diameters of anchorage dowels. Anchorage dowels were provided on all faces of infills of the strengthened specimen as viewed in **Figure 5.104**.

Figure 5.104. General Views from PC Panel Application to 3D Specimen

Table 5.1. Designation and Descriptions of the 3D Test Specimens

Specimen	Description	Ilustration
SR	Reference specimen with hollow brick infills in central-bay of longitudinal frame in both first and second storeys.	
SS	Central-bay of both longitudinal frames were strengthened by rectangular PC panel application.	
SS-LR	On the specimen **SS**, the lap-spliced reinforcement of the columns at the foundaton level were retrofitted and then covered by epoxy mortar.	
SS-LRM	On the specimen **SS-LR**, in addition to the retrofit in lap-splices on the foundation level, new masses were placed in both floor levels.	
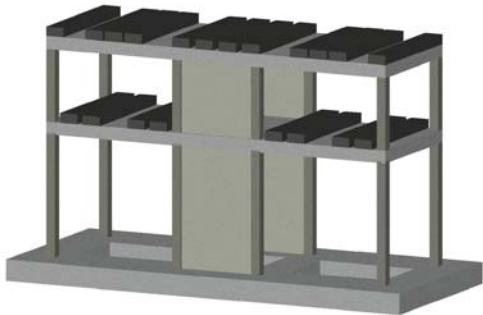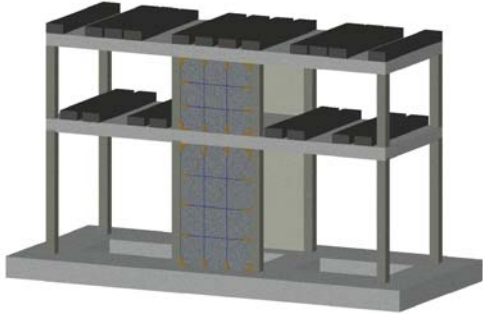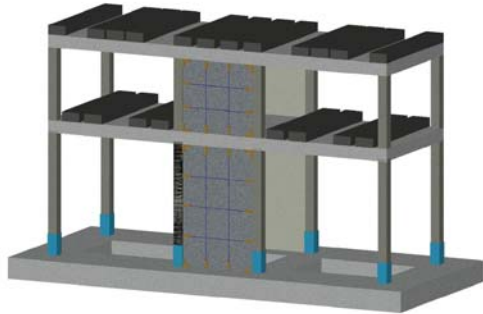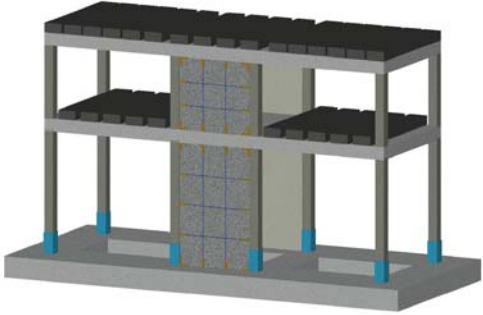
5.5.2. Applied Dynamic Loadings and Test Results

Dynamic loading tests were realized in IZIIS, using the DYNLAB dynamic loading system. Excitations were applied to the models along the longitudinal frame direction. (**Garevski et.al, 2004**) E-W direction earthquake record of 1999 İzmit Earthquake, presented in **Figure 5.105**, was applied to both specimens **SR** and **SS** as series of dynamic loadings by scaling. The applied excitations and corresponding response of specimen **SR** are presented in **Table 5.2**.
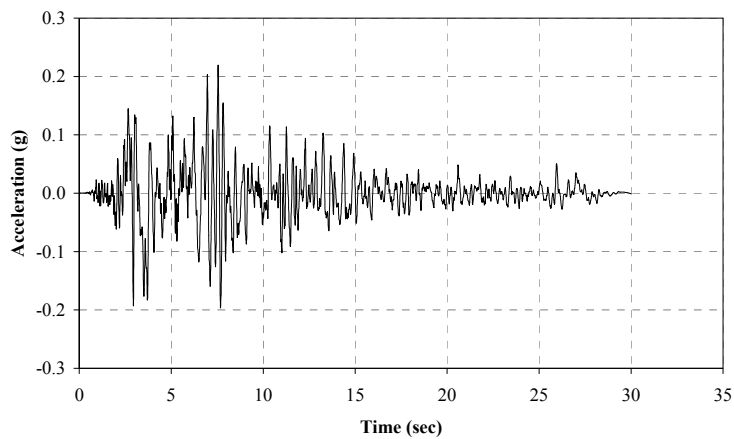
Figure 5.105. Original 1999 İzmit Earthquake Acceleration Record in E-W Direction

Table 5.2. Maximum Values of Input Excitations and Corresponding Response of Reference Specimen **SR**

Excitation ID	input (system)		first floor		second floor	
	abs. acc. (g)	displ. (mm)	abs. acc. (g)	rel. displ. (mm)	abs. acc. (g)	rel. displ. (mm)
Span 35	0.02	3.27	0.03	6.10	0.05	6.14
Span 90	0.06	8.82	0.08	17.67	0.12	17.30
Span 180	0.11	16.25	0.15	32.64	0.18	32.85
Span 360	0.20	33.77	0.28	69.39	0.31	70.64
Span 500	0.26	48.63	0.34	105.50	0.40	106.87
Span 750	0.45	73.01	0.35	163.01	0.42	168.25

Soon after the series of dynamic loading presented in **Table 5.2** applied, specimen **SR** failed by crushing of hollow brick infills and occurence of plastic hinges at beam and column ends as depicted in **Figure 5.106.** The test series of this specimen was terminated as the specimen experienced 0.45g of input acceleration with almost 11% of interstorey drift ratio measured for the first floor.

Figure 5.106. Views of Specimen **SR** at the end of Series of Dynamic Loadings

Table 5.3 presents the summary of dynamic loading data and corresponding response of strengthened specimen **SS**. The first two steps of dynamic loading applied to specimen **SR** was initially applied specimen **SS.** Since, these tests resulted in very low level of storey displacements compared to that of specimen **SR**, the magnitude of the following dynamic loadings was then directly increased as can be seen in **Table 5.3.**

Table 5.3. Maximum Values of Input Excitations and Corresponding Response of Specimen **SS**

Excitation ID	input (system)		first floor		second floor	
	abs. acc. (g)	displ. (mm)	abs. acc. (g)	rel. displ. (mm)	abs. acc. (g)	rel. displ. (mm)
Span 35	0.03	3.88	0.04	0.56	0.05	0.56
Span 90	0.08	8.51	0.07	1.96	0.10	2.80
Span 620	0.43	70.66	0.39	11.01	0.53	14.24
Span 650	0.50	79.28	0.41	11.51	0.65	16.36
Span 700	0.53	85.39	0.39	14.33	0.53	22.40

It was clearly observed that, PC panel application considerably improved seismic behaviour of the 3D model when the lateral displacement response of specimen **SS** is compared with that of specimen **SR.** However, the inadequate lap-splice lengths of the column longitudinal bars at foundation level resulted in rocking of the central-bay as shown in **Figure 5.107.** In order to eliminate this deficiency, the cover concrete was removed and then the lap-splices on first storey column bases were retrofitted by point welding of a Φ12 deformed bar to both pieces of the lapped reinforcements. Soon after the welded points cooled, the section was covered by epoxy mortar and this modified specimen was named **SS-LR**. **Table 5.4**. shows the summary of applied dynamic loadings and corresponding response of the retrofitted specimen **SS-LR**.

Figure 5.107. Seperations of the Mid-bay Base due to Rocking

Table 5.4. Maximum Values of Input Excitations and Corresponding Response of Specimen **SS-LR**

Excitation ID	input (system)		first floor		second floor	
	abs. acc. (g)	displ. (mm)	abs. acc. (g)	rel. displ. (mm)	abs. acc. (g)	rel. displ. (mm)
Span 650	0.40	65.28	0.33	11.01	0.48	14.33
sinesweep 4-7 Hz	0.09	4.00	0.12	13.09	0.17	23.38
sinesweep 5.5-7 Hz	0.07	3.34	0.12	13.95	0.20	23.71
sinesweep 3-7.72 Hz	0.08	4.01	0.13	14.92	0.20	25.06

Specimen **SS-LR** was first subjected to scaled Izmit acceleration record by reaching 0.40g system acceleration. The maximum interstorey drift ratio for the first floor reached to 0.73% without any remarkable damage. The system was then loaded to three series of sinusoidal loadings, one of which is illustrated in **Figure 5.108**. At the end of these loadings, the first storey interstorey drift ratio reached almost 1%. At this drift level, no remarkable damage was observed over the PC panel strengthened specimen.
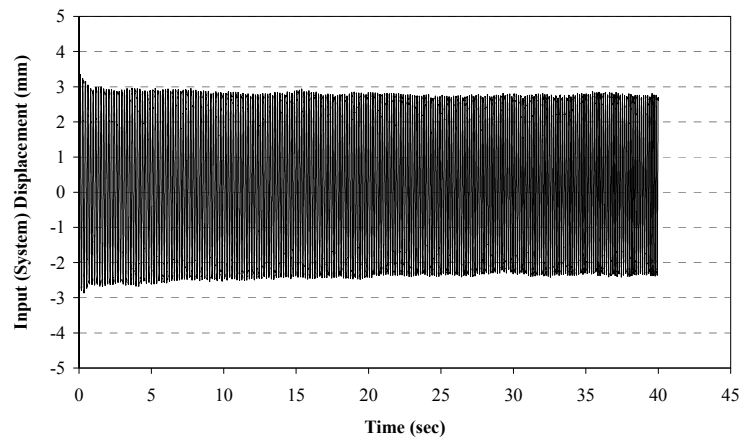
Figure 5.108. Sinusoidal Loading for Specimen **SS-LR** for
Loading Case of Sinesweep 5.5 – 7 Hz

Since two series of dynamic loading did not result in a considerable level of structural damage together with storey displacements, the 3D model of **SS-LR** was further modified. The test specimens were regarded as the model of a four storey prototype structure and the mass simulation was realized by locating the ballast blocks as illustrated in **Table 5.1.** (**Garevski et.al, 2004**). In order to excite the PC panel strengthened specimen to result in considerable level of damages, the mass was increased to simulate a six storey building and this modified specimen is called as **SS-LRM**. Since, sinusoidal loadings and Izmit earthquake records were previously applied to the specimen, two types of impulsive loadings were further applied to specimen **SS-LRM** as shown in **Figure 5.109**. The summary of the applied loading and response of specimen **SS-LRM** are presented in **Table 5.5**. The specimen reached almost 3% of first storey interstorey drift ratio at the fourth dynamic loading together with flexural cracks at the beam levels and plastic hinging at the beam and column ends. However, no structural damage to strengthened infill was observed. The test was terminated at this stage.
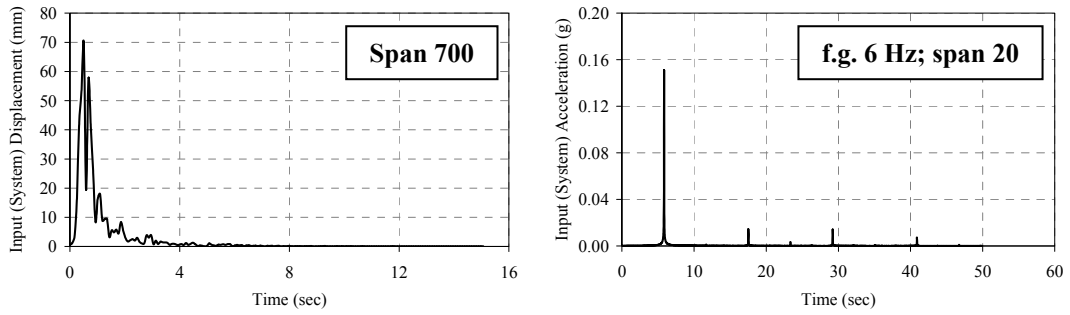
Figure 5.109. Loading Schemes for Specimen **SS-LRM**

Table 5.5. Maximum Values of Input Excitations and Corresponding Response of Specimen **SS-LRM**

Excitation ID	input (system)		first floor		second floor	
	abs. acc. (g)	displ. (mm)	abs. acc. (g)	rel. displ. (mm)	abs. acc. (g)	rel. displ. (mm)
Span 650	0.02	66.20	0.03	1.19	0.04	2.58
Span 700	0.02	69.50	0.03	1.62	0.04	3.41
f.g. 6 Hz; span 20	0.15	9.03	0.07	4.45	0.19	3.65
f.g. 6 Hz; span 50	0.32	22.68	0.11	44.42	0.24	90.26

Front and rear side views of PC panel strengthened specimen **SS** at the end of the above mentioned modifications and dynamic testing series are presented in **Figure 5.110**.

Figure 5.110. Front and Rear Side views of PC panel strengthened specimen **SS** at the end of Dynamic Testing Series

204

5.5.3. Conclusions

Hollow brick infilled reference and rectangular shaped PC panel strengthened 3D frame specimens were subjected to dynamic loading in order to verify the effectiveness of PC panel application under dynamic loading conditions. The following conclusions can be drawn from dynamic shake table test results of 3D model specimens.

- PC panel application considerably improved the seismic behaviour of 3D frame specimens with structural deficiencies. At the dynamic load level at which the hollow brick infilled specimen **SR** failed (0.45g of input acceleration and 11% of first floor interstorey drift), the PC panel strengthened specimen **SS** experienced (0.43g of input acceleration and 0.73% of first floor interstorey drift ratio) without any observable structural crackings or damage.
- As the dynamic loading intensity was increased, the lap-splice deficiency of the longitudinal column bars started to dominate the behaviour by rocking the strengthened central-bay. The retrofit of the lap-splice deficiency at first storey column bases avoided rocking action and resulted in monolithic behaviour of the PC panel strengthened bay together with the remaining of the 3D frame system.
- PC panel strengthened specimen did not experience remarkable level of damage on the structural elements by the end of the tests conducted over specimen **SS-LR**. As the mass increased and the loading was applied in impulsive manner, structural damage was observed on the frame elements
- It can be concluded that, PC panel application has been shown to be also very effective for also deficient 3D frame systems subjected to severe dynamic loading conditions. The effectiveness of the method can be increased by proper lap-splice retrofits over the column longitudinal bars.

CHAPTER 6

EVALUATION OF TEST RESULTS

6.1. General

In this chapter, the RC frame test results are evaluated in terms of lateral strength, stiffness, energy dissipation, ductility and interstorey drift characteristics. Each set of test data is compared with that of upper and lower bound references for all specimen groups. Summary of all test results are presented in **Table 6.1.** Total lateral load – top displacement curves of all specimens, are drawn to a common scale and presented in **Figure 6.1**. Furthermore, front and rear side crack patterns of all specimens are also presented in **Figure 6.2** and **Figure 6.3**, respectively.

6.2. Response Envelopes

Response envelope curves are generated by connecting the peak points of each forward and backward cycles of the hysteretic total lateral load-top displacement curves of the specimens. These curves, drawn to a common scale for all, are valued to make comparisons of lateral strength in both forward and backward directions and to evaluate the post-peak behaviour and effect of test variables such as panel type. Response envelope curves of all specimens are plotted in **Figure 6.4**. In addition, response envelope curves were also generated for each narrower, standard and wider series of specimens and presented in **Figure 6.5**, **Figure 6.6** and **Figure 6.7**, respectively.

Table 6.1. Summary of Test Results

| Specimen | Panel Type | Axial Load Level (N/No) | Compressive Strength (MPa) | | | Forward Loading | | | Backward Loading | | | Initial Stiffness Indicator (kN/mm) | Cumul. Energy Dissip. (kN.m) | Disp. Ductility Ratio (Δ_u/Δ_y) |
			Frame	Panel	Mortar	Max. Load (kN)	1st Storey Drift Ratio (Δ_1/h_1)	2nd Storey Drift Ratio ($(\Delta_2-\Delta_1)/h_2$)	Max. Load (kN)	1st Storey Drift Ratio (Δ_1/h_1)	2nd Storey Drift Ratio ($(\Delta_2-\Delta_1)/h_2$)			
NB	-	0.15	7.9	-	-	8.4	0.0189	0.0151	7.6	0.0189	0.0134	1.1	2.1	5.7
NR	-	0.08	19.0	-	5.0	34.5	0.0032	0.0055	35.1	0.0088	0.0073	10.9	2.5	6.4
NRP	rec.	0.10	14.5	48.0	5.0	66.4	0.0098	0.0164	64.0	0.0092	0.0164	15.2	18.8	8.7
NSP	strip	0.10	13.8	48.0	5.0	64.3	0.0045	0.0061	62.0	0.0045	0.0068	26.1	13.7	9.2
NRC	RC infill	0.09	16.0	16.0	-	68.4	0.0106	0.0108	70.1	0.0104	0.0091	21.7	15.7	7.8
SB	-	0.10	13.7	-	-	13.6	0.0130	0.0115	13.4	0.0173	0.0138	1.2	3.7	5.0
SR	-	0.11	12.2	-	5.5	78.3	0.0076	0.0035	75.5	0.0056	0.0059	57.5	6.2	6.0
SRP	rec.	0.12	11.9	55.7	3.5	187.5	0.0151	0.0149	177.4	0.0164	0.0165	128.9	35.1	6.3
SSP	strip	0.09	16.1	58.0	5.8	172.0	0.0178	0.0167	175.4	0.0148	0.0194	137.4	33.7	7.9
SRC	RC infill	0.10	15.0	23.1	-	189.7	0.0096	0.0068	189.4	0.0087	0.0093	232.9	26.0	8.4
WB	-	0.10	14.9	-	-	15.4	0.0295	0.0109	13.8	0.0221	0.0085	1.4	4.2	2.9
WR	-	0.09	17.6	-	5.1	87.8	0.0048	0.0034	82.3	0.0047	0.0055	122.3	12.8	8.0
WRP	rec.	0.09	16.2	55.8	5.4	166.6	0.0046	0.0004	160.1	0.0046	0.0057	188.2	25.9	9.9
WSP	strip	0.11	12.8	62.1	5.3	178.1	0.0048	0.0039	164.7	0.0036	0.0064	240.2	37.4	7.4
WRC	RC infill	0.11	13.6	16.4	-	186.8	0.0164	0.0126	163.1	0.0171	0.0121	267.3	41.6	7.4
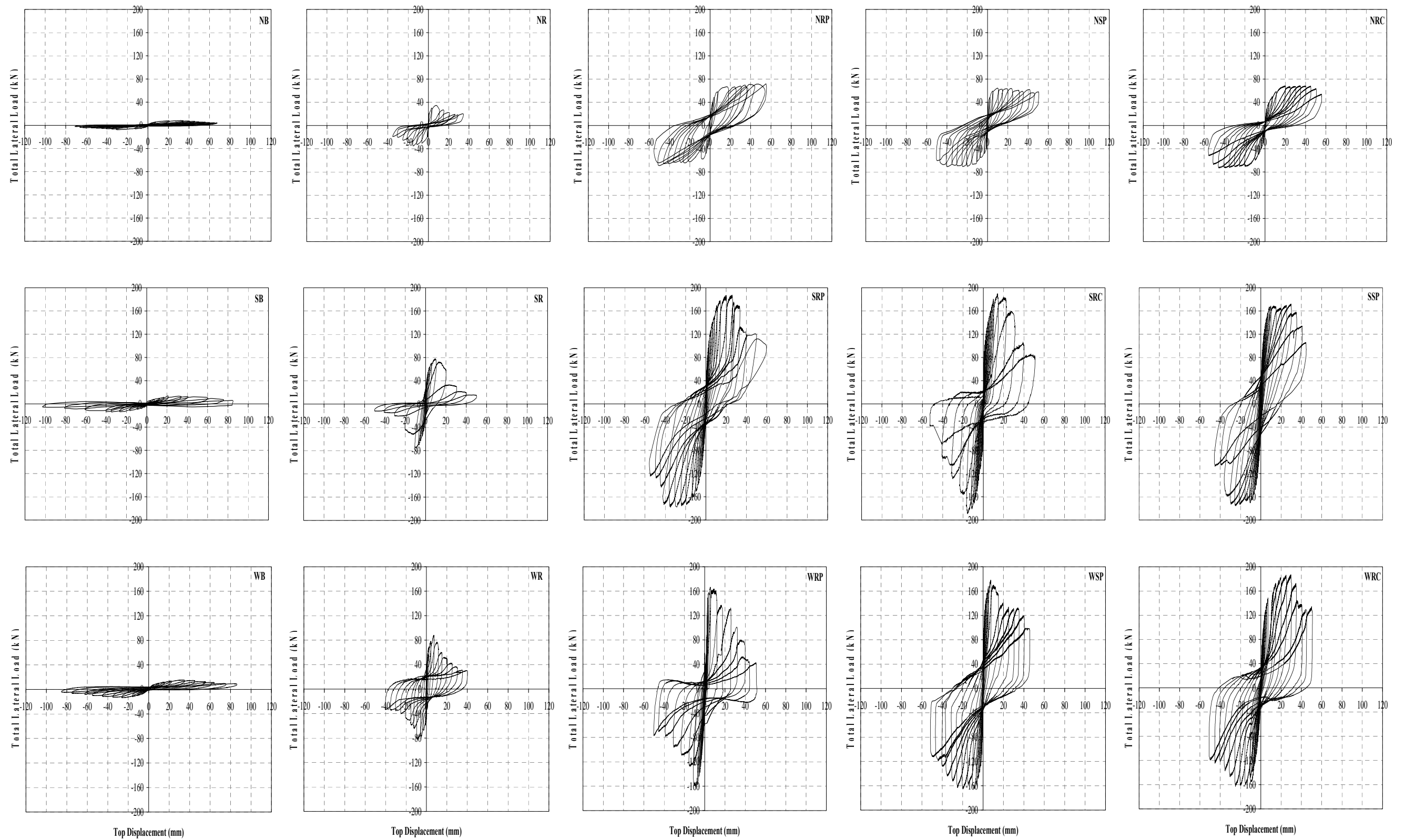
Figure 6.1. Total Lateral Load – Top Displacement Curves of All Series of Specimens
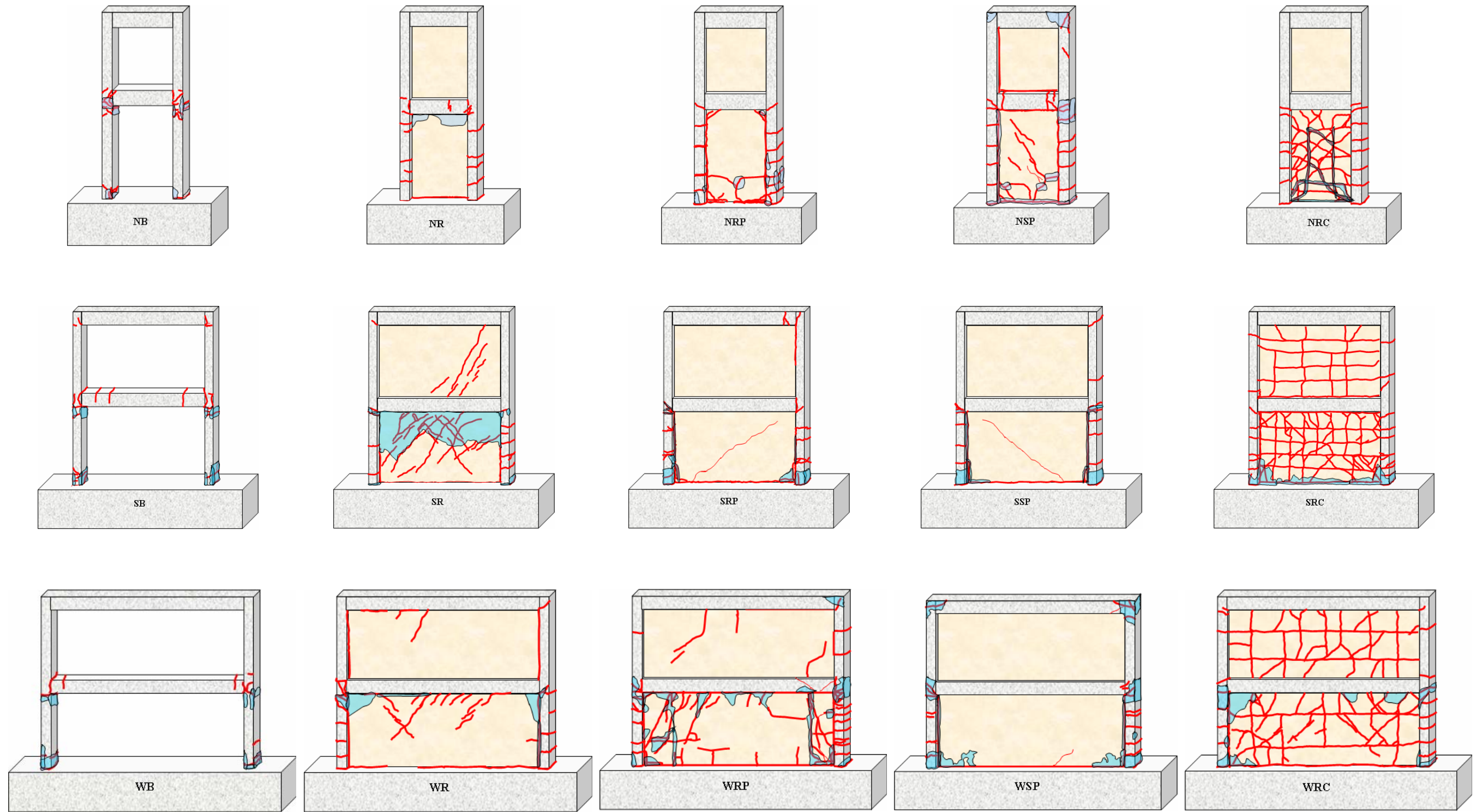
Figure 6.2. Front Side Crack Patterns of All Series of Specimens
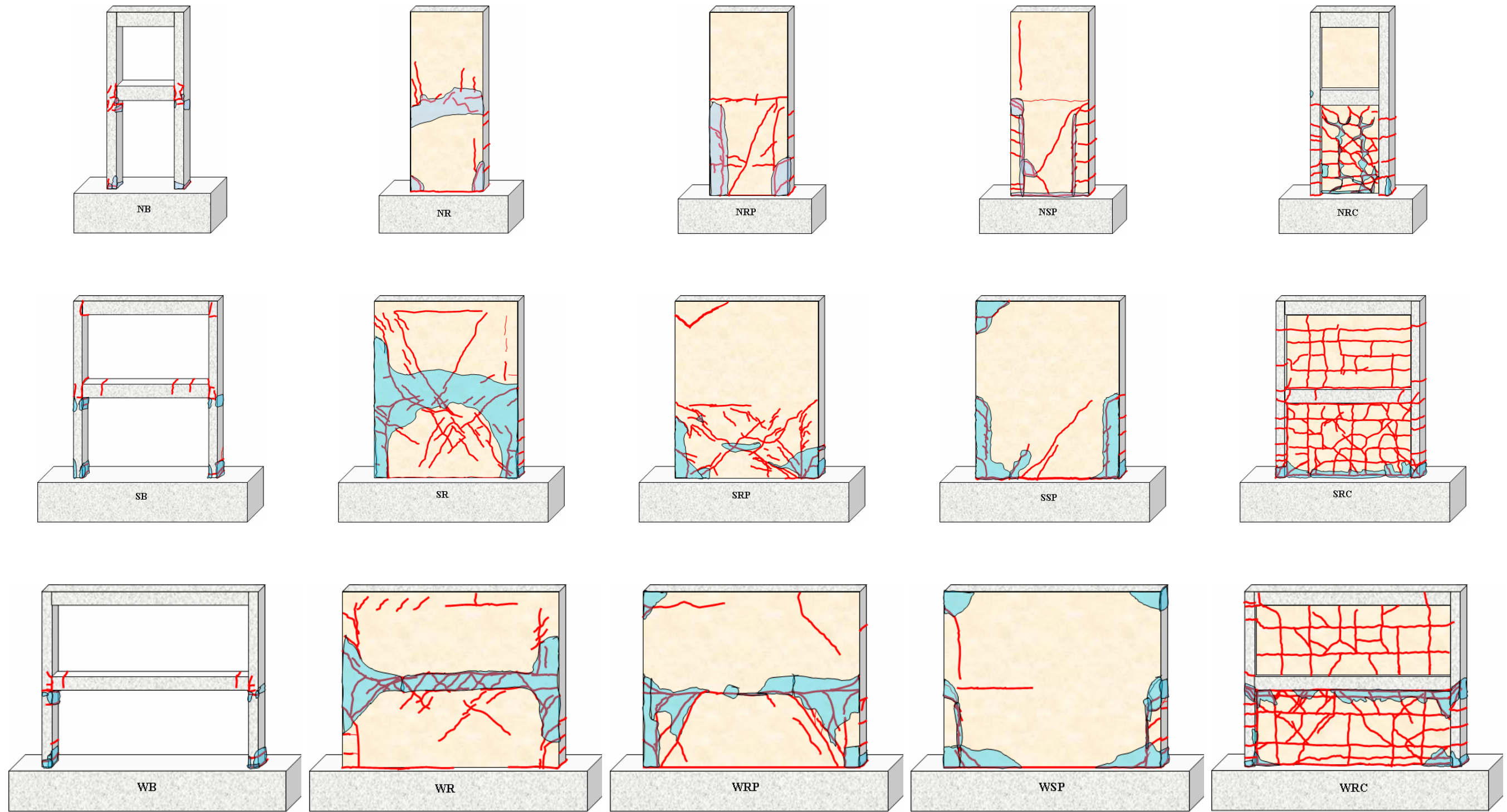
Figure 6.3. Rear Side Crack Patterns of All Series of Specimens

210
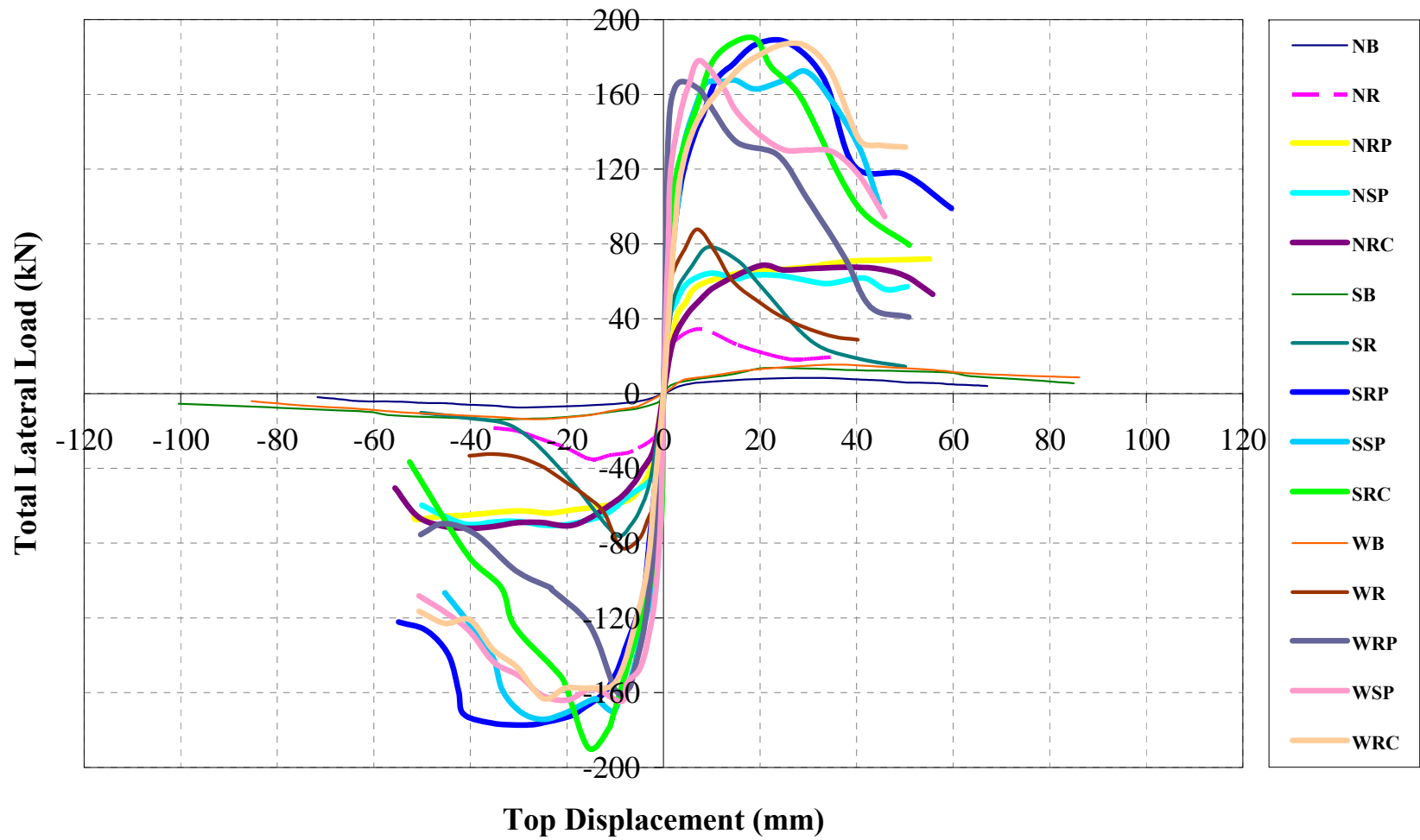
Figure 6.4. Response Envelope Curves of All Groups of Specimens

Response envelope curves clearly indicate the contribution of infill to overall frame behaviour when the bare frames and hollow brick infilled specimens are compared. Furthermore, the significant improvement of lateral strength and stiffness of the specimens as a result of PC panel application is also evident in **Figure 6.4**.

The specimen behaviour in both forward and backward directions was almost the same for all specimens. However, in evaluation of lateral load capacities of forward and backward directions, it is generally observed that the capacity over the backward direction lowers from that of the forward direction by ~2% for narrower and standard series and 8% for wider series of specimens. This behaviour may be attributed to incremental damage caused by each cycle of loading. Since the loading started first over the forward direction in the experiment, the specimen was naturally subjected to a pre-deformation (strain) prior to the opposite, backward, direction loading. This effect may have provided lower lateral load capacities of backward direction when compared to that of forward direction.

In **Figure 6.5**., response envelope curves of narrower series specimens are all plotted together. It is obvious that, specimen **NR** exhibits the RC frame behaviour with the strength degradation after reaching the ultimate load carrying capacity due to separation of infill from the column surfaces and crushing of the brittle hollow brick infill. As the infill wall separated from the columns, the frame almost lost its rigidity. Lateral strength increase of the two PC panel strengthened specimens **NRP** and **NSP** with respect to the lower bound reference, **NR**, is clearly observed in both forward and backward directions. Moreover, the strength increase with PC panel application for specimens **NRP** and **NSP** is almost the same as the cast-in-place RC infilled, upper bound reference specimen **NRC**. Specimen **NSP** initially behaved stiffer than both strengthened specimens **NRP** and **NRC**, while the post-peak behaviour of strengthened specimens **NRP** and **NSP** are nearly the same as specimen **NRC**; all providing almost no strength degradation. None of the specimens **NRP**, **NSP** and **NRC** provided significant strength degradation beyond the peak by 15% of its lateral load carrying capacity, reflecting the ductile frame behaviour.
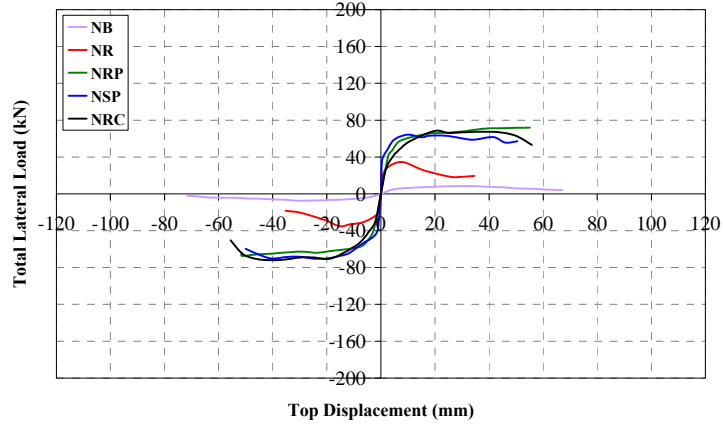
Figure 6.5. Response Envelope Curves of Narrower Series of Specimens
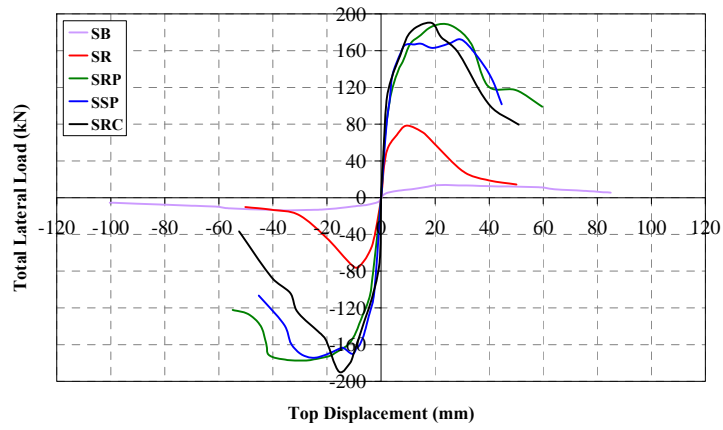
Figure 6.6. Response Envelope Curves of Standard Series of Specimens

Figure 6.7. Response Envelope Curves of Wider Series of Specimens

213
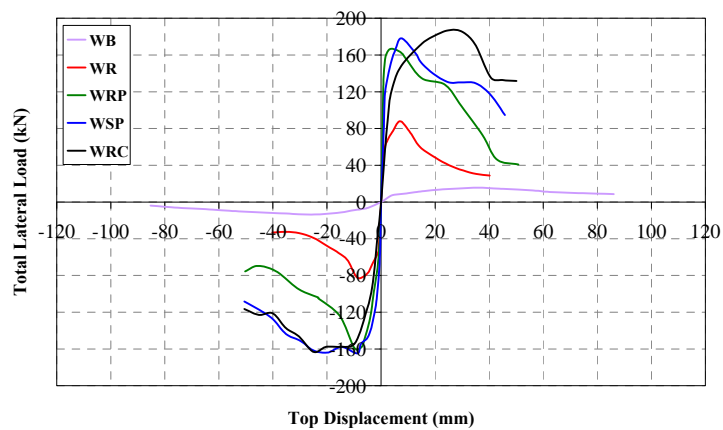
In **Figure 6.6**, response envelope curves of standard series specimens are all plotted together. The lower bound reference specimen, **SR**, exhibits the RC frame behaviour with post-peak strength degradation due to diagonal cracking and crushing of the hollow brick infill. It also proved the positive contribution of infill on the performance of the RC frame under lateral loading when compared to specimen **SB**. The behaviour of PC panel strengthened specimens **SRP** and **SSP** are clearly superior to the lower bound reference specimen, **SR**. Lateral stiffness of specimen **SRC** is observed to be higher than that of PC panel strengthened specimens, since this specimen reached its lateral loading capacity at lower levels of top displacements in both directions. Lateral strength improvement by rectangular PC panel application is observed to be higher than that of strip panel when specimens **SRP** and **SSP** are compared. This may be attributed to the better anchoring properties in between the frame elements and PC panels of specimen **SRP** when compared to specimen **SSP**. Furthermore, the lateral strength of PC panel strengthened specimen **SRP** is almost equal as the upper bound reference, specimen **SRC** in the forward direction while the lateral load carrying capacity of specimen **SRP** is slightly lower in the backward direction. All strengthened specimens displayed strength degradation in the post-peak range due to diagonal shear cracks either on the PC panel surface or plaster, and infill crushing. The strength degradation rate of specimen **SRC** is higher than the other PC panel strengthened specimens **SRP** and **SSP**; while this rate is observed to be minimum for specimen **SRP**.

In **Figure 6.7.**, response envelope curves of wider series specimens are all plotted together. Similar to other group of specimens, lower bound reference specimen **WR** provided RC frame behaviour with post-peak strength degradation due to diagonal shear cracking on the infill surface and crushing of the infill. In addition, the contribution of infill on overall RC frame behaviour is remarkable when the specimens **WB** and **WR** considered. Response envelope curves of specimens **WRP** and **WSP** clearly indicate the superior behaviour gained with PC panel application over the lower bound reference, **WR**.

Among the PC panel strengthened specimens, specimen **WRP** provided a little less lateral strength improvement when compared to specimen **WSP**. This behaviour can be

attributed to existence of lateral lap joints of rectangular PC panels together with less number of anchorage dowels on the storey basement and upper beam levels compared to specimen **WSP**. Post-peak strength degradation of specimen **WRP** is also relatively faster, especially in the backward direction. Specimen **WSP** provided a lateral load carrying capacity in both forward and backward directions being almost equal to upper bound reference specimen **WRC**. Post-peak strength degradation of both specimens **WSP** and **WRP** are almost coinciding with each other in the backward direction, while specimen **WRC** performs relatively better in the forward direction.

Response envelope curves of bare frames are presented in **Figure 6.8** with a larger vertical scale. The response envelope curves of hollow brick infilled frames, strip PC panel strengthened frames, rectangular PC panel strengthened frames and cast-in-place RC infill strengthened frames are depicted in **Figure 6.9.**
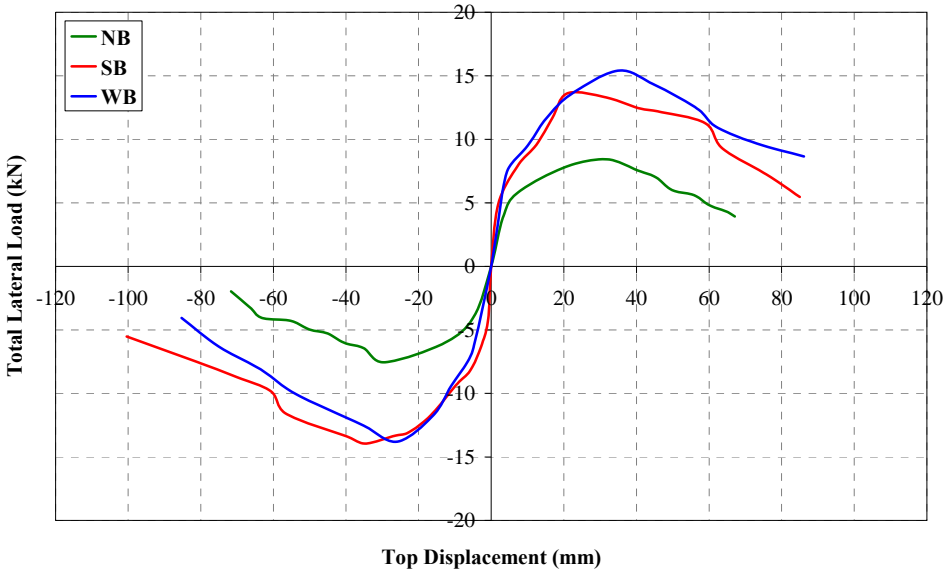
* 10 times larger vertical scale compared to the presentations in **Figure 6.9**.

Figure 6.8. Response Envelope Curves of Bare Frames

The lateral load carrying capacity of the bare frames inceases as the aspect ratio increases as can be seen in **Figure 6.8**. The difference is not that significant between standard and wider series of specimens, while it is considerable for narrower series. This observation is almost the same for other groups of specimens presented in **Figure 6.9**. In case of hollow brick infilled and strip PC panel strengthened specimens the order of the lateral load carrying capacity is in the same fashion as the aspect ratio; the higher aspect ratio, the higher lateral load carrying capacity. For rectangular PC panel strengthened specimens, standard series of specimen have slightly higher lateral load carrying capacities compared to that of wider series specimens and similar to the other groups, narrower series of specimen has the least lateral load carrying capacities.
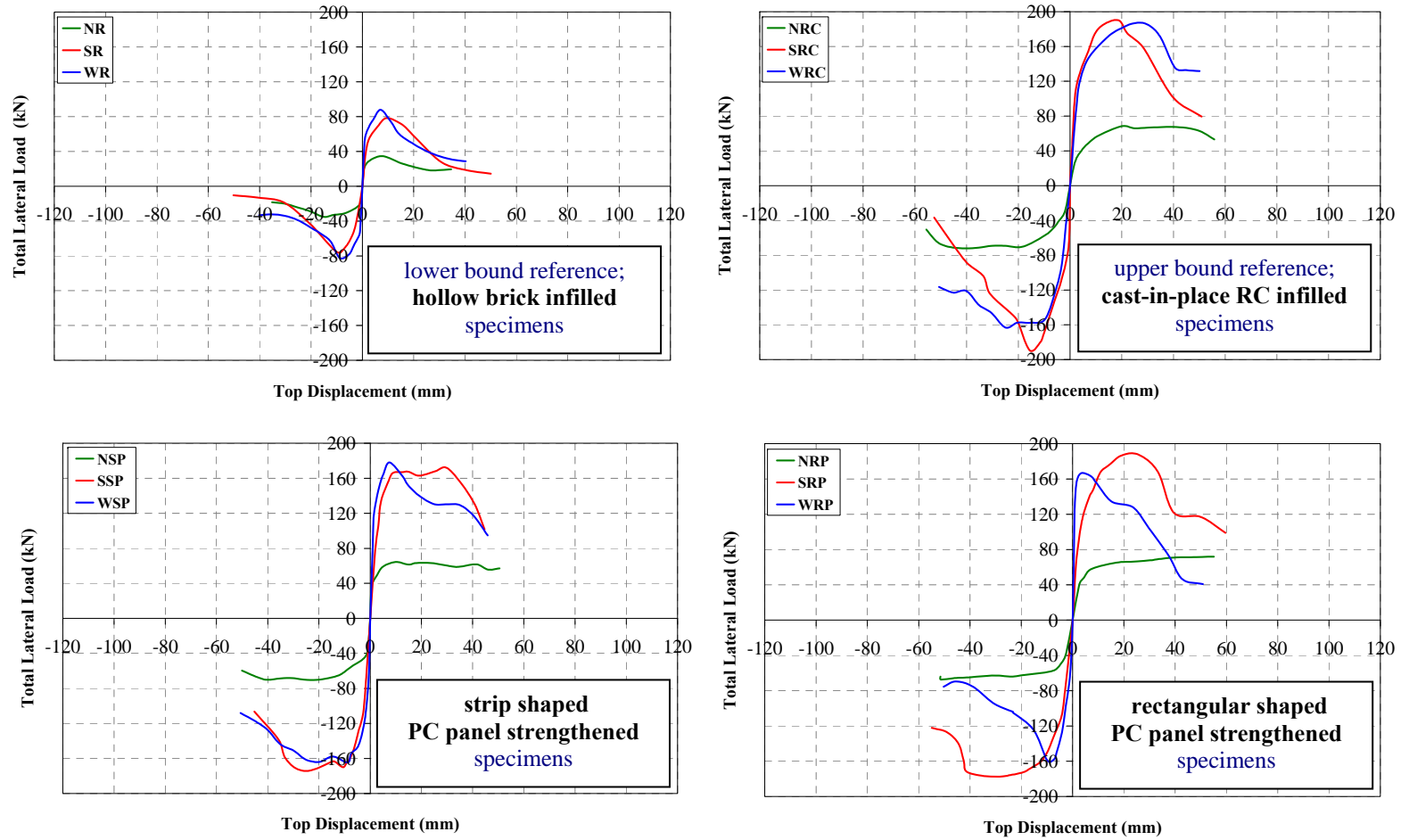
Figure 6.9. Response Envelopes for Upper and Lower Bound Reference and PC Panel Strengthened Specimens

6.3. Strength

Lateral strength improvement with respect to that of hollow brick infilled frame system is one of the major aims of the proposed pre-quake strengthening technique. Since PC panel method is investigated as an alternative to cast-in-place RC infill application, comparison of the lateral strength of the PC panel strengthened specimens with respect to the lateral load carrying capacity of the cast-in-place RC infilled frame is of major importance. The lateral load carrying capacities were investigated in order to evaluate the strength characteristics of the frame specimens. As the base shear-top displacement curves are analyzed, it can be clearly seen that PC panel application considerably increased the lateral strength of RC frame for all three series of specimens. Numerical values of lateral load carrying capacities and the comparisons with respect to the lower and upper bound references are presented in **Table 6.2**.

Table 6.2. Comparison of Lateral Load Carrying Capacities of All Series of Specimens

Specimen	Maximum Forward Load (kN)	Ratio of max. forward load to that of reference specimen		Maximum Backward Load (kN)	Ratio of max. backward load to that of reference specimen	
		Lower Bound*	Upper Bound**		Lower Bound*	Upper Bound**
NB	8.4	0.24	0.12	7.6	0.22	0.11
NR	34.5	1.00	0.50	35.1	1.00	0.50
NRP	66.4	1.92	0.97	64.0	1.82	0.91
NSP	64.3	1.86	0.94	62.0	1.77	0.88
NRC	68.4	1.98	1.00	70.1	2.00	1.00
SB	13.6	0.17	0.07	13.4	0.18	0.07
SR	78.3	1.00	0.41	75.5	1.00	0.40
SRP	187.5	2.39	0.99	177.4	2.35	0.94
SSP	172.0	2.20	0.91	175.4	2.32	0.93
SRC	189.7	2.42	1.00	189.4	2.51	1.00
WB	15.4	0.18	0.08	13.8	0.17	0.08
WR	87.8	1.00	0.47	82.3	1.00	0.50
WRP	166.6	1.90	0.89	160.1	1.95	0.98
WSP	217.3	2.47	1.16	207.2	2.52	1.27
WRC	186.8	2.13	1.00	163.1	1.98	1.00

* : Hollow brick infilled specimen; **NR**, **SR** and **WR**

** : Cast-in-place RC infilled specimen; **NRC**, **SRC** and **WRC**

Experimental results indicate that, hollow brick infill improves the lateral load carrying capacity of bare frame almost four times for narrower series specimens. Both strip and rectangular shaped PC panels enhanced lateral strength of the narrower series of specimens, nearly to the level of improvement by cast-in-place RC infill application. Specimen **NRP** provided relatively higher lateral strength improvement compared to specimen **NSP**. This may be attributed to existence of anchorage dowels between PC panels and columns such that, these dowels prevented the separation of infill composite from the surrounding columns and provided a better monolithical nature, similar to specimen **NRC**.

In case of standard series of specimens, it is observed that hollow brick infill improves lateral strength of bare frame almost six times of that of bare frame. The contribution of PC panel application to lateral strength gain for standard series of specimens is evident when specimens **SRP** and **SSP** are considered. Both PC panel strengthened specimens displayed superior load carrying capacities compared to the lower bound reference specimen **SR**. Moreover, the lateral load carrying capacity of specimen **SRP** is almost equal to upper bound reference specimen **SRC**. This result is not surprising; since the PC panels of specimen **SRP** were effectively connected to frame members due to its anchorage configuration and thus a successful monolithical nature was created similar to specimen **SRC**.

Hollow brick infill improves lateral load carrying capacity of bare frame almost six times that of bare frame for wider series of specimens, being similar to that of the standard series. Lateral load carrying capacities of the strengthened specimens **WRP** and **WSP** are almost equal to upper bound reference specimen **WRC**, in the backward direction; whereas specimen **WRP** has relatively less lateral load carrying capacity in the forward direction when compared to the other two. Specimen **WSP** reached nearly the same lateral strength as specimen **WRC** in the forward direction. This can be attributed to the existence of more numbers of anchorage dowels on the storey basement and upper beam levels, as the behaviour is dominated by shear.

The contribution of PC panel application on shear behaviour of RC frames can be investigated on total lateral load-first storey infill shear displacement curves for all series of specimens as presented in **Figure 6.10**. The first storey shear deformation curves of strengthened specimens of narrower series, as given in **Figure 6.10** clearly indicate the improved flexural behaviour with wider loops and quite visible shear deformations as compared to the lower bound reference specimen **NR**. In addition, the shear deformations of strengthened narrower series specimens are higher, than that of strengthened standard and wider series specimens.

In case of standard and wider series of specimens, the positive contribution of PC panel application on shear deformation behaviour of the first storey infill panels can also be seen in **Figure 6.10**, as well. Strip shaped PC panels significantly decreased the shear deformations due to applied base shear for both strengthened specimens **SSP** and **WSP** Rectangular shaped PC panels provided higher cyclic shear deformations for specimens **SRP** and **WRP** when compared to their anchorage dowel configurations.
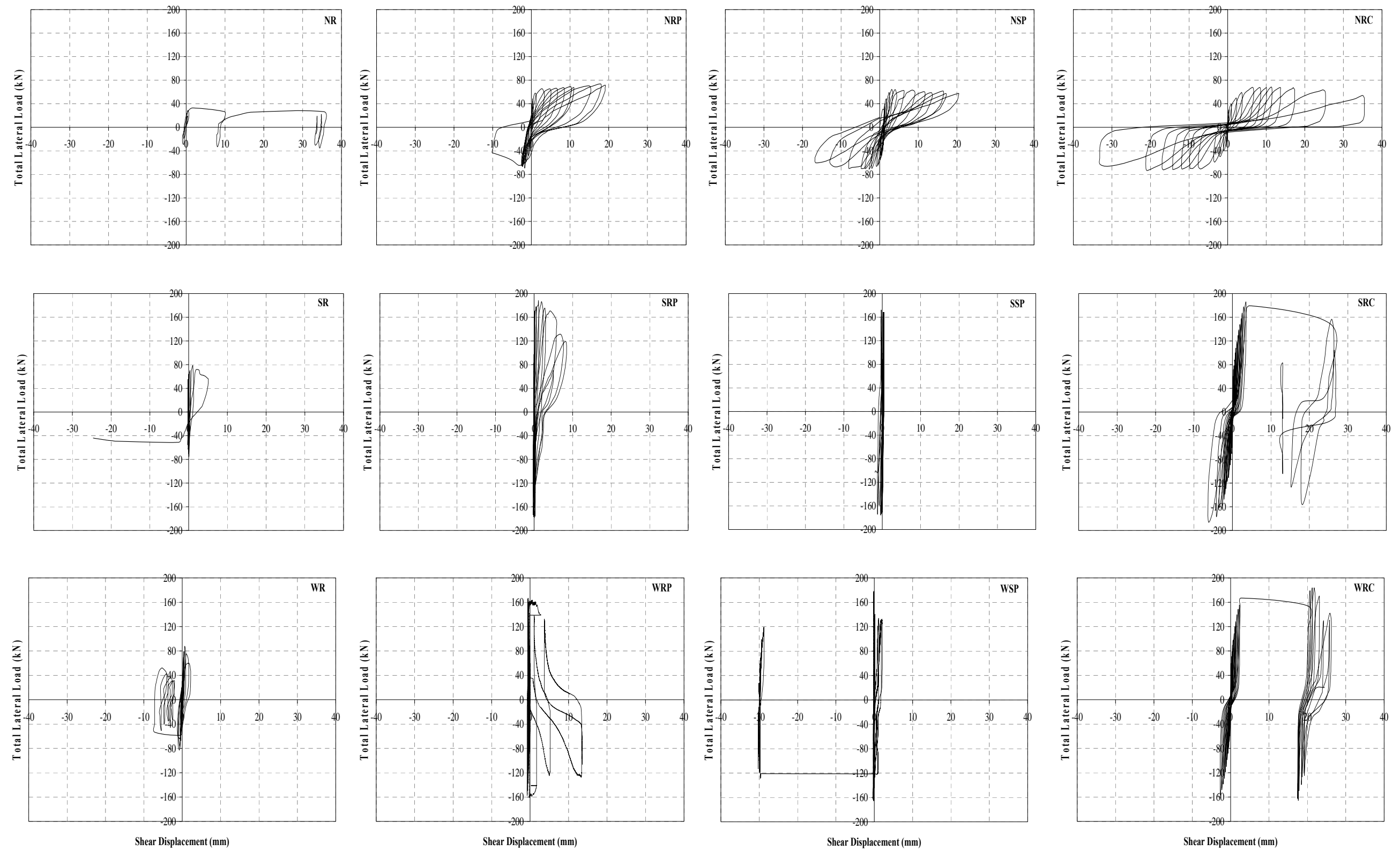
Figure 6.10. Total Lateral Load – First Storey Shear Displacement Curves of All Series of Specimens

221

6.4. Stiffness

Stiffness of a structure defines the resistance of the structure against deformations. As the stiffness of the structure is higher, it is expected the structure to undergo smaller deformations under the same load. Stiffness of a structure is a very important structural performance indicator of the non-structural damage under seismic action. Insufficient lateral stiffness is the major cause of excessive deformation leading to excessive structural damage. This problem was clearly observed in many buildings damaged major earthquakes experienced in Turkey over the last two decades.

Excessive lateral displacements may amplify the load effects on vertical load bearing elements by creating second-order effects which can even lead to failure. In order to limit the interstorey drift of a structure as a result of ground motion, enough lateral stiffness should be provided. The lack of enough lateral stiffness may cause severe damage to non-structural elements, even if it does not cause structural failure. This is another important economic loss. When both structural failure and economic loss due to damage of non-structural elements are of concern, it becomes an important issue to improve stiffness of the structure in case of pre-quake seismic strengthening. Therefore, one of the major aims of PC panel method is to improve lateral stiffness behaviour of the structure. Experimental data were, therefore, investigated in terms of lateral stiffness properties.

Tangent slopes of the experimental hysteretic base shear-top displacement curves were calculated as the stiffness indicator of each cycle. This approach is considered to be acceptable since evaluation of the relative values is essential rather than the absolute values **(Duvarcı, 2003)**. The procedure is depicted in **Figure 6.11** and was also preferred to provide consistency with the previous PC panel method related studies. Stiffness of each cycle was calculated for every specimen and the obtained data were used to draw stiffness degradation curves. The initial stiffness values of all series of specimens are presented in **Table 6.3** together with comparisons with respect to that of reference specimens. In addition, stiffness degradation curves of narrower, standard and

wider series of specimens are presented in **Figure 6.12**, **Figure 6.13** and **Figure 6.14**, respectively.
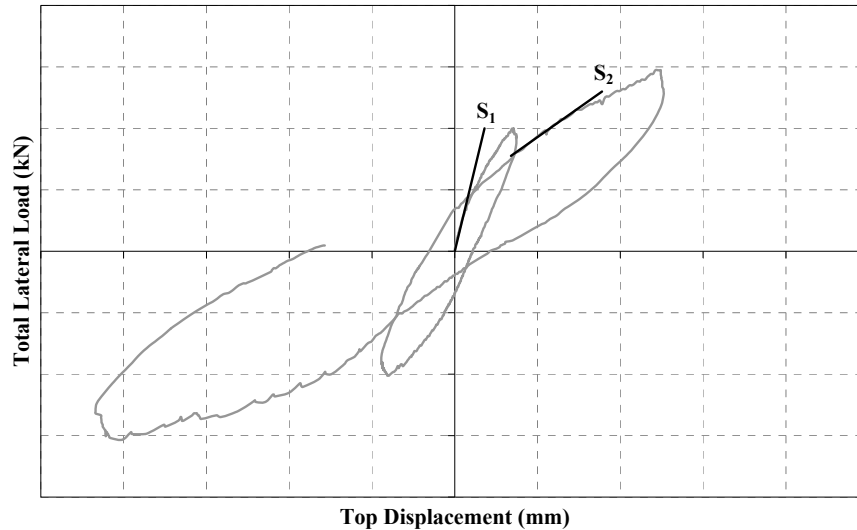
Figure 6.11. Representative Cycle Slopes for Stiffness Calculations

The numerical initial stiffness indicator values given in **Table 6.3** show the significant contribution of hollow brick infill existence to lateral stiffness of RC frames. Hollow brick infill walls increased lateral stiffness of bare frame of narrower series specimen almost ten times; while this ratio is nearly fifty for standard series specimen and ninety for wider series of specimen. As the RC frame behaviour is dominated by shear due to the increase in the aspect ratio, the lateral stiffness improvement by hollow bricks becomes quite remarkable.

Experimental results clearly show the improvement of lateral stiffness of RC frames by PC panel application, for all series of specimens. In all series of specimens, the lateral stiffness improvement by rectangular PC panel application is lower than that of strip shaped PC panel strengthening. This behaviour can be explained by existence of lateral lap joints on infill surface due to panel-to-panel connections and anchorage dowels in between the PC panels and surrounding columns, which can be stated to improve flexibility of the system rather than the lateral rigidity.
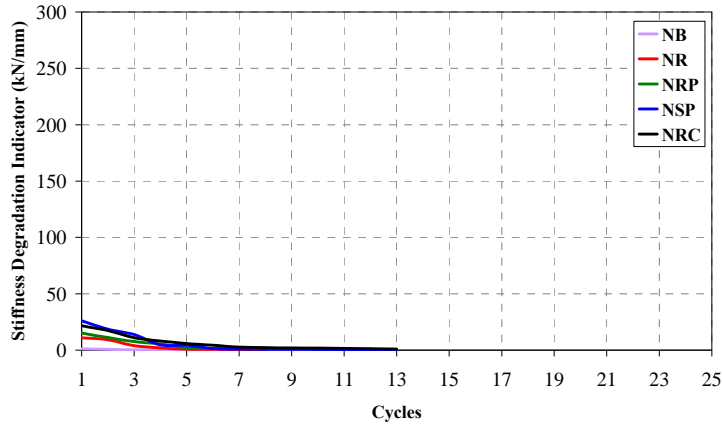
Figure 6.12. Stiffness Degradation Curves for Narrower Series of Specimens
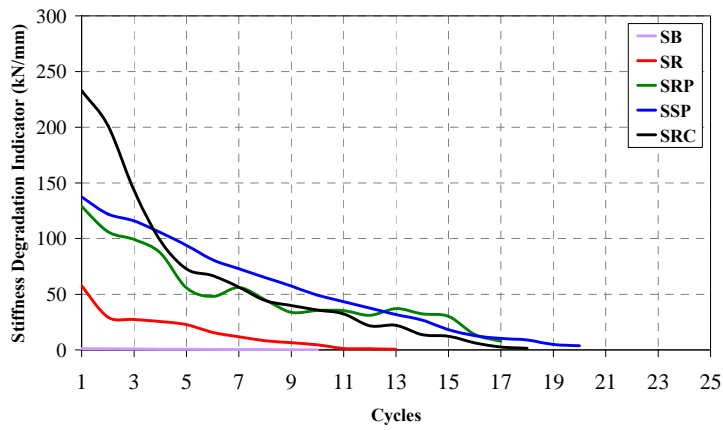
Figure 6.13. Stiffness Degradation Curves for Standard Series of Specimens
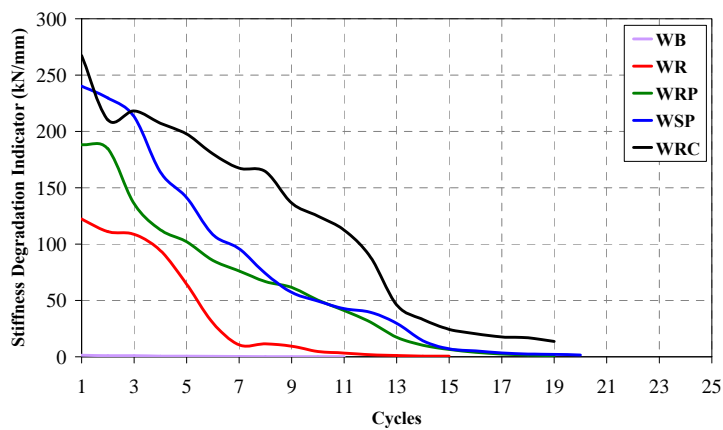
Figure 6.14. Stiffness Degradation Curves for Wider Series of Specimens

Table 6.3. Comparison of Initial Stiffness Indicator Values of All Series of Specimens

Specimen	Initial Stiffness Indicator Value (kN/mm)	Ratio of initial stiffness indicator to that of reference specimen	
		Lower Bound*	Upper Bound**
NB	1.1	0.10	0.05
NR	10.9	1.00	0.50
NRP	15.2	1.39	0.70
NSP	26.1	2.39	1.20
NRC	21.7	1.99	1.00
SB	1.2	0.02	0.01
SR	57.5	1.00	0.25
SRP	128.9	2.24	0.55
SSP	137.4	2.39	0.59
SRC	232.9	4.05	1.00
WB	1.4	0.01	0.01
WR	122.3	1.00	0.46
WRP	188.2	1.54	0.70
WSP	240.2	1.96	0.90
WRC	267.3	2.19	1.00

*　: Hollow brick infilled specimen; **NR**, **SR** and **WR**

** : Cast-in-place RC infilled specimen; **NRC**, **SRC** and **WRC**

In case of narrower series, specimen **NRP** provided initial stiffness improvement almost one and half times of that of lower bound reference specimen **NR**. Strip shaped PC panel strengthened specimen **NSP** had the highest initial stiffness being almost six times of lower bound reference specimen **NR** and three times of that of upper bound reference specimen **NRC**. The upper bound reference specimen of narrower series, **NRC** showed initial stiffness improvement as almost two times of that of lower bound reference **NR**. Stiffness degradation curves of narrower series specimens depicted in **Figure 6.12** also show the significant initial stiffness improvement by strip shaped panels. The stiffness degradation curves of the other strengthened specimens **NRP** and **NRC** are almost parallel to each other. Since the panel strength of specimens **NRP** and **NSP** are the same, the superior initial stiffness behaviour of specimen **NSP** may be

directly linked to the absence of lateral lap joints of PC panels and anchorage dowels to the columns that can be stated to improve the flexibility of the whole RC frame-infill system rather than the lateral rigidity.

Cast-in-place RC infill application provided the highest initial stiffness for standard series of specimens as the numerical values given in **Table 6.4** fortify. The initial stiffness of upper bound reference specimen **SRC** is almost four times of that of lower bound reference specimen **SR**. However, the stiffness degradation rate of specimen **SRC** is significantly higher at the initial cycles, and then almost coincides with the other two PC panel strengthened specimens **SRP** and **SSP** as can be seen in **Figure 6.13**. Strip shaped PC panel application improved the lateral stiffness of the specimen SSP being almost more than two times of that of lower bound reference specimen **SR**. Moreover, stiffness degradation curve of specimen **SSP** is almost linear and parallel to that of specimen **SRC**. Lateral stiffness improvement by rectangular shaped PC panel application is slightly less than that of specimen **SSP**. The higher initial stiffness value of specimen **SSP** may be attributed to not only the absence of lateral lap joints and anchorages to the columns, but also having higher mortar, frame and panel compressive strength.

Strip shaped PC panel strengthened specimen **WSP** and upper bound reference, cast-in-place RC infilled specimen **WRC** had nearly the same initial stiffness values which were almost two times of that of lower bound reference specimen **WR**. Specimen **WRP** gained the least initial stiffness improvement with respect to lower bound reference specimen **WR** with almost 50% of that of specimen **WR**. Stiffness degradation curves of wider series of specimens are presented in **Figure 6.14**. Stiffness degradation rate of PC panel strengthened specimens **WRP** and **WSP** are observed to be higher than that of specimen **WRC**.

6.5. Storey Drift Index

Storey Drift Index is a dimensionless indicator calculated by dividing relative displacements of two storey by storey height and it is preferred to be used as a measure of non-structural damage and controlling second order effects in earthquake engineering terminology. Under seismic excitations, the damage of non-structural elements is mainly indexed to the capacity of the structure to resist excessive relative storey displacements. If the interstorey drift ratios are not controlled by proper structural elements such as shear walls, a moment-resisting RC framed structure may also experience severe damage to the non-structural elements even if it satisfies all requirements of lateral strength, stiffness and ductility provisions. Therefore, storey drift index values of test specimen were also evaluated as one of the seismic performance indicators.

Turkish Seismic Code (TSC) 2007 limits the maximum storey drift index value of the vertical load bearing elements such as columns and shear walls of any storey to 0.02, *in case of seismic design*. **(TSC, 2007)** Total lateral load – first storey drift ratio and drift index curves with respect to the cycles of the test frames are presented in **Figure 6.15** and **Figure 6.16**, respectively to evaluate storey drift behaviour of specimens. The TSC 2007 storey drift index design limit of 0.02 is also shown in both graphical representations as the reference limit.

Storey drift index values corresponding to maximum forward and backward direction load carrying capacities and post-peak storey drift index ratio values in both directions corresponding to the load level with 15% reduction of the maximum load are tabulated in **Table 6.4.** Besides, TSC 2007 also, provides the storey drift index limits for vertical load bearing elements *in case of seismic performance evaluation* of RC framed structures as presented in footnote format for **Table 6.4.**

Since one of the major aims of the proposed pre-quake retrofitting method is also to improve drift properties of the system; it was also intended to evaluate the storey drift index values of the test specimens considering the code provided performance

evaluation limits. The effect of hollow brick infills on first storey drift index ratio quantities for all series of specimens is obvious in **Figure 6.15**. Large amounts of storey drift ratios of bare frames are reduced by existence of hollow brick infills. It can be clearly seen that, lower bound reference specimens **NR**, **SR** and **WR** reached the ultimate lateral load carrying capacities at lower storey drift levels compared to the corresponding bare frames as can be seen in **Table 6.4**. The first storey drift ratios of the lower bound reference specimens at the ultimate are all less than immediate occupancy performance limit of 0.01 as can be seen in **Table 6.4**.

Table 6.4. Storey Drift Ratio Values at Maximum Lateral Load Levels for All Series Specimens

Specimen	Forward Direction				Backward Direction			
	@ F_{max}		@0.85* F_{max} Beyond Peak		@ F_{max}		@0.85* F_{max} Beyond Peak	
	1st Storey	2nd Storey	1st Storey	2nd Storey	1st Storey	2nd Storey	1st Storey	2nd Storey
NB	0.019	0.015	0.036	0.010	0.019	0.013	0.023	0.014
NR	0.003	0.006	0.009	0.004	0.009	0.007	0.012	0.002
NRP	0.010	0.016	0.018	0.020	0.009	0.016	0.026	0.041
NSP	0.005	0.006	0.024	0.025	0.005	0.007	0.025	0.028
NRC	0.011	0.011	0.040	0.016	0.010	0.009	0.036	0.020
SB	0.013	0.012	0.054	0.011	0.017	0.014	0.052	0.016
SR	0.008	0.004	0.014	0.006	0.006	0.006	0.007	0.006
SRP	0.015	0.015	0.017	0.023	0.016	0.017	0.025	0.025
SSP	0.018	0.017	0.025	0.019	0.015	0.019	0.021	0.020
SRC	0.010	0.007	0.021	0.011	0.009	0.009	0.016	0.009
WB	0.030	0.011	0.048	0.017	0.022	0.009	0.040	0.010
WR	0.005	0.003	0.007	0.006	0.005	0.006	0.005	0.007
WRP	0.005	0.001	0.020	0.004	0.005	0.006	0.004	0.007
WSP	0.005	0.004	0.012	0.006	0.004	0.006	0.002	0.013
WRC	0.016	0.013	0.037	0.007	0.017	0.012	0.016	0.022

* Storey drift index limits in TSC 2007 for performance evaluation of vertical load bearing elements for immediate occupancy (IO) 0.01, life safety (LS) 0.03, collapse prevention (CP) 0.04

It should be initially underlined that as the storey drift index values are related to the damage of the non-structural elements like hollow brick infills, any evaluation over the drift properties of an individual bare frame specimen would be therefore meaningless. The drift values of bare frames were basically evaluated as the references values to see the contribution of hollow brick infills on drift properties of the infilled system. Higher storey drift index values were observed for the bare frames of all series, as expected. This behaviour can be explained not only by absence of infill that improves lateral stiffness of the system, but also with the bond-slip phenomenon. Since plain bars were used as longitudinal reinforcement together with low strength of concrete, higher levels of lateral displacement observations due to bond-slip effect were initially expected. Existence of hollow brick infills are observed to decrease lateral displacements corresponding to the lateral strength in both directions considerably when compared to that of bare frames, as the storey drift index values stated in **Table 6.4** show.

PC panel application significantly improved storey drift index properties of RC frame system for all series of strengthened specimens as can be seen in **Table 6.4** and **Figure 6.15**. This conclusion can be made by considering the storey drift index values corresponding to the lateral load carrying capacity of the system. For instance; specimens **SB** and **SRP** reached their ultimate load carrying capacities almost at the same level of storey drifts, being beyond of immediate occupancy performance limit. However, the load carrying capacity of strengthened specimen **SRP** is almost fourteen times of that of specimen **SB**.

In case of narrower series of specimens, rectangular PC panel strengthened specimen **NSP** behaved quiet stiff and reached its lateral load carrying capacity with very low levels of storey drift index values as can be seen in **Table 6.4**. Specimen **NRP** and **NRC** reached their load carrying capacities at very closer storey drift index values, just beyond the immediate occupancy performance limit. However, the post-peak first storey drift ratio corresponding to 85% of the lateral strength for specimen **NRC** is beyond the collapse prevention and life safety performance levels in forward and backward directions, respectively.

In case of standard series of specimens, PC panel strengthened specimens **SRP** and **SSP** reached their load carrying capacities at almost equal storey drifts which are just beyond the immediate occupancy performance level. In addition, the upper bound reference specimen **SRC** reached its lateral load carrying capacity with fewer amounts of storey drifts compared to the other PC panel strengthened specimens.

Since the behaviour is dominated by shear with the increasing frame aspect ratio, the positive contribution of PC panel application on storey drift index characteristics of the system becomes quite remarkable for wider series of specimens as numerical values given in **Table 6.4** indicate. PC panel strengthened wider series of specimens **WSP** and **WRC** reached their load carrying capacities in both directions with very low storey drift index values; even being less than the TSC 2007 limit for immediate occupancy performance level. However, cast-in-place RC infilled upper bound reference specimen **WRC** reached its lateral load carrying capacities in both directions with storey drift index ratios beyond the immediate occupancy performance level.

As another view, positive contribution of PC panel application on displacement behaviour of RC frames for all series of specimens can be seen on **Figure 6.16**. Storey drift index history for each specimen is presented as dimensionless indicators of displacement history. Since the higher deformations of RC frame indicate less stiffness, these charts may also give idea about the lateral stiffness of the RC frame specimens.
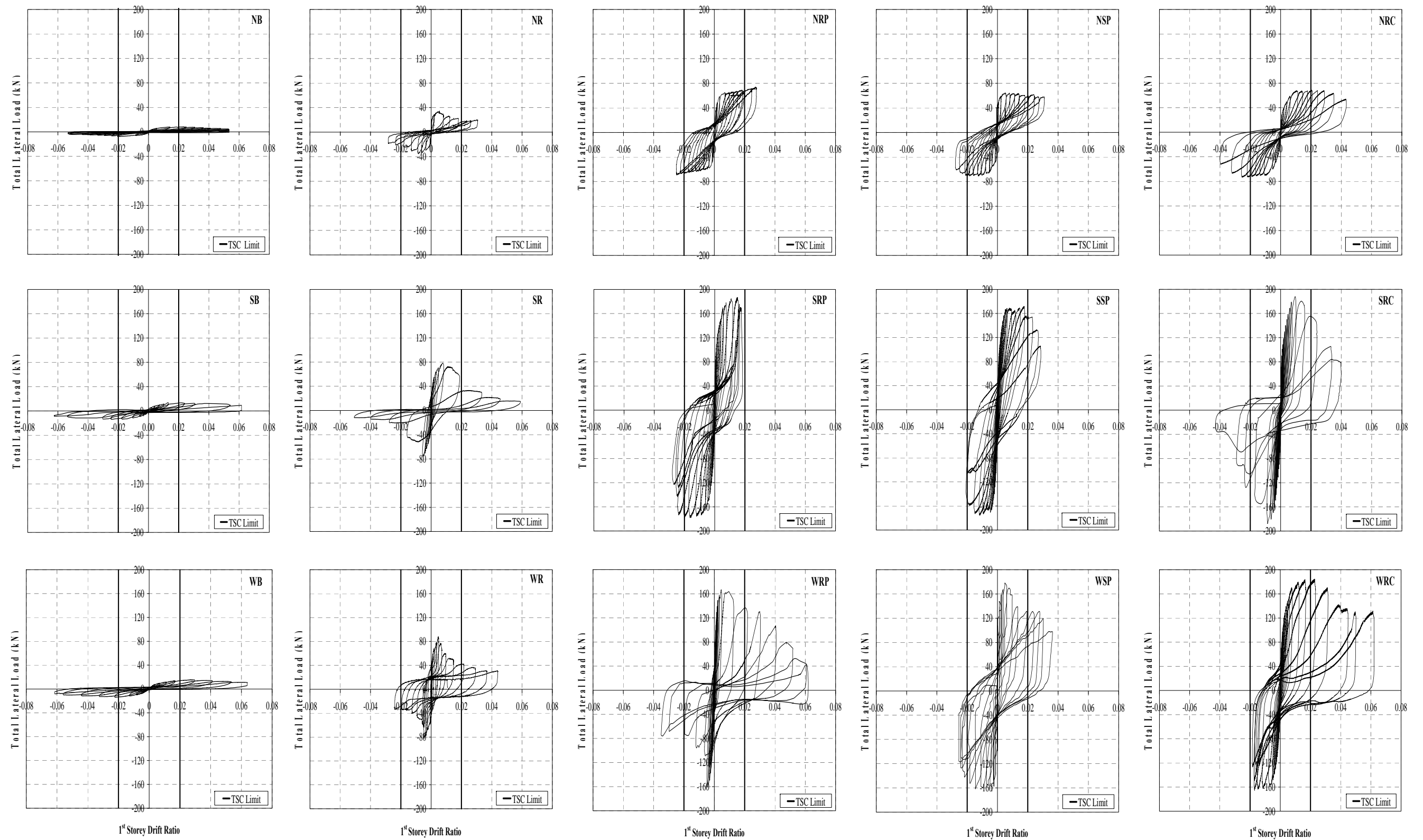
Figure 6.15. Total Lateral Load – First Storey Drift Ratio Curves for All Series of Specimens

231
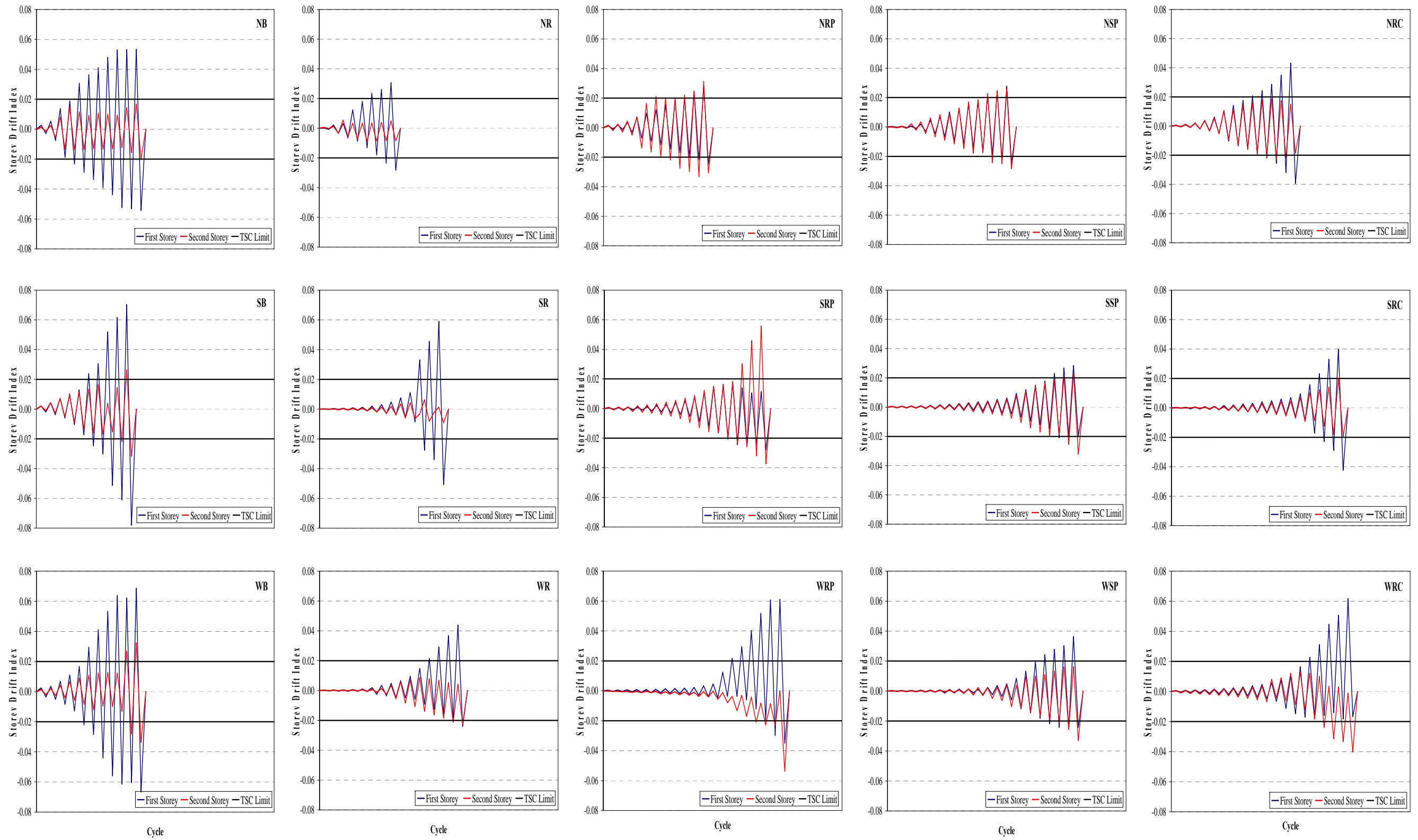
Figure 6.16. Storey Drift Index Curves for All Series of Specimens

6.6. Energy Dissipation

The conventional approach to seismic resistant design relies on the ductile behaviour of the structural members for energy dissipation such that; the capacity of a structure to resist large hysteretic effects created by earthquake without collapse depends on its capacity to dissipate energy. A reasonable pre-quake strengthening method is, therefore, required to positively contribute not only to the load carrying capacity of the structure, but also to its energy dissipating capability.

Energy dissipation is an important indicator of ductility of the member. The amount of dissipated energy can be calculated from the area enclosed within each loop of a loading-unloading cycle in a hysteretic load-deformation curve, for a specific cycle. Cumulative energy dissipation of the system is calculated by addition of all amounts of the dissipated energies in all of the full cycles. It should be underlined that, the energy dissipation characteristics strongly depend on the loading history of the specimen. In the experimental study, the loading histories of the specimens were intended to be as similar as possible. The specimens loaded up to its lateral load carrying capacity by a load controlled fashion and beyond this point, displacement controlled loading was applied by imposing the same second storey level displacements in both forward and backward half cycles.

The energy dissipated by the specimen was calculated from the experimental hysteretic base shear-top displacement curves of first and second storey levels considering the lateral load sharing (one-third of the applied lateral load is considered for the first storey level and two-third of the applied lateral load is considered for the second storey level) and plotted against each cycle. Cumulative energy dissipation curves of narrower, standard and wider series of specimens are depicted in **Figure 6.17**, **Figure 6.18** and **Figure 6.19**, respectively. Total amount of dissipated energy of each specimen and comparisons with respect to lower and upper bound references of each series are tabulated in **Table 6.5**.
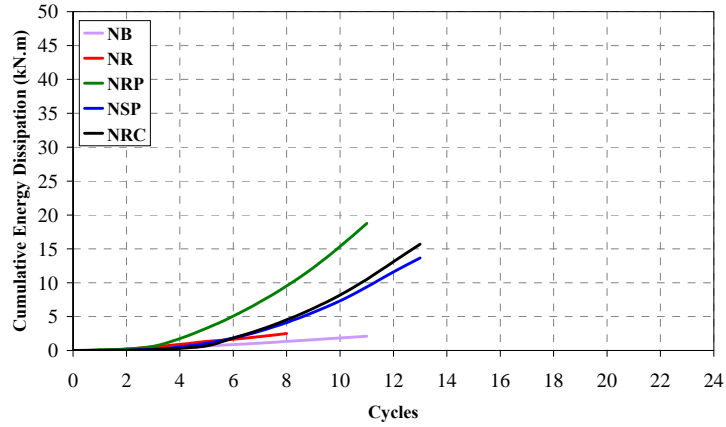
Figure 6.17. Cumulative Energy Dissipation Curves for Narrower Series of Specimens
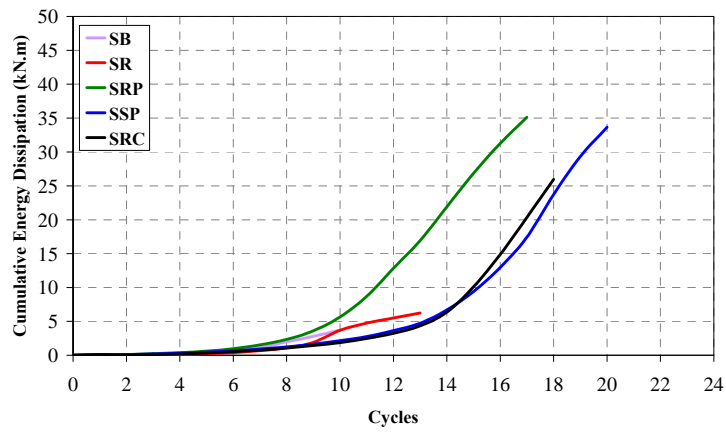
Figure 6.18. Cumulative Energy Dissipation Curves for Standard Series of Specimens
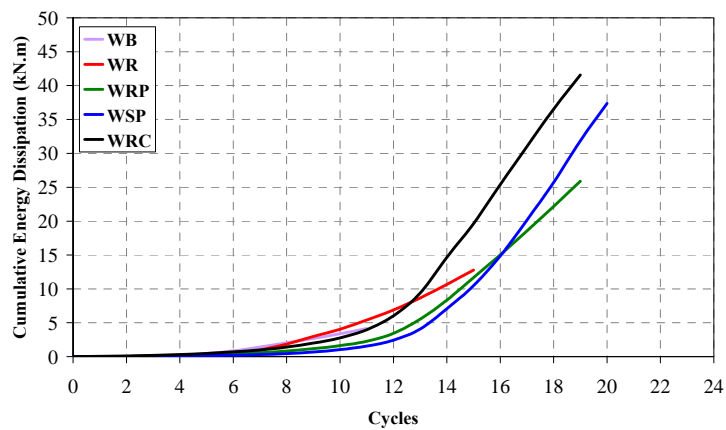
Figure 6.19. Cumulative Energy Dissipation Curves for Wider Series of Specimens

Table 6.5. Comparison of Cumulative Energy Dissipation Capacities of All Series of Specimens

Specimen	Cumulative Energy Dissipation (kN.m)	Ratio of cumulative energy dissipation to that of reference specimen	
		Lower Bound*	Upper Bound**
NB	2.1	0.84	0.13
NR	2.5	1.00	0.16
NRP	18.8	7.50	1.20
NSP	13.7	5.46	0.87
NRC	15.7	6.27	1.00
SB	3.7	0.60	0.14
SR	6.2	1.00	0.24
SRP	35.1	5.65	1.35
SSP	33.7	5.41	1.30
SRC	26.0	4.17	1.00
WB	4.2	0.33	0.10
WR	12.8	1.00	0.31
WRP	25.9	2.02	0.62
WSP	37.4	2.92	0.90
WRC	41.6	3.25	1.00

*   : Hollow brick infilled specimen; **NR**, **SR** and **WR**

** : Cast-in-place RC infilled specimen; **NRC**, **SRC** and **WRC**

It is important to emphasize that, the loading history has great influence on the energy dissipation characteristics. Considering this fact, the cumulative energy dissipation characteristics should be carefully evaluated and should not be misinterpreted for each of the specimen series.

As the numerical values of cumulative energy dissipation are investigated, it is clearly observed that PC panel application considerably increased the total dissipated energy when compared to the lower bound reference specimens, for all series. In addition, PC panel strengthened specimens of narrower and wider series even dissipated more energy when compared to the upper bound reference specimens. Energy dissipation curves of the specimens initially follow a relatively linear trend showing linear action until the slope suddenly changes. This slope change is more pronounced as

the aspect ratio increases. Start of increased dissipation rate marks the point where plasticization starts and higher curves mean higher total energy dissipation.

In case of narrower series, brittle hollow brick infills did not contribute a lot to the energy dissipation characteristics, when bare frame **NB** and lower bound reference specimen **NR** are compared. The cumulative energy dissipation of lower bound reference specimen **NR** is almost equal to that of bare frame **NB**. Since the behaviour of narrower series specimen is obviously dominated by flexure, this result can be attributed to the brittle fashion of the infill; of course the less numbers of cycles that specimen **NR** was subjected to should also be considered. PC panel strengthened specimens **NRP** and **NSP** dissipated energy almost seven times of that of lower bound reference specimen **NR**, in average, which is approximately same as the total amount dissipated by the upper bound reference, specimen **NRC**. As a remarkable result, specimen **NRP** dissipated energy 20% higher than that of specimen **NRC**, although specimen **NRP** was subjected to less numbers of loading cycles compared to upper bound reference specimen **NRC**, as can be seen in **Figure 6.17**.

The effect of hollow brick infills on cumulative energy dissipation capacity is more pronounced for standard series specimens compared to narrower series specimens. The cumulative energy dissipation of lower bound reference specimen **SR** is almost two times of that of bare frame **SB**. As can be seen in **Figure 6.18**, specimen **SRP** and **SSP** dissipated energy approximately six times of that of lower bound reference specimen **SR** and this ratio is almost four for upper bound reference specimen **SRC**. Either rectangular or strip shape PC panel application provided higher cumulative energy dissipation for standard series specimens **SRP** and **SSP**, when compared to the upper bound reference specimen **SRC**. Both PC panel strengthened specimens dissipated energy approximately 30% higher than that of specimen **SRC**. Cumulative energy dissipation of specimen **SRP** is relatively higher than that of specimen **SSP**, which may be explained by existence of anchorage dowels in between PC panels and surrounding columns that provided a better monolithical nature.

236

In case of wider specimens, the contribution of hollow brick infills on energy dissipation characteristics of RC frame is more remarkable than that of standard series specimens. The cumulative energy dissipation of lower bound reference specimen **WR** is almost three times of that of bare frame **WB**. As can be seen in **Figure 6.19,** specimens **WRP** dissipated energy almost two times of that of specimen **WR**, while this ratio is almost three for strip panel strengthened specimen **WSP**. In wider series, upper bound reference specimen **WRC** dissipated energy more than three times of that of specimen **WR**, being higher than that of PC panel strengthened specimens **WRP** and **WSP**.

6.7. Ductility

Ductility is a very important consideration in the areas requiring analysis and design for seismic loading. This is because of the present philosophy of seismic design codes so that; it is required to design the structures as to behave elastically during the relatively moderate earthquakes and reliance is placed on availability of sufficient ductility after yielding to enable the structure to survive without collapse. Therefore, seismic design code requirements can be satisfied only if the structure has sufficient ductility to absorb and dissipate energy by post-elastic deformations when subjected to several cycles of loading well into the yield range. (**Park and Paulay, 1975)**

The inelastic deformation of a section or member is commonly quantified by ductility parameters, in case of seismic design. Some ductility parameters such as curvature and displacement ductility factors, cumulative ductility amounts calculated over curvature and displacement values which represent the deformability of concrete section and member, respectively, can be stated as commonly preferred ductility indicating parameters. Displacement ductility ratio, μ_Δ values were calculated in order to evaluate the ductility indicators of all series of specimens of the present research using **Equation 6.1**, the details of which are as below expressed.

$$\mu_\Delta = \frac{\Delta_y}{\Delta_u}$$

<div align="right">(6.1)</div>

where;

μ_Δ : Displacement ductility ratio

Δ_y : Yield displacement taken from bilinear representation of the response envelope curve on the forward loading direction

Δ_u : Ultimate displacement taken from bilinear representation of the response envelope curve on the forward loading direction which corresponds to post-peak load level corresponding to 15% strength loss

Displacement ductility ratio values of all series of specimens were calculated first by generating the bilinear representation of response envelope curve of the specimen in the forward loading direction as depicted in **Figure 6.20.** Ductility is defined as *"the capability of undergoing large deformations without a significant reduction in the strength"*. Significant reduction can approximately be defined as strength loss of more than 15%. **(Ersoy, Özcebe and Tankut, 2003)** Therefore, the post-peak data of the response envelope curve beyond 85% of the lateral loading capacity, F_{max}, were ignored in the calculations. Bilinear representation of the capacity curve is the second stage to define the yield and ultimate displacements. The approach suggested in *Displacement Coefficient Method* **(FEMA-356, 2000)** was used to generate the bilinear representation of the response envelope curve. A secant line, representing effective elastic stiffness, K_e, was first drawn by judgement such that it intersects the response envelope curve at 60% of the yield base shear, F_y. Since, the yield base shear is not known at the beginning, this procedure requires some trials in order to find the yield base shear value that equates the areas below the actual capacity curve and its bilinear representation as shown in **Figure 6.20**.
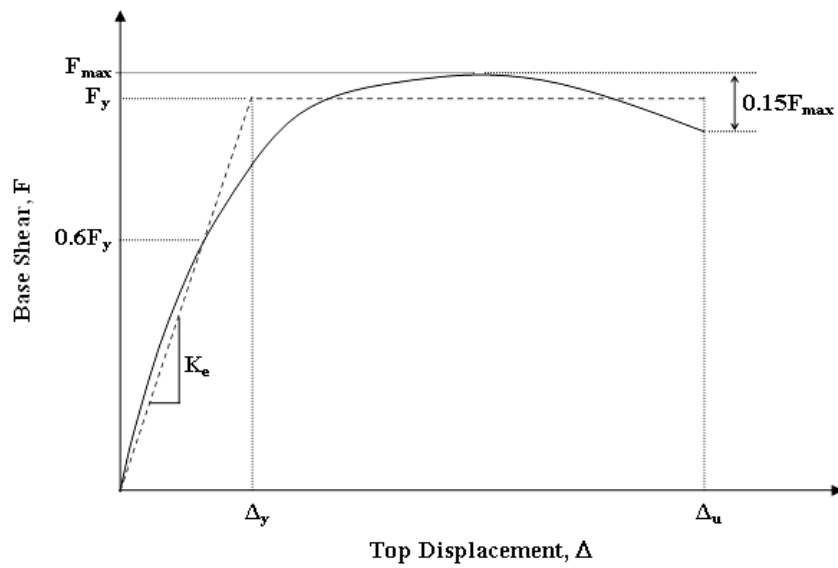
Figure 6.20. Bilinear Representation of Response Envelope Curve

Displacement ductility ratio values of all series of specimens are presented in **Table 6.6**. Since, ductility demand of the specimen for an assigned ground motion is not known, the displacement ductility values can not be compared to that of demand values. However, the displacement ductility values depicted in **Table 6.6** are remarkable such that; PC panel application provides a stiffer system compared to that of lower bound references also by providing the ductility with almost no reduction compared to that of lower bound reference. Therefore, it may be stated that PC panel application not only positively contributes to the pre-peak system behaviour by improving lateral load carrying capacity and initial stiffness; but also provides ductility for the specimen to survive in the post-peak range. Furthermore, it is clearly observed that hollow brick infills also improve ductility of the bare frames for all series of specimens by significantly lowering the yield displacements.

Table 6.6. Comparison of Displacement Ductility Ratio Values of All Series of
Specimens

Specimen	Displacement Ductility Ratio $(\mu_\Delta = \Delta_u/\Delta_y)$	Ratio of displacement ductility ratio to that of reference specimen	
		Lower Bound*	Upper Bound**
NB	5.7	0.89	0.73
NR	6.4	1.00	0.82
NRP	8.7	1.36	1.11
NSP	9.2	1.43	1.17
NRC	7.8	1.22	1.00
SB	5.0	0.84	0.60
SR	6.0	1.00	0.71
SRP	6.3	1.06	0.75
SSP	7.9	1.32	0.94
SRC	8.4	1.41	1.00
WB	2.9	0.36	0.39
WR	8.0	1.00	1.08
WRP	9.9	1.24	1.35
WSP	7.4	0.93	1.01
WRC	7.4	0.92	1.00

  * : Hollow brick infilled specimen; **NR**, **SR** and **WR**

 ** : Cast-in-place RC infilled specimen; **NRC**, **SRC** and **WRC**

In case of narrower series specimen, both of PC panel strengthened specimens had higher displacement ductility ratios than upper bound reference specimen **NRC**. Strip shaped PC panel strengthened specimen **NSP** provided the highest ductility which can be linked to lower amount of yield displacement compared to the other strengthened specimens.

In case of standard series of specimens, both of PC panel strengthened specimens provided higher displacement ductility ratios compared to that of lower bound reference **SR**. The upper bound reference specimen **SRC** had the highest displacement ductility ratio among the other PC panel strengthened specimens which can be directly attributed to lower yield displacement. However, the displacement ductility ratio of strengthened specimen **SSP** slightly differs from the upper bound reference specimen **SRC**.

In case of wider series of specimens, the positive contribution of hollow brick infills on ductility of bare frame is more pronounced compared to that of standard and narrower series specimens. Both PC panel strengthened specimens **WRP** and **WSP** gained higher displacement ductility ratios compared to that of upper bound reference specimen **WRC**. Rectangular shaped PC panel strengthened specimen **WRP** provided the largest displacement ductility ratio compared to that of other strengthened specimens due to lower yield displacement.

6.8. Summary of Evaluation of the Test Results

The effectiveness of the proposed PC panel method is briefly and quantitatively summarised in **Table 6.7** to **Table 6.9**. Performance improvement is displayed numerically with respect to the bare frame, hollow brick infilled frame and cast-in-place RC infilled frame in the three columns of each table.

The performance improvement, indicated by the values given in these tables, is self evident. However, two general observations appear to be strikingly important. Putting minor differences aside,

- The performance improvement provided by the proposed panel technique is almost equal to that provided by the cast-in-place RC infill.
- The performance improvement appears to be almost the same in the three series of different aspect ratios, indicating validity of the proposed technique for infill walls of all aspect ratio series.

Table 6.7. Behaviour Improvement on **Narrower** Series Specimens

by PC Panel Application

SEISMIC PERFORMANCE INDICATOR	With reference to		
	bare frame	specimen with hollow brick infill	specimen with cast-in-place RC infill
Lateral Load Carrying Capacity	~7.8 times	~1.9 times	~1.0 times
Lateral Stiffness	~18.6 times	~1.9 times	~0.9 times
Ductility	~1.6 times	~1.4 times	~1.2 times
Cumulative Energy Dissipation	~7.7 times	~6.5 times	~1.0 times

Table 6.8. Behaviour Improvement on **Standard** Series Specimens

by PC Panel Application

SEISMIC PERFORMANCE INDICATOR	With reference to		
	bare frame	specimen with hollow brick infill	specimen with cast-in-place RC infill
Lateral Load Carrying Capacity	~13.2 times	~2.3 times	~1.0 times
Lateral Stiffness	~110.0 times	~2.3 times	~0.6 times
Ductility	~1.4 times	~1.2 times	~0.9 times
Cumulative Energy Dissipation	~9.2 times	~5.5 times	~1.3 times

Table 6.9. Behaviour Improvement on **Wider** Series Specimens

by PC Panel Application

SEISMIC PERFORMANCE INDICATOR	With reference to		
	bare frame	specimen with hollow brick infill	specimen with cast-in-place RC infill
Lateral Load Carrying Capacity	~11.2 times	~ 2.0 times	~ 0.9 times
Lateral Stiffness	~153.0 times	~1.8 times	~0.8 times
Ductility	~3.0 times	~1.1 times	~1.2 times
Cumulative Energy Dissipation	~7.6 times	~2.5 times	~0.8 times

CHAPTER 7

ANALYTICAL STUDIES

7.1. General

This chapter presents the details of the analytical modelling studies of the quasi-static RC frame tests. Narrower, standard and wider series of specimens were all modelled in OpenSees software package and nonlinear static pushover analyses were performed in order to obtain the capacity curves analytically.

Three main approaches have been reported in the capacity curve assessment of frames with continuous infill panels, to date; such as equivalent diagonal strut concept, the theory of plasticity based methods and the numerical methods. The equivalent diagonal strut concept is based on the behaviour of an infilled frame in early stages of loading when the composite system is subjected to in-plane lateral loading at the floor or roof levels. The infill and frame stay in contact over the limited lengths near the loaded corners, in the early stages of loading. During this phase, the composite system behaves as if it were diagonally braced. The infill is, therefore, replaced by this bracing which can only resist in-plane axial loads. Researchers like **Wood (1978)** and **Liauw and Kwan (1983)** developed design approaches based on plastic mechanisms of such composite systems of RC infilled frames, based on the observed failure mechanisms developed in infilled frames during various test programmes. Numerical methods like finite element analysis are, currently, extensively applied to masonry structures in general and to infilled frames in particular, due to progress in the computational field.

Although such numerical method choices are available, the increased complexity, cost and time consumption make the detailed finite element analysis and plasticity based

method applications unattractive design and assessment procedures of infilled frames. A simple analytical method may be appropriate in initial stages of assessment/analysis process of RC frames with infill panels. Considering this point, the infills of RC infilled test specimens of the present research were modelled by using equivalent diagonal strut concept with appropriate modifications.

RC frame specimens of the present research were modelled in OpenSees software for analytical evaluation. The infills were, therefore, simulated with equivalent diagonal struts; the geometric and material properties of which are defined in the light of the individual infill panel tests (**See Appendix-D**) and proposed code equations. Since plain bars and lower strength concrete were used in RC frames, bond-slip effects were also taken into consideration in the analytical evaluation. Nonlinear static pushover analysis was performed on analytical RC frame models to obtain the capacity curves. Experimental response envelopes gathered in the present research are compared to that of the analytical modelling results.

The details of RC frame modelling and analysis, application of equivalent diagonal strut concept for infill simulations, analytical evaluation of bond-slip action and the analysis results of the test specimens are presented in this chapter.

7.2. RC Frame Modelling and Pushover Analysis

RC frame specimens were modelled in OpenSees software; Open System for Earthquake Engineering Simulation, **(OpenSees, 2008)**. OpenSees is not a code. It is an object-oriented software framework for simulation applications in earthquake engineering using finite element solution methods. OpenSees has the potential for a community code for earthquake engineering, as an open-source software. There exists a communication mechanism within PEER (Pacific Earthquake Engineering Research Centre) for exchanging and building upon research accomplishments.

The analytical RC frame models were generated and analyzed in 2D, since the frames were also tested in 2D. Six nodes were initially assigned to represent the frame elements as shown in **Figure 7.1**; where node-1 and node-6 are fixed. "`nonlinearBeamColumn`" element command was used to model beam and column elements, while "`Truss`" element command was assigned to simulate the equivalent diagonal struts for infilled frames. P-Δ effects were included in beam and column element definition. Beam and column sections were modelled as fibre sections using "`Fiber`" section command considering confined and unconfined concrete regions. Uniaxial material object of "`Concrete01`" was used for concrete material definition which ignores the concrete contribution in tension with degraded linear loading/unloading stiffness. Uniaxial material object of "`Steel02`" was used for steel material definition which considers the isotropic strain hardening in tension.
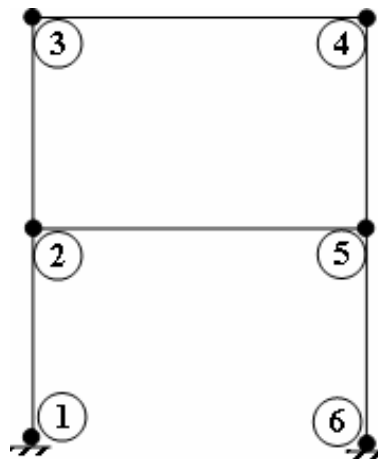
Figure 7.1. Node Definition in OpenSees 2D Frame Model

Bond-slip action, mainly, observed on column bases resulted in higher roof displacements of bare frames. The bond-slip effect was noticeably observed in case of narrower specimen series together with relatively higher pinching. This effect was also introduced into the analytical RC frame models to avoid overestimations in strength and stiffness indicators, as explained in **Section 7.3,** in detail. Definition and determination of equivalent diagonal strut section and material parameters for infilled RC frames are also presented in **Section 7.4**.

In case of analysis of RC frames, the constant column axial load was first applied on node-3 and node-4 and then the displacement controlled nonlinear pushover analysis was performed in order to obtain the capacity curves, analytically. Push-over analysis is a type of nonlinear static analysis method which is applied to examine the performance of the structures under lateral loads. (**Sonuvar, 2001**) In this type of analysis, first a load pattern is selected and then applied to the structure over the defined nodes in small increments. Displacement versus corresponding base shearing forces is graphed to obtain the capacity curve of the structure. Since numerical problems may occur due to stiffness deteriorations in load controlled type of loading, the displacement controlled loading was applied to the models in the present study. A lateral roof displacement pattern was assigned over node-3 and node-4 of the model frames with very small increments up to the target displacement which was reached in the experiment and the data for capacity curve was recorded. The pushover analysis procedure is simply illustrated in **Figure 7.2.**
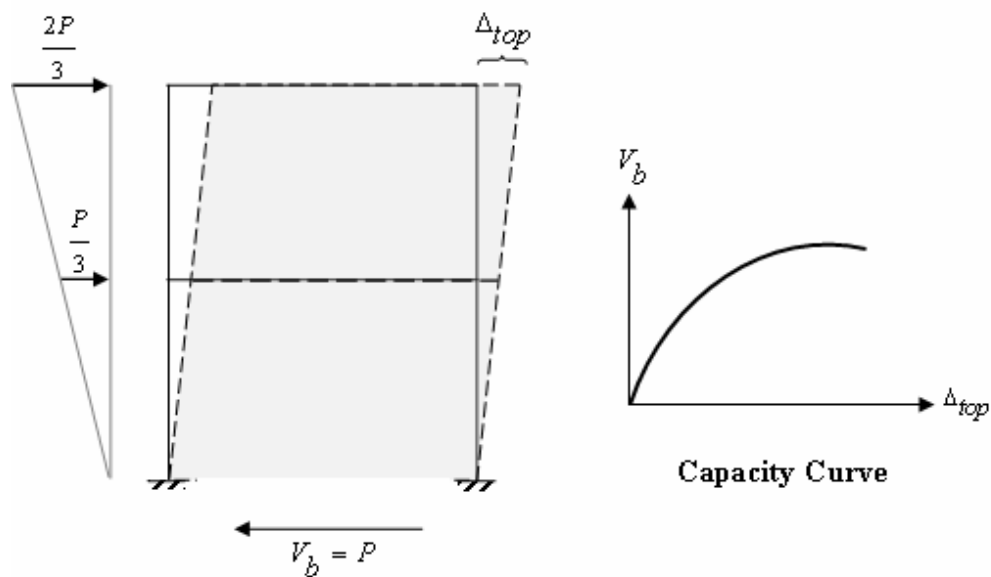
Figure 7.2. Pushover Analysis Procedure

7.3. Evaluation of Bond-Slip Effect

RC frame structures which are subjected to extreme lateral loadings experience localized inelastic deformations occurring at the member end regions as illustrated in **Figure 7.3**. These member end deformations consist of two components. The first component is the flexural deformation that causes inelastic strains in the longitudinal bars and concrete and the second one is the member end rotation, as indicated by arrows in **Figure 7.3**, due to reinforcement slip. Since plain bars and low strength of concrete were used in RC frame construction of the present research, bond-slip effects were also considered in analytical RC frame modelling studies.
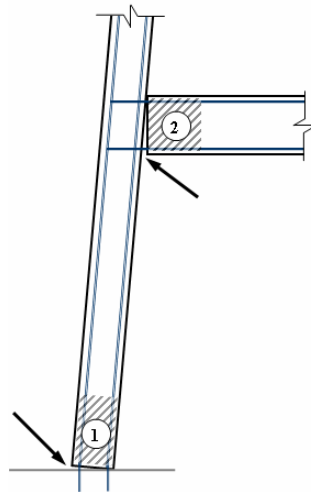
Figure 7.3. Schematic Representation of Typical Inelastic Regions in RC Frame

This bond-slip, which is characteristically different from the slip that occurs to the entire bar embedment length due to poor anchorage condition, results from strain penetration along a portion of the fully anchored bars into the adjoining concrete members such as footings and joints during the elastic and inelastic response of a structure. Longitudinal bar slip at the end zones of the RC members results in additional member end rotation which is not a part of flexural deformations. The contribution of these member end rotations to total lateral deformations can be relatively large; in some cases even as large as the flexural deformations. If the

deformations resulting from longitudinal bar slip are ignored in the analysis or member modelling, the predicted member deformations may be significantly smaller or the predicted lateral member stiffness may be larger than the existing member stiffness. **(Sezen and Moehle, 2003)** In the existence of bond-slip action, the loaded end of the anchored bar exhibits slip at the connection interface resulting from the accumulative strain difference between the bar and concrete within the connecting member. As a result, a crack forms at the connection interface and an end rotation occurs to the flexural member. The flexural and bond-slip deformations of a column under lateral loading are illustrated in **Figure 7.4** and **Figure 7.5,** respectively**. (Elwood, et. al, 2006)**

$$\Delta_{flex} = \frac{L^2}{6}\phi_y \longrightarrow$$ Does not account for end rotations due to bar slip!
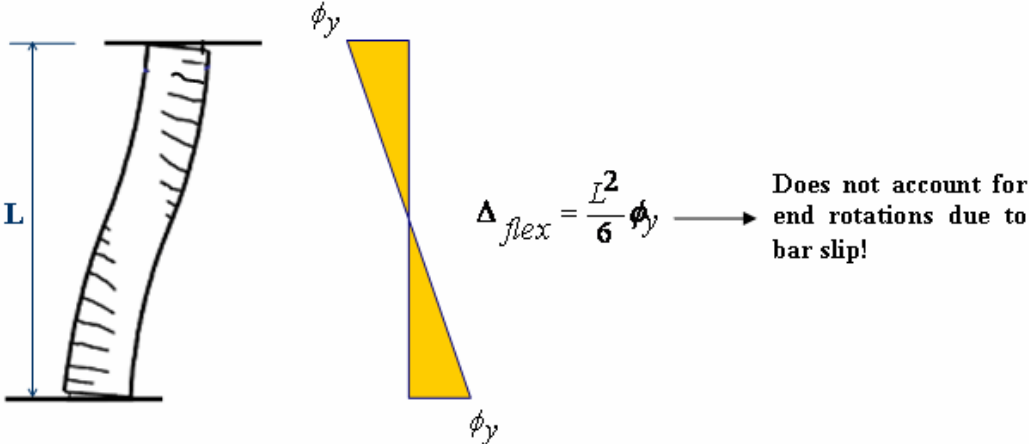
Figure 7.4. Flexural Deformation of a Column under Lateral Loading

$$\Delta_{slip} = \frac{Ld_b f_s \phi_y}{8u}, \quad u = 6\sqrt{f_c^l}$$
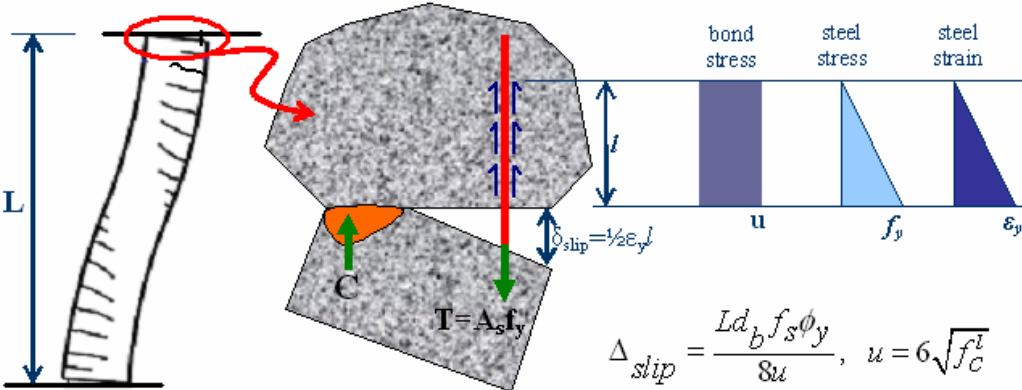
Figure 7.5. Bond – Slip Deformations of a Column under Lateral Loading

The anchorage behaviour of reinforcing bars has been experimentally investigated by researchers and a number of bond stress-slip models were proposed to estimate the lateral deformations due to bond slip. **(Sezen and Moehle, 2003)** Springs were commonly used to represent the bond-slip behaviour of the loaded longitudinal bars in the analytical model. Rotational springs at the column bases require the reliable moment-rotation relationships to simulate the bond-slip behaviour, similarly the 1D springs at the column bases do. Another approach is to model special interface elements, again commonly by means of springs, over the longitudinal bar as illustrated in **Figure 7.6**. The deficiencies of the spring model concept may be attributed to the following; the assumed bond stress distribution along the bar is not experimentally justified, the bond slip estimated at the loaded end of the bar is strongly influenced by the theoretical stress-strain model used for the reinforcing steel and the end rotations are underestimated at small displacements due to the use of a constant neutral axis depth. In addition, the spring models may not be reliably extended to capture the bond-slip rotation of a generalized flexural member that has an arbitrary cross-section and is subjected to bidirectional loading. **(Zhao and Sritharan, 2007)**

Rotational Spring   1D Spring   Special Interface Element
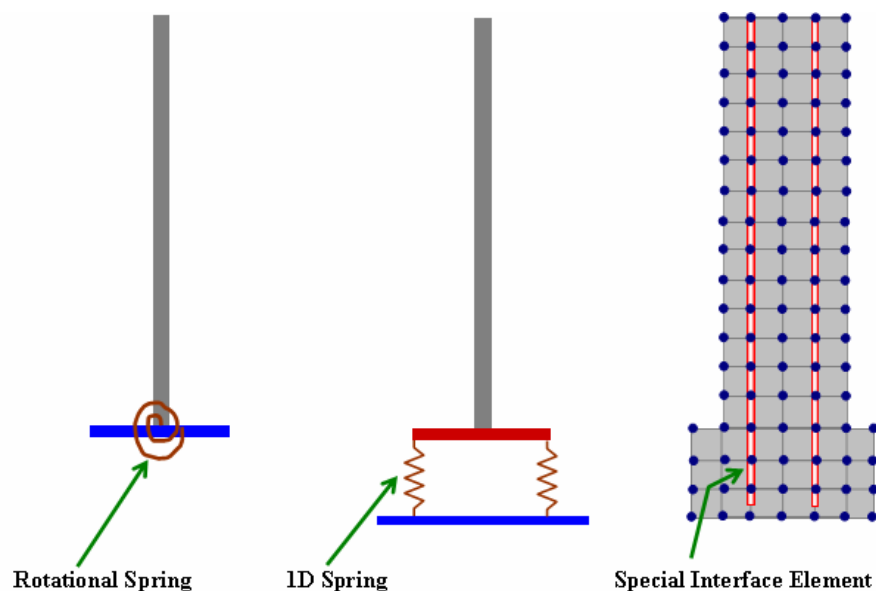
Figure 7. 6. Some Approaches to Model Bond-Slip Effect

The deformations due to member end rotations caused by bond-slip action were taken into account during the analytical RC frame modelling work of the present research since plains bars and low strength concrete were used in specimen production. The OpenSees command proposed by **Zhao and Sritharan (2007)** to model the bond-slip effect was introduced to the analytical frame models, at the first storey column bases. The proposed OpenSees command is only applicable to the models with the sections defined by fibre elements as the ones of the present research. Briefly to incorporate the bond-slip effects to the analytical model; a "**zeroLengthSection**" element is first defined at the column base and subsequently the material model of "**uniaxialMaterial Bond_SP01**" is assigned to the longitudinal reinforcement of the zero-length section as illustrated in **Figure 7.7**.
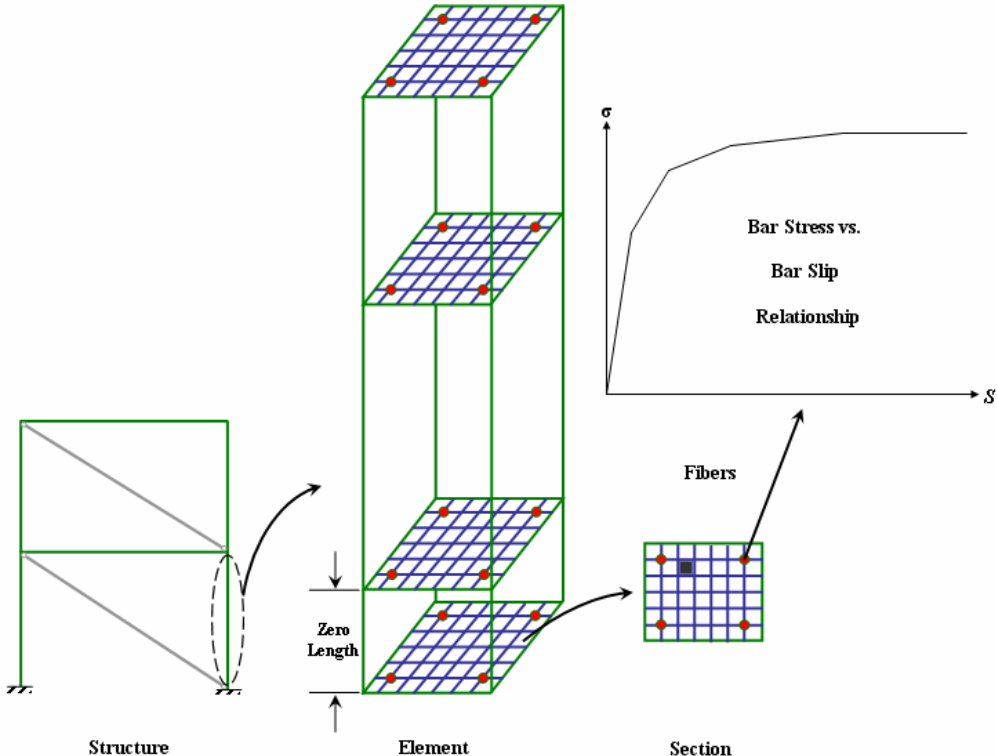
Figure 7.7. Zero-length Section Element Definition for Bond-Slip Effect

As stated above, a zero-length section element at the column-foundation joint (node-1 and node-6) is initially defined, as shown in **Figure. 7.7** to incorporate the fixed-end

rotation caused by strain penetration to the beam-column element by using the "**zeroLengthSection**" command. At this stage, a duplicate node is required to create a zero-length section element in OpenSees. Moreover, the translational degree-of-freedom of the duplicated nodes should be constrained to each other to prevent sliding of the beam-column element at the common node under lateral loads because the shear resistance is not included in the zero-length section.

The zero-length section element definition is realized for bond-slip effect inclusion; so that the zero-length section element in OpenSees is assumed to have a unit length such that the element deformation (e.g., rotation) is equal to the section deformation (e.g., curvature). Because of the fibre representation of the section at the member interface, the proposed approach is stated to model the bond-slip of the longitudinal bars individually during the state determination of the zero-length section element. Hence, this approach is amenable to the fibre analysis concept and allows the strain penetration effects to be captured during flexural analysis of concrete members regardless of the cross-sectional shape and direction of the lateral load. The concept of using a zero-length section element to capture strain penetration effects is reported to be equally applicable to beam bars anchored into interior buildings joints. However, such application of the proposed concept is stated to require further research. **(Zhao and Sritharan, 2007)** Therefore, it was only applied to the column elements in this study.

The unit length assumption also implies that the material model for the steel fibres in the section element would represent the bar *slip* instead of *strain* for a given bar stress. Focusing on capturing the bond-slip due to strain penetration along fully anchored bars into concrete footings; bar stress-slip model used for "**uniaxialMaterial Bond_SP01**" command is presented in **Figure 7.8**. This uniaxial material is assigned to the longitudinal reinforcement of the zero-length section element, as above stated.
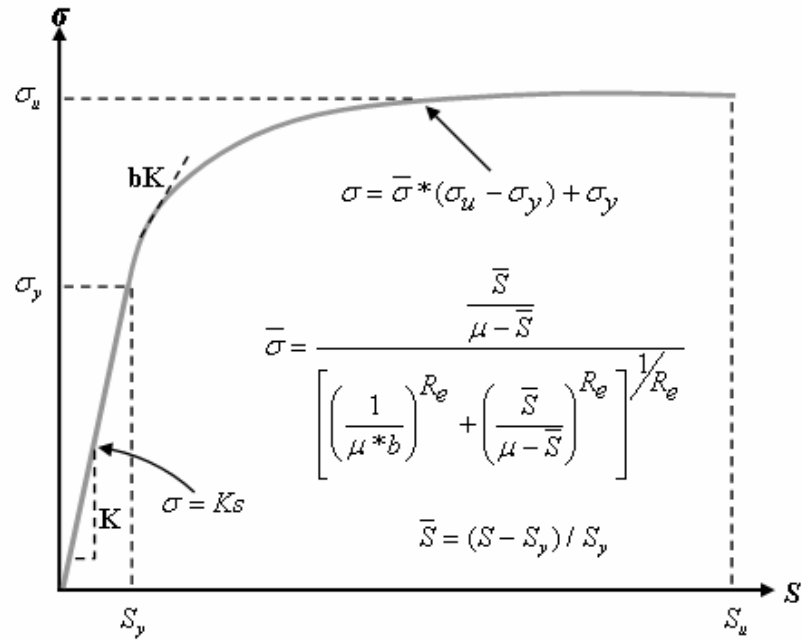
Figure 7.8. Monotonic Bar Stress - Slip Response as Represented by "**uniaxialMaterial Bond_SP01**" command

The bar stress-slip model of "**uniaxialMaterial Bond_SP01**" command requires the slip values at yield and ultimate strength values of the longitudinal reinforcement. The slip values at yield and ultimate strength of the longitudinal column reinforcement were calculated using the **Equation 7.1** and **Equation 7.2** proposed by **Zhao and Sritharan (2007)**.

$$S_y(mm) = 0.4 \left(\frac{d_b(mm)}{4} * \frac{f_y(MPa)}{\sqrt{f_c^l(MPa)}} (2\alpha_i + 1) \right)^{1/\alpha_i} + 0.34 \qquad (7.1)$$

$$S_u = 35 * S_y \qquad (7.2)$$

where the parameters are defined as;

d_b : Longitudinal bar diameter

f_y : Yield strength of the longitudinal reinforcement

f_c : Compressive strength of the concrete

α_i : Parameter used in the local bond-slip relation and was taken as 0.4 in this study in accordance with CEB-FIP Model Code 90 (MC90) (**CEB-FIP, 2000**)

S_y : Slip corresponding to yield strength of longitudinal reinforcement

S_u : Slip corresponding to ultimate strength of longitudinal reinforcement

The effect of the bond-slip deformations were analytically evaluated on bare frames by applying the above presented procedure and the resulting capacity curves are presented in **Figure 7.9**, together with the experimental response envelopes. The experimental and analytical predictions of lateral load carrying capacities for bare frames are presented in **Table 7.1.**

Table 7.1. Experimental and Analytical Lateral Load Capacities for Bare Frame Specimens **NB**, **SB** and **WB**

Specimen	Lateral Load Carrying Capacities in the Forward Direction (kN)		
	Experimental (F_{max})	Analytical	
		with bond-slip effect	without bond-slip effect
NB	8.2	10.5 (~1.3 times of F_{max})	18.9 (~2.3 times of F_{max})
SB	13.6	16.1 (~1.2 times of F_{max})	18.1 (~1.3 times of F_{max})
WB	15.3	16.5 (~1.1 times of F_{max})	17.2 (~1.1 times of F_{max})
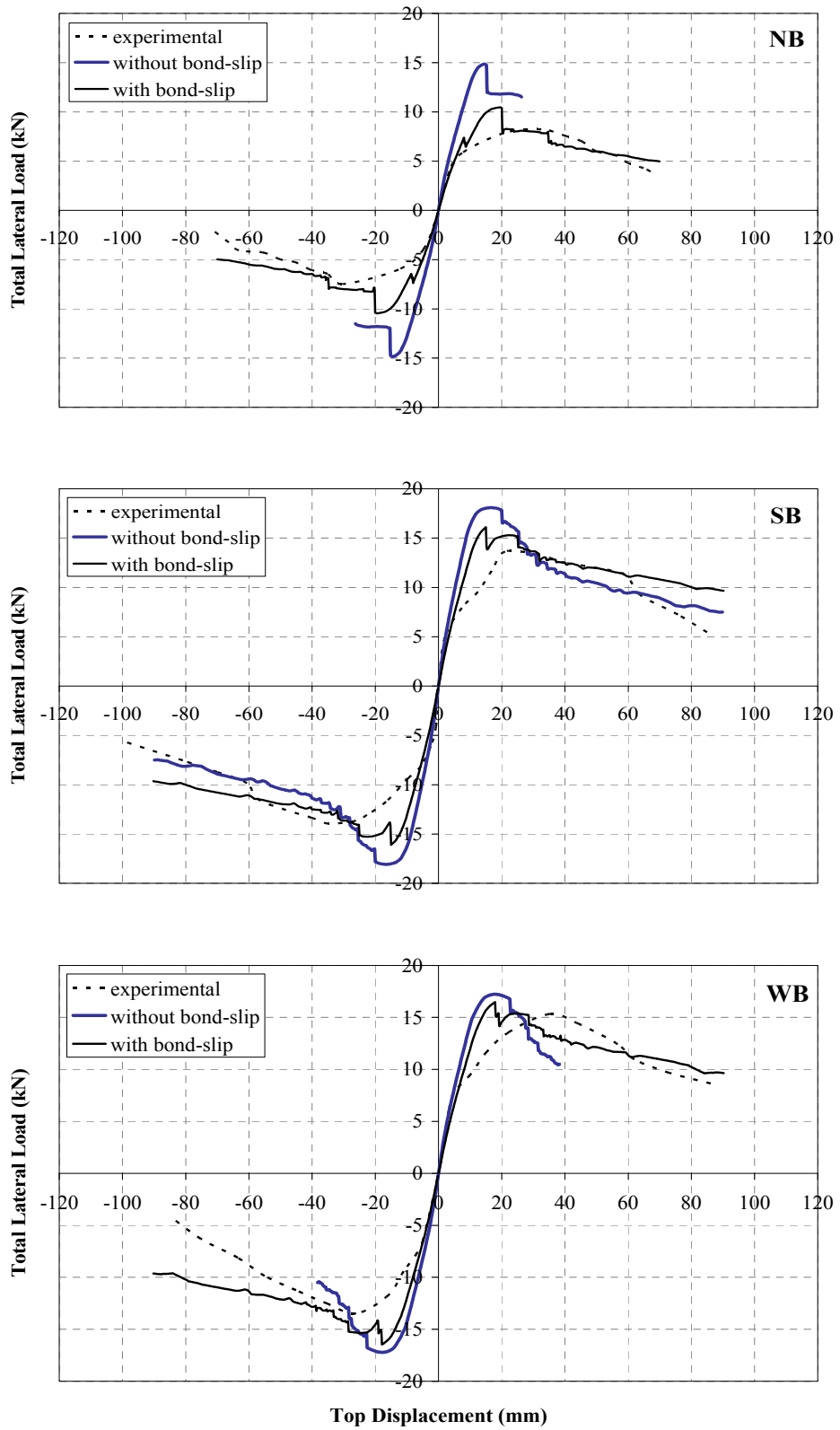
Figure 7. 9. Effect of Bond-Slip Deformations for Specimens **NB, SB** and **WB**

254

Since plain bars and low strength concrete were used in frame preparations to reflect the present state of the target building, the bond-slip effect was predominantly observed by means of higher lateral displacements. The analysis results indicate that without bond-slip effect consideration, the ultimate lateral loading capacities are overestimated more when compared to the model with the inclusion of bond-slip effect. This overestimation is more pronounced when the aspect ratio of the RC frame decreases. As presented in **Figure 7.10**, when the axial tensile force, T, in column occurring due to lateral loading increases, so do the bond-slip effect and the pinching becomes more pronounced. For instance, at the maximum lateral load levels axial tensile force in columns are calculated as 18.5 kN, 13.9 kN and 10.7 kN for specimens **NB**, **SB** and **WB**, respectively. The effect of the smaller aspect ratio and therefore, higher tension forces in columns resulted in more pronounced bond-slip effect to overestimate the lateral loading capacity as can be seen in **Table 7.1** and **Figure 7.9**.
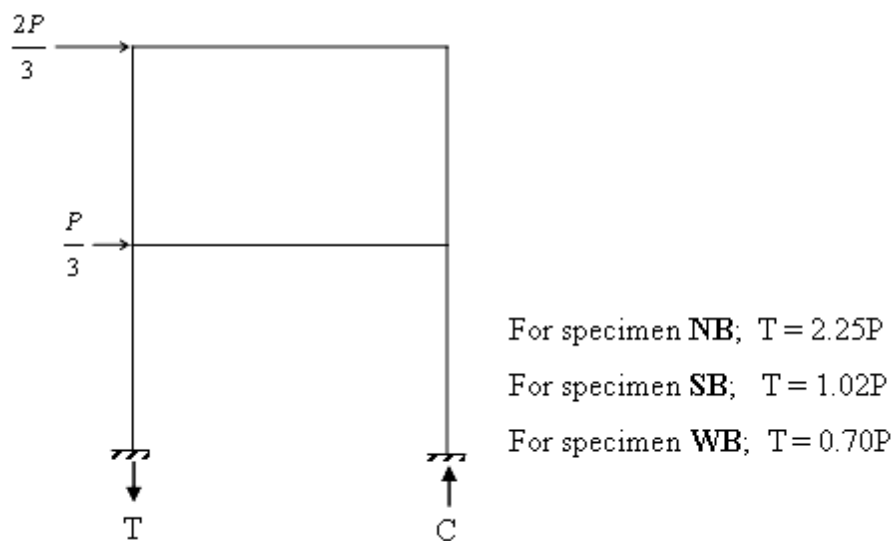
Figure 7. 10. Axial Forces in Columns due to Lateral Loading

7.4. Equivalent Diagonal Strut Concept and Application for Test Specimens

Infilled frames of the present research were modelled by means of equivalent diagonal strut method. This concept was originally mentioned by **Polyakov (1956)** which later on became the most widely used analytical method to model the structural behaviour of the infilled frames under monotonic or cyclic lateral loading. **Polyakov (1956)** suggested that, an infilled frame system could be idealized as a frame with a diagonal strut which will be replaced by the infill. This concept was later adopted and studied by **Holmes (1961, 1963).** Primarily **Smith (1962)** and his colleagues subsequently carried out extensive theoretical and experimental investigations on small scale infilled frames and extended the concept to include the effect of relative stiffness values of infill and frame. This concept was generalized to be applicable to any configuration of infilled frames including multi-storey systems**. (Smith, 1962, 1966a, 1966b, 1967, 1968) (Smith and Carter, 1969)** Further, **Mainstone (1971)** studied the definition of geometric properties of the equivalent diagonal strut which is also one of the main references of the procedure proposed in **FEMA-356, (2000)**

This concept proposes to replace existing infill by a diagonal compression strut like a truss element. The analogy is simple as illustrated in **Figure 7.11.** When the lateral load is applied to the frame, the infill wall is separated from the frame along a certain length of the beam or the column and the contact between the frame and the infill wall remains at the other two opposite corners. At this stage, a line drawn from one corner to the other, at which there is connection between the frame and the infill wall, shows the direction of compression. The infill transfers compression along this line. For this reason, the infill can be modelled as an equivalent virtual diagonal strut.

Previous M.E.T.U. researchers like **Altin (1990)** and **Sonuvar (2001)** used equivalent diagonal strut concept for analytical evaluation of RC infill wall panels as compression struts. **Sevil (2010)** modelled fibre reinforced mortar strengthened RC infilled frames following the diagonal strut concept by proposing two struts; one for the existing infill and the second for the new fibre reinforced mortar layer. **Baran (2005)** analytically investigated the contribution of PC panel application on standard sized RC frames by

two different methods. The first procedure was the equivalent column method in which the whole frame system with infill is converted into an equivalent column and the equivalent thickness of the new element is defined by considering the modulus of elasticity values of all existing material components. The second method was the equivalent diagonal strut concept. The strengthened infill was modelled with two diagonal struts; one for plastered hollow brick infill wall and the other for PC panels. **Baran (2005)** reported that, the equivalent diagonal strut concept to give better results than the equivalent column method in analytical evaluation of PC panel strengthened RC frames, by means of lateral load carrying capacities.
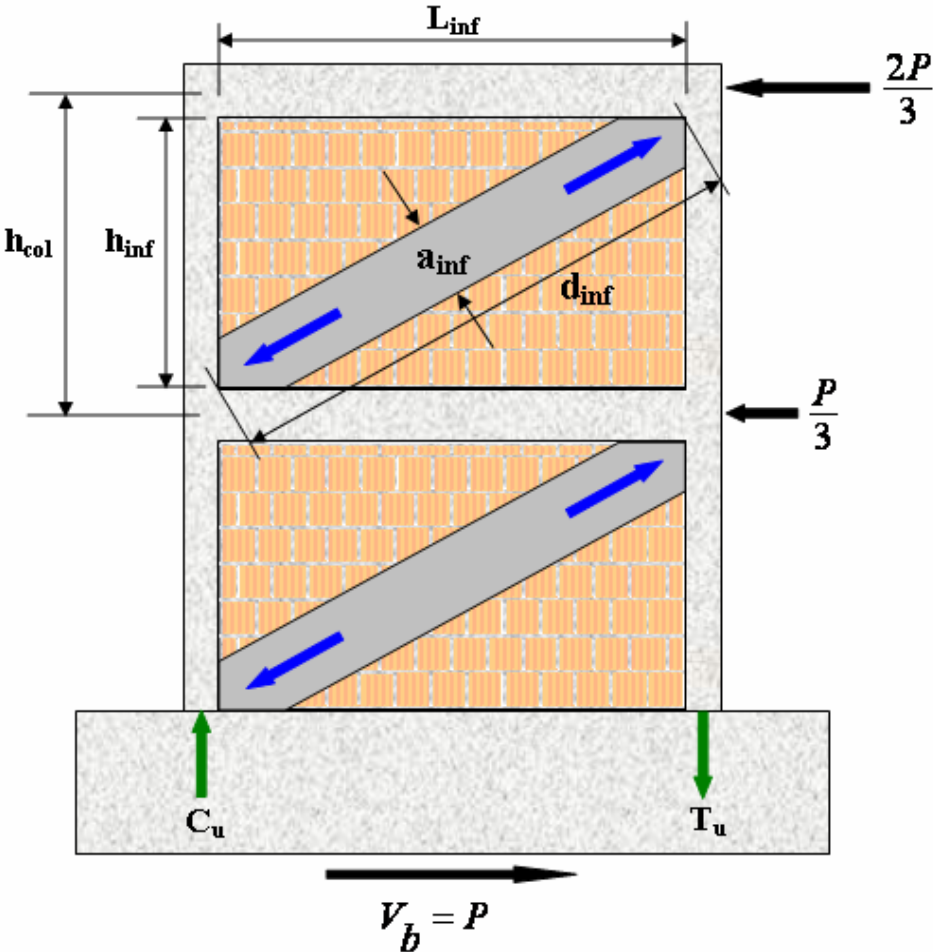
Figure 7.11. Equivalent Diagonal Strut Analogy

In the present research, each infill was modelled as a unique diagonal compression strut the mechanical properties of which were estimated from the individual infill panel tests. (**See Appendix-D**) The mathematical model for the infilled frames is presented in **Figure 7.12.**
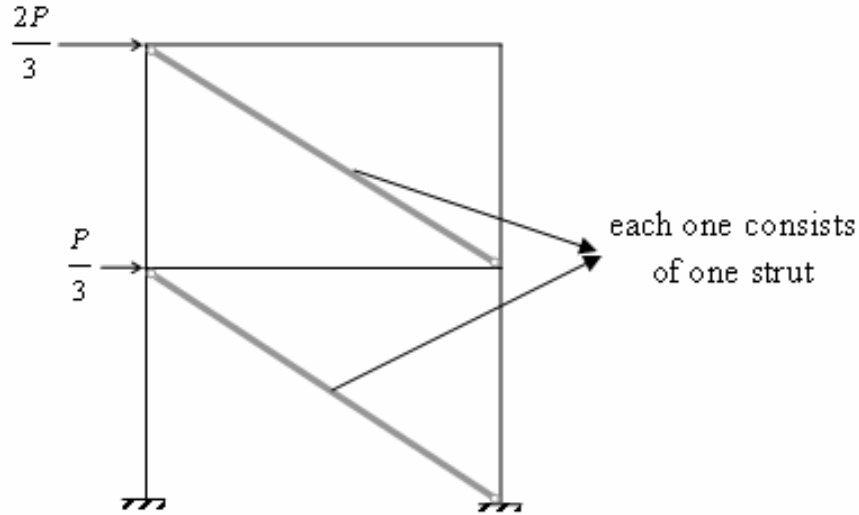
Figure 7.12. Mathematical Model for Infilled RC Frames

The main challenge of the diagonal compression strut approach was to determine the geometric properties of the diagonal strut. The procedure proposed by **FEMA-356 (2000)** and **TSC (2007)** for rectangular section definition of the virtual compression strut width was initially followed by using **Equation 7.3** and **Equation 7.4**, while the strut thickness was taken as the existing infill thickness.

$$\lambda_1 = 4\sqrt{\frac{E_{\text{inf}} t_{\text{inf}} \sin 2\theta}{4 E_{fe} I_{col} h_{\text{inf}}}} \tag{7.3}$$

$$a_{\text{inf}} = 0.175(\lambda_1 h_{col})^{-0.4} d_{\text{inf}} \tag{7.4}$$

where the parameters are defined as;

λ_1 : Coefficient used to determine equivalent width of strut.

E_{inf} : Expected modulus of elasticity of infill material, in MPa.

E_{fe} : Expected modulus of elasticity of frame material, in MPa.

I_{col} : Moment of inertia of column, in mm^4.

t_{inf} : Thickness of infill panel and equivalent strut, in mm.

h_{inf} : Height of the infill panel, in mm.

θ : Angle whose tangent is the infill height-to-length aspect ratio, in radians.

a_{inf} : Width of diagonal compression strut, in mm.

d_{inf} : Diagonal length of infill panel, in mm.

The expected modulus of elasticity of frame material, concrete, was defined using **Equation 7.5**. (**ACI-318, 1995**)

$$E_{fe} = 4750\sqrt{f_{c,frame}} \tag{7.5}$$

where the parameter is defined as;

$f_{c,frame}$: The compressive strength of the frame concrete, in MPa.

Individual infill wall panels which are similar to that of the infills of the test frames were tested under diagonal compression. (**See Appendix-D**) Average compressive strength and modulus of elasticity values for the infills are calculated over the mentioned test results as presented in **Table 7.2.**

Table 7.2. Diagonal Compressive Strength and Modulus of Elasticity Estimations for Infills

Infill Type	Compressive Strength (MPa), $f_{c,strut}$	Modulus of Elasticity (MPa), E_{inf}
Hollow brick infill	2.6	5000
Rectangular PC panel strengthened hollow brick infill	4.5	8000
Strip PC panel strengthened hollow brick infill	5.8	8500
RC infill	15.2	12500

The compressive strength and modulus of elasticity values of the strut materials realized for the present research are also presented in **Table 7.3** in terms of concrete, plaster/mortar strength values of the infill materials.

Table 7.3. Compressive Strength and Modulus of Elasticity Values of the Strut Material in Terms of $f_{c, panel}$ and $f_{c, plaster}$

Infill Type	Diagonal Compressive Strength (MPa), $f_{c,strut}$	Modulus of Elasticity (MPa), E_{inf}
Hollow brick infill	$0.49 * f_{c,plaster}$ or $(f_{c,plaster})^{0.58}$	$2200\sqrt{f_{c,plaster}}$
Rectangular PC panel strengthened hollow brick infill	$0.09 * f_{c,panel}$ or $(f_{c,panel})^{0.38}$	$1100\sqrt{f_{c,panel}}$
Strip PC panel strengthened hollow brick infill	$0.11 * f_{c,panel}$ or $(f_{c,panel})^{0.44}$	$1150\sqrt{f_{c,panel}}$
RC infill	$0.85 * f_{c,panel}$ or $(f_{c,panel})^{0.95}$	$2950\sqrt{f_{c,panel}}$

where the parameters are defined as;

$f_{c, panel}$: Compressive strength of PC panel concrete, in MPa

$f_{c, plaster}$: Compressive strength of infill plaster/mortar , in MPa

The material model below presented in **Figure 7.13** was used to define the compressive strut material with no tensile strength. The thickness of the strut is taken to be equal as the infill thickness. The strut width was initially calculated by **Equation 7.4** and assigned to the analytical model. However, the strut width calculated by the code equation does not incorporate the effects of the anchorage dowels. Therefore, the initial values underestimated the lateral load carrying capacities. Coefficient of $C_{w,strut}$ was introduced to calculate the strut width which best fits with the experimental data for each of the infilled specimen as given in **Equation 7.6**. The coefficient $C_{w,strut}$ varied with the frame aspect ratio, **α**.. The best-fit line equations for all infilled RC frames are tabulated in **Table 7.4**. The aspect ratio-strut width coefficient relationships for all types of infills are also presented in **Figure 7.13**.

$$w_{strut} = C_{w,strut} * a_{inf} \tag{7.6}$$

where the parameters are defined as;

w_{strut} : Best-fitting strut width with the experimental data, in mm

$C_{w,strut}$: Strut width coefficient

a_{inf} : Strut width calculated by **Equation 7.4**, in mm

Table 7.4. Aspect Ratio – Strut Width Coefficient Relationships

Infill Type	Relationship
Hollow brick infill	$C_{w,strut} = -0.6085\alpha^2 + 1.646\alpha + 1.4603$
Rectangular panel strengthened hollow brick infill	$C_{w,strut} = -1.5165\alpha^2 + 4.7107\alpha - 0.7556$
Strip panel strengthened hollow brick infill	$C_{w,strut} = -0..4415\alpha^2 + 1.5379\alpha + 0.5216$
RC infill	$C_{w,strut} = -0.6587\alpha^2 + 2.0227\alpha + 0.0852$
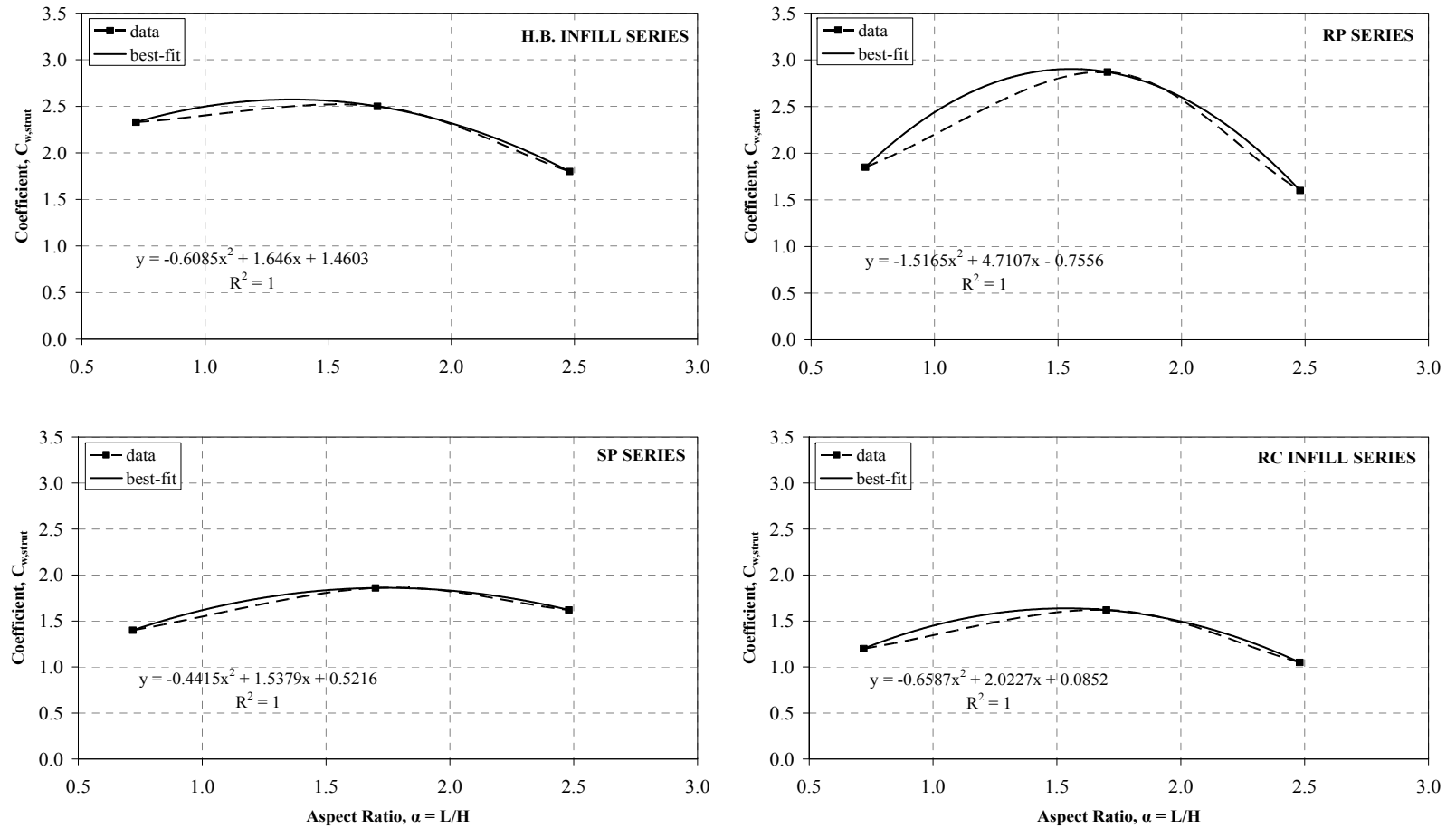
Figure 7.13. Aspect Ratio – Strut Width Coefficient Relationships for All Types of Infills

A uniaxial material model was proposed and used for the strut material simulation in the analytical models as presented in **Figure 7.14**. The uniaxial material models in OpenSees require the maximum stress, ultimate stress and the corresponding strain values. The compressive strength values obtained from the infill panel tests, presented in **Table 7.2**, were assigned as the maximum stress and the elastic modulus values were used to calculate the corresponding maximum strain. The average material strength values of RC frame specimens are given in **Table 7.5** together with the material strength values of the individual infill wall panel tests. Since, these average values for RC infilled frames and individual infill panel tests differ from each other in acceptable range (±10%), the required properties of the strut material were directly taken as the ones obtained from the individual infill wall panel tests. In case of the strain calculations for the strut material model, two coefficients were assigned for various infills as tabulated in **Table 7.6**. Tensile strength of the strut material was ignored.

Table 7.5. Average Compressive Strength Values for the Materials of RC Test Frames and Infill Wall Panels

Material of	**Compressive Strength (MPa)**				
	Frame Concrete	**Mortar/ Plaster**	**Rectangular Panel concrete**	**Strip Panel Concrete**	**RC Infill**
RC Test Frames	14.6	5.2	53.2	54.3	18.5
Infill Wall Panels	-	5.3	50.0	50.0	18.0
Difference (%)	-	1.19	-6.00	-7.9	-2.70
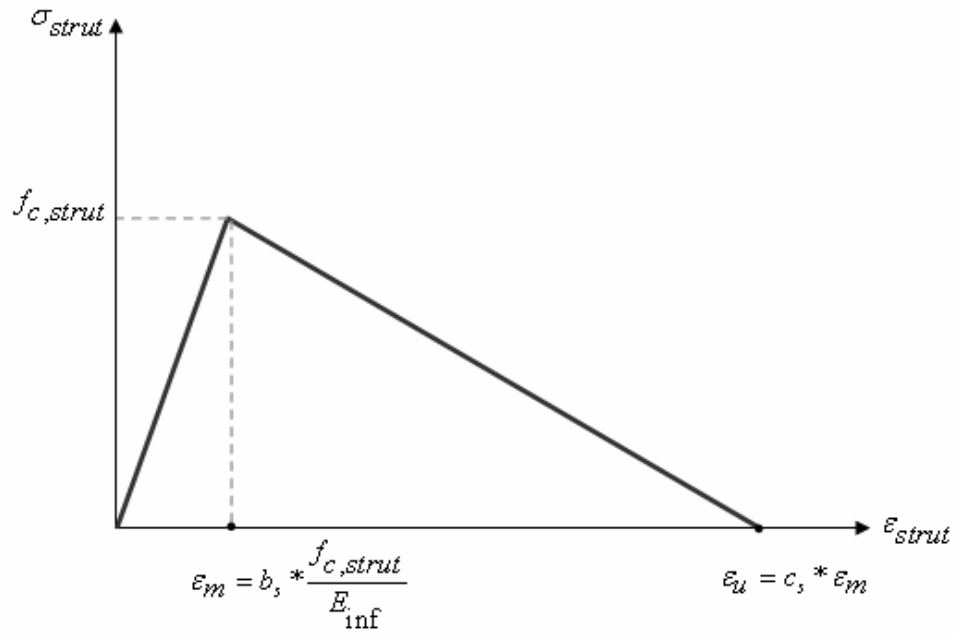
Figure 7.14. Proposed Material Model for Equivalent Diagonal Strut

Table 7.6. Coefficients for Strain Calculations of the Strut Material Model

Infill Type	b_s	c_s
Hollow brick infill	1.20	25
Rectangular panel strengthened hollow brick infill	1.20	85
Strip panel strengthened hollow brick infill	1.20	85
RC infill	1.64	20

Modelling of equivalent diagonal strut briefly consists of two stages; first as the definition of the section properties of the strut and second as the definition of the strut material properties. To summarize, the following steps were followed and suggested in equivalent diagonal strut modelling for infilled RC frames of the present research:

1. Section properties of the equivalent diagonal strut are defined in the first stage. Strut thickness is taken to be equal as the infill thickness. Strut width is calculated by **Equation 7.6**; for which the code proposed strut width is calculated by **Equation 7.4** and then modified with the strut width coefficient by using the proper equation presented in **Table 7.4**.

2. Material properties of the diagonal strut are defined in the second stage by using the proposed compression-only material model presented in **Figure 7.14**. Compressive strength and modulus of elasticity of the strut material can be calculated by using the appropriate equations, presented in **Table 7.3**, which are given in terms of the compressive strength values of the PC panel and the existing plaster. Similarly, strain values corresponding to the maximum and ultimate strength points can be calculated by using the appropriate coefficients presented in **Table 7.6**.

Moreover, the axial load carrying capacity of a compression strut can be calculated using **Equation 7.7.** In addition, the axial rigidity of the strut can be calculated using **Equation 7.8.**, in accordance with **FEMA-356 (2000).**

$$F_{strut} = f_{c,strut} * C_{w,strut} * b_{inf} * a_{inf} \tag{7.7}$$

$$k_{strut} = \frac{w_{strut} * b_{inf} * E_{inf}}{d_{inf}} \tag{7.8}$$

The analytical and experimental capacity curves for all RC frame specimens are presented in **Figure 7.15**.
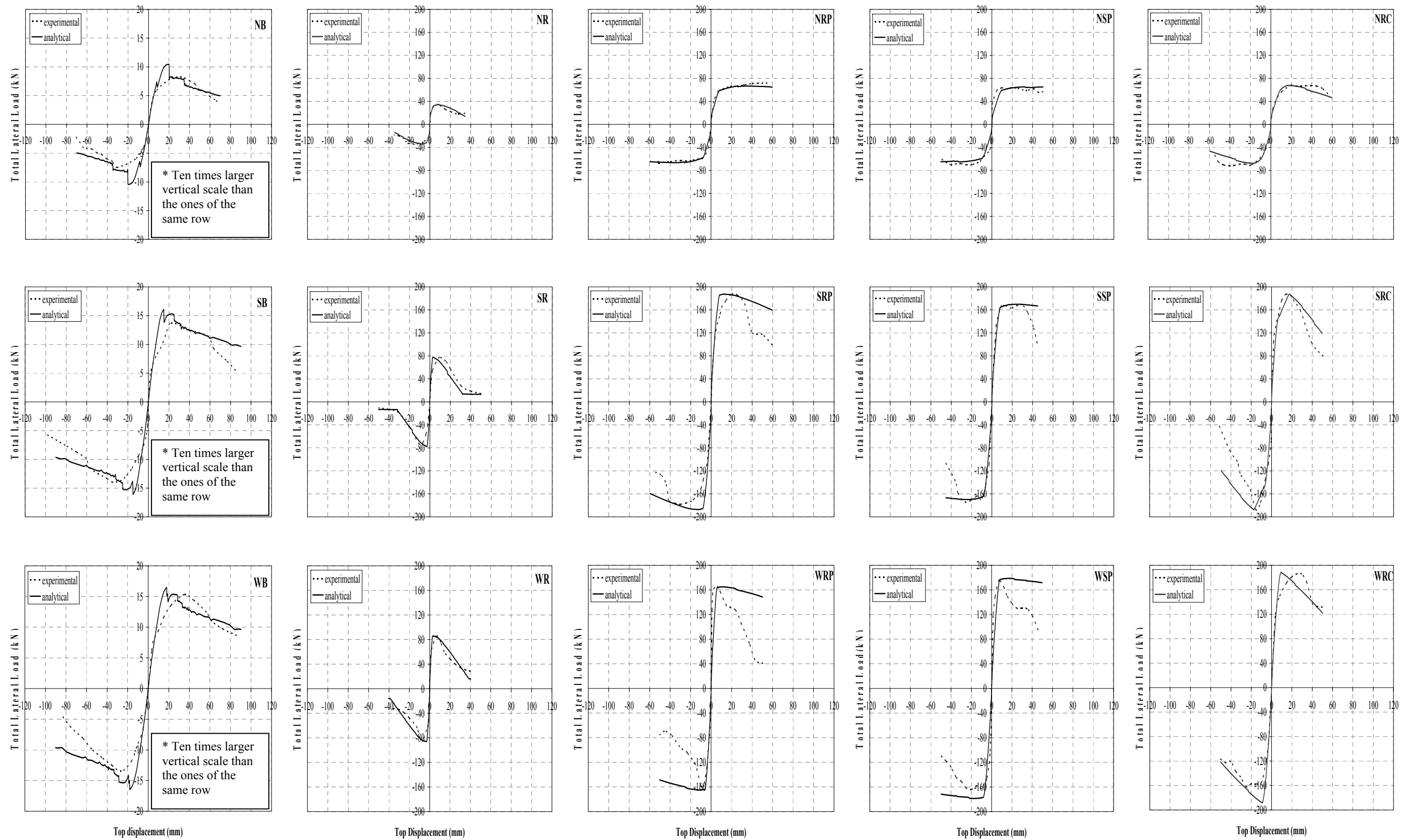
Figure 7.15. Experimental and Analytical Response Envelope Curves for All Series of Specimens

266

7.5. Summary and Concluding Remarks of the Analytical Studies

RC frame tests were analytically modelled and analyzed in OpenSees software. Bond-slip effect was considered and introduced to the analytical models. Equivalent diagonal strut concept was used to simulate the contribution of infill to the behaviour of RC frame subjected to lateral loadings. The main conclusions of the analytical study can be stated as below.

- Bond-slip effect is suggested to be taken into consideration in case of analytical RC frame analysis in order to avoid the overestimations of lateral strength and stiffness of RC frames with plain bars and low strength concrete. This effect is more pronounced for smaller aspect ratio frames together with pinching. As the tensile force in column due to lateral loads increases, the slip of the plain bar from the low strength concrete becomes more pronounced. Thus, the total lateral deformation becomes higher than the calculated flexural deformations.

- **Baran (2005)** suggests to use the equivalent column method and equivalent diagonal strut concept for analytical investigation of PC panel strengthened specimens, emphasizing the better results of the equivalent diagonal strut concept with two struts to simulate the PC panel strengthened hollow brick infill. The equivalent diagonal strut concept was preferred for this study by modelling only a unique strut to simulate the whole infill. One compression strut is defined to represent the infill contribution in each storey; tensile strength of the strut material was ignored.

- Non-linear static pushover analysis was performed for each specimen. It was observed that the equivalent diagonal strut concept well coincides with the lateral loading capacities obtained in the experimental study. Moreover, the post-peak behaviour of strength degradation was able to be simulated, as possible.

- The existing RC framed structures with infills can be analyzed by equivalent diagonal strut method in case of either to see the contribution of existing hollow brick infills, cast-in-place RC infills or seismic performance improvement by PC panel application. This method provides the time and work consumption for quick determination of lateral strength capacities of the RC frames with PC panels.

- It is necessary to underline that, these observations are limited to 1:3 scaled RC frame tests of the present study. Generalization of the conclusions should be done carefully in accordance with the model-prototype relationships presented in **Appendix-A**.

CHAPTER 8

CONCLUSIONS AND RECOMMENDATIONS

8.1. General

PC panel application has been developed in M.E.T.U. Structural Mechanics Laboratory for pre-quake seismic strengthening of existing building structures. The basic idea behind the method is to simply convert the existing non-structural hollow brick infills into load bearing structural elements by covering the surfaces with precast concrete panels using epoxy mortar and enabling shear transfer between the bounding frame and infill with proper anchorage dowel configurations.

The seismic performance of PC panel strengthened RC frames compared to that of the hollow brick infilled RC frames was experimentally proved in the previous studies referring to test data and observations obtained from a number of experiments over which important parameters of the proposed procedure were evaluated. The performance improvement by PC panel application was experimentally investigated in the present research for frames of various aspect ratios.

Total of fifteen RC frames were tested in three different groups of three different aspect ratios. Two different shapes of PC panels were used and the main variable of the frames tests was the frame aspect ratio. Bare frame, hollow brick infilled frame, rectangular and strip shaped PC panel strengthened frames and cast-in-place RC infilled frames were tested for each aspect ratio series. The test results were evaluated considering strength, stiffness, energy dissipation, ductility and story drift characteristics. In the analytical part of the research, the infills of the frames were modelled by equivalent diagonal struts and bond-slip effect localized at the column bases was also considered.

269

Besides, total of eighteen individual wall panel tests were realized in order to study the behaviour of strength of different infill wall types and experimental estimations were obtained for material properties of infills to be used in the analytical studies.

8.2. Conclusions

The conclusions based on the limited experimental data obtained from total of fifteen RC frame and eighteen infill wall panel tests conducted in M.E.T.U. Structural Mechanics Laboratory and analytical studies are presented below:

- PC panel application significantly improved the seismic behaviour of RC frames with hollow brick infills in terms of strength, stiffness, and energy dissipation, ductility and storey drift characteristics for all series of specimens with varying aspect ratios. It can be concluded that PC panel application improved the seismic performance of deficient RC frames both in the elastic and inelastic ranges. The comparisons were made by referring to the hollow brick infilled specimens as lower bound references and to the cast-in-place RC infilled specimens as upper bound references.

- PC panel application can be stated to provide seismic performance improvement almost equal to that of cast-in-place RC infill application. Performance improvements provided by the panel technique and that by the cast-in-place RC infill wall technique are summarised in **Table 8.1**. The following six conclusions are evident from this table.

Table 8.1. Behaviour Improvement by PC Panel Technique and Cast-in-place RC Infill Application

SEISMIC PERFORMANCE INDICATOR	By **PC PANEL TECHNIQUE**								By **CAST-IN-PLACE RC INFILL APPLICATION**							
	With Reference To								With Reference To							
	Bare Frame				Hollow Brick Infilled Frame				Bare Frame				Hollow Brick Infilled Frame			
	Narrower	Standard	Wider	Average	Narrower	Standard	Wider	Average	Narrower	Standard	Wider	Average	Narrower	Standard	Wider	Average
Lateral Load Carrying Capacity	~7.8 times	~13.2 times	~11.2 times	**~10.7 times**	~1.9 times	~2.3 times	~2.0 times	**~2.1 times**	~8.1 times	~13.9 times	~12.1 times	**~11.4 times**	~2.0 times	~2.4 times	~2.1 times	**~2.2 times**
Lateral Stiffness	~18.6 times	~110.0 times	~153.0 times	**~93.9 times**	~1.9 times	~2.3 times	~1.8 times	**~2.0 times**	~19.2 times	~192.5 times	~190.9 times	**~134.2 times**	~2.0 times	~4.0 times	~2.2 times	**~2.7 times**
Ductility	~1.6 times	~1.4 times	~3.0 Times	**~2.0 times**	~1.4 times	~1.2 times	~1.1 times	**~1.2 times**	~1.4 times	~1.7 times	~2.5 times	**~1.9 times**	~0.7 times	~1.4 times	~0.9 times	**~1.0 times**
Cumulative Energy Dissipation	~7.7 times	~9.2 times	~7.6 times	**~8.2 times**	~6.5 times	~5.5 times	~2.5 times	**~4.8 times**	~7.4 times	~7.0 times	~10.0 times	**~8.1 times**	~6.3 times	~4.2 times	~3.2 times	**~4.6 times**

- The performance improvement provided by the proposed panel technique is almost equal to that provided by the cast-in-place RC infill.

- The performance improvement appears to be almost the same in the three series of different aspect ratios, indicating validity of the proposed technique for infill walls of all aspect ratio series.

- PC panel application increased lateral load carrying capacity by 2.1 times of that of hollow brick infilled RC frame, in average of all aspect ratios. This improvement is calculated to be 2.2 times for cast-in-place RC infill application with respect to the hollow brick infilled specimen.

- PC panel application increased lateral stiffness by 2.0 times of that of hollow brick infilled RC frame; while cast-in-place RC infill application increased lateral stiffness by 2.7 times of that of the hollow brick infilled RC frame, in average of all aspect ratios.

- Displacement ductility ratios of PC panel and cast-in-place RC infill strengthened specimens are calculated to be 1.0 times of that of hollow brick infilled RC frame, in average of all aspect ratios.

- Cumulative energy dissipation amounts of PC panel strengthened specimens were calculated to be 4.8 times of that of hollow brick infilled specimen; while cast-in-place RC infill strengthened specimens provided cumulative energy dissipation amounts 4.6 times of that of hollow brick infilled specimen, in average of all aspect ratios.

- Interstorey drift characteristics are acceptable for all strengthened specimens. The PC panel application controlled the drift effectively.

- Epoxy mortar provided sufficient connection in between PC panels and existing infills, separation was not observed in any of the strengthened specimens. Besides, panel-to-panel connections were also successful to provide monolithic behaviour.

- PC panel application is occupant friendly. Even under laboratory conditions, the preparation of cast-in-place RC infills was quiet difficult than strengthening any specimen with PC panels. The strengthening application was realized on the specimens in vertical position to reflect the conditions in practice.

- PC panel method can be practically applied in short times of construction. There is no need of extra formwork and evacuation; therefore the revenue loss

is reduced. It can be said that the pre-quake retrofitting by PC panel application is cost effective.

- Bond-slip effect is suggested to be taken into consideration in case of analytical RC frame analysis in order to avoid overestimations of lateral strength and stiffness of RC frames with plain bars and low strength concrete.

- The experimental material property estimations from the individual wall panel tests were used in analytical studies in case of strut modelling.

- The existing RC framed structures with infills can be satisfactorily analyzed by equivalent diagonal strut method for strengthening design by the panel technique.

8.3. Recommendations

Conversion of non-structural infills into load-bearing structural elements by the use of epoxy glued PC panels is a very effective technique for improving lateral strength, stiffness, ductility and energy dissipation whereas decelerating post-peak stiffness and strength degradation. The performance improvement by PC panel application is almost equal to that of cast-in-place RC infill replacement method. Besides, the method does not require evacuation; needs shorter construction time and causes very little disturbance to the occupants. When all these advantages and performance improvement achieved are considered, the technique is cost effective.

8.3.1. Recommendations for Further Research

PC panel technique was comprehensively investigated by experimental studies. Numbers of parameters related to either RC frame or PC panel geometry and application types were evaluated. In addition, an experimental material research was also conducted in order to investigate the possibility of using high strength semi-lightweight concrete and fibres as panel reinforcement for PC panel production. (**Okuyucu et.all, 2011**) The main objectives of the research were to evaluate the possibility of lowering the panel weight and simplifying the panel production by using

fibres instead of steel mesh as panel reinforcement. The results of this study showed that material properties of high strength, structural, semi-lightweight concrete made of unexpanded perlitte aggregate does not differ much than that of normal weight concrete, except relatively lower elastic modulus. Moreover, use of polypropylene fibres was observed to be more successful than use of steel fibres of same aspect ratio as panel reinforcement. In addition, use of fibre-reinforced mortar as second plaster layer over the existing wall surface was experimentally investigated as a seismic strengthening method. (**Sevil, 2010**) The plastering application with 20 mm thick steel fibre-reinforced mortar of ~20 MPa compressive strength is stated to provide lateral strength improvement by almost two times of that of hollow brick infilled and plastered frame specimen. Considering the results of the above mentioned studies, the following recommendations can be stated for further research of PC panel technique:

- Experimental investigation of seismic performance improvement by PC panel application using the panels made of high strength semi-lightweight concrete.
- Experimental investigation of seismic performance improvement by PC panel application using the panels made of fibre-reinforced high strength concrete.

8.3.2. Recommendations for Practice

PC panel technique is recommended by Turkish Seismic Code (**2007**) as a method to strengthen the existing structure with some limitations. The following recommendations may be stated for practice by also discussing the Turkish Seismic Code (**2007**) limitations.

- Turkish Seismic Code (**2007**) limits the number of storey of the building in which the PC panel technique can be applied up to maximum three storeys, excluding the basement. Since PC panel technique is observed to be as effective as cast-in-place RC infill application, it can be stated that PC panel technique can be applied to the mid-rise buildings with more than three storeys.

- Turkish Seismic Code (**2007**) limits the aspect ratio of the frame system to which PC panel application is applicable to be between 0.5 and 2.0. However, the results of the present research show that PC panel technique can successfully be applied to the frame systems with the aspect ratio of higher than 2.0.

- Turkish Seismic Code (**2007**) only allows inner side PC panel application in which the panels remain within the frame boundaries; eccentrical application is not allowed. Although the present study includes only the inner side applications, it should be stated that the outer surface applications realized in previous PC panel studies also provided successful results of seismic performance improvement.

- The first stage of the pre-quake seismic strengthening is the performance evaluation of the existing building. If the decision of retrofitting is given together with the owner and technical team, the PC panel application can be introduced to the computer model of the building and the performance evaluation is repeated for the case with PC panel application.

- It is suggested to distribute the frames to be strengthened with PC panel technique symmetrically in both plan directions of the building. The application should also be continuous along the height of the building for each of strengthened frame opening.

- Turkish Seismic Code (**2007**) proposes the analytical modelling bases of PC panel technique and suggests simulating the strengthened infills by means of equivalent diagonal struts. In the code, the strut thickness is proposed to be equal to the PC panel thickness. However, in the present research it is suggested to take the strengthened infill thickness to be equal to the thickness of equivalent diagonal strut. Furthermore, the strut width equation proposed in Turkish Seismic Code (**2007**) was modified by a coefficient that is dependent on the aspect ratio of the system and specific to the PC panel type. The infill material properties that are used in strut width calculations are also proposed in this research, while Turkish Seismic Code (**2007**) proposes only to use the panel concrete properties as strut material properties.

- Turkish Seismic Code (**2007**) proposes material properties of the equivalent diagonal strut by only considering the panel material and ignoring the

contribution of existing infill and panel reinforcement. Strut material models with respect to the PC panel type are proposed in this study considering the test results of individual infill panel tests and analytical frame evaluations.

- During the PC panel production, the building can be prepared for the application to reduce the total construction time.

- Prior to PC panel application, the wall surface is suggested to be slightly roughened for better adherence of epoxy mortar. It is very important the application surface to be clean, dry and dust-free.

- The manageable sized PC panels can be easily applied to the infill surface by two workers. The key point of the PC panel placing is to provide full contact in between panels and walls. Soon after the panel is located manually, a number of plastic hammer blows are suggested to remove voids in epoxy mortar.

REFERENCES

ACI-318-95, "Building Code Requirements for Reinforced Concrete", American Concrete Institute, Detroit, Michigan, 1995.

Akın, E., "Strengthening of Brick Infilled RC Frames with CFRP Reinforcement – General Principles", A Doctor of Philosophy Thesis in Civil Engineering., Middle East Technical University, Ankara, Turkey, 2011.

Akın, L.A., "Behaviour of Reinforced Concrete Frames with Masonry Infills in Seismic Regions", A Doctor of Philosophy Thesis in Civil Engineering, Purdue University, West Lafayette, Indiana, U.S.A., 2006.

Altın, S., "Strengthening of Reinforced Concrete Specimens with Reinforced Concrete Infills", A Doctor of Philosophy Thesis in Civil Engineering, Middle East Technical University, Ankara, Turkey, 1990.

Altin, S., Ersoy, U, and Tankut, T., "Hysteretic Response of Reinforced Concrete Infilled Frames", Journal of Structural Engineering, Vol. 118, No 8, August 1992.

Anıl, Ö., "Strengthening of Reinforced Concrete Frames by Reinforced Concrete Infill with Openings", A Doctor of Philosophy Thesis in Civil Engineering, Gazi University, Ankara, Turkey, 2002. (In Turkish)

Armin B. M., Shing, P.B., Schuller, M. P., and Noland, J. L., "Experimental Evaluation of Masonry Infilled Frames", Journal of Structural Engineering, pp. 228-237, March 1996.

Asteris., P.G., "Lateral Stiffness of Brick Masonry Infilled Plane Frames", Journal of Structural Engineering, ASCE, pp. 1071-1079, August 2003.

ASTM E519/E519M, "Standard Test Method for Diagonal Tension (Shear) in Masonry Assemblages",, ASTM International, West Conshohocken, U.S.A., 2007.

Baran, M., "Precast Concrete Panel Reinforced Infill Walls for Seismic Strengthening of Reinforced Concrete Framed Structures", A Doctor of Philosophy Thesis in Civil Engineering, Middle East Technical University, Ankara, 2005.

Benjamin, J. R., and Williams, H.A., "The Behaviour of One Storey Brick Shear Walls", Proceedings of ASCE, v. 84, ST4, pp. 1723-1-1723-30, July1958.

Benjamin, J.R., and Williams, H.A.., "The Behaviour of One Storey Reinforced Concrete Shear Walls", Journal of the Structural Division, ST 3, Vol. 83, pp. 1-49, 1957.

Bertero, V., and Brokken, S., "Infills in Seismic Resistant Building", Journal of Structural Engineering, Vol. 109, No. 6, June 1983.

Binici, B., Özcebe, G., "Analysis of Infilled Reinforced Concrete Frames Strengthened with FRPs", Advances in Earthquake Engineering for Urban Risk Reduction, Wasti, S.T., Özcebe, G. (Editors), Springer Publications, The Netherlands, 2006.

Caccese, V., and Harris, H. G., "Earthquake Simulation Testing of Small-Scale Reinforced Concrete Structures", ACI Structural Journal, Vol. 87, No. 1, pp. 72-80, January-February 1990.

Canbay, E., "Contribution of Reinforced Concrete Infills to the Seismic Behaviour of Structural Systems", A Doctor of Philosophy Thesis in Civil Engineering, Middle East Technical University, Ankara, Turkey, 2001.

Dawe, J., and Seah, C. K., "Behaviour of Masonry Infilled Steel Frames", Canadanian Journal of Civil Engineering, Vol. 16, pp. 865-876, 1989.

Deierlein, G., Elwood, K., Wallace, J., and Lehman, D., (as instructors), "Seismic Performance of Existing Concrete Buildings", 100th Anniversary Earthquake Conference Commemorating the 1906 San Francisco Earthquake, 2006.

Dönmez, S., "Deprem Etkisinde Betonarme Binalarda Hasarın Oluşmasında Dolgu Duvarların Modellenmesi ve Taşıyıcı Sisteme Katkısı", A Master of Science Thesis in Civil Engineering, İstanbul Technical University, İstanbul, Turkey, 2006. (In Turkish)

Dukuze, A., "Behaviour of Reinforced Concrete Frames Infilled With Brick Masonry Panels", A Doctor of Philosophy Thesis in Civil Engineering, University of Alberta, Alberta, Canada, 2000.

Duvarci, M. "Seismic Strengthening of Reinforced Concrete Frames with Precast Concrete Panels", A Master of Science Thesis in Civil Engineering, Middle East Technical University, Ankara, Turkey, 2003.

Erdem, İ., "Strengthening of Existing Reinforced Concrete Frames", A Master of Science Thesis in Civil Engineering, Middle East Technical University, Ankara, Turkey, 2003.

Erduran, E., "Behaviour of Reinforced Concrete Frames Strengthened CFRP Reinforcement: Phase II", A Master of Science Thesis in Civil Engineering, Middle East Technical University, Ankara, Turkey, 2002.

Ersoy U., and Uzsoy S., "The Behaviour and Strength of Infilled Frame", TUBITAK MAG-205 report. Ankara ,Turkey, 95 pages, 1971. (In Turkish)

Ersoy, U., Özcebe, G., and Tankut, T., "Reinforced Concrete", M.E.T.U. Press, Ankara, Turkey, 2003.

FEMA-356, "NEHRP Guidelines for the Seismic Rehabilitation of Buildings", Federal Emergency Management Agency, November 2000.

FIB, Bulletin 10, "Bond of Reinforcement in Concrete", State of the art report prepared by Task Group Bond Models, former CEB, Task Group 5.2. fib, Case Postale 88, CH-1015 Lausanne , 427 pages, August 2000.

Fiorato, A.C., Sözen, M.A., and Gamble, W., "An Investigation of the Interaction of Concrete Frames with Masonry Filler Walls", Structural Research Series Report No. 370, University of Illinois, Urbana, November 1970.

Frosch, R.J., "Panel Connections for Precast Concrete Infill Walls", ACI Structural Journal, Vol. 96, No. 4, July-August 1999.

Garevski, M., Hristovski, V., Talaganov, K., and Stojmanovska, M., "Experimental Investigation of 1/3 Scale R/C Frame with Infill Walls Buildings Structures", 13th World Conference on Earthquake Engineering, Vancouver, B.C., Canada, Paper No. 772, August 2004.

Govindan, P., Lakshmipathy, M. And Santhakumar, A., R., "Ductility of Infilled Frames", ACI Journal, Technical Paper, Title No:83-50, pp. 567 – 576, 1986.

Higashi, Y., Endo, T., Shimizu, Y., "Experimental Studies on Retrofitting of Reinforced Concrete Building Frames", 8th World Conference on Earthquake Engineering, Vol.1, pp. 477-484, San Francisco CA, 1984.

Holmes, M., "Combined Loading on Infilled Frames", Proceedings of the Institution of Civil Engineers, 25:31-38, 1963.

Holmes, M., "Steel Frames with Brickwork and Concrete Infillings", Proceedings of the Institution of Civil Engineers, 19:473-478, 1961.

Kahn, L., F., "Reinforced Concrete Infilled Shear Walls for Aseismic Strengthening", A Doctor of Philosophy Thesis in Civil Engineering, University of Michigan, Michigan, U.S.A. 1976.

Kahn, L.F., and Hanson, R.D. "Infilled Walls for Earthquake Strengthening", Journal of the Structural Division, Proceedings of the American Society of Civil Engineering, Vol. 105, No. ST2, February 1979.

Kara, M.E., "Sünek Olmayan Betonarme Çerçevelerin Betonarme Parçasal Dolgu Duvarlarıyla Güçlendirilmesi", A Doctor of Philosophy Thesis in Civil Engineering, Gazi University, Ankara, Turkey, 2006. (In Turkish)

Keskin, R.S.O., "Behaviour of Brick Infilled Reinforced Concrete Frames Strengthened by CFRP Reinforcement: Phase I", A Master of Science Thesis in Civil Engineering, Middle East Technical University, Ankara, Turkey, 2002.

Kligner, R. E., and Bertero, V. V., "Earthquake Resistance of Infilled Frames", Journal of the Structural Division, Proceedings of the American Society of Civil Engineers, Vol. 104, No.ST6, pp. 973-989, June 1978.

Klingner, R. E., and Bertero, V. V., "Earthquake Resistance of Infilled Frames", Journal of Structural Division, Proceedings of the American Society of Civil Engineers, Vol. 104, No. ST6, June 1976.

Liauw, T.C., "Test on Multi-storey Infilled Frames Subject to Dynamic Lateral Loading", ACI Journal, pp. 551-563, April 1979.

Liauw, T.C., and Kwan, K.H., "Plastic theory of infilled frames with finite interface shear strength." Proceedings of the Institution of Civil Engineers, Part 2, V. 75, No. 3, pp. 707-723, 1983.

Mainstone, R., "On the Stiffness and Strength of Infilled Frames", Proceedings Instution of Civil Engineers, Supplement, Vol. 48, pp. 57-90, 1971.

Makino, M., Kawano, A., and Kurobane, Y., "An Investigation for the Design of Framed Structures with Infill Walls", Proceedings of the 7th WCEE, Vol.4, Istanbul, Turkey, pp. 369-372, September 1980.

Mallick, D. V., and Garg, R. P., "Effect of Openings on the Lateral Stiffness of Infilled Frames", Proceedings Instution of Civil Engineers, Struct. Build., 49, pp. 193–209, 1971.

Mallick, D., "Dynamic Characteristics of Single Story Infilled Frames with Brick Panels", Bulletin of the Indian Society of Earthquake Technology, pp. 193-210, 1972.

Mertol, H.C., "Carbon Fibre Reinforced Masonry Infilled Reinforced Concrete Frame Behaviour", A Master of Science Thesis in Civil Engineering, Middle East Technical University, Ankara, Turkey, 2002.

Mosalam, K. M., White, R. M. and Gergely, P., "Static Response of Infilled Frames Using Quasi-Static Experimentation", Journal of Structural Engineering, ASCE, Vol. 123, No. 11, pp. 1462-1469, November 1997.

Ockleston, A., "Load Tests on a Three Story Reinforced Concrete Building in Johannessburg", The Structural Engineer, Vol. 33(10), pp. 304-322, 1955.

Okuyucu, D., and Tankut, T., "Effect of Panel Concrete Strength on Seismic Performance of RC Frames Strengthened by Precast Concrete Panels", WCCE-ECCE-TCCE Joint Conference: Earthquake& Tsunami, Istanbul, Turkey, IMO Publication Nr.: E/09/03, June 2009.

Okuyucu, D., Turanlı, L., Uzal, B., and Tankut, T., "Some Characteristics of Fibre Reinforced Semi-Lightweight Concrete with Unexpanded Perlite", Magazine of Concrete Research, Article in Press, 2011.

OpenSees Simulation User Manual and Software, Pacific Earthquake Engineering Research Center, University of California, Berkeley, 2008.

Özcebe, G., et. al., "Seismic Assessment and Rehabilitation of Existing Buildings, NATO SfP 977231, 2005.

Park, R., and Paulay, T., "Reinforced Concrete Structures", New York : Wiley, 1975.

Polyakov, S. V., "On the Interaction Between Masonry Filler Walls and Enclosing Frame When Loaded in the Plane of the Wall", Translation in Earthquake Engineering, Earthquake Engineering Research Institute, San Francisco, pp 36-42, 1956.

Popov, E. P., "Engineering Mechanics of Solids", Prentice Hall, New Jersey, U.S.A., pp. 46-47, 1999.

SAP2000 Nonlinear V.11, Computer and Structures, Inc.," California, U.S.A., Licenced to M.E.T.U.

Sevil, T., "Seismic Strengthening of Masonry Infilled R/C Frames with Steel Fiber Reinforcement", A Doctor of Philosophy Thesis in Civil Engineering, Department of Civil Engineering, Middle East Technical University, Ankara, 2010.

Sezen H., and Moehle J. P., "Bond-Slip Behaviour of Reinforced Concrete Members." fib - Symposium (CEB-FIP); Concrete Structures in Seismic Regions, Athens, Greece, May 2003.

Sikadur-31 Two Component Thixotropic Epoxy Mortar Product Data Sheet, Specifications certificated by ISO9001, Sika Construction Chemicals, İstanbul, Turkey, 2009.

Smith, B., S., "Lateral Stiffness of Infilled Frames", Journal of the Structural Division, Proceedings of ASCE, 88: 182-197, 1962.

Smith, B., S., "Behaviour of Square Infilled Frames", Journal of the Structural Division, Proceedings of ASCE 92, ST. 1, 1966a.

Smith, B. S., "Behaviour of Square Infilled Frames", Journal of the Structural Division, Proceedings of ASCE, Building Science, Vol. 91, pp. 381-403, 1966b.

Smith, B. S., "Methods for Predicting the Lateral Stiffness and Strength of Multi-Storey Infilled Frames". Building Science, 2: 247-257, 1967.

Smith, B. S., "Model Test Results of Vertical and Horizontal Loading of Infilled Specimens", ACI Journal, pp. 618-624, August 1968.

Smith, B.S., and Carter, C. A., "Method of Analysis for Infilled Frames", Proc. ICE., pp. 44: 31-48, 1969.

Sonuvar, M., O., Özcebe, G., and Ersoy, U., "Rehabilitation of Reinforced Concrete Frames with Reinforced Concrete Infills", ACI Structural Journal, V.101, No.4, pp. 494-500, July-August 2004.

Sonuvar, O., "Hysteretic Response of Reinforced Concrete Specimens Repaired by Means of Reinforced Concrete Infills", A Doctor of Philosophy Thesis in Civil Engineering, Middle East Technical University, Ankara, Turkey, 2001.

Spit Epcon Embedding System Epoxy Product Data Sheet, Specifications accepted by SOCOTEC, Bourg-Lés Valence, France, July 2005.

StrainSmart Data Acquisition System 5000, Vishay Precision Group, Wendell, U.S.A., 2006.

Süsoy, M., "Seismic Strengthening of Masonry Infilled Reinforced Concrete Frames with Precast Concrete Panels", A Master of Science Thesis in Civil Engineering, Middle East Technical University, Ankara, 2004.

Thomas, F., "The Strength of The Brickwork", The Structural Engineer, Vol. 31, pp. 35-41, 1955.

Turkish Seismic Code, Ministry of Public Work and Settlement, Government of Republic of Turkey, Ankara, 2007.

Wood, R. H., "The Stability of Tall Buildings", Proceedings of Institutions of Civil Engineers, 11:69-102, 1958.

Yoichi, H., Toneo, E., Masamichi, O., "Experimental Study on Strengthening Reinforced Concrete Structure by Adding Shear Wall", Proceedings of the 7th WCEE, Vol.6, Istanbul, Turkey, pp. 263-270, September 1980.

Yüzügüllü, O., "Repair of Reinforced Concrete Frames with Reinforced Concrete Precast Panels", TUBITAK Report, No. MAG-494, Nov, 1979. (In Turkish)

Zhao, J., and Sritharan, S., "Modelling of Strain Penetration Effects in Fiber-Based Analysis of Reinforced Concrete Structures", ACI Structural Journal, 104(2), pp. 133-141, 2007.

APPENDIX – A

SIMILITUDE FOR THE QUASI-STATIC TEST SPECIMENS

The physical conditions and test setup capabilities of the laboratories mostly limit the experimental investigations on the scaled models of the target prototypes in the field. The model is generally in smaller sizes than the prototype and further sometimes constructed from different materials. In this case, it is difficult to predict the prototype behavior from the model test results. The law of similitude must be, therefore, followed in order to first model the prototype structure for experimentation in the laboratory and more significantly to transfer the observed beahvior of the tested model to the prototype structure.

The relationship in between the prototype and the model for the length, volume, point force, displacement and modulus of elasticity are presented in **Table A.1**. In the table, subscript **m** represents the model and similarly subscript **p** represents the prototype.

Table A.1. Model – Prototype Relationship

Variables	Similitude Law
Length	$L_p = \lambda_s * L_m$
Moment of Intertia	$I_p = \lambda_s{}^4 * I_m$
Volume	$V_p = \lambda_s{}^3 * V_m$
Density	$\gamma s = \mathbf{(c)} * \gamma m$
Point Force	$F_p = \lambda_s{}^2 * (s)*F_m$
Modulus of Elasticity	$E_p = (s)*E_m$
Displacement	$\delta p = \lambda_s * \delta m$

where the parameters are defined as:

λ_s : Length factor which is equal to 3 for the research

c&s : Coefficients depend on material properties of the model and prototype

The length scale λ_s is equal to **3** for the present research. Since concrete was used for the model specimens and was already used for the prototype structure, the coefficients of **c** and **s** were assumed to be 1.0. The error introduced by this assumption is small, although this is not 100% correct. Some of the relations in between the prototype and the model are also derived for stiffness (**K**), mass (**M**) and the period (**T**) below:

Derivation of relationship for Stiffness (K) :

$$K = \frac{Force}{Displacement} = \frac{F}{\delta}$$

$$K_p = \frac{F_p}{\delta_p} = \frac{\lambda_s^2 * s * F_m}{\lambda_s * \delta_m} = \lambda_s * s * K_m$$

assuming s=1 and $E_m = E_p$, the equation yields to the following expression:

$$K_p = \lambda_s * K_m \tag{A.1}$$

Derivation of relationship for Mass (M) :

$$M = \frac{Weight}{S\tan dard\ Gravity} = \frac{W}{g} \qquad \text{and} \qquad Weight = Volume * Density = V * \gamma$$

$$W_p = V_p * \gamma_p = \lambda_s^3 * V_m * (c)$$

Assuming c=1 and $\gamma_p = \gamma_m$, the following equation is obtained:

$$W_p = \lambda_s^3 * (V_m * \gamma_m) = \lambda_s^3 * W_m$$

$$M_p = \frac{\lambda_s^3 * W_m}{g} \qquad \Rightarrow \qquad M_p = \lambda_s^3 * M_m \qquad \text{(A.2)}$$

Derivation of relationship for Period (T) :

$$T = \frac{2\Pi}{\sqrt{\dfrac{K}{M}}} \qquad \text{and} \qquad T_m = \frac{2\Pi}{\sqrt{\dfrac{K_m}{M_m}}} \qquad \& \qquad T_p = \frac{2\Pi}{\sqrt{\dfrac{K_p}{M_p}}}$$

$$T_p = \frac{2\Pi}{\sqrt{\dfrac{\lambda_s * K_m}{\lambda_s^3 * M_m}}} = \frac{2\Pi}{\sqrt{\dfrac{K_m}{\lambda_s^2 * M_m}}} = L_s \frac{2\Pi}{\sqrt{\dfrac{K_m}{M_m}}}$$

$$T_p = \lambda_s * T_m \qquad \text{(A.3)}$$

APPENDIX – B

EVALUATION OF INFILL PANEL SHEAR DEFORMATIONS

Shear deformations on infill panels of test frames were measured by diagonally placed dial gages and recorded during the test. It is possible to determine the shape of the panel, since there exits two displacement readings taken along the diagonals of the infill panel. This appendix presents the shear deformation computation of the infill panel.

The approximate shear deformation of the infill panel can be calculated condisdering the approximate deformed shape of the panel presented in **Figure B.1**, as follows.
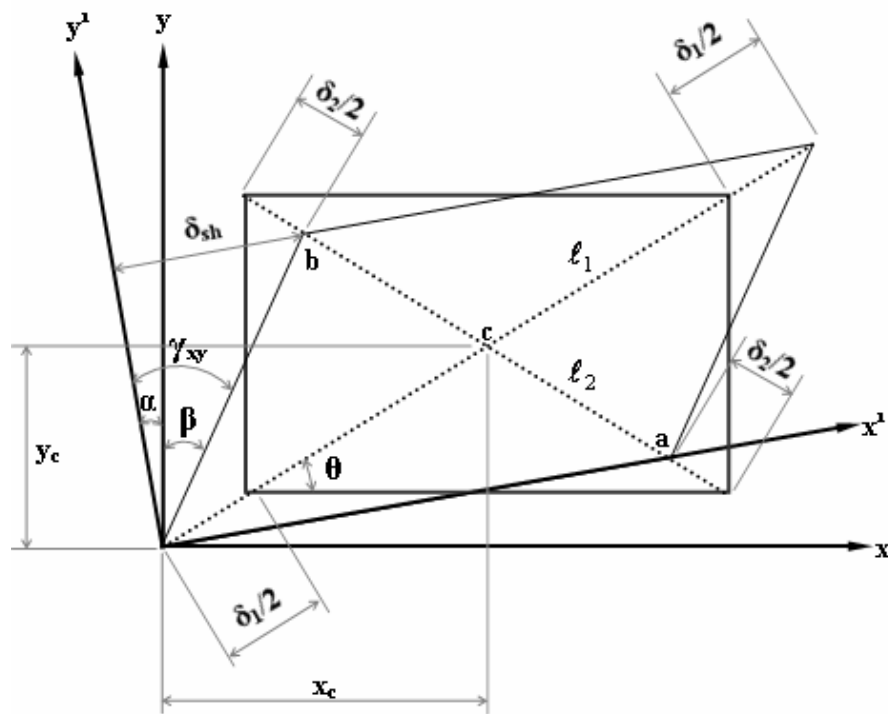
Figure B.1. Rectangular Shape Distortion

where the parameters are defined as:

h : height of the rectangle

w : width of the rectanlg

ℓ_1 : length of the diagonal 1

ℓ_2 : length of the diagonal 2

ℓ'_1 : length of the diagonal 1 after deformation

ℓ'_2 : length of the diagonal 2 after deformation

ε_1 : strain in diagonal 1 direction

ε_2 : strain in diagonal 2 direction

δ_1 : total elongation in diagonal 1 direction

δ_2 : total elongation in diagonal 2 direction

$$\theta = \arctan(\frac{h}{w}) \tag{B1}$$

$$\ell'_1 = \ell_1 + \delta_1 = \ell_1(1 + \varepsilon_1) \tag{B2}$$

$$\ell'_2 = \ell_2 + \delta_2 = \ell_2(1 + \varepsilon_2) \tag{B3}$$

$$x_c = \frac{\ell'_1}{2}\cos(\theta) \tag{B4}$$

$$y_c = \frac{\ell'_1}{2}\sin(\theta) \tag{B5}$$

$$x_a = x_c + \frac{\ell'_2}{2}\cos(\theta) = \left(\frac{\ell'_1 + \ell'_2}{2}\right)\cos(\theta) \tag{B6}$$

$$y_a = y_c - \frac{\ell'_2}{2}\sin(\theta) = \left(\frac{\ell'_1 - \ell'_2}{2}\right)\sin(\theta) \tag{B7}$$

$$x_b = x_c - \frac{\ell'_2}{2}\cos(\theta) = \left(\frac{\ell'_1 - \ell'_2}{2}\right)\cos(\theta) \tag{B8}$$

$$y_b = y_c + \frac{\ell'_2}{2}\sin(\theta) = \left(\frac{\ell'_1 + \ell'_2}{2}\right)\sin(\theta) \tag{B9}$$

The shear deformation of the panel is defined with the angle of γ_{xy} as shown in Figure A1, which is the sum of the angles $\boldsymbol{\alpha}$ and $\boldsymbol{\beta}$. These angles can be easily calculated using the following expressions.

$$\gamma_{xy} = \alpha + \beta \tag{B10}$$

Calculation of α :

$$\alpha = \arctan\left(\frac{y_a}{x_a}\right) = \arctan\left(\frac{\left(\frac{\ell_1^t - \ell_2^t}{2}\right)\sin(\theta)}{\left(\frac{\ell_1^t + \ell_2^t}{2}\right)\cos(\theta)}\right) = \arctan\left(\frac{\ell_1^t - \ell_2^t}{\ell_1^t + \ell_2^t}\tan(\theta)\right) \tag{B11}$$

$$\alpha = \arctan\left(\frac{\ell_1^t - \ell_2^t}{\ell_1^t + \ell_2^t}\left(\frac{h}{w}\right)\right) = \arctan\left(\frac{\varepsilon_1 - \varepsilon_2}{2 + \varepsilon_1 + \varepsilon_2}\left(\frac{h}{w}\right)\right)$$

Calculation of β :

$$\beta = \arctan\left(\frac{x_b}{y_b}\right) = \arctan\left(\frac{\left(\frac{\ell_1^t - \ell_2^t}{2}\right)\cos(\theta)}{\left(\frac{\ell_1^t + \ell_2^t}{2}\right)\sin(\theta)}\right) = \arctan\left(\frac{\ell_1^t - \ell_2^t}{\ell_1^t + \ell_2^t}\cot(\theta)\right) \tag{B12}$$

$$\beta = \arctan\left(\frac{\ell_1^t - \ell_2^t}{\ell_1^t + \ell_2^t}\left(\frac{w}{h}\right)\right) = \arctan\left(\frac{\varepsilon_1 - \varepsilon_2}{2 + \varepsilon_1 + \varepsilon_2}\left(\frac{w}{h}\right)\right)$$

The shear displacement value, $\boldsymbol{\delta_{sh}}$, can be computed using **Equation B13**. Geometrical representation of $\boldsymbol{\delta_{sh}}$ is clearly provided in Figure A1, as well.

$$\delta_{sh} = \gamma_{xy}.h \tag{B13}$$

The shear displacement value $\boldsymbol{\delta_{sh}}$ calculated for each infill panel was the interstorey shear displacement for that storey. Total shear-displacement curve can be calculated by summing the shear-displacements of each panel.

It must be realized that the sensitivity and placement of the instrumentation was not sufficient to obtain accurate values of the shear distortions at infill panel. It is difficult to get accurate measurements of shear deformations due to uncertainties introduced by panel cracking.

APPENDIX – C

ADDITIONAL TEST RESULTS

Detailed evaluation and test results of RC frame tests are provided in **Chapter 5**. Some of the additional test results as total lateral load-column base vertical displacement curves for both north and south columns and total lateral load-second storey infill shear displacement curve are presented in this appendix for each specimen.

Two dial gages were located at the column bases in order to measure the variations in column base rotations. Total lateral load-column base deformation graphs were obtained by using data measured by these dial gages and the lateral load measuring load cell. The displacement of the dial gage with deformation at the south column base is depicted in **Figure C.1.** Both of the dial gauges were installed at some distance from the outer faces of the columns; therefore, measurements of these gages include the rotation of columns at the foundation level. It should also be stated that, the measurements of these gages are affected by cracking of the concrete and yielding of steel under tension and crushing of the concrete under compression of later stages.
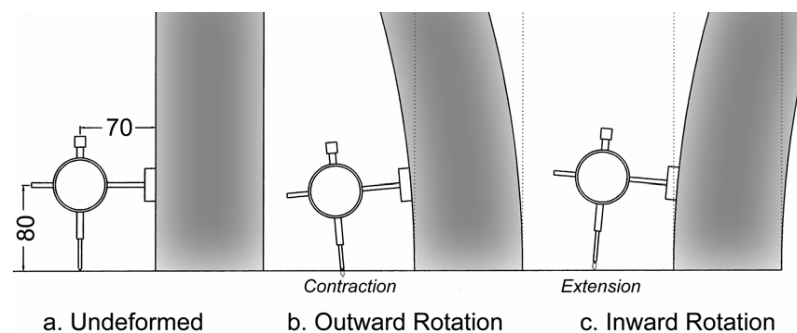
Figure C.1. Measurement of South Column Deformation at the Base (units in mm)

(**Süsoy, 2004**)

As can be seen on **Figure C.1.**, lateral loading in the forward direction caused the south column to rotate outwards and the north column to rotate inwards with respect to the infill. Similarly, loading in the backward direction caused deformation in the opposite directions. Contraction of the dial gauges was measured as positive displacement and extension was measured as negative displacement. In the graphs of total lateral load-column base vertical displacement of, for instance, specimen **NR**, curves are lying in a wider range at one side, according to the loading direction. The curves for both north and south columns of specimen **NR** are wider at the negative side of the graphs. This means that, column bases experience much more deformation towards the opposite direction of the infill, since the infill provides a local restraint reducing column base rotation.

The total lateral load-column base vertical displacement graphs also indicate the starting stage of infill crushing as significant increase in displacements in the negative direction. Column bases rotate in both directions without significant restraint after crushing of the infill. This rotational freedom at column bases indicates a frame behaviour and loss of effectiveness of the infill. The lower bound reference specimens of hollow brick infilled RC frames provided the typical sway frame behaviour; when the infill was separated from the column, the frame almost lost its lateral rigidity that can also be seen in total lateral load-column base vertical displacement graphs.

It can be seen in all series of specimens that, strengthened specimens showed quiet higher column base displacements compared to that of the hollow brick infilled lower bound reference specimens. It can be stated that PC panel application was so effective for all aspect ratios of RC frames such that the PC panel strengthened specimens almost failed in flexure by showing monolithic behaviour. In PC panel strengthened specimens, flexural behaviour indicators such as yielding of the column longitudinal reinforcement in tension side and crushing of the concrete in compression side were observed at the column base where the moment is maximum. As the measurements of the dial gages at the column bases also affected by cracking of the concrete and yielding of steel under tension and crushing of the concrete under compression, the wider loops of total lateral load-column base vertical displacement curves can be evaluated as the indications of flexural failure. Any brittle, shear failure of the specimen was observed in the experimental studies.

C1. Additional Test Results for Specimen NB
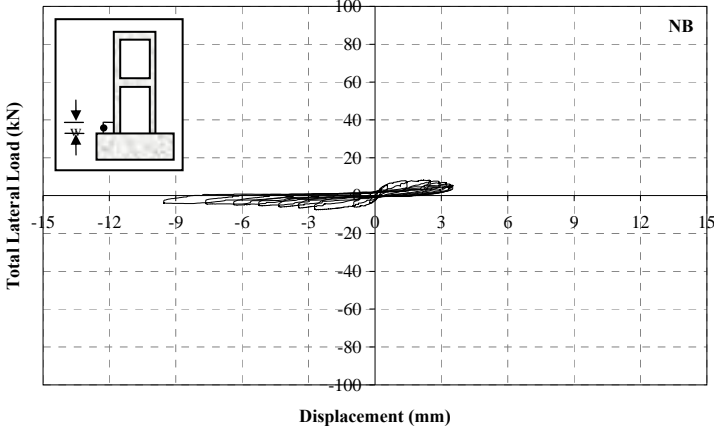
Figure C.2. Total Lateral Load - South Column Base Vertical Displacement,
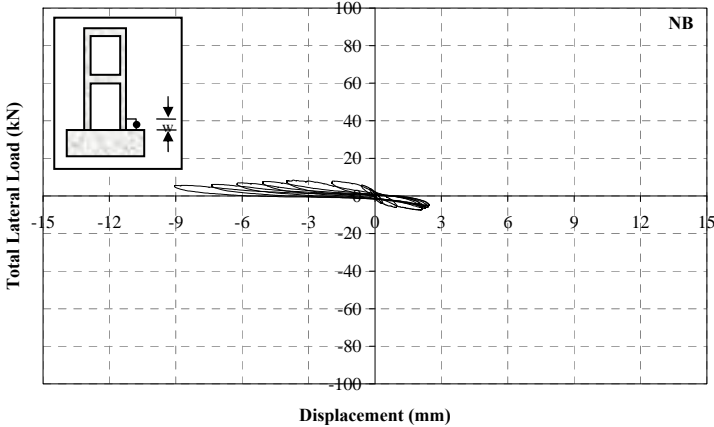
Specimen **NB**

Figure C.3. Total Lateral Load - North Column Base Vertical Displacement,

Specimen **NB**

C2. Additional Test Results for Specimen NR
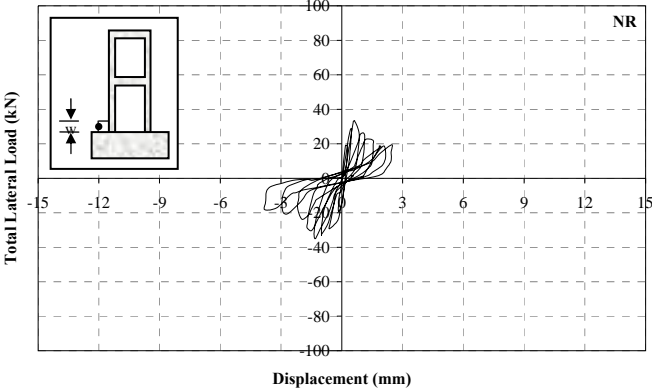
Figure C.4 Total Lateral Load - South Column Base Vertical Displacement, Specimen **NR**
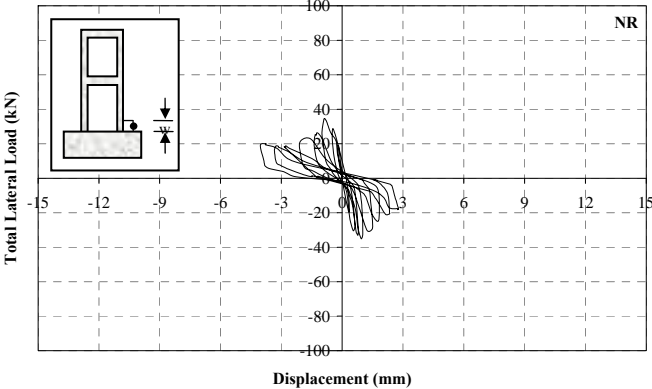
Figure C.5. Total Lateral Load - North Column Base Vertical Displacement, Specimen **NR**
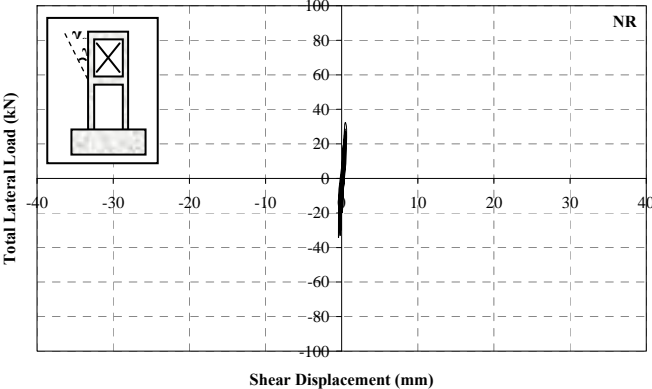
Figure C.6. Total Lateral Load – Second Storey Infill Shear Displacement Curve, Specimen **NR**

C3. Additional Test Results for Specimen NRP
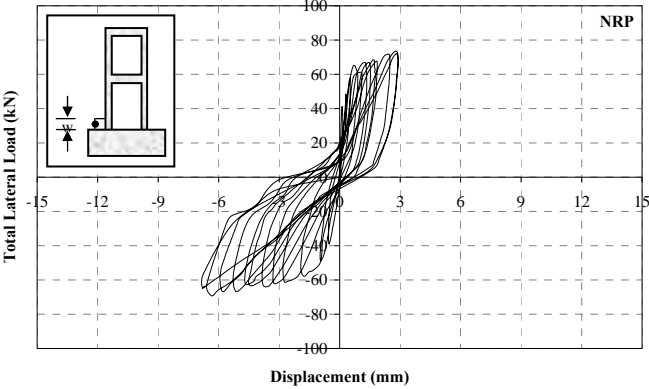
Figure C.7. Total Lateral Load - South Column Base Vertical Displacement Curve, Specimen **NRP**
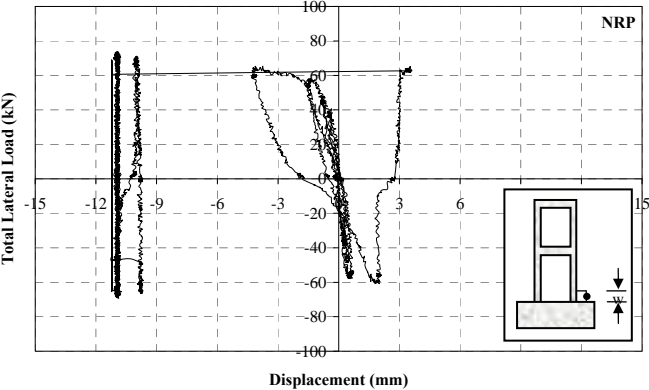
Figure C.8. Total Lateral Load - North Column Base Vertical Displacement Curve, Specimen **NRP**
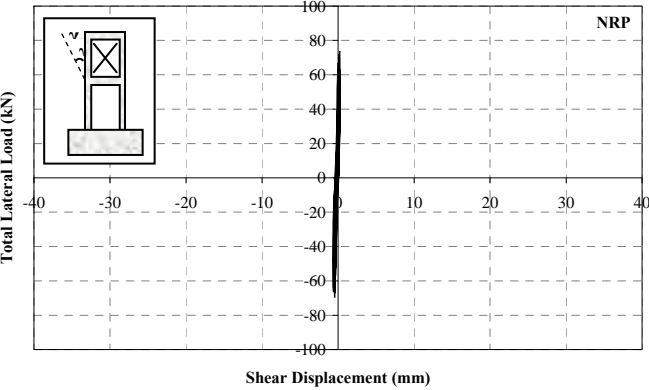
Figure C.9. Total Lateral Load – Second Storey Infill Shear Displacement Curve, Specimen **NRP**

C4. Additional Test Results for Specimen NSP
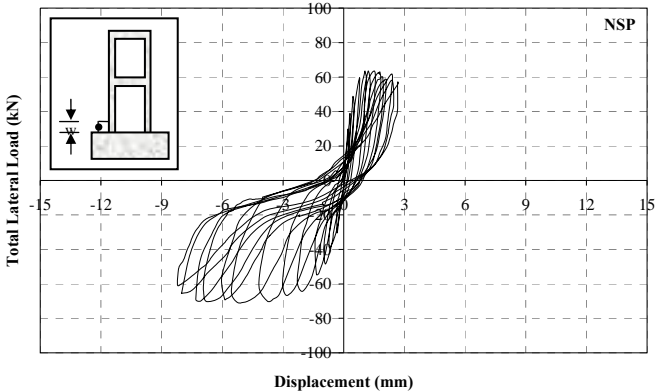
Figure C.10. Total Lateral Load - South Column Base Vertical Displacement Curve, Specimen **NSP**
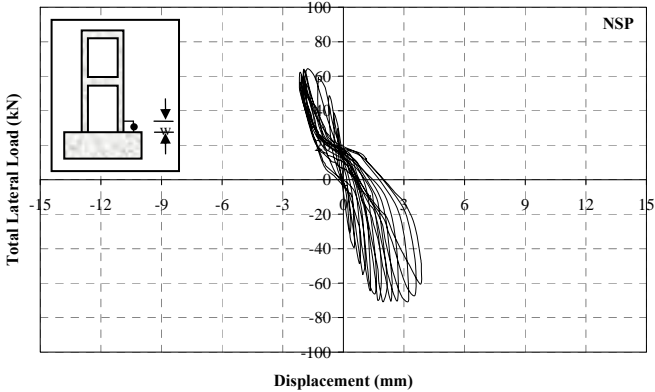
Figure C.11. Total Lateral Load – North Column Base Vertical Displacement Curve, Specimen **NSP**
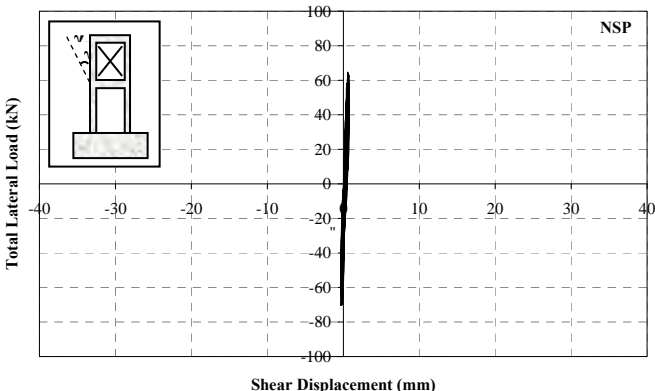
Figure C.12. Total Lateral Load – Second Storey Infill Shear Displacement Curve, Specimen **NSP**

C5. Additional Test Results for Specimen NRC
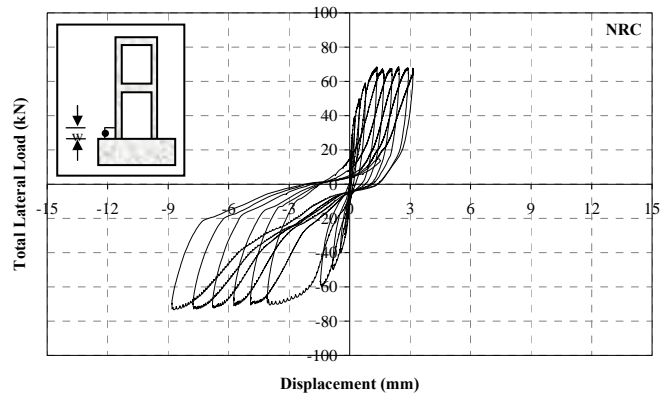
Figure C.13. Total Lateral Load - South Column Base Vertical Displacement Curve, Specimen **NRC**
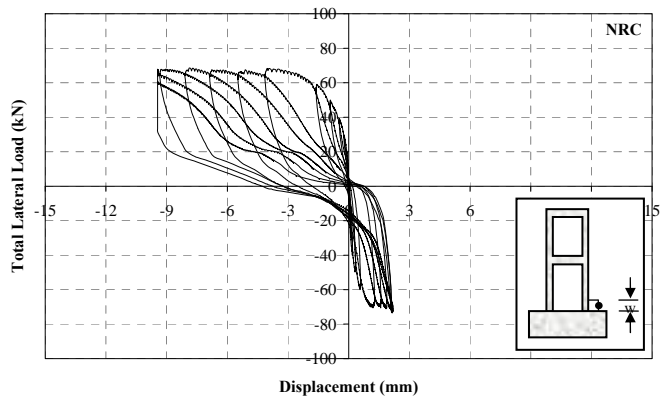
Figure C.14. Total Lateral Load – North Column Base Vertical Displacement Curve, Specimen **NRC**
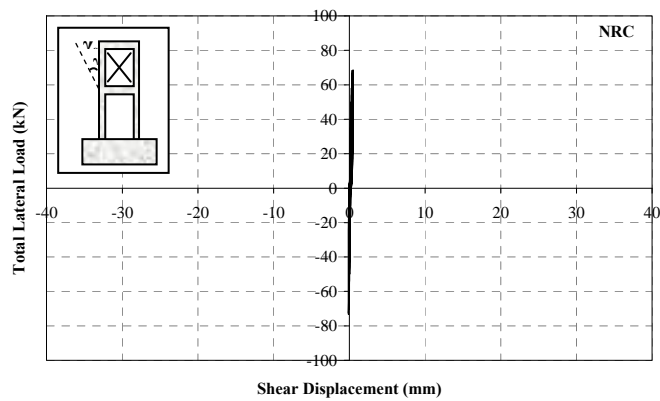
Figure C.15. Total Lateral Load – Second Storey Infill Shear Displacement Curve, Specimen **NRC**

C6. Additional Test Results for Specimen SB
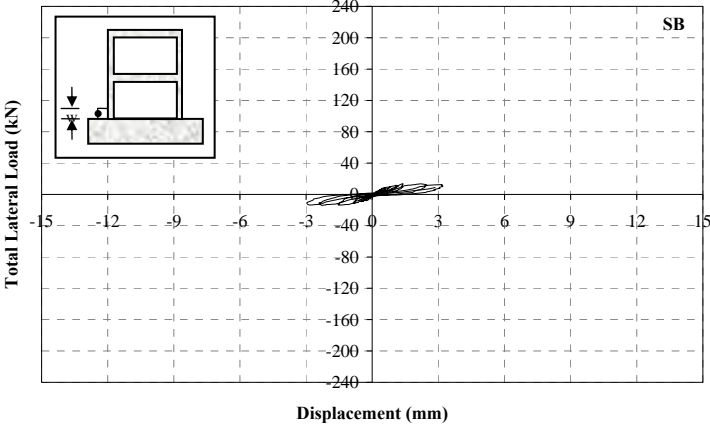
Figure C.16. Total Lateral Load – South Column Base Vertical Displacement Curve, Specimen **SB**
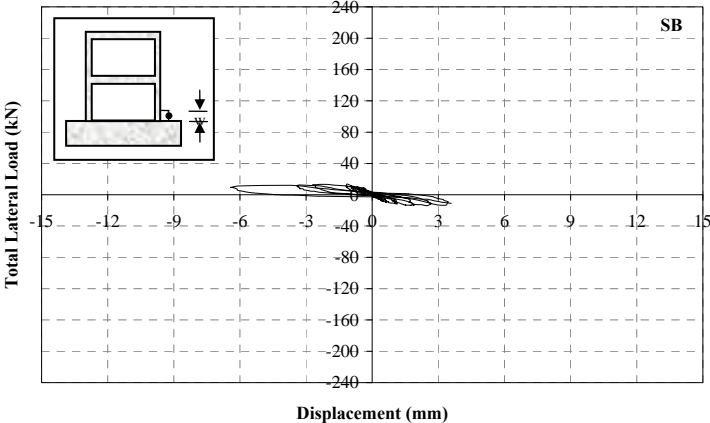
Figure C.17. Total Lateral Load - North Column Base Vertical Displacement Curve, Specimen **SB**

C7. Additional Test Results for Specimen SR
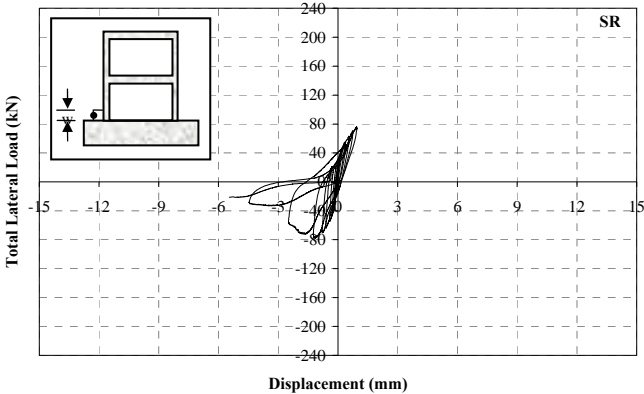
Figure C.18. Total Lateral Load - South Column Base Vertical Displacement Curve, Specimen **SR**
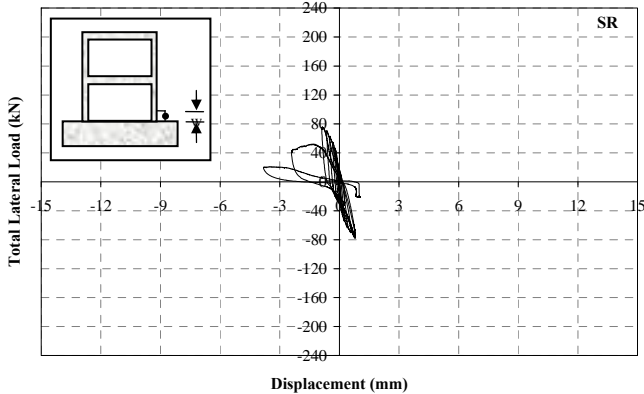
Figure C.19. Total Lateral Load - North Column Base Vertical Displacement Curve, Specimen **SR**
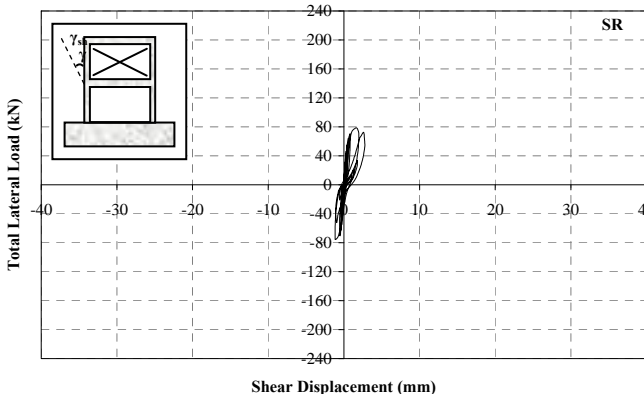
Figure C.20. Total Lateral Load – Second Storey Infill Shear Displacement Curve, Specimen **SR**

301

C8. Additional Test Results for Specimen SRP
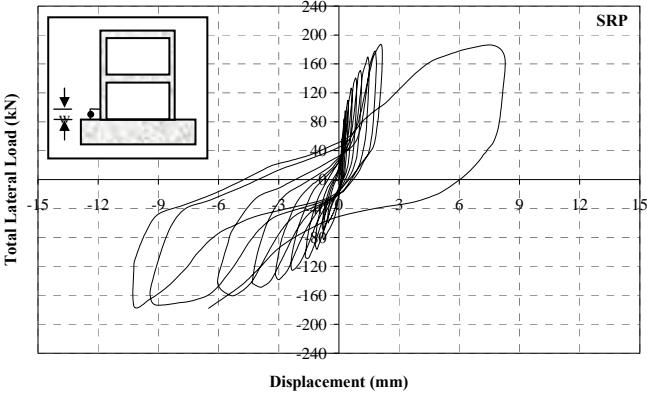
Figure C.21. Total Lateral Load - South Column Base Vertical Displacement Curve, Specimen **SRP**
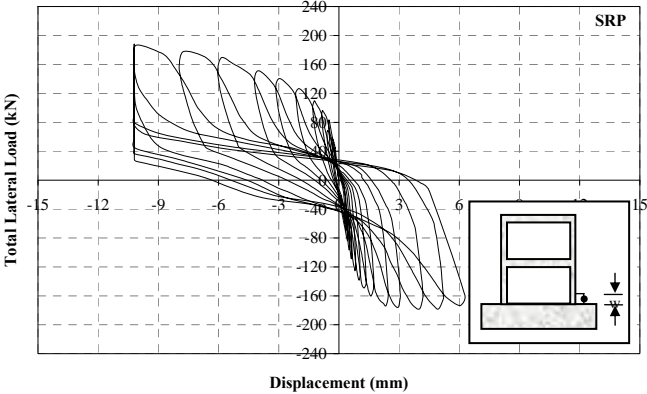
Figure C.22. Total Lateral Load – North Column Base Vertical Displacement Curve, Specimen **SRP**
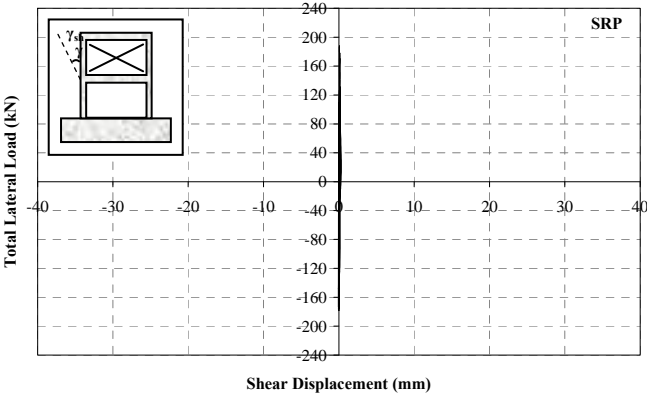
Figure C.23. Total Lateral Load – Second Storey Infill Shear Displacement Curve, Specimen **SRP**

C9. Additional Test Results for Specimen SSP
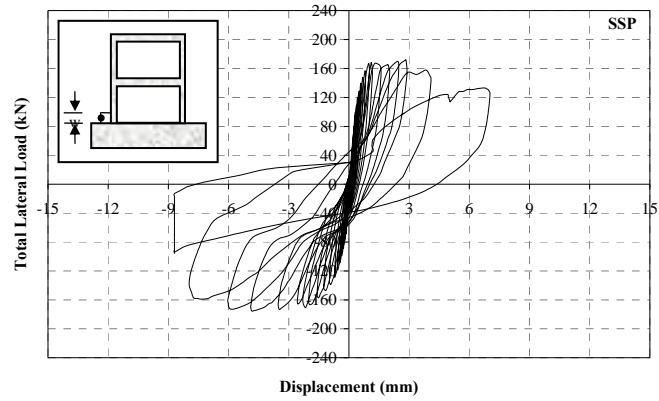
Figure C.24. Total Lateral Load - South Column Base Vertical Displacement Curve, Specimen **SSP**
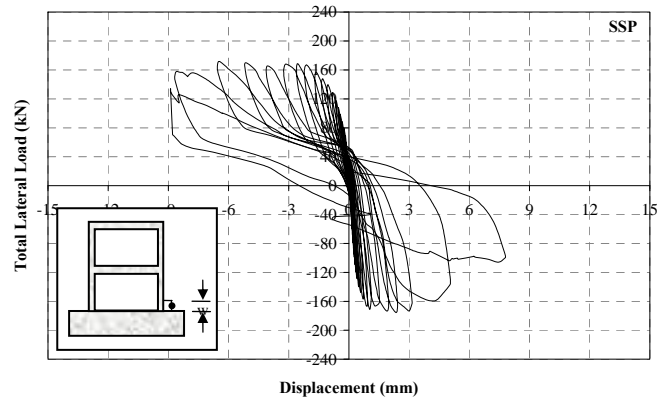
Figure C.25. Total Lateral Load – North Column Base Vertical Displacement Curve, Specimen **SSP**
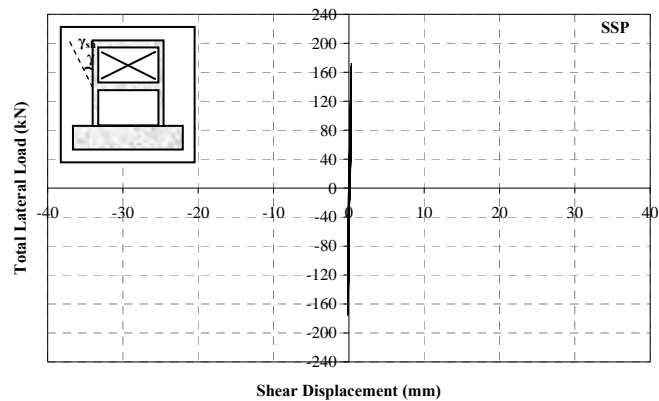
Figure C.26. Total Lateral Load – Second Storey Infill Shear Displacement Curve, Specimen **SSP**

C10. Additional Test Results for Specimen SRC
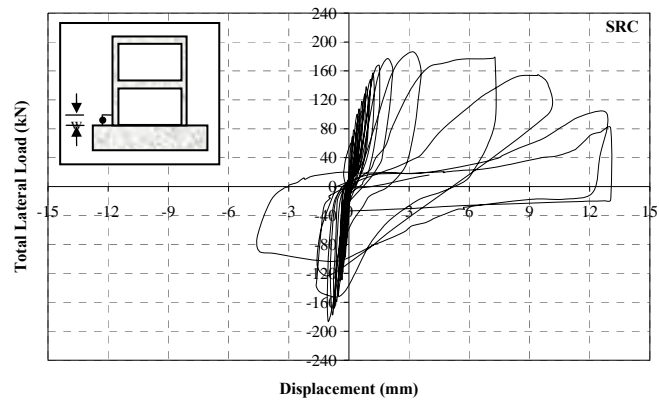
Figure C.27. Total Lateral Load - South Column Base Vertical Displacement Curve, Specimen **SRC**
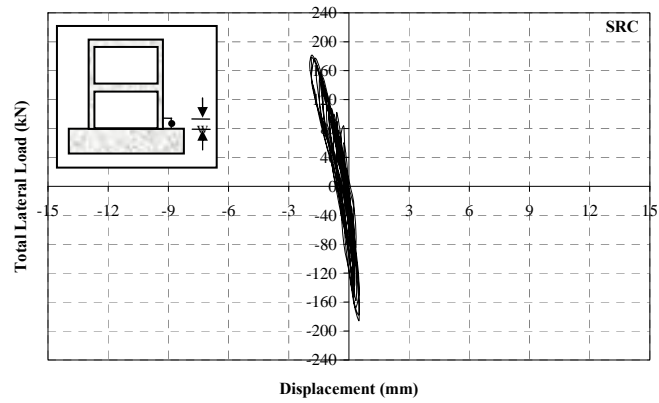
Figure C.28. Total Lateral Load – North Column Base Vertical Displacement Curve, Specimen **SRC**
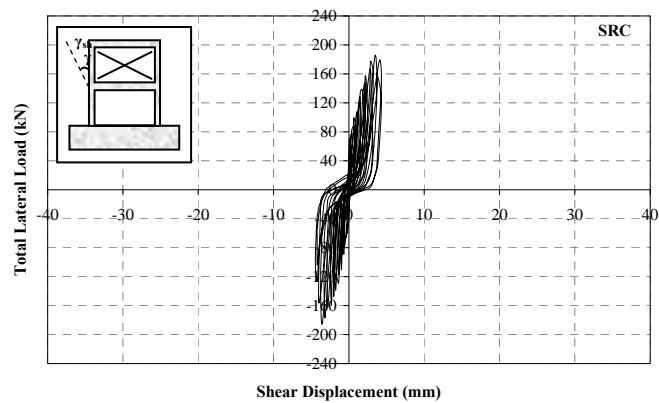
Figure C.29. Total Lateral Load – Second Storey Infill Shear Displacement Curve, Specimen **SRC**

C11. Additional Test Results for Specimen WB
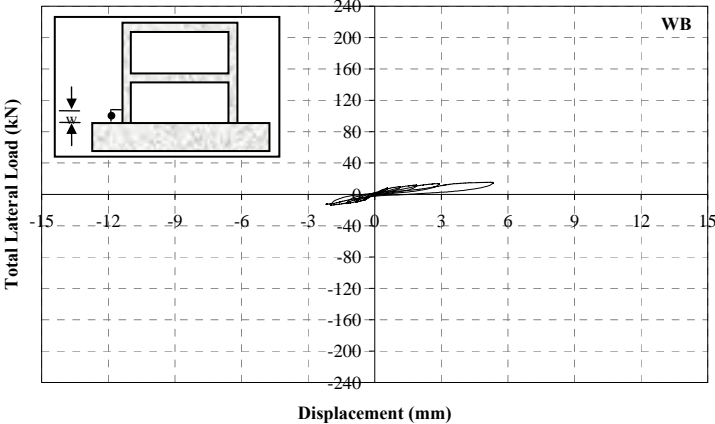
Figure C.30. Total Lateral Load - South Column Base Vertical Displacement Curve, Specimen **WB**
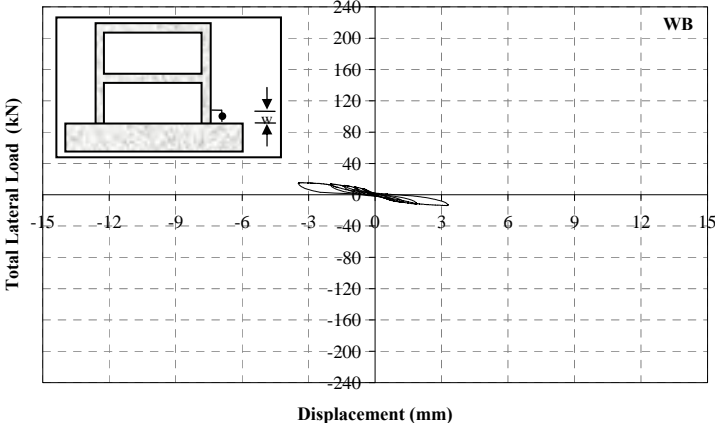
Figure C.31. Total Lateral Load - North Column Base Vertical Displacement Curve, Specimen **WB**

305

C12. Additional Test Results for Specimen WR
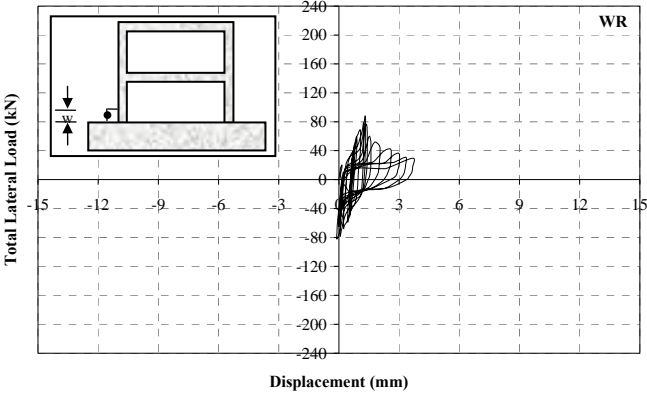
Figure C.32. Total Lateral Load - South Column Base Vertical Displacement Curve, Specimen **WR**
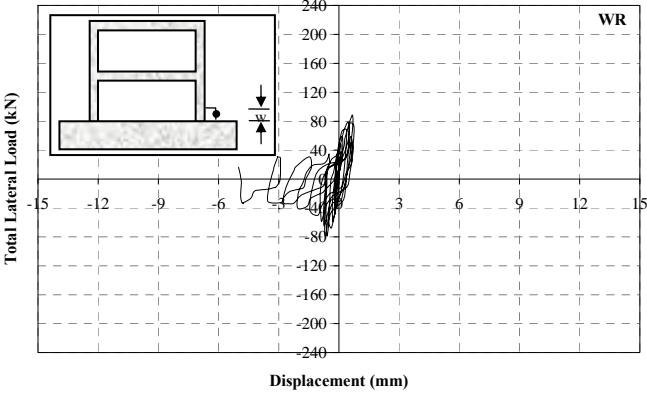
Figure C.33. Total Lateral Load - North Column Base Vertical Displacement Curve, Specimen **WR**
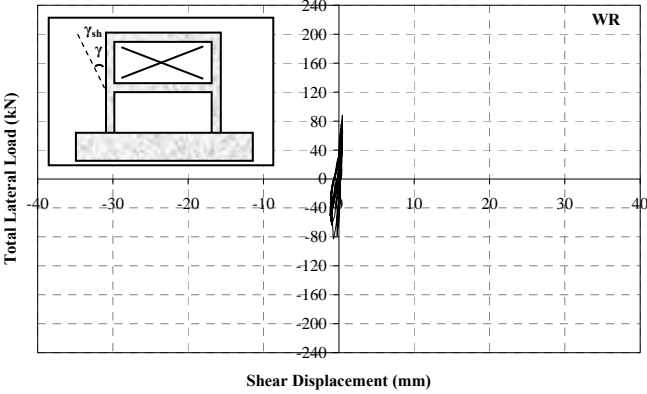
Figure C.34. Total Lateral Load – Second Storey Infill Shear Displacement Curve, Specimen **WR**

C13. Additional Test Results for Specimen WRP
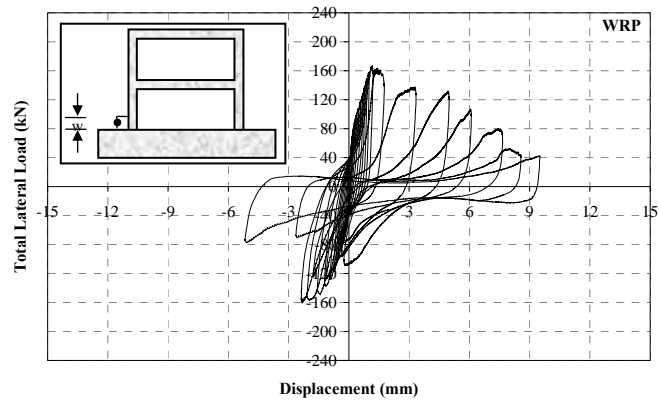
Figure C.35. Total Lateral Load - South Column Base Vertical Displacement Curve, Specimen **WRP**
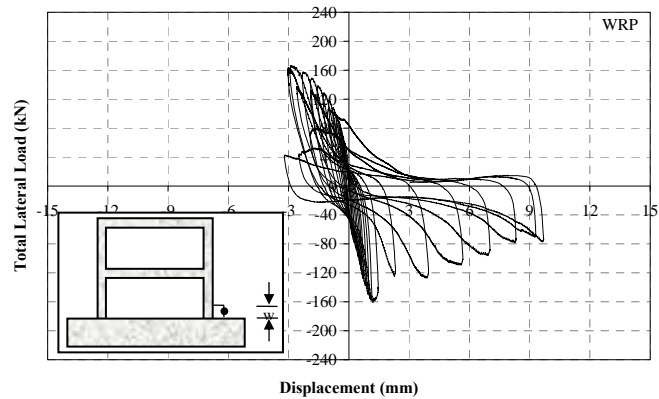
Figure C.36. Total Lateral Load - North Column Base Vertical Displacement Curve, Specimen **WRP**
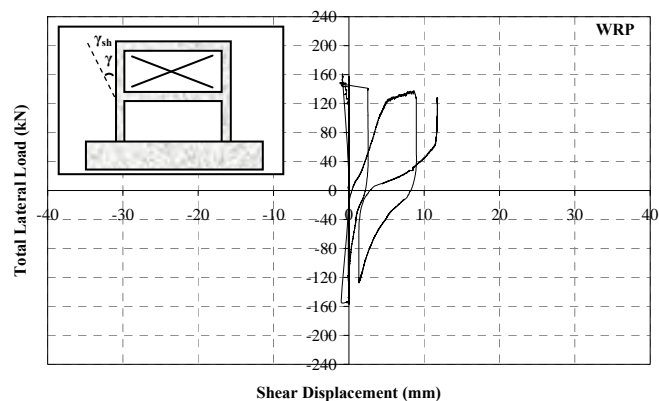
Figure C.37. Total Lateral Load –Second Storey Infill Shear Displacement Curve, Specimen **WRP**

C14. Additional Test Results for Specimen WSP
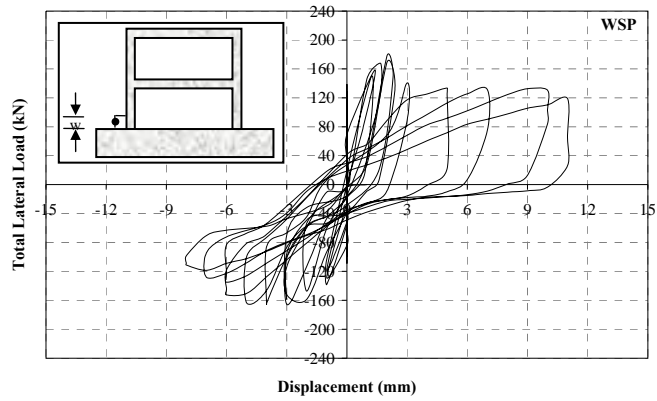
Figure C.38. Total Lateral Load - South Column Base Vertical Displacement Curve, Specimen **WSP**
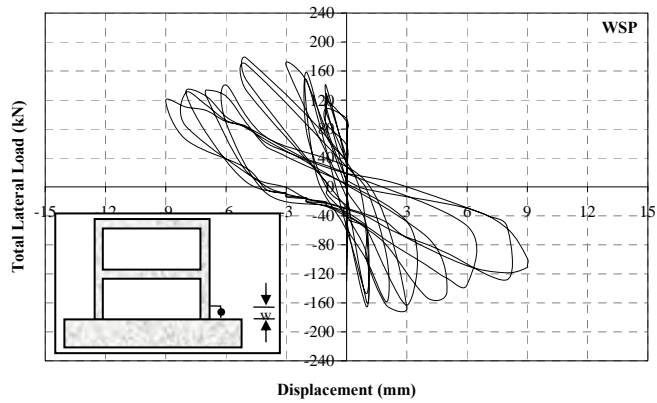
Figure C.39. Total Lateral Load - North Column Base Vertical Displacement Curve, Specimen **WSP**
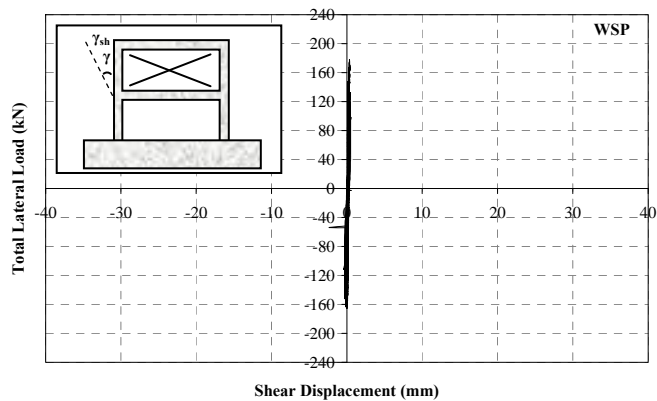
Figure C.40. Total Lateral Load – Second Storey Infill Shear Displacement Curve, Specimen **WSP**

C15. Additional Test Results for Specimen WRC
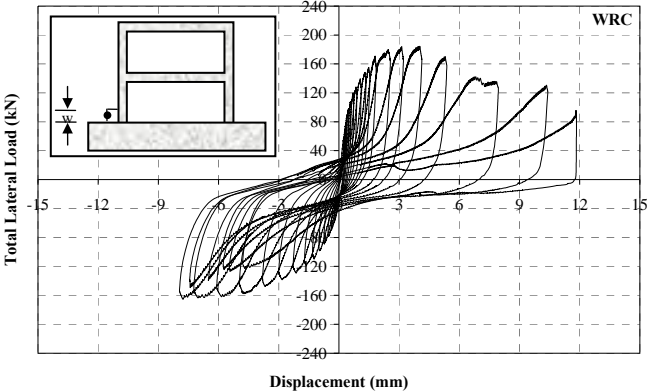
Figure C.41. Total Lateral Load - South Column Base Vertical Displacement Curve, Specimen **WRC**
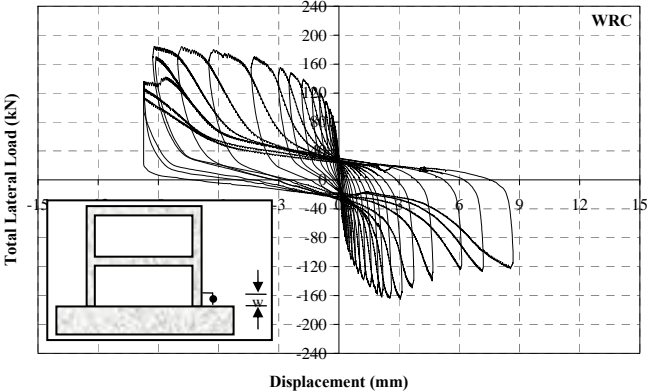
Figure C.42. Total Lateral Load - North Column Base Vertical Displacement Curve, Specimen **WRC**
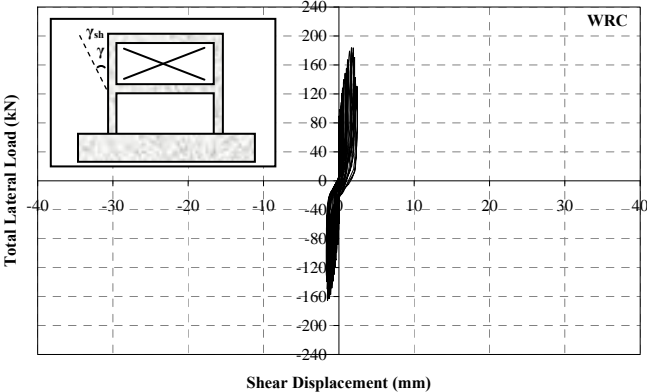
Figure C.43. Total Lateral Load – Second Storey Infill Shear Displacement Curve, Specimen **WRC**

APPENDIX - D

INFILL PANEL TESTS

D.1. General

Behaviour of individual infill wall panels which were similar as the infills of RC frame specimens of the present research were investigated by infill panel tests, prior to the RC frame experiments. Infill panels were prepared in the laboratory and tested under monolithic diagonal compression in accordance with ASTM E 519-81 standards. **(ASTM E519/E519M – 10, 2007)** Hollow brick infills, PC panel strengthened infill walls and RC infill panels were of the test specimens. The information gathered in panel tests was valued to model the RC frame tests in analytical evaluation. The details of infill panel tests are presented in this chapter.

D.2. Test Specimens

The infill panel experiments were performed on 1:3 scale model walls. All masonry wall panels were square in dimensions of 700 x 700 mm. Thickness of the hollow brick walls, PC panel strengthened panels and RC infills were ~90 mm, ~110 mm and ~60 mm, respectively.

Infill panel test specimens were all prepared in the METU Structural Mechanics Laboratory. Hollow brick infill wall panels were constructed in the same manner as the RC frame infills. Strip and rectangular shaped panels were also cast, being same as the ones used in PC panel application for RC frames. The PC panel details are presented in **Chapter 4**. RC infills simulating the cast-in-place RC infill material were also prepared

same as that of the frame application. **Table D.1** presents the appellation of the infill panel test specimens and **Figure D.1** provides an illustration of cross section of all groups of specimens.

Table D.1. Appellation and Definitions of Infills Panel Test Specimens

Hollow Brick Infill Specimens	
HBP1	Hallow brick wall panel with 10 mm thick plaster on both side
HBP2	
HBP3	
HBP4	
Rectangular PC Panel Strengthened Hollow Brick Infill Specimens	
RPS1	10 mm plastered hallow brick wall panel strengthened with 20 mm thick rectangular PC panels on one side
RPS2	
RPS3	
RPS4	
Strip PC Panel Strengthened Hollow Brick Infill Specimens	
SPS1	10 mm plastered hallow brick wall panel strengthened with 20 mm thick strip PC panels on one side
SPS2	
SPS3	
SPS4	
RC Infill Specimens	
RC1	60 mm thick reinforced concrete infill panel with two layers of steel mesh reinforcement of $\Phi6/150mm$
RC2	
RC3	
RC4	
RC5	
RC6	

Figure D.1. Sectional View Illustrations of All Series of Specimens

D.2.1. Hollow Brick Infill Panel Specimens, HBS Series

Total of four hollow brick infill panels were prepared and tested under diagonal compression. Test data of the three **HBS** specimens could be reliably taken into consideration; however one of the test data could not be properly recorded due to technical reasons.

HBS series of specimens resemble the main reference specimens of the infill panel tests. 1:3 scaled hollow bricks and common mortar were used for wall construction as explained in **Chapter 4.** The specimens were first prepared; 10 mm thick plastering was applied on both sides; cured by wet burlap coating and tested 28 days after the construction. Cylinder mortar samples of 75 mm in diameter and 150 mm in height were tested on the day of experiment in order to obtain the compressive strength of the mortar/plaster material. Mix design and compressive strength values of mortar/plaster are presented in **Table D.2** and **Table D.3**, respectively. Compressive test results of the tiles are tabulated in **Table D.4**. General views of the hollow brick infill specimens are presented in **Figure D.2.**

Figure D.2. Views of the Specimen **HBS** before the Experiment

Table D.2. Mix Design of Mortar and Concrete by Weight Percentage (%)

Material used for	Cement	Lime	Water	Super plasticizer	Sand (0-3 mm)	Fine Aggregate (3-7 mm)
RC Infill	17*	-	9	-	39	35
PC Panel	19**	-	10	1***	38	33
Mortar/Plaster	11*	7	14	-	68	-

*   : PC 32.5

** : PC 42.5

*** : Percentage by cement weight

Table D.3. Compressive Strength of Mortar and Concrete Samples

Mortar and Plaster (MPa)	PC Panel Concrete (MPa)	RC Infill Concrete (MPa)
5.3	50	18

Table D.4. Hollow Brick Tile Compressive Strength Test Results

No	Maximum Load (kN)	Net Area (mm^2)	Net Compressive Strength (MPa)	Gross Area (mm^2)	Gross Compressive Strength (MPa)
1	64.7	2815	23.0	5865	11.0
2	81.5	2815	29.0	5865	13.9
3	65.5	2815	23.3	5865	11.2
4	78.0	2815	27.7	5865	13.3
5	82.5	2815	29.3	5865	14.1
6	77.5	2815	27.5	5865	13.2
7	88.2	2815	31.3	5865	15.0
8	76.3	2815	27.1	5865	13.0
9	81.8	2815	29.1	5865	13.9
10	73.2	2815	26.0	5865	13.1
		average :	**27.3**	average :	**13.1**
		cov* :	**0.10**	cov* :	**0.10**

* : coefficient of variation

D.2.2. Rectangular PC Panel Strengthened Hollow Brick Infill Specimens, RPS Series

Total of four **RPS** specimens were prepared and tested under diagonal compression in order to see the contribution of rectangular PC panel application on the shear behaviour of hollow brick infill wall panel. All tests of **RPS** series of specimens were successful and whole data of four **RPS** specimens were investigated.

PC panel strengthening procedure, as explained in **Chapter 4**, was regularly followed in specimen preparation. Hollow brick infill wall panels were first prepared together with **HBS** specimens, using the same hollow bricks and mortar batch. Rectangular PC panels were prepared in 20 mm thickness and reinforced by one layer of welded wire steel mesh of Φ3/50 mm. Both of the strip and rectangular PC panels were moulded from the same concrete batch. After curing of both rectangular PC panels and hollow brick infill panel, PC panels were epoxy glued to the infill wall using the same epoxy mortar as the one for RC frame specimens, Sikadur-31. Cylinder mortar samples of 75 mm in diameter and 150 mm in height and PC panel concrete samples of 150 mm in diameter and 300 mm in height were tested on the day of experiment in order to obtain the compressive strength values of the materials. Mix design and compressive strength values of mortar/plaster and PC panel concrete are presented in **Table D.2** and **Table D.3**, respectively. Compressive test results of the tiles and mechanical properties of PC panel reinforcement are given in **Table D.4** and **Table D.5**, respectively. Views of the rectangular PC panels strengthened hollow brick infill specimens are presented in **Figure D.3.**

Table D.5. Properties of Steel Mesh Reinforcement

Material used for	Diameter (mm)	Mesh Spacing (mm)	Yield Strength (MPa)	Ultimate Strength (MPa)
RC Infill Panel	6	150	340	460
PC Panel	3	30	-	680

Figure D.3. Views of the Specimen **RPS** before and during the Experiment

D.2.3. Strip PC Panel Strengthened Hollow Brick Infill Specimens, SPS Series

Total of four **SPS** specimens were prepared and tested under diagonal compression in order to see the contribution of strip shaped PC panel application on the shear behaviour of hollow brick infill wall panel. Since, a technical problem occurred in the setup during the test of specimen **SPS3**, the test was terminated and reliable data could not be taken. Experimental data of remaining three **SPS** specimens were evaluated.

The specimen preparation for **SPS** series is same as the preparation of **RPS** series of specimens as explained in **Section D.2.2**. Mix design and compressive strength values of mortar/plaster and PC panel concrete of **SPS** series are presented in **TableD.2** and **Table D.3**, respectively. Cylinder mortar samples of 75 mm in diameter and 150 mm in height and PC panel concrete samples of 150 mm in diameter and 300 mm in height were tested on the day of experiment in order to obtain the compressive strength values of the materials. Compressive test results of the tiles and mechanical properties of PC panel reinforcement are given in **Table D.4** and **Table D.5**, respectively. Views of the strip PC panel strengthened hollow brick infill specimens are presented in **Figure D.4.**

Figure D.4. Views of Specimen **SPS** before the Experiment

D.2.4. Reinforced Concrete Infill Specimens, RC Series

Total of six **RC** infill panels were prepared and tested under diagonal compression. Five **RC** infill tests were successful, only one premature failure was experienced and therefore, five of the test data were realized for evaluation. **RC** infill panels had the same thickness of ~60 mm and reinforcement with that of cast-in-place RC infills of RC frame tests as two layers of steel mesh of Φ6/150 mm. Preparation views of this group of specimens are provided in **Figure D.5.** Wooden moulds were used for concrete moulding on the floor of the laboratory.

Figure D.5. Views from **RC** Infill Panel Specimen Preparations

All of **RC** infill panel specimens were cast from the same concrete batch. Moist curing was applied to the specimens by wet burlap coating and specimens were tested ~28 days after moulding. Cylinder concrete samples of 150 mm in diameter and 300 mm in height were tested on the day of experiment. Mix design and compressive strength value of the **RC** infill concrete are presented in **Table D.2** and **Table D.3**, respectively. Mechanical properties of RC infill reinforcement are given in **Table D.5.** Views of the **RC** specimens are presented in **Figure D.6.**

Figure D.6. Views of the Specimen **RC** before the Test

D.3. Test Setup and Instrumentation

The setup for panel specimens was constructed in a vertical load bearing stiff steel frame. Test setup illustration and general view is provided in **Figure D.7** and **Figure D.8,** respectively**.** A hydraulic jack was used for load application and a load cell of 500 kN capacity with ±2.5 kN precision was placed to measure the applied load. Dial gages of 20 mm measurement capacity with ±0.01 mm precision were used for displacement measurements in two perpendicular diagonal directions.
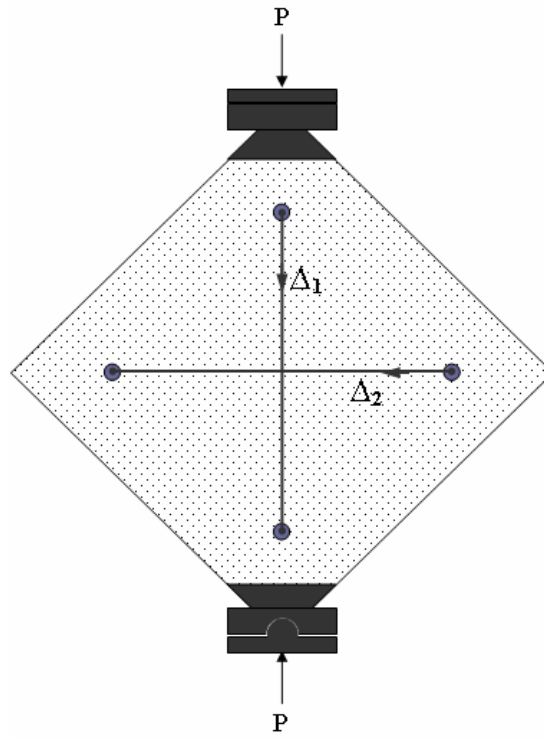
Figure D.7. Infill Panel Test Setup Illustration

Figure D.8. General Views of Infill Panel Test Set-up

318

Steel caps were fixed to the specimen corners by gypsum mortar to prevent local crushing and to uniformly distribute the applied load. Since the specimens were of different thickness, two different size steel caps were used as provided in **Figure D.9.** All specimens were white washed to observe crack patterns better and were tested under load controlled monolithic loading through the vertical diagonal up to failure. An electronic data-acquisition system recorded the applied load and deformations measured over the two diagonals continuously.
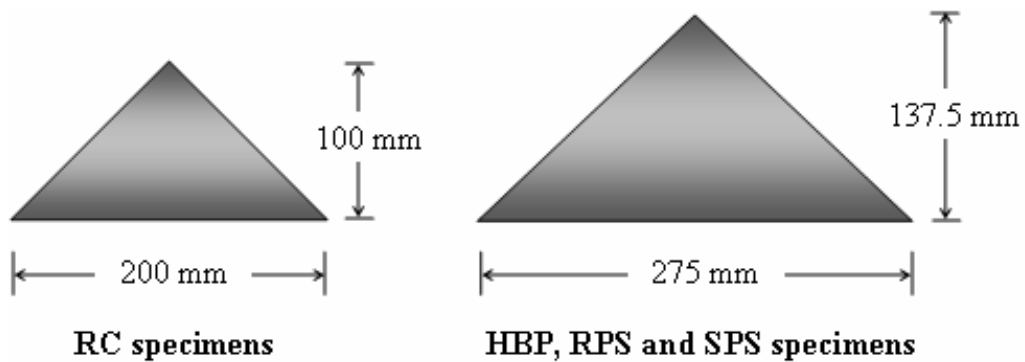
Figure D.9. Steel Cap Dimensions

D.4. Test Results and Observations

Infill wall panels were located on the setup and loaded by monolithical diagonal compression. Applied load was measured by a loadcell. Shortening of the loaded diagonal and elongation of the transverse diagonal were measured by dial gages and recorded. Load – deformation graphs of all specimen groups are presented in **Figure D.10, Figure D.11, Figure D.12,** and **Figure D.13.** It should be explained that, the post-peak data of each specimen was ignored beyond 80% of the maximum load. Load carrying capacities of all specimens are summarized in **Table D.6**, damage observations of all specimens are presented in **Table D.7,** and comparison of test results are provided in **Table D.8**.

Specimen	Mortar/Plaster Strength (MPa)	PC Panel / RC Infill Strength (MPa)	Load Carrying Capacity (kN)	Average Load Carrying Capacity (kN)
Hollow Brick Infill Specimens				
HBP1	5.3	-	61.9	64.7
HBP2	5.3	-	64.7	
HBP3	5.3	-	67.6	
HBP4*	5.3	-	-	
Rectangular PC Panel Strengthened Hollow Brick Infill Specimens				
RPS1	5.3	50.0	118.9	137.0
RPS2	5.3	50.0	114.6	
RPS3	5.3	50.0	178.3	
RPS4	5.3.	50.0	136.3	
Strip PC Panel Strengthened Hollow Brick Infill Specimens				
SPS1	5.3	50.0	163.6	176.0
SPS2	5.3	50.0	168.4	
SPS3**	5.3	50.0	-	
SPS4	5.3	50.0	196.0	
RC Infill Specimens				
RC1	-	18.0	167.6	182.8
RC2	-	18.0	175.9	
RC3	-	18.0	166.3	
RC4	-	18.0	194.3	
RC5***	-	18.0	-	
RC6	-	18.0	209.8	

* : Technical problem in data recording

** : Problem in the test setup

*** : Premature failure
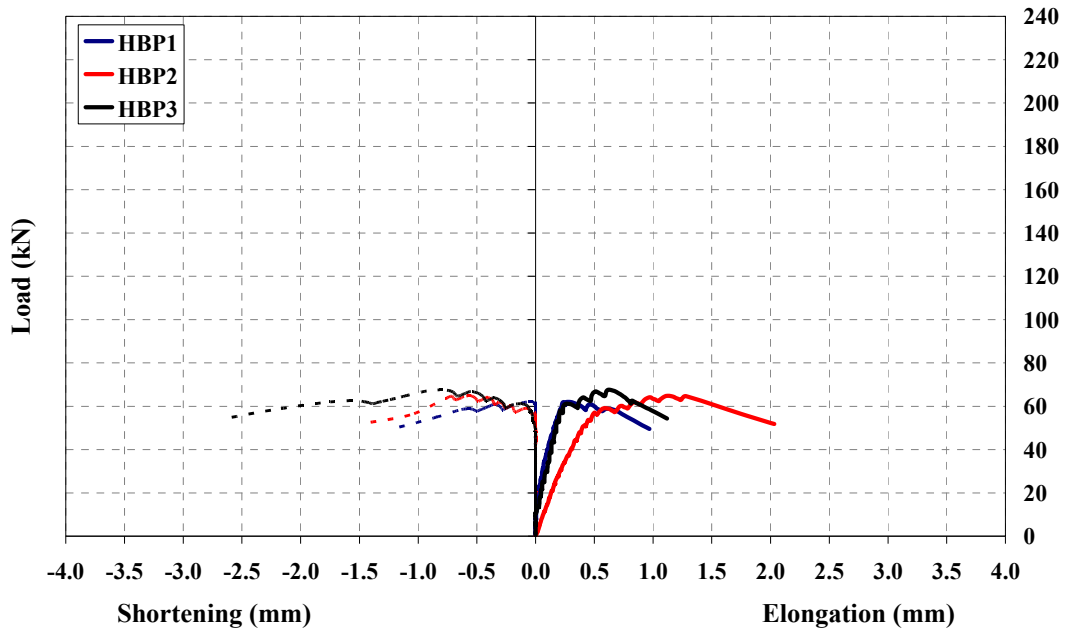
Figure D.10. Load vs. Elongation/Shortening of **HBP** Specimens
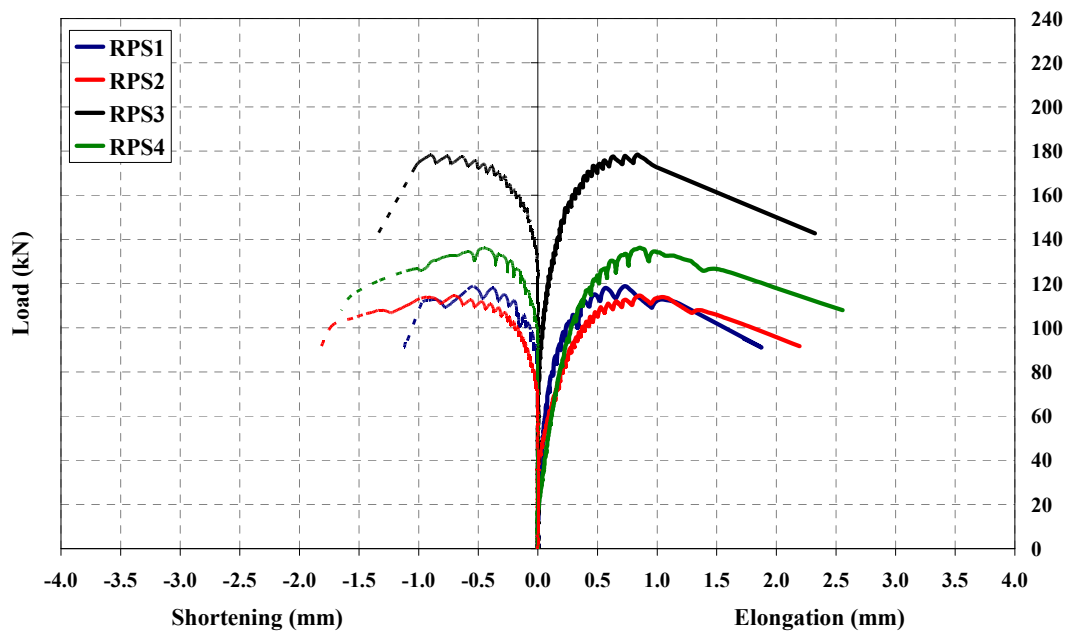
Figure D.11. Load vs. Elongation/Shortening of **RPS** Specimens
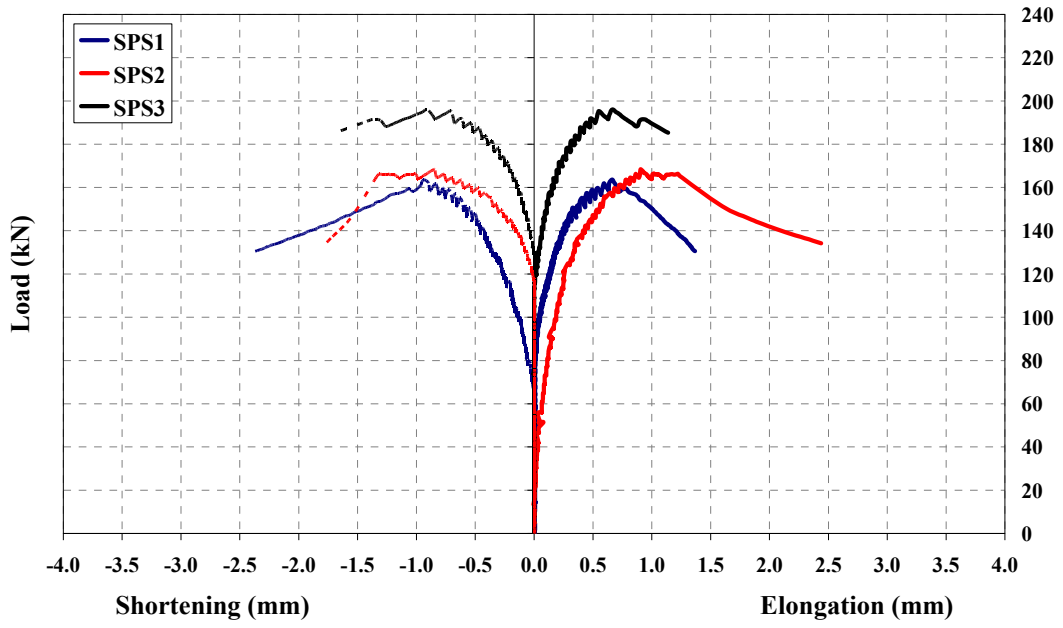
Figure D.12. Load vs. Elongation/Shortening of **SPS** Specimens
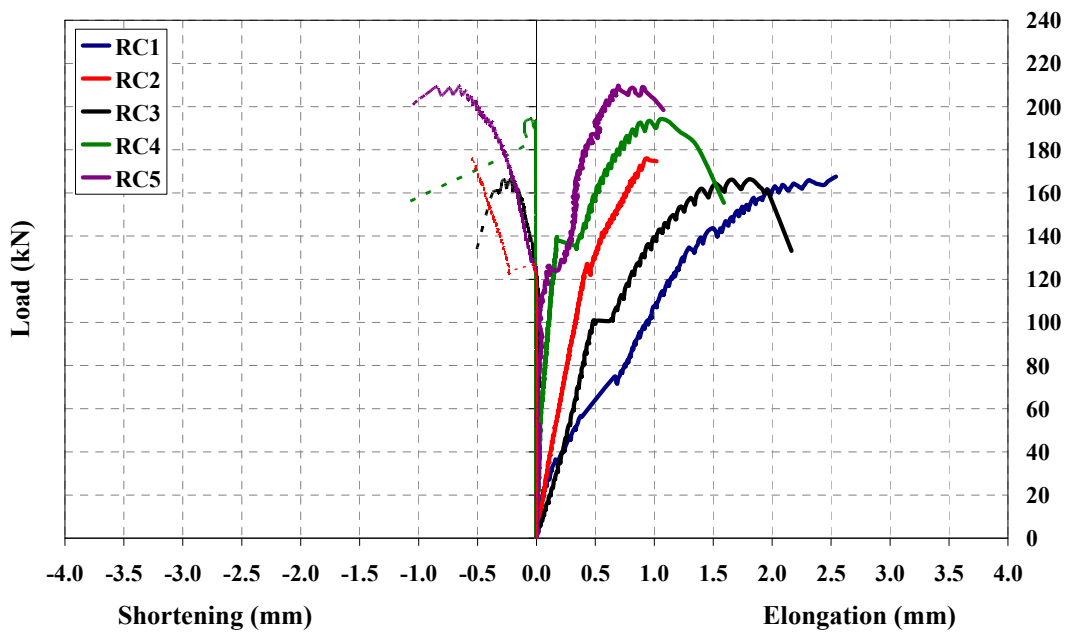
Figure D.13. Load vs. Elongation/Shortening of **RC** Specimens

322

Table D.7. Damage Observations of Infill Panel Tests

Specimen	Observation
HBP1	Diagonal cracking along the loading direction.
HBP2	Diagonal cracking along the loading direction and appearance of cracks lying from steel cap corners to the main diagonal crack.
HBP3	Diagonal cracking along the loading direction.
HBP4*	-
RPS1	Cracks on the PC panels perpendicular to the loading direction mostly on the upper cap side; openings on the epoxy connections of both free corner PC panels which are also observable on the plaster surface; two wide, diagonal and symmetrical cracks on the plaster lying from ~one brick distance away from top steel cap corner to the bottom cap edges; crushing on the bricks.
RPS2	Cracks on the PC panels perpendicular to the loading direction mainly on the bottom side; localized concrete crushing of the PC panel corners closer to the loading caps; wide diagonal cracks along the loading direction on the plaster side; crushing of the brick closer to the top loading steel cap and separation of the plaster over the crushed brick surface.
RPS3	Cracks on the PC panels perpendicular to the loading direction being very closer to the upper loading cap; separation of corner PC panel on which the upper loading cap is bonded; diagonal plaster crack on the loading direction in between the edges of both steel caps; crushing of the bricks at the upper loading steel cap and separation of plaster around the crushed bricks.
RPS4	Cracks on the PC panels perpendicular to the loading direction being very closer to the bottom loading cap, crushing and separation of the PC panel just above the bottom loading cap; a wide diagonal plaster crack in the loading direction in between the edges of the loading steel caps and separation of approximately half of the hollow brick infill wall from the PC panel layer following the mentioned diagonal crack
SPS1	Cracks on the PC panels perpendicular to the loading direction being very closer to the bottom loading cap; crushing of the PC panel concrete just above the bottom loading cap edges; a number of diagonal plaster cracks on the loading direction; crushing of the hollow bricks above the bottom loading cap and separation of the plaster over the crushed bricks.
SPS2	Cracks on the PC panels perpendicular to the loading direction being very closer to the upper loading cap and crushing of the PC panel concrete over the crack zone; a wide, diagonal plaster crack in the loading direction; no plaster separation.
SPS3**	-
SPS4	Crushing of the hollow bricks around the bottom loading cap and bending/buckling cracks on the PC panels perpendicular to the loading direction; separation of plaster and spalling of the crushed bricks.
RC1	Diagonal crackings along the loading direction; spalling of the concrete around the top loading cap and the dial gage measuring the deformation on the loading direction lifted up with concrete.

Table D.7. (Continued) Damage Observations of Infill Panel Tests

RC2	A wide diagonal cracking along the loading direction; spalling of the concrete around the bottom loading cap and the dial gage measuring the deformation on the loading direction lifted up with concrete.
RC3	A wide diagonal cracking together with a number of fine cracks along the loading direction; spalling of the concrete around the bottom loading cap and consequently, separation of the metal disc which bounds the gage length of the dial gage measuring the deformation on the loading direction.
RC4	A wide diagonal crack lying from the corner of the upper loading cap to the cross corner of the bottom loading cap; spalling of the concrete on miscellaneous points along the crack and around the cross corners of the loading caps on rear side.
RC5***	-
RC6	A wide diagonal crack lying from the corner of the upper loading cap to the cross corner of the bottom loading cap; a number of fine cracks on the loading direction; spalling of the concrete on miscellaneous points along the wide crack and around the left corner of the bottom loading cap on the rear side.

*   : Technical problem in data recording

** : Problem in the test setup

*** : Premature failure

The tests were performed in accordance with ASTM E519/E519M – 10 standards. (**ASTM E519/E519M, 2010**) This specification proposes equations also to prepare the shear strain-shear stress graphs for diagonally loaded infill panels. Shear strain and shear stress are calculated using below presented equations of **Equation D.1**, **Equation D.2** and **Equation D.3.**

$$\gamma = \frac{\Delta V + \Delta H}{g} \tag{D.1}$$

$$S_s = \frac{0.707 F_d}{A_n} \tag{D.2}$$

$$A_n = \frac{(b+h)}{2} * t * n \qquad \qquad \text{(D.3)}$$

where the parameters defined as;

$\gamma:$ Shearing strain, in mm/mm

$S_s:$ Shearing stress, in MPa

$\Delta V:$ Vertical shortening, in (mm)

$\Delta H:$ Horizontal extension, in (mm)

$g:$ Vertical gage length, in (mm) so that ΔV must be based on the same gage length as ΔH

$F_d:$ diagonal compression force, in N

$A_n:$ net area of the specimen, in mm^2

$b:$ Width of the specimen, in mm

$h:$ Height of the specimen, in mm

$t:$ Thickness of the infill panel, in mm

$n:$ The percent of the gross area of the unit that is solid, expressed as a decimal. **n** is calculated to be 0.936, 0.947 and 1.0 for the specimens **HBP**, **RPS, SPS** and **RC**, respectively.

The shear strain-shear stress graphs obtained by above presented equations are also depicted in **Figure D.14**, **Figure D.15**, **Figure D.16** and **Figure D.17** for all series of specimens. It should be underlined that, the post-peak data of each specimen were ignored beyond 80% of the maximum load. In addition, views of the infill panel specimens are presented from **Figure D.18** to **Figure D.29**.
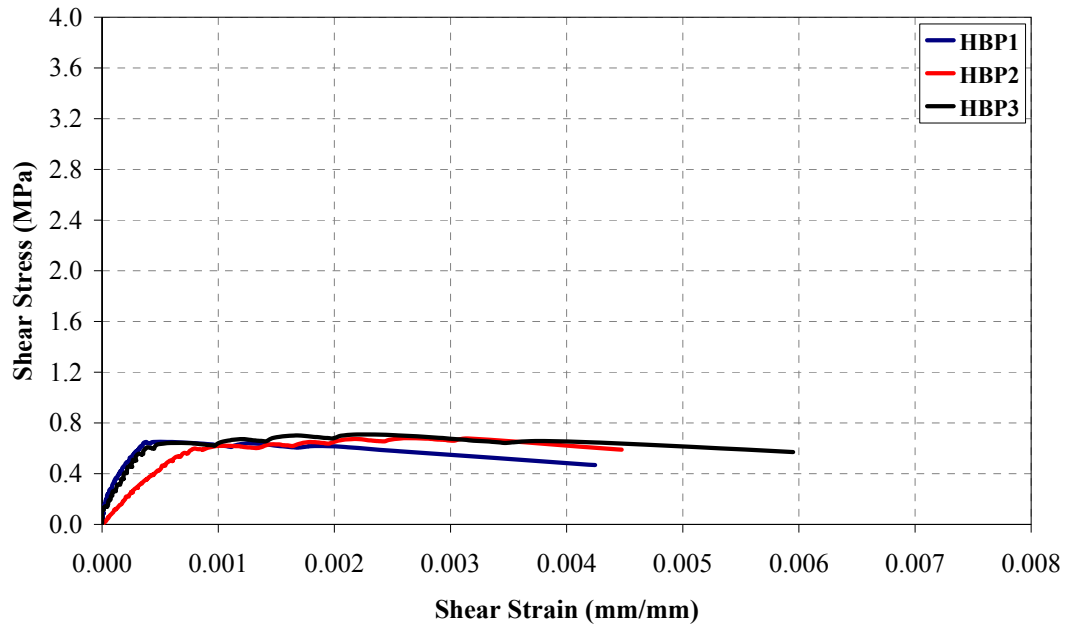
Figure D.14. Shear Strain-Shear Stress Graphs for **HBP** Specimens
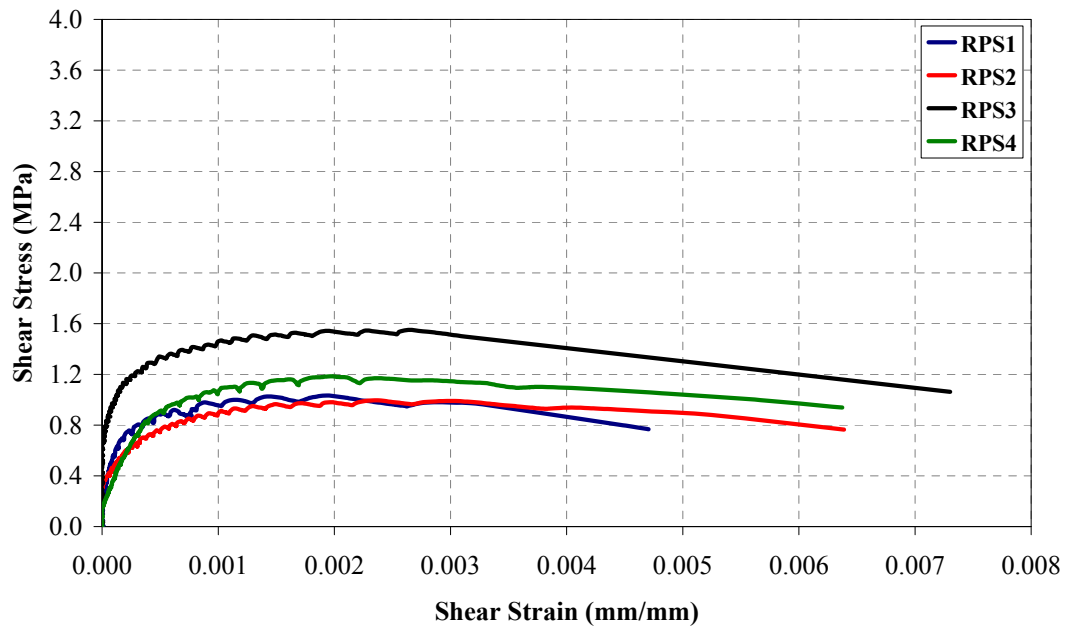
Figure D.15. Shear Strain-Shear Stress Graphs for **RPS** Specimens
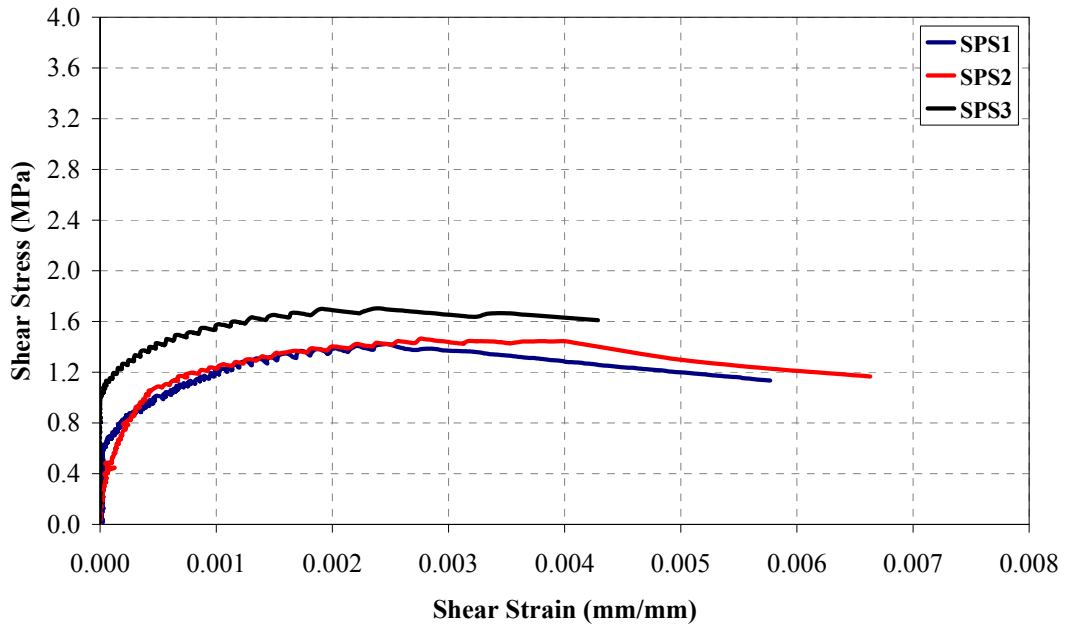
Figure D.16. Shear Strain-Shear Stress Graphs for **SPS** Specimens
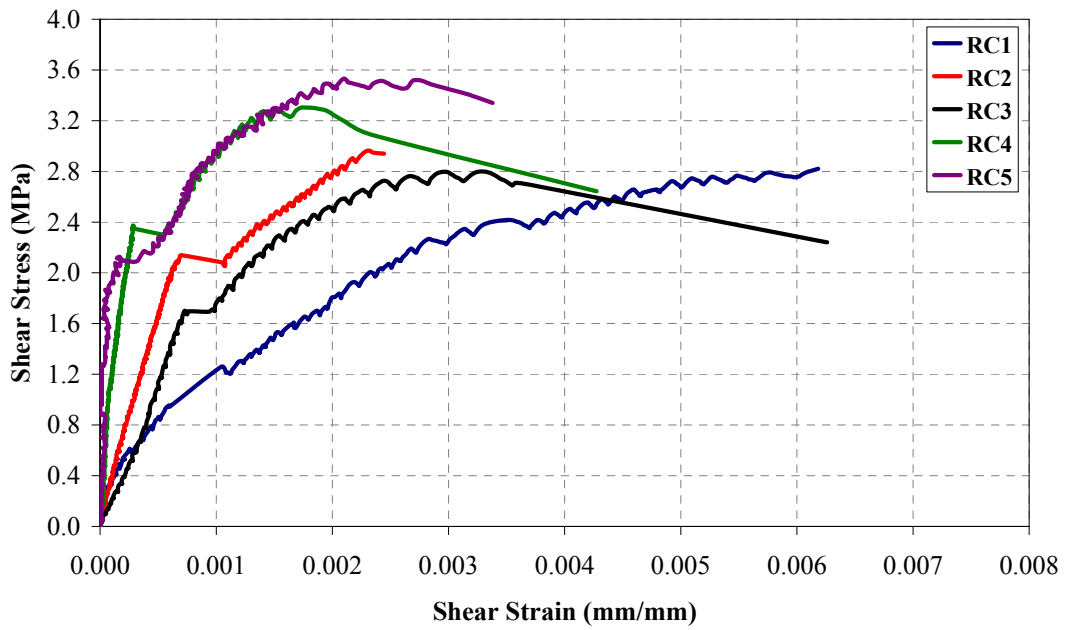
Figure D.17. Shear Strain-Shear Stress Graphs for **RC** Specimens

327
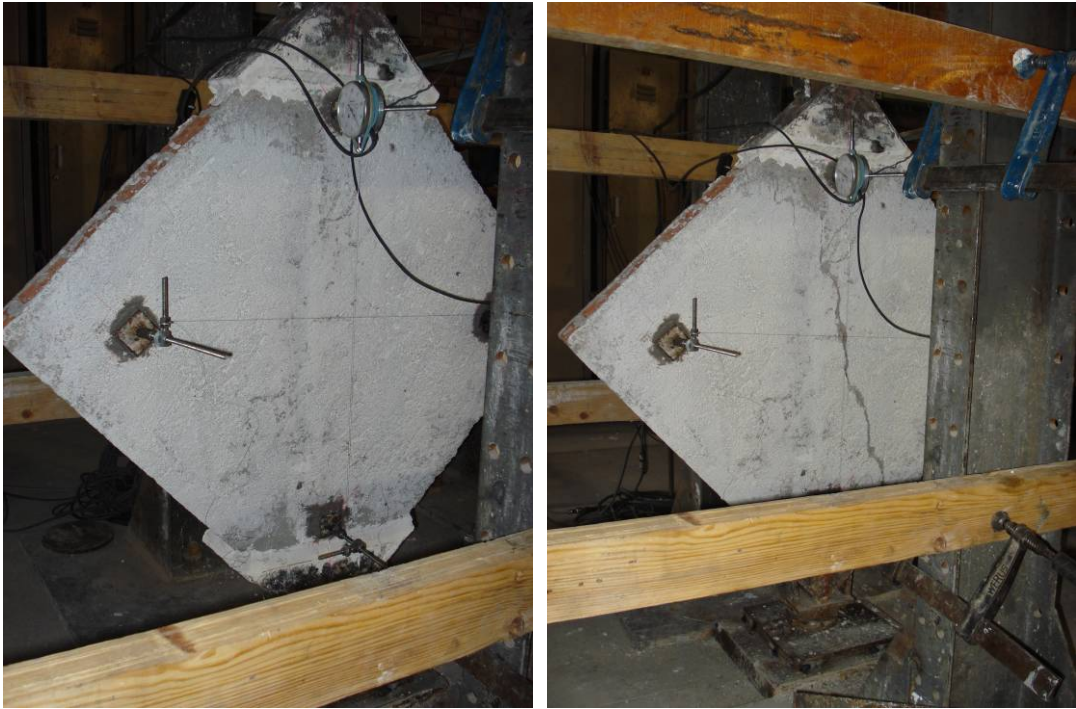
Figure D.18. Views of Specimen **HBP1** Before and after Test

Figure D.19. Front and Rear Side Views of Specimen **HBP2** after Test

Figure D.20. Front and Rear Side Views of Specimen **HBP3** after Test

Figure D.21. Front and Rear Side Views of Specimen **RSP1** after Test
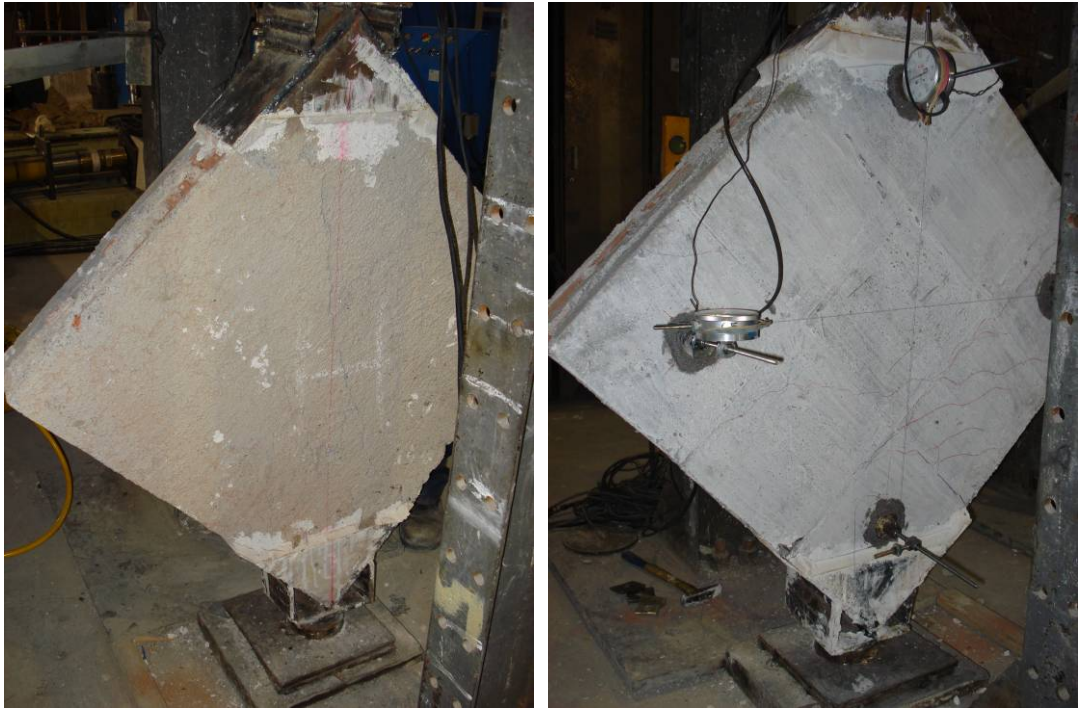
Figure D.22. Front and Rear Side Views of Specimen **RSP2** after Test

Figure D.23. Front and Rear Side Views of Specimen **RSP3** after Test

Figure D.24. Front and Rear Side Views of Specimen **RSP4** after Test

Figure D.25. Front and Rear Side Views of Specimen **SPS1** after Test

Figure D.26. Front and Rear Side Views of Specimen **SPS2** after Test

Figure D.27. Front and Rear Side Views of Specimen **SPS3** after Test

Figure D.28. Front and Rear Side Views of Specimen **SPS4** after Test

Figure D.29. Views of **RC** Specimens after the Experiment

334

D.5. Evaluation of Test Results

Total of 18, 1:3 scaled infill panels with varying properties were prepared and tested in the scope of the infill panel tests. Due to the technical problems realized in data recording and test set-up, three of the test data were not able to be processed reliably. Since the infill panels were of non-homogenous structure, it was very difficult to obtain the modulus of elasticity for the tested specimens. Rough estimations of compressive strength and modulus of elasticity values of specimen series were realized and presented in **Table D.8** and the tabulated values were valued for analytical RC frame modelling studies. In addition, diagonal load carrying capacities were primarily evaluated as the performance indicator, as tabulated in **Table D.9.** In this section, the infill panel test results are evaluated by means of failure modes and strength characteristics.

Table D.8. Compressive Strength and Modulus of Elasticity Estimations for Infill Panel Test Specimens

Specimen Series	Compressive Strength (MPa)	Modulus of Elasticity (MPa)
HBP	2.61	5000
RPS	4.53	8000
SPS	5.82	8500
RC	15.23	12500

Table D.9. Comparison of the Load Carrying Capacities of Infill Panel Series

Specimen	Average Load Carrying Capacity (kN)	Comparison to that of HBP Specimen
HBP	64.7	~1.0 times
RPS	137.0	~2.1 times
SPS	176.0	~2.7 times
RC	182.8	~2.8 times

335

D.5.1. Failure Modes

Test data and behaviour observations of total of 15 infill panel specimens were evaluated. Mortar and plaster thicknesses were ~10 mm for all hollow brick wall covering specimens. Average load carrying capacity results and comparisons of the panel tests are presented in **Table D.9**.

Hollow brick infill panels were the reference specimens of the panel tests since; they represent the existing infill system in most of the RC framed structures in Turkey. All **HBP** specimens failed due to the diagonal cracking along the loading direction reaching the average diagonal compression capacity of **64.7 kN**. The behaviour of **HBP** specimens clearly indicated that tensile stresses perpendicular to the diagonal crack of the loading direction caused the failure.

RPS specimens were the first group of the strengthened hollow brick infill wall panels. The test data showed that rectangular PC panel application increased the diagonal loading capacity of hollow brick infill panels considerably, ~2.1 times that of **HBP** specimen by reaching **137.0 kN** of diagonal compression capacity, in average. RPS specimens failed in a more ductile manner compared to **HBP** specimens. Diagonal plaster cracks parallel to the loaded diagonal and PC panel crushing cracks mostly localized around the loaded diagonal corners were observed prior to failure of **RPS** specimens. In addition, separation cracks on the loaded corner panel-to-panel connections were monitored.

SPS specimens provided a superior performance against **RPS** specimens by achieving **176.0 kN** of average loading capacity that corresponds to ~2.7 times that of **HBP** specimen. The difference in the diagonal load carrying capacities of **RPS** and **SPS** specimens can be attributed to the panel lap joint configurations. Since the principal stresses are concentrated around the loading cap regions, as also analytical model representation is depicted in **Figure D.39,** sliding of the corner panel from the infill in **RPS** specimens became easier due to existence of lap joint for rectangular PC panel

and this action decreased the diagonal load carrying capacity by disrupting the integrity of the panel layer.

RC specimens reached **181.8 kN** average diagonal load carrying capacity which corresponds to ~2.8 times that of **HBP** specimen. **RC** panel specimens failed by diagonal cracking along the loaded direction which was completed by crushing of the concrete around the loading cap corners. Spalling of the concrete on the edges of the bottom loading cap was also observed. Stress analysis performed by running SAP2000 (**SAP2000, V.11**) software provides the principal stress directions over the loaded infill panel under diagonal compression as presented in **Figure D.31**. **Figure D.30** provides the front and rear side views of the **RC2** specimen after the experiment. The localized concrete crushing and spalling occurred on the corner zones of the specimen **RC2,** over which the stress concentrations were also analytically obtained and presented in **Figure D.31.**

One representative test data from each specimen group are presented in **Figure D.32** for load vs. elongation/shortening relationship and the other for shear stress – shear strain behaviour in **Figure D.33**.

Figure D.30. Front and Rear Side Views of Specimen **RC2** after the Experiment
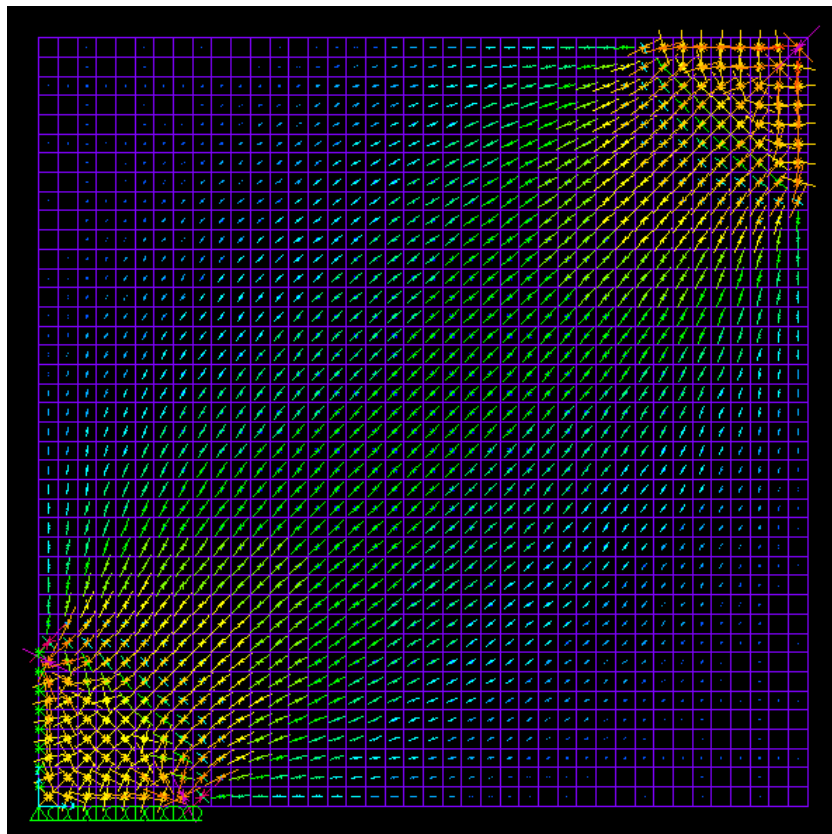
Figure D.31. Principal Stress Directions for **RC** Series Specimens Loaded by
Distributed Diagonal Compression
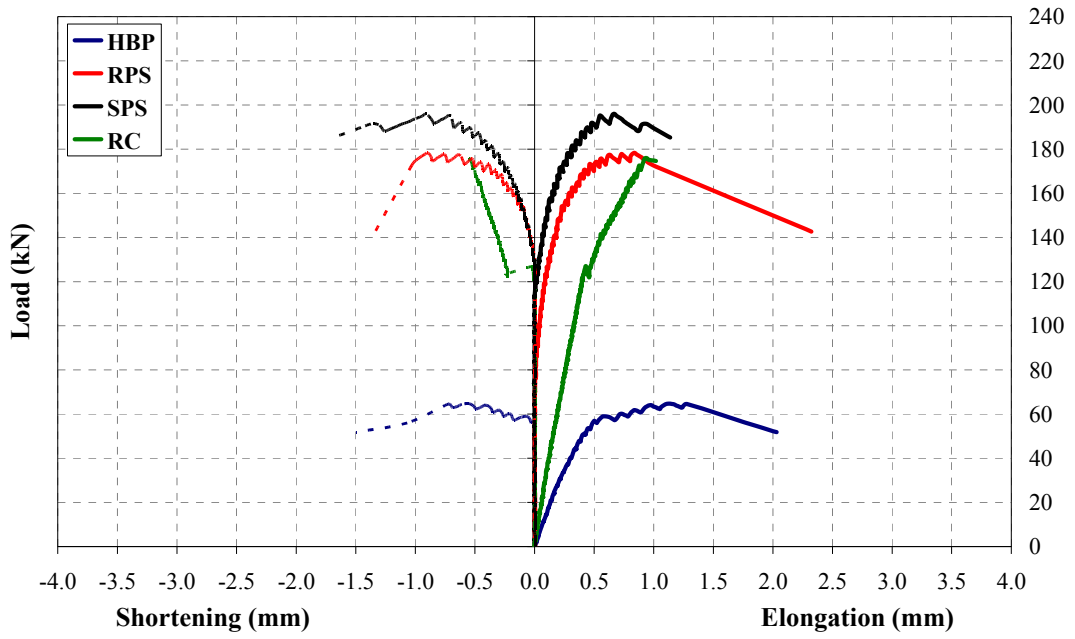
Figure D.32. Representative Load vs. Elongation/Shortening Graphs for All Series of Specimens
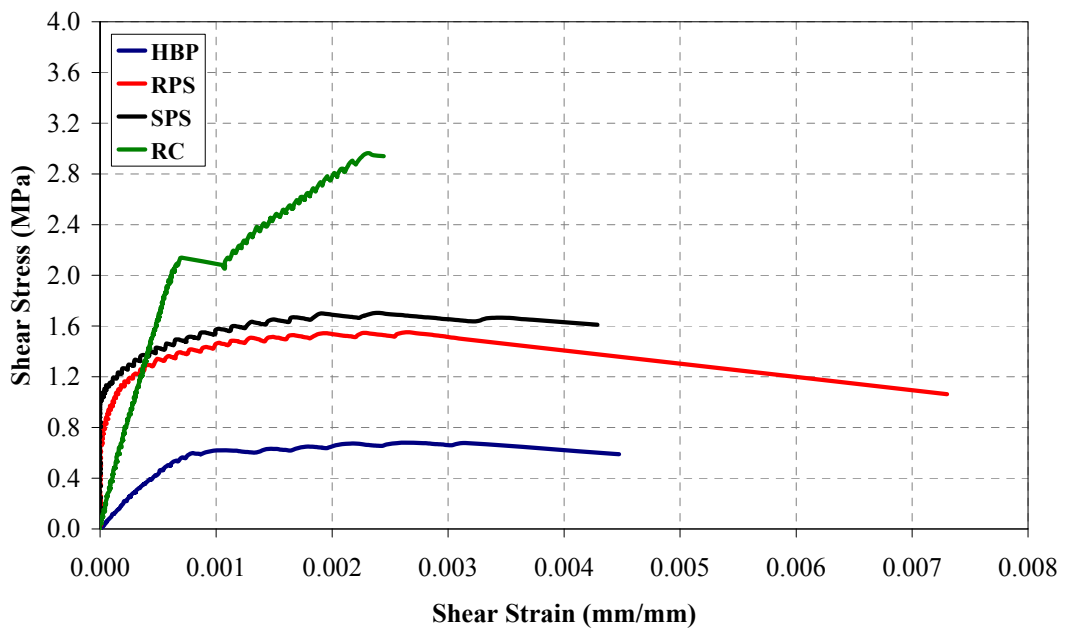
Figure D.33. Representative Shear Strain-Shear Stress Graph for All Series of Specimens

339

D.5.2. Strength Characteristics

Infill panels were tested under diagonal compression were further modelled and analyzed in SAP2000 **(SAP2000, V.11)** computer software for analytical investigations. Panels were modelled as thin shell elements and finely meshed into 40x40 (total of 1600) sub-elements. The infill panels were assumed to be modelled as isotropic, linearly elastic and globally homogenous. The primary objective of computer model analysis was to obtain the principal stress directions of the diagonally loaded specimens.

Stress analysis of infill panels were carried out on two different analytical models. In the first model, the specimens were analyzed under concentrated diagonal compression force as shown in **Figure D.34** Centre point stresses of the panels were obtained and also presented in **Figure D.34**. The stresses are normalized for average stress, τ_{ave} as given in **Equation D.4**. The Mohr's Circle representation of the midpoint stresses and principal stress directions for this model is presented in **Figure D.35** and **Figure D.36**, respectively.

$$\tau_{ave} = \frac{0.707F_d}{bt}$$

(D.4)

where the parameters are defined as:

F_d : diagonal compression force, in N

b : Width of the specimen, in mm

t : Thickness of the infill panel, in mm
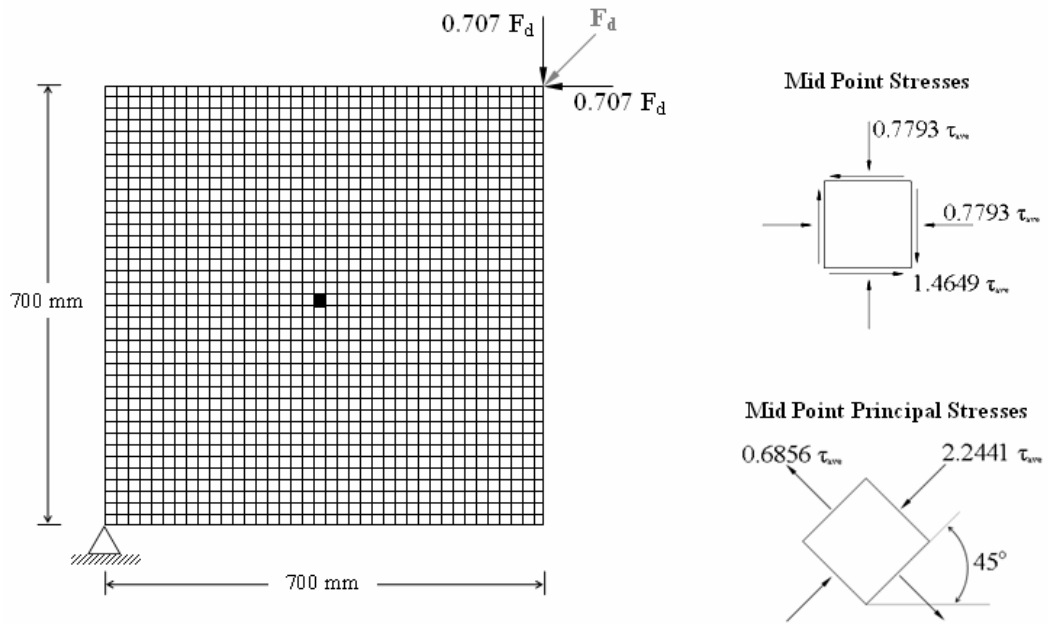
Figure D.34. Finite Element Model of the Panel Specimen with Concentrated Diagonal Force
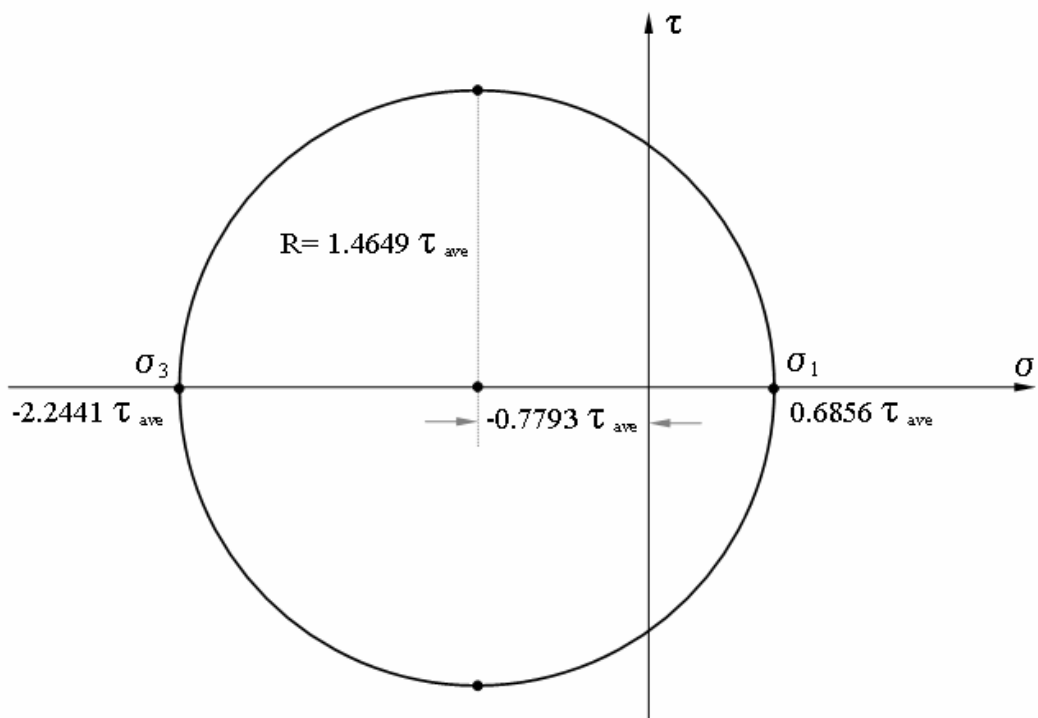
Figure D.35. Mohr's Circle Representation of Midpoint Stresses for the First Panel Finite Element Model
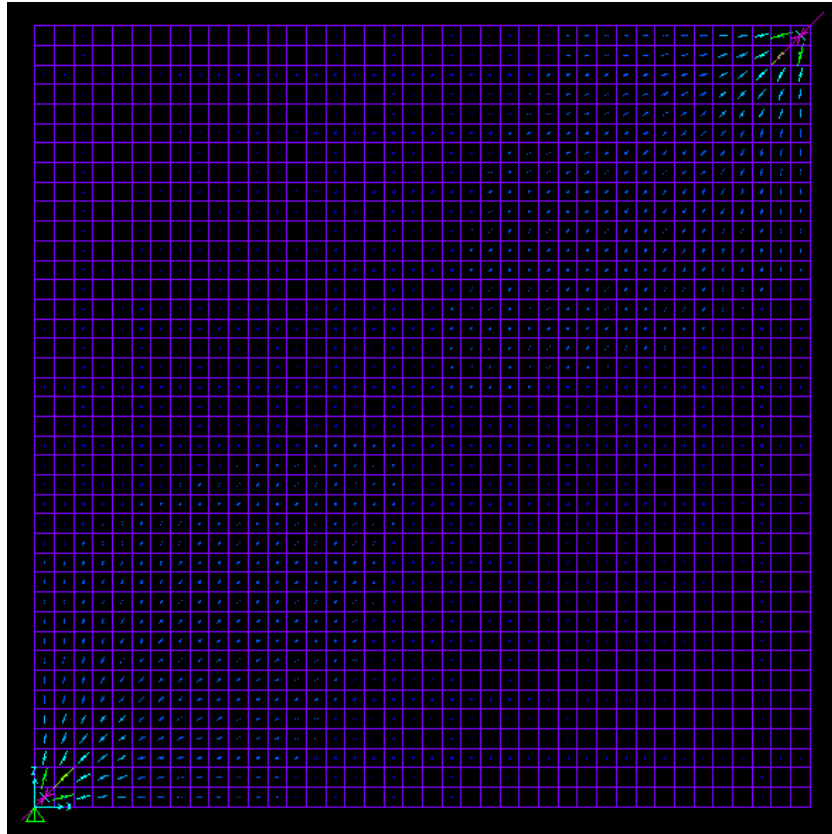
Figure D.36. Principal Stress Directions of Panel Loaded by Concentrated Diagonal Compression

In the second finite element model of the infill panels, the load and support were distributed over the steel cap length, since the panels were supported and loaded over the steel caps on both upper and bottom corners. The analytical model, midpoint stress distributions and τ_{ave} normalized midpoint principal stresses for all specimens are illustrated in **Figure D.37**. Mohr's Circle representation of mid-point stresses for the second panel model with distributed load and support is presented in **Figure D.38.**

The midpoint stresses in between two models did not vary a lot, however the second model provided more realistic stress distributions which also coincides with the experimental damage observations. The model assumes the panel as isotropic, linearly elastic and homogenous. Compressive stresses are shown as negative and tensile stresses are shown as positive.
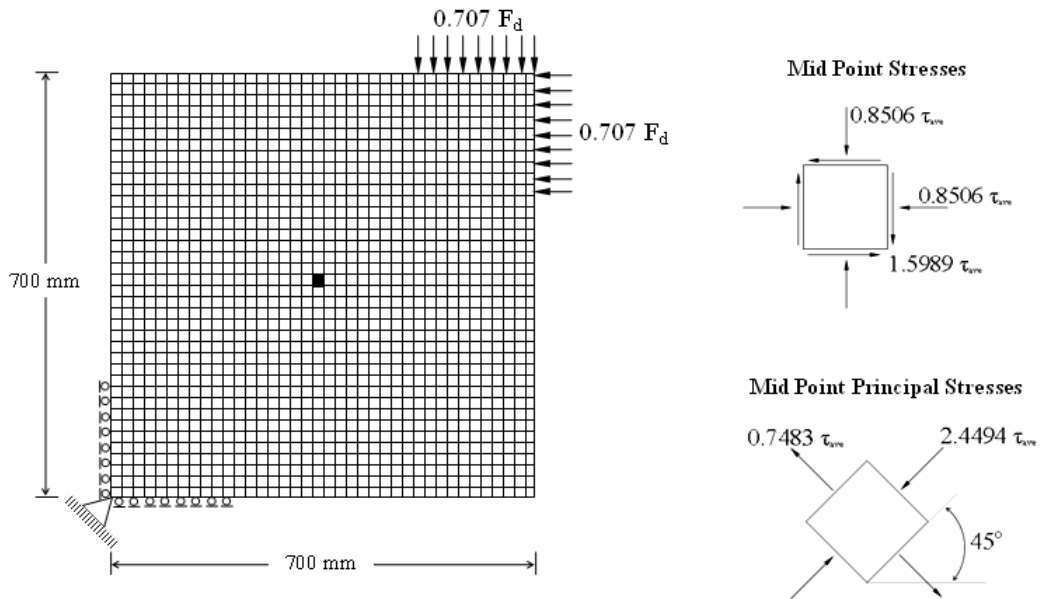
Figure D.37. Finite Element Model of the Panel Specimen with Distributed Diagonal Force and Support
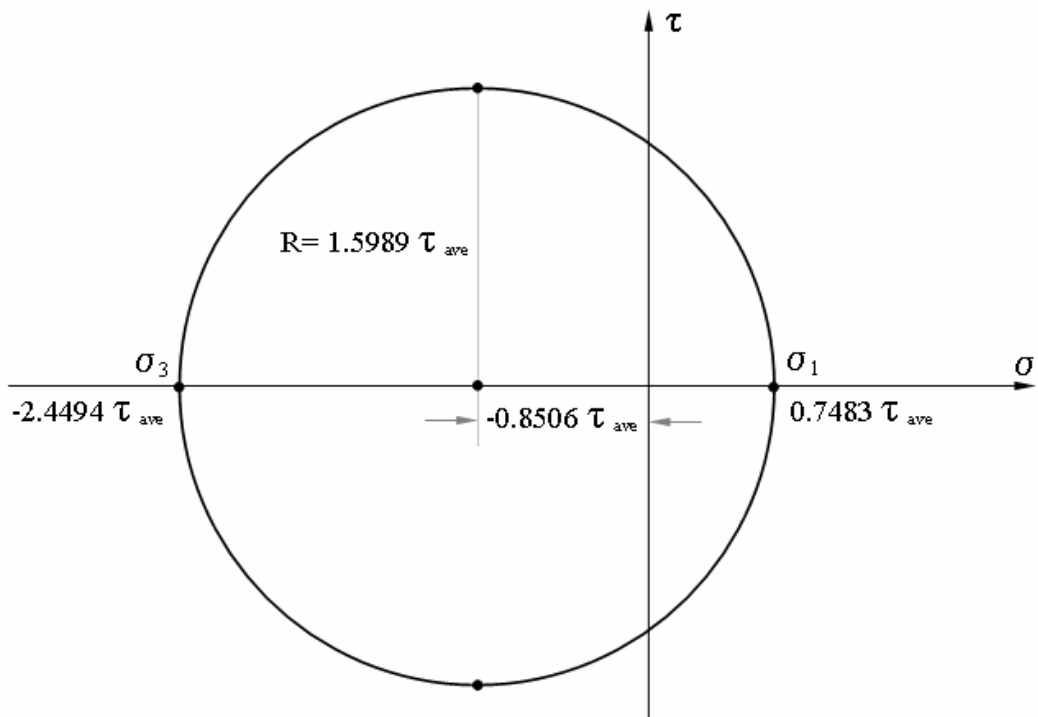
Figure D.38. Mohr's Circle Representation of Mid-point Stresses for Second Panel Model

343

Smaller sized steel caps were used for RC infills so that they were in ~60 mm thickness; while all the remaining panels were subjected to the diagonal loading using the larger sized steel caps. The difference in steel cap dimensions did not affect the midpoint principal stresses; however, the principal stress directions varied slightly which also well coincides with the damage observations of RC specimens. The principal stress directions of the second model for RC specimens is formerly presented in **Figure D.31** and the other one for **HBP**, **RPS** and **SPS** specimens are provided in **Figure D.39**.
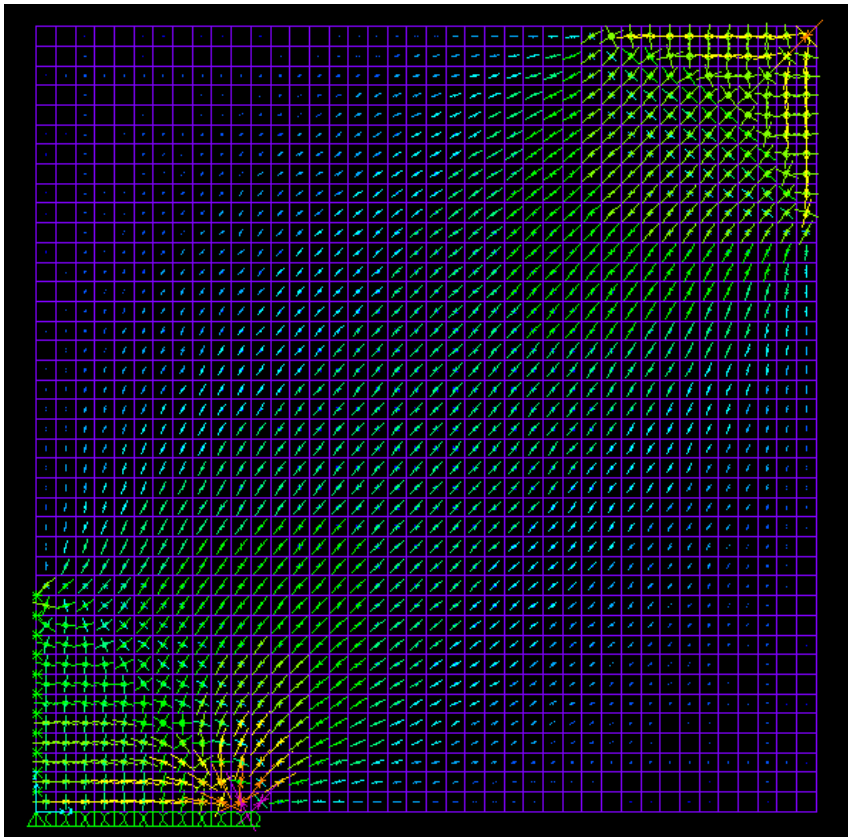
Figure D.39. Principal Stress Directions for **HBP, RPS** and **SPS** Series Specimens Loaded by Distributed Diagonal Compression

In case of analytical capacity predictions, Mohr – Coulomb failure hypothesis was used for calculating the cracking strength, since the failure was brittle and the diagonal cracking initiated at or near the centre of panel. (**Popov, 1998**) Failure of the non-plastered panels was reported to be basically occurred in the brick lying mortar and therefore, the mortar strength was used for the calculation of the capacity. (**Sevil, 2010**)

Considering Mohr-Coulomb failure surface for the biaxial state of stress presented in **Figure D.40** for the second infill panel model, tensile strength of the mortar can be calculated below, as also **Sevil (2010)** stated.
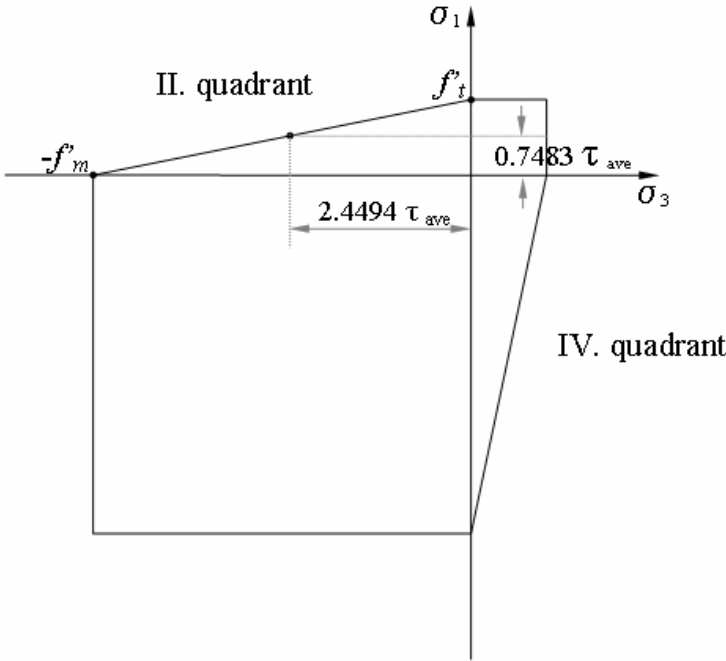
Figure D.40. Mohr – Coulomb Yield Surface for Second Panel Model

Equation of the line in the second quadrant is given in **Equation D.5**. Compressive strength of the material, f'_m, and the test results obtained from the diagonal compression test of the panels are the two points known on the line of second quadrant.

$$\sigma_1 = a\sigma_3 + c \tag{D.5}$$

$$@ \quad \sigma_1 = 0 \quad \rightarrow \quad \sigma_3 = f'_m \quad \Rightarrow \quad a = -\frac{c}{f'_m} \tag{D.6}$$

$$@ \quad \sigma_1 = 0.7483\tau_{ave} \quad \rightarrow \quad \sigma_3 = -2.4494\tau_{ave} \quad \Rightarrow \quad c = \frac{0.7483\tau_{ave}f'_m}{f'_m + 2.4494\tau_{ave}} \tag{D.7}$$

where the parameters are defined as:

a : Slope of the line in the second quadrant

c : Intersection point on σ_1 axis, being the tensile strength of the material, f'_t

f'_m **:** Compressive strength of the material

When the average shear stress, $\boldsymbol{\tau_{ave}}$, defined in **Equation D.4** formerly is substituted in **Equation D.7**, the following expression is obtained for the tensile strength of the material being the intersection point on σ_1 axis.

$$c = f'_t = \frac{0.5290 f'_m F_d}{f'_m bt + 1.7317 F_d} \tag{D.8}$$

The Mohr-Coulomb criteria yield in the second quadrant to **Equation D.9**, with the known compressive and tensile strength of the mortar/plaster.

$$\frac{\sigma_1}{f'_t} - \frac{\sigma_3}{f'_m} = 1 \tag{D.9}$$

The finite element analysis gives $\sigma_1 = 0.7483\tau_{ave}$ and $\sigma_2 = 2.4494\tau_{ave}$ for the principal stresses. When these values are substituted into the Mohr-Coulomb criteria and the average shearing stress is considered as cracking stress, the following equation is obtained for cracking stress.

$$\tau_{cr} = \frac{f^l{}_t f^l{}_m}{0.7483 f^l{}_m - 2.4494 f^l{}_t} \tag{D.10}$$

The brick lying mortar and plaster strength was 5.3 MPa for all **HBP**, **RPS** and **SPS** specimens. The corresponding tensile strength obtained by **Equation 8.8** overestimated the calculated diagonal load capacity of the corresponding panels. A line can be proposed for tensile strength of the mortar considering that the line should intersect the origin as also stated by **Sevil (2010)**

$$f^l{}_t = 0.05 f^l{}_m \tag{D.11}$$

The above stated equation is only valid for the brick lying mortar. The regular equation for direct tensile strength of the concrete is used for tensile strength of the plaster and tensile strength of the concrete for **RC** and **RPS** panels as presented in **Equation D.12** and **Equation D.13**, respectively. (**Ersoy, Özcebe, Tankut, 2003**) In case of **SPS** panels, direct tensile strength value of the concrete obtained by **Equation D.13** underestimates the calculated diagonal loading capacity when compared to that of experimental data. **Equation D.14**, which is also the splitting tensile strength function for normal strength concrete, is proposed for calculation of the tensile strength value for concrete component of **SPS** panels. (**Ersoy, Özcebe, Tankut, 2003**)

$$f^l{}_{t,p} = 0.35\sqrt{f^l{}_{c,plaster}} \tag{D.12}$$

$$f^l_{t,c} = 0.35\sqrt{f^l_{c,concrete}} \quad \text{(for RC and RPS panels)} \tag{D.13}$$

$$f^l_{t,c} = 0.50\sqrt{f^l_{c,concrete}} \quad \text{(for SPS panels)} \tag{D.14}$$

where the parameters are defined as:

$f^l_{c,plaster}$:   Compressive strength of the plaster, in MPa

$f^l_{c,concrete}$ Compressive strength of the panel concrete, in MPa

$f^l_{t,p}$:   Tensile strength of the plaster, in MPa

$f^l_{t,c}$:   Tensile strength of the panel concrete, in MPa

When the tensile strength of the material is determined, the cracking shear strength of the material is calculated and than the force contribution is easily calculated from the average shear stress definition. Contribution of steel reinforcement is also involved in case of capacity calculation for **RC** panel. The experimental load carrying capacities and that of theoretically calculated values are tabulated in **Table D.10**.

Table D.10. Comparison of Calculated vs. Experimental Load Carrying Capacities of Infill Panels

Specimen	Strength (MPa)		Force Contribution (kN)			Calculated Capacity (kN)	Test Result (kN)	Ratio *
	Mortar/ Plaster	Concrete	Brick	Plaster	Concrete			
HBP	5.3	-	20.5	42.4	-	63.0	64.7	1.03
RPS	5.3	50.0	20.5	42.4	78.2	141.1	137.0	0.97
SRS	5.3	50.0	20.5	42.4	121.7	184.7	176.0	0.95
RC	5.3	18.0	-	-	185.5	185.5	181.8	0.98

* Ratio is defined to be experimental / calculated load carrying capacity.

D.6. Conclusions

The contribution of PC panel application on individual hollow brick infill panels was experimentally investigated in this study. Conclusions from the evaluated test data and observations can be stated as follows.

- PC panel application with either rectangular or strip shaped panels improves the diagonal load carrying capacity of hollow brick infill panels considerably when compared to that of plain hollow brick infill panels, as presented in **Table D.9**.

- **SPS** series specimens provided a superior performance against **RPS** series specimens by means of load carrying capacities, **SPS** series panels reached ~2.7 times and **RPS** panels reached ~2.1 times of reference specimens, respectively.

- **RC** series specimens reached the diagonal load carrying capacity of ~2.8 times of the **HBP** specimens. The load carrying capacity is very close to that of the **SPS** panels.

- Mohr-Coulomb failure hypothesis was used to calculate cracking strength. Since the tensile strength function obtained from the second quadrant of the Mohr-Coulomb failure surface for the biaxial state of stress overestimated the cracking capacity; **Equation D.11** was suggested for tensile strength of the mortar and regular concrete equations were proposed for tensile strength of plaster and concrete elements.

- The calculated diagonal load carrying capacities lied in the error range of ± 5% of the experimental values, which can be considered as acceptable.

- The modulus of elasticity and compressive strength value estimations obtained by infill panel tests were used in the analytical RC frame capacity evaluations.

VITA

Dilek OKUYUCU was born in Erzurum, on August 11, 1980. She recieved her B.Sc. degree from Atatürk University in 2002 and was qualified to start direct Ph.D Programme of Department of Civil Enginering, METU in the name of Atatürk University. During her Ph.D. studies, she took permission from the university in 2008 and visited Kassel University, Germany for one year period to make research on seismic control systems and their applications to historical masonry structures for earthquake protection. She worked as research assisstant in between 2002 and 2011. During her Ph.D. in 2011, she recieved Prof. Dr. Uğur Ersoy Experimental Mechanics Scholarship. She finished her Ph.D in 2011. Her main area of interest is seismic performance improvement of RC framed structures and historical masonry buildings.

She started competitive judo in 1985, in Erzurum and participated in numbers of national and international competitions. She is a national team level judo competitior with black belt degree and currently has regional judo referee licence. She also deals with judo related scientific studies. She is also interested and involved in winter sports. She is currently acting as executive board member of Turkish Ice Skating Federation; in chair of education commitee and members of international relations and referee commissions. Her main areas of interest in sport are sport management, olypmic qualification procedures of individual sports and biomechanics related sport performance improvement and evaluation studies.